

CONTROL OF TRANSMISSION SYSTEM POWER FLOWS

A Dissertation
Presented to
The Academic Faculty

By

Frank Kreikebaum

In Partial Fulfillment
Of the Requirements for the Degree
Doctor of Philosophy in Electrical and Computer Engineering

Georgia Institute of Technology

December 2013

Copyright © Frank Kreikebaum 2013

CONTROL OF TRANSMISSION SYSTEM POWER FLOWS

Approved by:

Dr. Deepak Divan, Advisor
School of Electrical and Computer
Engineering
Georgia Institute of Technology

Dr. Ronald Harley
School of Electrical and Computer
Engineering
Georgia Institute of Technology

Dr. Miroslav Begovic
School of Electrical and Computer
Engineering
Georgia Institute of Technology

Dr. Sakis Meliopoulos
School of Electrical and Computer
Engineering
Georgia Institute of Technology

Dr. Valerie Thomas
School of Industrial and Systems
Engineering
Georgia Institute of Technology

Date Approved: November 15, 2013

to Liz

ACKNOWLEDGEMENTS

I am overwhelmed by the support that has enabled this research.

Dr. Deepak Divan is the source of the questions upon which the research is based. His dedication inspired the effort required.

Dr. Miroslav Begovic, Dr. Santiago Grijalva, Dr. Tom Habetler, Dr. Ron Harley, Frank Lambert, Dr. Sakis Meliopoulos, Dr. Valerie Thomas, and Dr. Fumin Zhang provided the necessary techniques and encouragement.

AWS Truepower, Bruce Bailey, Baltimore Gas and Electric, the Begovic family, Michele and John Bleichert, Tom and Mary Frances Carlson, Dominic Caserta and Mafalda Soares, Yongnam Cho, Dong Gu Choi, the Colella family, Jess and Rich Conley, Maria Cortes and the Cortes-Singleton family, Erica Cowell, Micah Cranman, Heather Cunningham, Debrup Das and Pamela Patra, the Dazols Albers family, the Department of Energy, the Divan family, the Dupin family, Patty Durand, Hamza and Ayesha Faraz, Anne Fitzgerald, Donna Florek, the Ford Motor Company, Diana Fouts, General Electric, Sharon Greene, Stefan Grubic, Sangtaek Han, Jean Carlos Hernandez, Jorge Hernandez, Dustin Howard, Munuswamy Imayavaramban, the Intelligent Power Infrastructure Consortium, Amrit Iyer, Harjeet Johal, Rajendra Prasad Kandula, Rye Kennedy and family, Hervé Kieffel, Debbie King, Tyler and Kate King, Jason Kreiselman, Katie Lesko, DeJim Lowe, Nat MacHardy, the Szwedek-Mackiewicz family, Kiran Malancharuvil, Renfro Manning, Greg McPheeters, Siri Melkote, Tiffany Meyer Aljure, Rohit Moghe and family, Marilou Mycko, the National Electric Energy Testing Research

and Applications Center, the National Rural Electric Cooperative Association, the National Science Foundation, Chris Gillham and Mary Nolan-Gillham, Lyneka Porter, the Power Systems Engineering Research Center (PSERC), Andrew Paquette and family, Akanksha Prakash and family, Anish Prasai and Jyoti Sastry, Curtis Roe and Becky Krenz-Roe, Martin Sanchez and family, Joe Schatz, Mitch and Betty Simpson, Brian Smith, Smart Wire Grid, Southern Company, Daniela Staiculescu, James Steinberg, the Tennessee Valley Authority, James Thomas, Jacqueline Trappier, Varentec, Eric White, Rochelle Williams, Whitney Wilson, Yi Yang, Jacob Yunis, and my family filled in the gaps.

TABLE OF CONTENTS

ACKNOWLEDGEMENTS	iv
LIST OF TABLES	xii
LIST OF FIGURES	xiv
NOMENCLATURE	xx
SUMMARY	xxv
CHAPTER 1: INTRODUCTION	1
CHAPTER 2: ORIGIN AND HISTORY OF THE PROBLEM	5
2.1. Introduction	5
2.2. Current State of Transmission Operation	5
2.2.1. Reliability	5
2.2.2. Congestion	6
2.2.3. Methods of Control	11
2.3. Drivers for Additional Transmission Capability	12
2.3.1. Metrics of Transmission Capability	12
2.3.2. Load Growth	12
2.3.3. Historic Transmission Investment Levels	13
2.3.4. Integration of Renewable Generation	14
2.3.5. Discussion	19
2.4. Transmission Planning and Regulation	19

2.4.1.	Centralized Transmission Planning	19
2.4.2.	Merchant Transmission Planning	25
2.5.	Potential Mechanisms to Increase Transmission Capability	27
2.5.1.	Aggregating Control and Market Areas	27
2.5.2.	Incenting Additional Transmission Investment	28
2.5.3.	New Transmission Cost Allocation Methods	30
2.5.4.	Consolidation of Transmission Ownership and Operation	32
2.5.5.	Increased Controllability of Power Flows	33
2.6.	Potential Methods to Reduce Need for Additional Transmission Capability	34
2.6.1.	Locating Generation in Load Centers	34
2.6.2.	Energy Storage	35
2.6.3.	Demand Side Management	36
2.6.4.	Packetized Energy	36
2.7.	Power Flow Controllers	38
2.7.1.	Shunt Controllers	39
2.7.2.	Series Controllers	48
2.7.3.	Shunt-Series Controllers	53
2.7.4.	HVDC Controllers	59
2.7.5.	Level of Power Flow Control in the Current Grid	63
2.7.6.	Modeling Power Flow Controllers	64
2.8.	Methods of Transmission Planning Optimization	69

2.9.	Operation and Regulation of Natural Gas Transportation Pipelines	70
2.9.1.	Fundamentals of Planning and Operation of Natural Gas Pipelines	70
2.9.2.	Natural Gas Regulation	72
2.9.3.	Relevance for Electricity Markets	73
2.10.	Discussion	74
CHAPTER 3: METHOD OF INCREMENTAL POWER FLOW CONTROL		75
3.1.	Introduction	75
3.2.	Concept of Incremental Power Flow Control	76
3.3.	Converter Rating Required for Incremental Power Flow Control	80
3.3.1.	Problem Setup	80
3.3.2.	Results	81
3.3.3.	Discussion	84
3.4.	Impact of Power Flow Control and Incremental Power Flow Control on the Cost of RPS Compliance	85
3.4.1.	Motivation	85
3.4.2.	Problem Setup	85
3.4.3.	Results	93
3.5.	Viability of Realizing Incremental Power Flow Control using a Hybrid Centralized-Localized Control Scheme	96
3.5.1.	Motivation	96
3.5.2.	Problem Setup	97
3.5.3.	Results	102
3.5.4.	Discussion	107

3.6. Discussion	107
CHAPTER 4: CORRECTIVE SECURITY-CONSTRAINED OPTIMAL POWER FLOW WITH POWER FLOW CONTROL AND INCREMENTAL POWER FLOW CONTROL	109
4.1. Introduction	109
4.2. CSCOPF Method	109
4.2.1. Power Flow Equations for Circuits with Power Flow Controllers	110
4.2.2. Corrective Security-Constrained Optimal Power Flow Leveraging Power Flow Control and Incremental Power Flow control	113
4.3. CSCOPF Tool Development	119
4.4. Demonstration	121
4.5. Incremental Packetized Energy	125
4.6. Discussion	131
CHAPTER 5: TRANSMISSION PLANNING WITH POWER FLOW CONTROL AND INCREMENTAL POWER FLOW CONTROL	133
5.1. Introduction	133
5.2. Proposed Transmission Planning Frameworks	133
5.2.1. Revised Centralized Transmission Planning Framework	134
5.2.2. Merchant Electrical Pipeline Framework	135
5.2.3. Hybrid Transmission Planning Framework	138
5.3. Implementation	139
5.3.1. General Structure of the Planning Tool	140
5.3.2. Planning Tool Design Specific to each Planning Framework	152
5.4. Comparison of Frameworks and Demonstration of Planning Tool	157
5.4.1. Metrics	158

5.4.2.	Propositions	158
5.4.3.	Test System	159
5.4.4.	Unit Cost of Transmission Investment	162
5.4.5.	Results	165
5.5.	Discussion	172
CHAPTER 6: CONTRIBUTIONS, FUTURE WORK, AND CONCLUSIONS		174
6.1.	Contributions	174
6.1.1.	Merchant Electrical Pipeline Framework	175
6.1.2.	Hybrid Transmission Planning Framework	175
6.1.3.	CSCOPF Methodology	176
6.1.4.	CSCOPF Tool Development	176
6.1.5.	Automated Transmission Planning Methodology	176
6.1.6.	Automated Transmission Planning Tool	177
6.1.7.	Demonstration of Benefit of Packetization	177
6.2.	Future Work	179
6.2.1.	Explore the Feasibility of Merchant Electrical Pipelines	179
6.2.2.	Scale the CSCOPF Tool to Realistic Systems	180
6.2.3.	Scale the Planning Tool to Realistic Systems and Assess Propositions	180
6.2.4.	Augment the CSCOPF Tool to Model Incremental Power Flow Transactions and the Controllability Market	181
6.2.5.	Improve the Modeling of Stability Constraints in the CSCOPF tool	181

6.2.6. Improve the Modeling of Planning Tool Choices	182
6.3. Conclusions	183
APPENDIX A: SUPPLEMENTAL INFORMATION FOR CHAPTER ONE	185
APPENDIX B: SYSTEM PARAMETERS FOR QUANTIFICATION OF CONVERTER RATING REQUIRED TO REALIZE INCREMENTAL POWER FLOW CONTROL	189
APPENDIX C: SYSTEM PARAMETERS FOR THE RPS COMPLIANCE STUDY	193
APPENDIX D: RESULTS FROM THE RPS COMPLIANCE STUDY	199
APPENDIX E: SYSTEM DETAILS FOR THE CSCOPF AND PLANNING TOOL DEMONSTRATION SYSTEMS	207
APPENDIX F: SYSTEM DETAILS FOR THE PLANNING TOOL DEMONSTRATION SYSTEM	212
REFERENCES	214

LIST OF TABLES

Table 1: Summary of transmission investment costs for wind generation.	18
Table 2: Details on power flow controllers deployed in the United States by type.	64
Table 3: Natural gas pipelines built between 2000 and 2005.	73
Table 4: Voltage injections required to realize the IPF transaction.	80
Table 5: Pre-transaction currents on lines adjacent to the IPF transaction.	80
Table 6: Aggregate ratings and performance metrics.	83
Table 7: Comparison of total investments.	95
Table 8: CNT local controller parameters.	100
Table 9: Results of the CSCOPF demonstration.	125
Table 10: Max system load using incremental packetized energy relative to max secure load. The numerator includes secure load and flexible load.	131
Table 13: Centralized transmission planning process results.	166
Table 14: Revised centralized transmission planning framework results.	167
Table 15: Hybrid transmission planning framework results.	170
Table 16: Comparison of results across frameworks.	171
Table 17: Planning tool solution time and search efficiency by framework.	172
Table 18: Comparison of selected optimal transmission expansion papers.	185
Table 19: Circuit data for the quantification of IPF control effort.	189
Table 20: Load data for the quantification of IPF control effort.	191

Table 21: Generator data for the quantification of IPF control effort.	192
Table 22: Circuit data for the first year of the RPS compliance study.	193
Table 23: Bus data for the first year of the RPS compliance study for time periods one through three.	195
Table 24: Bus data for the first year of the RPS compliance study for time periods four through six.	196
Table 25: Generator data for the RPS compliance study.	198
Table 26: Breakdown of transmission upgrades required for the BAU case.	202
Table 27: Breakdown of the transmission upgrades required for the DSR case.	203
Table 28: Breakdown of the transmission upgrades required in the IPF control case.	204
Table 29: Generator parameters used for the CSCOPF demonstration cases.	208
Table 30: Circuit limits for the 39-bus CSCOPF demonstration system	211
Table 31: Plant capacity cost data.	213

LIST OF FIGURES

Figure 1: Uplift method of congestion measurement.	9
Figure 2: System redispatch method of congestion measurement.	10
Figure 3: Congestion revenue method of congestion measurement.	10
Figure 4: Historical and planned transmission investment by Investor Owned Utilities with planned investment in a lighter shade [21,22,23,24].	14
Figure 5: Map of wind and solar resources, major metropolitan areas, and transmission lines in the United States. Solar resources are shown from light yellow to brown, with the highest resource sites in brown. Wind resources are shown from light blue to dark blue, with the highest resource sites in dark blue. Only wind sites viable with current technology are shown. Major metropolitan areas are outlined in black. Grey lines in the background show high voltage transmission lines.	16
Figure 6: Annual average LMPs under Scenario Two, which meets 20% of annual demand in the Eastern Interconnection with wind energy.	17
Figure 7: Supply and demand curves showing the profit-maximizing operating point of an unregulated natural monopoly (A) and the deadweight loss of said operation (shaded region).	21
Figure 8: Congestion rent and congestion cost for a transfer between two areas.	26
Figure 9: Two-bus system connected by a single transmission line.	39
Figure 10: Phasor diagram of the power flow through the transmission line.	39
Figure 11: Connection of a shunt controller at Bus One.	40
Figure 12: Phasor diagram with a shunt controller installed at Bus One.	41
Figure 13: Connection of a shunt controller at the midpoint of the transmission line.	41

Figure 14: Phasor diagram with a shunt controller at the midpoint of the transmission line.	41
Figure 15: Mechanically switched capacitor (MSC).	42
Figure 16: Mechanically switched reactor (MSR).	42
Figure 17: Thyristor switched capacitor (TSC).	43
Figure 18: Thyristor controlled reactor (TCR).	44
Figure 19: Static VAR compensator (SVC).	45
Figure 20: Modular multilevel static synchronous compensator (StatCom).	46
Figure 21: Submodule of a modular multilevel StatCom.	46
Figure 22: Connection of a series controller at the Bus One side of the transmission line.	48
Figure 23: Phasor diagram with a series capacitive controller installed at the Bus One side of the transmission line.	49
Figure 24: Phasor diagram with a series inductive controller installed at the Bus One side of the transmission line.	49
Figure 25: Series mechanically switched reactor (MSR).	50
Figure 26: Series mechanically switched capacitor (MSC).	50
Figure 27: Thyristor controlled series capacitor (TCSC).	51
Figure 28: Static synchronous series compensator (SSSC).	52
Figure 29: Distributed series reactance (DSR).	52
Figure 30: Connection of a shunt-series controller to the power line.	54
Figure 31: Phasor diagram of a shunt-series controller connected to Bus One and the line between Bus One and Bus Two.	54

Figure 32: Unified power flow controller (UPFC).	55
Figure 33: Variable frequency transformer (VFT).	56
Figure 34: Controllable network transformer (CNT).	56
Figure 35: Fractionally-rated back-to-back (FR-BTB).	57
Figure 36: Three-phase diagram of a single core phase-shifting transformer (PST).	58
Figure 37: Three-phase diagram of a two core phase-shifting transformer (PST).	58
Figure 38: Phasor diagram of an HVDC controller connected between Bus One and Bus Three.	60
Figure 39: Phasor diagram of an HVDC controller connected to Bus One and supplying the line between Bus Three and Bus Two.	60
Figure 40: High voltage DC (HVDC) transmission system using line commutated converters.	61
Figure 41: High voltage DC (HVDC) transmission system using modular multilevel converters.	62
Figure 42: Submodule of a modular multilevel HVDC.	62
Figure 43: Back-to-back converter (BTB).	63
Figure 44: Flowchart for CSCOPF without PF controllers.	68
Figure 45: US natural gas transportation pipelines.	71
Figure 46: IEEE 39-bus system with desired incremental transaction shown in green.	78
Figure 47: An overview of the method to realize IPF control along a transaction path without changing power flows on adjacent circuits.	79
Figure 48: Locations and ratings of BTB converter to realize a 20 MW IPF transaction.	82

Figure 49: Locations and ratings of CNT converters to realize a 20 MW IPF transaction.	83
Figure 50: Generator Six output before and during the IPF transaction.	84
Figure 51: Power through Line ₂₁₋₂₂ before and during the IPF transaction.	84
Figure 52: Power through Line ₁₆₋₂₁ before and during the IPF transaction.	84
Figure 53: Power through Line ₁₆₋₂₄ before and during the IPF transaction.	84
Figure 54: IEEE 39-bus system with regional demarcations.	87
Figure 55: Diurnal variation of loads and wind potential production.	89
Figure 56: Flowchart for simulation methodology.	92
Figure 57: Four-bus system for study of centralized-localized IPF control.	98
Figure 58: CNT model using voltage and current sources.	98
Figure 59: CNT and local controller embedded in a transmission line.	101
Figure 60: Test-system with CNTs installed to execute transactions along one path.	102
Figure 61: Power flow through Line ₁₋₂ of the IPF transaction path.	103
Figure 62: Power flow through Line ₂₋₄ of the IPF transaction path.	103
Figure 63: Power flow through Line ₃₋₁ , which is not part of the IPF transaction path.	103
Figure 64: Power flow through Line ₃₋₂ , which is not part of the IPF transaction path.	104
Figure 65: Power flow through Line ₃₋₄ , which is not part of the IPF transaction path.	104
Figure 66: Power supplied by Generator One.	104
Figure 67: Power supplied by Generator Two.	104
Figure 68: Power supplied by Generator Three.	105

Figure 69: Power supplied by Generator Four.	105
Figure 70: Variation of the set points of CNT One.	106
Figure 71: Variation of the set points of CNT Two.	106
Figure 72: Flowchart for CSCOPF with PF controllers.	114
Figure 73: Topology of the Garver five-bus system.	122
Figure 74: System topology, generation capacity and load for the CSCOPF demonstration cases.	124
Figure 75: Planning tool overview flowchart.	140
Figure 76: Flowchart for the genetic algorithm.	147
Figure 77: Flowchart for the fitness function.	151
Figure 78: Base case system. The line values represent the admittance and max power flow. The generator types are designated by C, G, and W for coal, CCGT natural gas, and wind respectively. The generator values indicate the generator capacity. The load values indicate the peak load.	162
Figure 79: System topology, generation capacity and peak load at the end of the second decade under the centralized transmission planning process.	166
Figure 80: System topology, generation capacity and peak load at the end of the first decade under the revised centralized transmission planning framework. Transmission assets added in the first decade are shown in blue.	168
Figure 81: System topology, generation capacity and peak load at the end of the second decade under the revised centralized transmission planning framework. Transmission assets added in the second decade are shown in blue.	169
Figure 82: Model of a PF converter connected to Line $i-j$ per the power injection method.	185
Figure 83: Overview of transmission upgrades required in the BAU case.	199
Figure 84: Overview of the transmission upgrades required in the DSR case.	200

Figure 85: Overview of transmission upgrades required in the IPF control case.	201
Figure 86: Sample IPF transaction from Year Six.	202
Figure 87: Total non-discounted investment as function of time for the RPS compliance study.	205
Figure 88: Total discounted investment as function of time for the RPS compliance study.	206

NOMENCLATURE

BAU	business as usual
BTB	back-to-back
CAISO	California Independent System Operator
CCGT	combined-cycle gas turbine
CNT	controllable network transformer
COE	cost of energy
CSC	convertible static compensator
CSCOPF	corrective security-constrained optimal power flow
CTEP	centralized transmission expansion plan
DSR	distributed series reactance
EEP	exponential evolutionary programming
EIA	Energy Information Agency
ERCOT	Electricity Reliability Council of Texas
EWITS	Eastern Wind Integration and Transmission Study
FERC	Federal Energy Regulatory Commission
FC	fixed capacitor

FPC	Federal Power Commission
FR-BTB	fractionally-rated back-to-back
FTR	financial transmission right
GA	genetic algorithm
GEV	grid-enabled vehicle
HVDC	high-voltage direct current
IOU	investor-owned utilities
IPF	incremental power flow
ISO	independent system operator
ISONE	Independent System Operator New England
ITP	independent transmission provider
LMP	locational marginal price
LP	linear programming
LSE	load-serving entity
MEP	merchant electrical pipeline
MILP	mixed integer linear programming
MINLP	mixed integer non-linear programming

MP	master problem
MISO	Midwest Independent System Operator
MSC	mechanically switched capacitor
MSR	mechanically switched reactor
NLP	non-linear programming
NYISO	New York Independent System Operator
O&M	operations and maintenance
OCGT	open-cycle gas turbine
OPF	optimal power flow
PF	power flow
PJM	Pennsylvania-New Jersey-Maryland Interconnection
PPI	producer price index
PPO	power purchase option
PSCOPF	preventive security-constrained optimal power flow
PSO	particle swarm optimization
PST	phase-shifting transformer
PTC	production tax credit

PUC	public utility commission
PV	present value
	or
	real power and voltage
PURPA	Public Utility Regulatory Policies Act
RICC	reduction in congestion cost
RPS	renewable portfolio standard
RTO	regional transmission organization
SA	simulated annealing
SCOPF	security-constrained optimal power flow
SCUC	security-constrained unit commitment
SERC	SERC Reliability Corporation
SFV	straight-fixed-variable
SP	sub-problem
SPP	Southwest Power Pool
SSSC	static synchronous series compensator
StatCom	static compensator

SVC	static VAr compensator
TCE	total carbon emissions
TCR	thyristor controlled reactor
TCSC	thyristor controlled series capacitor
TLR	transmission line relief
TO	transmission owner
TransCo	transmission company
TSC	thyristor switched capacitor
TSR	thyristor switched reactor
TTC	total transfer capability
UPFC	unified power flow controller
USF	unscheduled flow
V2G	vehicle-to-grid
VFT	variable frequency transformer
VSC	voltage-source converter
WECC	Western Electricity Coordinating Council
WWSIS	Western Wind and Solar Integration Study

SUMMARY

Power flow (PF) control can increase the utilization of the transmission system and connect lower cost generation with load. While PF controllers have demonstrated the ability to realize dynamic PF control for more than 25 years, PF control has been sparsely implemented.

This research re-examines PF control in light of the recent development of fractionally-rated PF controllers and the incremental power flow (IPF) control concept. IPF control is the transfer of an incremental quantity of power from a specified source bus to specified destination bus along a specified path without influencing power flows on circuits outside of the path.

The objectives of the research are to develop power system operation and planning methods compatible with IPF control, test the technical viability of IPF control, develop transmission planning frameworks leveraging PF and IPF control, develop power system operation and planning tools compatible with PF control, and quantify the impacts of PF and IPF control on multi-decade transmission planning.

The results suggest that planning and operation of the power system are feasible with PF controllers and may lead to cost savings. The proposed planning frameworks may incent transmission investment and be compatible with the existing transmission planning process. If the results of the planning tool demonstration scale to the national level, the annual savings in electricity expenditures would be \$13 billion per year (2010\$). The proposed incremental packetized energy concept may facilitate a reduction in the environmental impact of energy consumption and lead to additional cost savings.

CHAPTER 1

INTRODUCTION

The electric power transmission system enables the arbitrage of electric generation costs and mitigates the amount of generation capacity required to meet reliability requirements. The existing transmission system was not designed to operate in a deregulated environment. In addition, the existing transmission system may not be sufficient to meet load growth and integrate renewable generation. However, even at peak demand and considering contingencies, utilization of the transmission system is incomplete. Power flow (PF) control can increase the utilization of the transmission system and connect lower cost generation with load. While PF controllers have demonstrated the ability to realize dynamic PF control for more than 25 years, PF control has been sparsely implemented.

This research re-examines PF control in light of the recent development of fractionally-rated PF controllers and the incremental power flow (IPF) control concept. Fractionally-rated PF controllers may have lower cost and better reliability than previous PF controllers. IPF control is the transfer of an incremental quantity of power from a specified source bus to specified destination bus along a specified path without influencing power flows on circuits outside of the path. In contrast to PF control, which is used to optimize overall system operation or conduct bulk merchant transactions, IPF control may be used to conduct incremental, bilateral power transactions.

In addition to poor transmission system utilization, existing transmission planning processes fail to realize economic investments. Centralized transmission planning is impeded by cost allocation challenges. These challenges have two sources. First, power flows are uncontrolled in the existing AC transmission system. Second, a single synchronous interconnect may have multiple transmission owners and regulators. The two realities lead to opportunities for free riders and the possibility of a welfare enhancing investment vetoed up by a stakeholder who would lose from the investment. The result is the requirement that the benefits of an investment exceed the cost of the investment by a greater amount than would be required if all transmission within an interconnection was owned by a single entity. Merchant transmission planning is impeded by the inability to provide long-term revenue certainty to the investment and the long lead-time for transmission construction.

The objectives of the research are to develop power system operation and planning methods compatible with PF control and IPF control, test the technical viability of IPF control, develop transmission planning frameworks leveraging PF and IPF control, develop power system operation and planning tools compatible with PF control, and quantify the impacts of PF and IPF control on multi-decade transmission planning. To support the objectives, the research:

- Reviews the history of transmission planning and regulation, the current state of the transmission system, drivers for additional transmission, alternatives to transmission, and PF control methods
- Assesses the potential benefits, costs and viability of IPF control

- Proposes a corrective security-constrained optimal power flow (CSCOPF) method compatible with PF control and IPF
- Develops a CSCOPF tool consistent with the proposed method and demonstrates the impact of PF control
- Proposes and demonstrates a method to reduce generation, transmission and distribution capacity by coupling IPF control with load flexibility
- Proposes transmission planning frameworks compatible with PF control and IPF control
- Proposes a method for automated transmission planning compatible with the proposed transmission planning frameworks
- Develops an automated transmission planning tool consistent with the proposed method
- Demonstrates the impact of the proposed transmission planning frameworks

The work is summarized in five chapters.

Chapter Two reviews transmission operation, planning, investment and regulation. It also enumerates the drivers for additional transmission capability and explores potential methods to increase transmission capability. PF control, a potential method to increase transmission capability, is explored in detail. The operation and regulation of natural gas transportation pipelines are reviewed to understand controllable networks.

Chapter Three describes the IPF control concept and presents preliminary analyses of the benefits, costs and viability of IPF. The first analysis assesses the control effort required to realize IPF using fully-rated and fractionally-rated PF controllers. The second

analysis compares the cost of renewable portfolio standard (RPS) compliance with and without IPF. The third analysis assesses the viability of IPF control in the absence of central control.

Chapter Four assesses the operational implications of PF control and IPF. It proposes a method of CSCOPF compatible with PF control and IPF. It describes the development and demonstration of a software tool based on the method. It also proposes the *incremental packetized energy* concept, which attempts to realize many of the benefits of packetized energy at a fraction of the cost.

Chapter Five assesses the planning implications of PF control and IPF. It proposes frameworks for transmission planning compatible with PF controllers. The chapter proposes the *merchant electrical pipeline* (MEP) framework for merchant transmission investment. The chapter also proposes a methodology to automate transmission planning that is compatible with PF control and IPF control. The methodology is developed into an automated planning software tool that can simultaneously deploy new transmission lines and multiple PF controller types and units. Case studies demonstrate the planning frameworks using the planning tool.

Chapter Six delineates the contributions, presents suggestions for future work, and summarizes the research.

CHAPTER 2

ORIGIN AND HISTORY OF THE PROBLEM

2.1. Introduction

This chapter begins with a discussion of the current state, future drivers for, and history of transmission planning, operation, and regulation. It then enumerates methods to increase transmission capability as well as methods to reduce the need for additional transmission capability. It then reviews available and emerging PF controllers and methods to model the operation of PF controllers. Next, it reviews methods to optimize transmission planning. Finally, it reviews the history and current state of natural gas transmission and regulation as natural gas pipelines are controllable and may inform the development of controlled electrical transmission. Most of the discussion will focus on the United States and details, unless noted otherwise, pertain to the US power system.

2.2. Current State of Transmission Operation

2.2.1. Reliability

No evidence was found that the reliability of the power system in the United States is degrading. One study found no statistical evidence that the frequency or size of large events is increasing in time [1]. While state-level reliability data are prevalent in the United States, data assessing the contribution of transmission system failure on overall system reliability were not identified. PG&E reports that between 1990 and 1999, transmission issues resulted in 14% of the outage hours and 11% of the outages [2]. The

2003 northeast blackout, 2008 Florida blackout, and 2011 Southern California blackout all involved transmission failures.

The transmission and generation systems are operated to ensure that the system is able to serve all load and operate within equipment ratings even if any event occurs. An event typically is one of the following types but may include a combination thereof

- loss of any single transmission asset,
- loss of any single generator, and
- any three-phase or phase-to-phase fault.

The system is classified as secure if it can serve all load within equipment ratings when an event occurs [3]. If the system is able to serve all load and operate within equipment ratings but is unable to continue to do so if another event occurs, the system is classified as normal but insecure [3].

2.2.2. Congestion

Congestion is the inability of the transmission system to realize the economic dispatch. The economic dispatch is found by optimizing generator set points while neglecting transmission constraints. The method used to quantify congestion depends on the jurisdiction in which the transfer occurs. Power is traded via bilateral transactions in non-market jurisdictions. In these areas, the level of congestion can be partially assessed by the number of times the system was unable to realize a scheduled transaction. In market-based jurisdictions, congestion can be measured via differences in energy prices across zones or nodes.

Most market jurisdictions have a financial mechanism so market participants can mitigate the uncertainty of congestion. In some markets, a transmission owner (TO) is granted a financial transmission right (FTR), in the form of an obligation or auction. If the price of energy at the receiving end of a transaction is higher than at the sending end of the transaction, the system operator pays a credit to the holder of the FTR. A TO can auction the FTR to monetize the congestion. In a functioning market, the auction price for the FTR will match the expected congestion revenue risk [4]. FTRs manage the variability of congestion but do not eliminate congestion. When a TO increases transmission capability, most market areas assign the incremental FTR to the TO.

2.2.2.1. Congestion outside Market Jurisdictions

In both the Eastern Interconnection and the Western Electricity Coordinating Council (WECC), operating procedures are used to curtail scheduled transactions if existing or imminent power flows will lead to insecure operation. In the Eastern Interconnection, operators use transmission line relief (TLR) orders to mitigate congestion. The TLR process has nine levels and sublevels. TLR levels two and higher involve curtailment of scheduled transactions. The number of level two and higher TLRs per year grew at an average rate of 35% between 1997 and 2010 [5]. The number of level five TLRs per year grew at an annual rate of 63% over 1999-2010 [5]. Meanwhile, annual demand grew at a rate of one per cent per year over both periods [6]. WECC uses the unscheduled flow (USF) process rather than TLRs. USF relieves congestion using both generator set points and adjustment of phase-shifting transformers (PSTs). A record of USF events over time was not identified.

2.2.2.2. Congestion in Market Jurisdictions

In market jurisdictions, bids and optimization techniques are used to maximize societal welfare or minimize the production cost. In a competitive market with both an energy and capacity market, the production cost is the variable cost of electricity generation. Most congestion appears as price differences between market zones or nodes. However, TLRs and USFs are still used in market jurisdictions to involve parties outside the market in the relief of the congestion [7]. A TLR is a crude tool to mitigate congestion, as it requires roughly three times more curtailment than the use of a market mechanism [7] and can be less timely and accurate [7].

The three basic methods of measuring congestion in market jurisdictions are the uplift method, the system redispatch method, and the congestion revenue method [8]. All three methods are described in relation to Figure 1 - Figure 3 assuming a 100 MW limit on flow between Area A and Area B. The figures are copied from [8]. The uplift method, as seen in Figure 1, calculates congestion as the difference in system production cost between the unconstrained case and the constrained case. This cost is spread across all customers pro rata. This technique was common in market jurisdictions but is less so now. The system redispatch method of Figure 2 calculates congestion as the difference in system production cost between the unconstrained case and the constrained case for a system that defines a locational marginal price (LMP) for each zone or bus. The congestion revenue method of Figure 3 calculates congestion as the difference between the amount paid to generators and the amount collected from consumers. Generators connected to Area A are paid the same LMP as loads in Area A. The LMP in Area B is higher than Area A because of congestion. Some of the power purchased by the system

operator in Area A is sold at a higher LMP in Area B. This creates congestion revenue for the system operator. Both the system redispatch and congestion revenue methods require estimation of the offer curves, impeding accurate estimation of congestion by market participants.

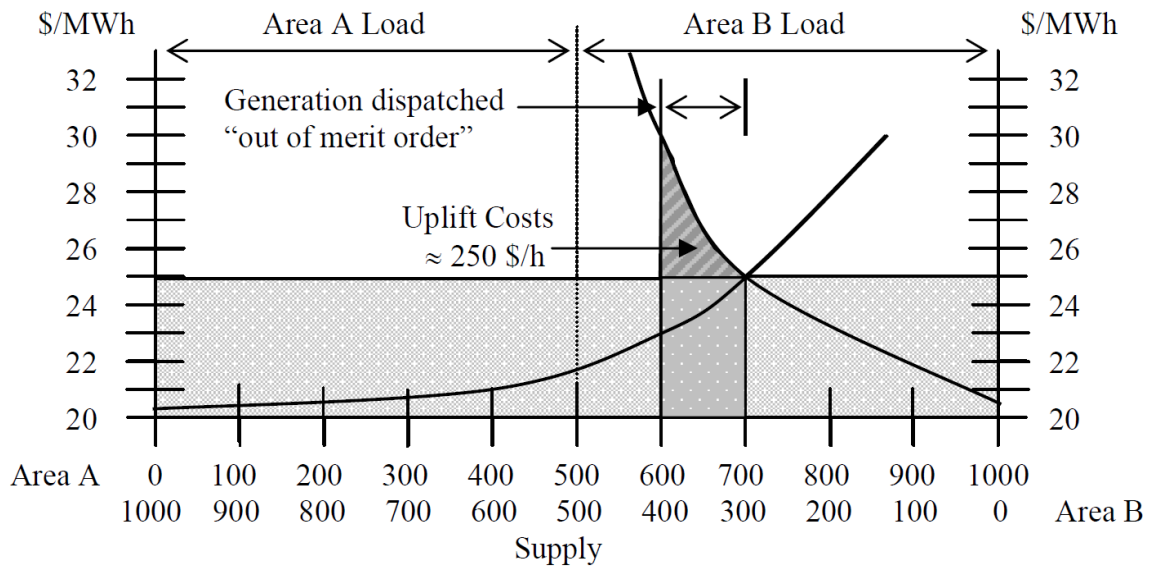


Figure 1: Uplift method of congestion measurement.

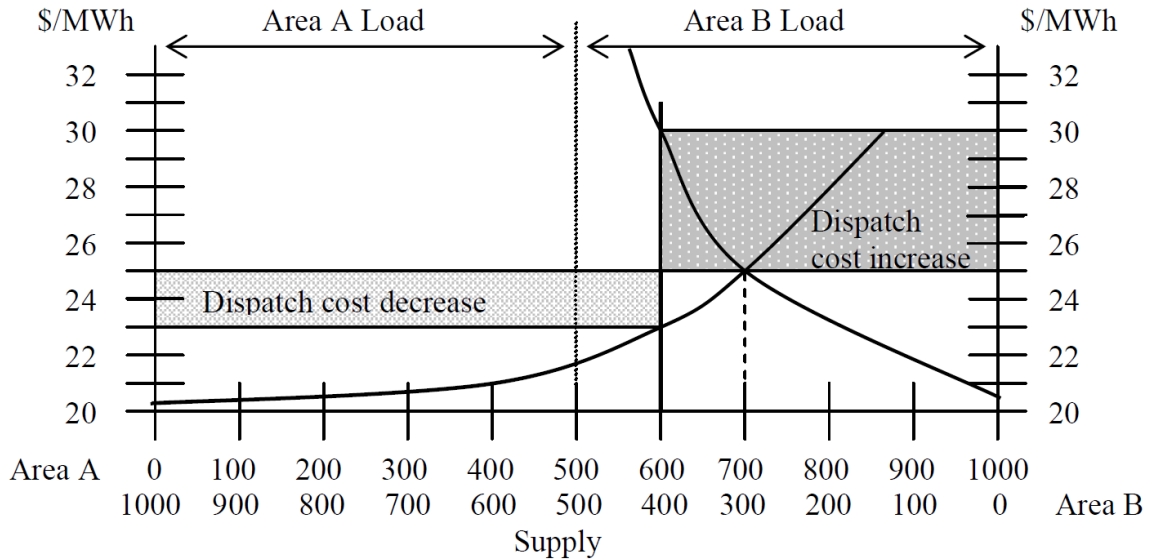


Figure 2: System redispatch method of congestion measurement.

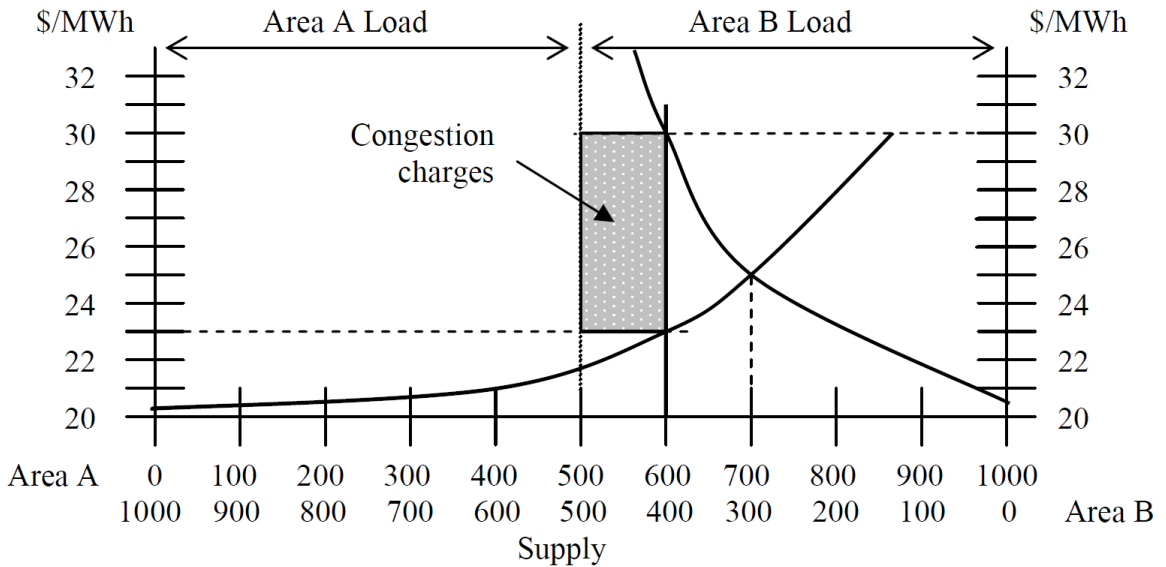


Figure 3: Congestion revenue method of congestion measurement.

Congestion cost in the Pennsylvania-New Jersey-Maryland Interconnection (PJM) was \$1,428 million in 2010 [9]. Congestion cost for the Midwest Independent System Operator (MISO) was \$312 million in 2009 [7]. Congestion cost in New York State was

\$442 million in 2009 [4]. Congestion cost for the California Independent System Operator (CAISO) was an estimated \$204 million in 2011 [10,11]. The congestion measurement methods and costs were not reviewed for the Independent System Operator New England (ISONE), Electricity Reliability Council of Texas (ERCOT), or the Southwest Power Pool (SPP). A 2002 study estimates that congestion costs totaled \$157-447 million per year in the PJM, California Independent System Operator (CAISO), New York Independent System Operator (NYISO) and ISONE jurisdictions, depending on the level of market power assumed [12]. The 2002 estimate appears low since congestion in PJM and NYISO totaled \$969 million in 2002. In 2009, congestion in PJM, NYISO, and MISO totaled \$1,473 million.

2.2.3. Methods of Control

System operators have a variety of methods to control the transmission system. They may change the set points of generators, VAr controllers, and PF controllers. They may call for demand response, shed load without consumer permission, or reconfigure the network. Optimal power flow (OPF) uses these control methods to minimize the production cost or maximize short-term societal welfare. The existence of congestion in the discussed jurisdictions means that existing control is insufficient to eliminate it. However, the existence of congestion does not mean that adding control to mitigate congestion would be cost optimal given that the OPF does not consider fixed costs like transmission and generation investment.

2.3. Drivers for Additional Transmission Capability

2.3.1. Metrics of Transmission Capability

The typical metric of transmission capability is total transfer capability (TTC). TTC is the amount of power that can be transferred between two points of a network under all $n-1$ conditions considering thermal, voltage, and stability requirements as seen in (Eq. 1) [13]. TTC is assessed for a specific combination of network configuration, generator dispatch, and load levels [13]. Calculation of TTC without modeling sufficient geographic range could result in inflated TTC values because of parallel flows. TTC is particular to a specific transaction and configuration and does not provide a single measurement of the overall capability of the system. MW-miles is another metric for transmission capability. MW-miles can be normalized and compared over time. However, the variation of MW-miles over time can conceal degrading capacity levels because of changes in grid operating practices. Average line utilization is a transmission capability metric useful for controllable systems, as high levels of utilization suggest little transmission capability remains. Unless otherwise noted, the term *transmission capability* refers to TTC for the balance of the document.

$$TTC = \min\{T_{thermal}, T_{voltage}, T_{stability}\} \quad (\text{Eq. 1})$$

2.3.2. Load Growth

The Energy Information Agency (EIA) expects American annual electricity demand to increase one percent each year until 2035, a 24% increase relative to 2010 demand [14]. As part of the demand projection, EIA estimates that grid-enabled vehicle

(GEV) penetration will comprise two percent of the light-duty vehicle fleet in 2035 [15]. Deutsche Bank projects GEVs will comprise 11% of model-year 2020 vehicles [16] while the Electrification Coalition shows a path for GEVs to comprise 90% of light-duty vehicle sales and 40% of the light-duty fleet in 2030 [17,18]. 100% GEV market share in 2050 would result in 25% more load growth than the case with no GEVs [19].

2.3.3. Historic Transmission Investment Levels

Transmission investment can be quantified in terms of dollars, MW-miles, or the ratio of transmission investment to total electrical demand. Transmission investment in real dollar terms declined among investor-owned utilities (IOUs) from 1975-1998 [20]. Investment in real dollar terms rose at an annual 12.8% growth rate from 1999-2010 [21,22,23,24]. Investment is expected to contract, in real dollar terms, starting in 2014 [23,24]. Historical and planned IOU transmission investments for 1999-2015 are shown in Figure 4. It is not clear if the recent increase in transmission investment is sufficient to meet future reliability requirements, minimize the levelized cost of energy, and ensure compliance with emerging drivers for additional transmission capability.

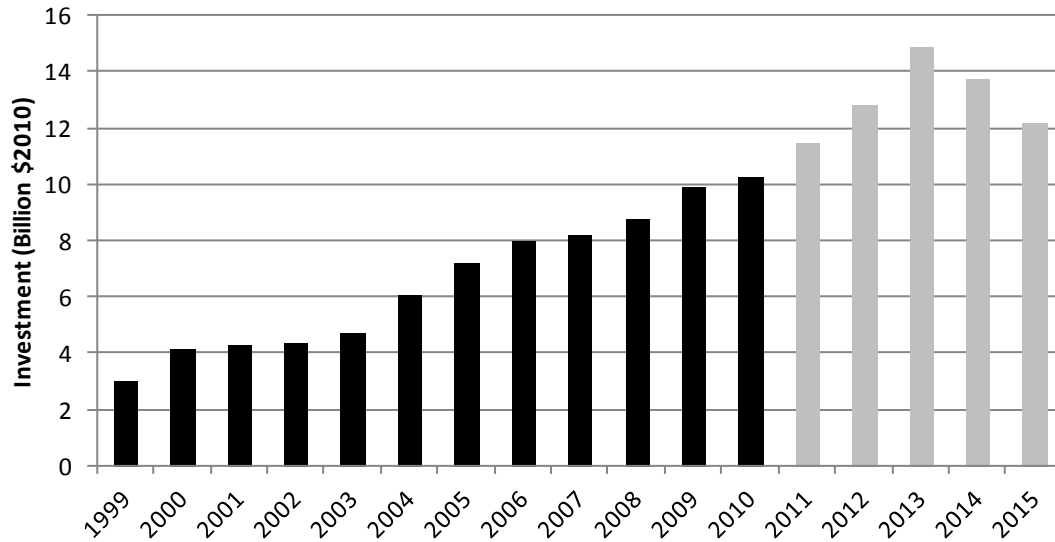


Figure 4: Historical and planned transmission investment by Investor Owned Utilities with planned investment in a lighter shade [21,22,23,24].

2.3.4. Integration of Renewable Generation

The addition of renewable generation has been facilitated by state-level RPSs and government incentives such as the production tax credit (PTC) and the US Treasury Section 1603 investment tax credit. Twenty-nine states, one territory and the District of Columbia have legally binding RPSs [25]. Eight additional states have goals for renewable energy procurement, with various incentives for utilities to meet the goals [25].

More wind generation has been deployed over the last decade than any other type of renewable generation, with 33.7 GW of new wind generation compared to 2.2 GW of solar generation [26,27]. In 2012, more wind generation was deployed than any other type of generation [28]. The majority of wind capacity is sited in resource-rich regions and solar developers are following this trend. As seen in Figure 5, generated in ArcGIS,

the resource-rich wind and solar regions are often in areas removed from load centers and with below average transmission density [29,30,31]. A number of integration studies have been performed to assess the transmission investment and system operation impacts of wind and solar generation [32,33,34,35,36,37,38,39,40,41,42,43,44,45]. Two studies covering large, multistate regions are the Eastern Wind Integration and Transmission Study (EWITS) [45] and the Western Wind and Solar Integration Study (WWSIS) [44]. EWITS examines five scenarios in which six percent to 30% of the electrical demand in 2024 is met with wind generation. Total wind capacity varies from 224-339 GW for scenarios sourcing 20 to 30% of energy from wind. EWITS calculates the transmission investments required to realize the scenarios via an iterated process conducted by a committee of stakeholders. The process is not optimized to minimize the levelized cost of energy and congestion exists with the transmission investments in place, as seen in Figure 6 [45]. Non-discounted transmission investment for the 20-30% scenarios were \$33-59 billion higher, in 2009 dollars, than the reference case. This amounts to \$300-447 of investment per kW of new wind capacity. With the transmission investment in place, wind curtailment averages seven to eleven percent. The benefit-to-cost ratio of the transmission investment varies from 0.79 to 1.22 depending on the scenario.

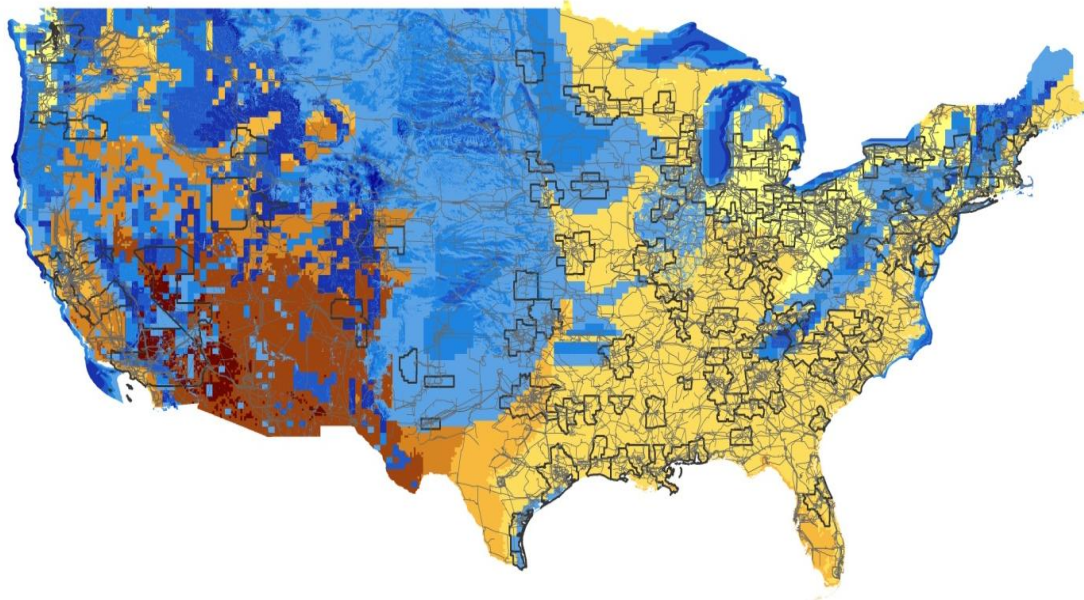


Figure 5: Map of wind and solar resources, major metropolitan areas, and transmission lines in the United States. Solar resources are shown from light yellow to brown, with the highest resource sites in brown. Wind resources are shown from light blue to dark blue, with the highest resource sites in dark blue. Only wind sites viable with current technology are shown. Major metropolitan areas are outlined in black. Grey lines in the background show high voltage transmission lines.

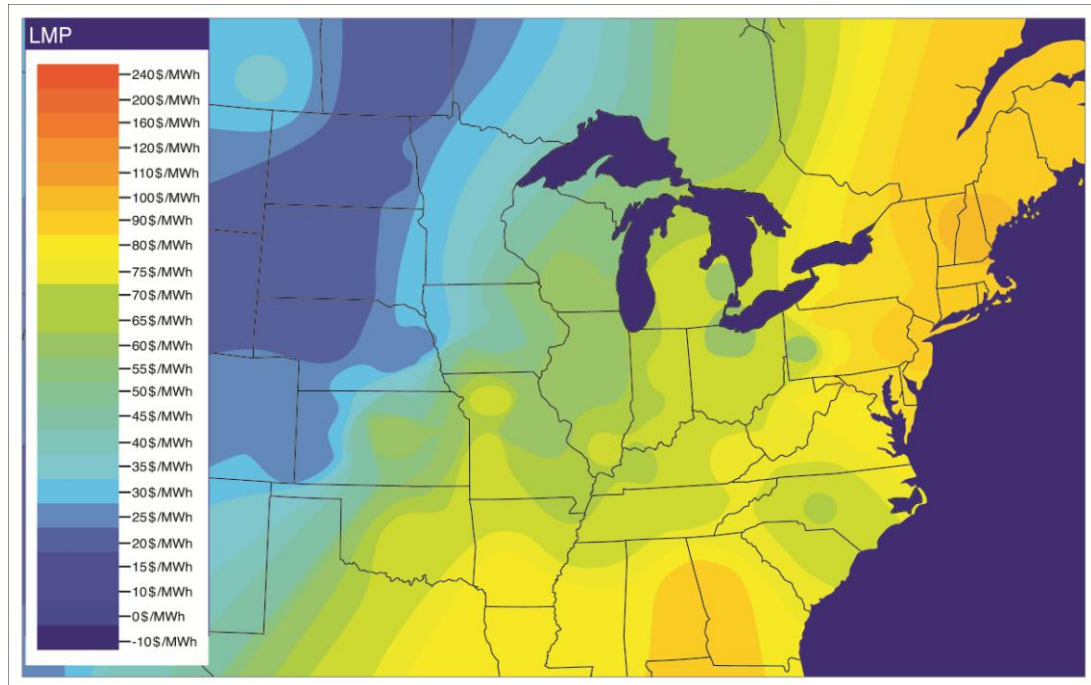


Figure 6: Annual average LMPs under Scenario Two, which meets 20% of annual demand in the Eastern Interconnection with wind energy.

The Western Wind and Solar Integration Study (WWSIS) examines the impact of wind and solar generation on the Western Interconnection. Unlike EWITS, the WWSIS does not assess scenarios in which a fixed percentage of interconnect-wide demand is sourced from renewable generation. Rather, the study focuses on the footprint of the WestConnect utilities, which roughly span WY, CO, MT, AZ, and NV. WWSIS scenarios source up to 35% of 2017 WestConnect demand from renewable generation, with 30% from wind and five percent from solar. Demand in the rest of the Western Interconnection is sourced with up to 23% renewable generation. For the 23% scenario, 20% of energy is sourced from wind and three percent from solar. Outside the WestConnect footprint, each state’s RPS is assumed to be met with in-state generation. The WWSIS transmission design is not iterated and non-cost-optimal. It quantifies the

cost of interstate transmission links within the WestConnect footprint and neglects the costs of transmission outside WestConnect and intrastate transmission within WestConnect. The interstate transmission links are centroid to centroid paths that assume the path can be fully utilized, similar to high-voltage direct current (HVDC) transmission or controllable AC lines. The study finds that \$11 billion of interstate transmission is required within the WestConnect footprint. The benefit-to-cost ratio of the transmission is 0.9 using a 15% carrying charge.

A summary of the transmission investment required to integrate renewable generation is seen in Table 1 [46]. Assuming these figures are applicable nationally and scale linearly, sourcing 20% of American electricity demand with 35% capacity factor wind generation in 2030 would cost \$44-1,036 billion [14,46] or an average of \$11 billion per year until 2030. In comparison, total IOU transmission investment in 2010 was \$10.2 billion [23].

Table 1: Summary of transmission investment costs for wind generation.

Study	Transmission Cost (\$/kW wind capacity)
EWITS	207
AEP	150-200
ISONE	1109-3575
JCSP	259
MISO ISO RGOS	833-1000
SPP	329
ERCOT CREZ	427

2.3.5. Discussion

Collectively, \$15-19 billion in transmission investments are projected to be required per year in the United States [21,23,47]. This estimate is based on EIA projections, which include 38 GW of new renewable generation and less than three percent GEV market penetration. However, sourcing 20% of 2030 electricity from wind generation would require 300 GW of new wind generation and GEVs may reach 40% of the light-duty fleet by 2030. Thus, actual investment may be higher than \$15-19 billion per year. Meanwhile, the peak annual investment during 2001-2010 was \$10 billion. Alternative solutions may emerge to meet transmission needs that do not require a doubling of annual investment.

2.4. Transmission Planning and Regulation

2.4.1. Centralized Transmission Planning

2.4.1.1. The History of Regulation

The electric utility has been classified as a natural monopoly because of its economies of scale. In a natural monopoly, the cost advantages of scale are so large that only a single large firm can earn a profit within a given jurisdiction. A natural monopoly pursuing monopolistic behavior will set the price higher than the marginal or average cost, as shown in Figure 7. Figure 7 is based on [48]. This leads to reduced societal welfare, called deadweight loss, as seen in the shaded region of Figure 7. The goal of a social welfare maximizing regulator is to drive the monopolistic entity to operate as close to point E as possible, where the marginal cost of delivering an incremental unit of electricity equals the marginal price [48]. Under constant returns to scale, social welfare

would be maximized at point E, where price equals marginal cost. However, for a natural monopoly, marginal cost is always less than price so regulating price at marginal cost would lead to long-term losses for the utility, requiring a government subsidy to keep the utility viable. Therefore, the lowest sustainable price is point F, where average cost equals price. Self-interested regulators may regulate price to a level above or below point F, depending on the relative strength of the utility and consumers [49]. There is evidence that prices are above average prices, and thus closer to monopolistic prices, because industry groups are more efficient per dollar expended than consumer groups at lobbying regulators [50,51].

Regulation of the electric power sector began in the 1910s at the request of the utilities [52]. Utilities were unable to expand because of overlap in service territories, competitive pricing, and an inability to benefit from economies of scale in transmission and distribution [52]. IOUs were granted monopolistic rights in exchange for regulation. As a consequence of regulation, technical advances, and other factors, the real cost of electricity in 1970 was 1/40th of the real cost in 1892 [52].

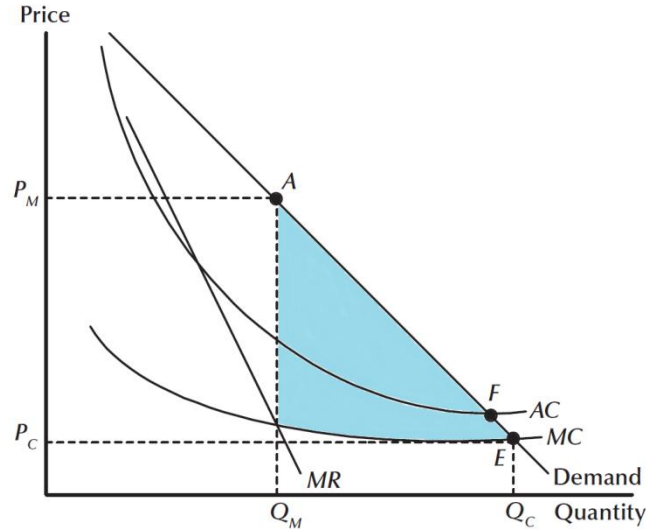


Figure 7: Supply and demand curves showing the profit-maximizing operating point of an unregulated natural monopoly (A) and the deadweight loss of said operation (shaded region).

Regulation can be split into two categories: rate-of-return regulation and performance-based regulation. Under rate-of-return regulation, the utility's profit is defined by a regulated return on invested capital. In theory, if a utility's costs are limited to capital and labor expenditures, the minimum rate-of-return is calculated as in (Eq. 2). In the equation, r is the minimum rate-of-return permitted by the regulator, P is the price paid by consumers per unit of electricity, Q is the quantity of electricity sold to consumers, p_L is the price paid by the utility for labor, L is the quantity of labor procured by the utility, and K is the amount of capital used. Rate-of-return regulation may lead to distorted incentives. According to the Averch-Johnson effect, the positive relationship between utility profit and capital stock causes the utility to use a higher ratio of capital-to-labor than a non-regulated entity [53]. Firms under rate-of-return regulation generally have higher than optimal capital-to-labor ratios but the reason for this is difficult to determine [54,55,56].

$$r \geq \frac{PQ - p_L L}{K} \quad (\text{Eq. 2})$$

Under performance-based regulation, firms may have better incentives than rate-of-return regulation to invest efficiently, operate efficiently, and align choices with societal welfare [57]. Despite deregulation, to be discussed next, the transmission and distribution sectors are still mostly regulated and rate-of-return regulation is still common. However, performance-based regulation has been used in at least 16 states [57].

2.4.1.2. History of Deregulation

Electricity costs increased 50% between 1970 and 1975, contributing to the deregulation of the electric power sector [52]. Among other factors, cost increases were ascribed to overinvestment by utilities, lack of technical and business knowledge in public utility commissions (PUCs), and conflicts of interest among PUCs [52].

The Public Utility Regulatory Policies Act (PURPA) of 1978 was an early act of deregulation. It allowed non-utility generators to compete against utility generators. Deregulation continued in the 1990s with the passage of the Energy Policy Act of 1992. The Energy Policy Act of 1992 relaxed restrictions that impeded utilities and non-utilities from functioning as independent power producers. It also granted the Federal Energy Regulatory Commission (FERC) more authority to force a TO to provide power-wheeling services on a case-by-case basis [58].

In 1996, FERC issued Orders 888 and 889. These orders are the foundation of transmission deregulation. In Order 888, FERC required TOs to adopt the contract-path framework. Also, it required open access, forcing TOs to allow use of their systems by third parties to execute contract-path transactions. Order 889, required each TO to establish an electronic system to make open access transparent. It also required vertically integrated utilities to create standards of conduct to functionally separate transmission, power marketing, and generation activities.

To support the development of regional wholesale power markets, FERC issued Order 2000 in 1999. Order 2000 suggested that utilities should relinquish operation of the transmission system to a regional transmission organization (RTO). Each TO was given the option to join an RTO or justify to FERC why they could not join an RTO.

Frustrated with the pace of implementation of Order 2000 implementation, FERC issued the Standard Market Design in 2002. The Standard Market Design required each TO to become an independent transmission provider (ITP) or relinquish operation of the transmission system. Each ITP was required to have no financial interest in any party within its region or neighboring region. Perhaps in response to resistance to the Standard Market Design, FERC issued a whitepaper effectively converting the Standard Market Design from a set of requirements to a set of suggestions. Thus, Standard Market Design is sometimes considered the high water mark for deregulation so far. The transmission sector remains mostly regulated but the overall electric power system is considered deregulated because of changes primarily in the generation sector [59].

2.4.1.3. Transmission Planning after Deregulation

Order 2000 charged RTOs with overseeing system planning. Eight years after Order 2000, many TOs had not joined RTOs. A TO not part of an RTO may lack incentives to invest in a welfare-enhancing transmission investment. To better align transmission planning with societal welfare in the absence of a migration to RTOs, FERC issued Order 890 in 2007. Order 890 required TOs and RTOs to include economic investments in the planning process [60,61]. In the presence of fragmented planning, FERC issued Order 1000 in 2011 [62]. Order 1000 required that interregional planning be coordinated, that economic investments with a benefit-to-cost ratio greater than 1.25 be built unless granted an exemption, and that planning be consistent with public policies such as RPSs [62,63]. Order 1000 proposed principles of cost allocation, including a requirement that only investment beneficiaries can be mandated to fund an investment. Order 1000 is controversial and it is unclear if will be fully enforced [64].

In the jurisdiction of an independent system operator (ISO) or RTO, the ISO or RTO and the member TOs conduct separate planning processes with various degrees of integration [65]. Economic investments identified in the ISO or RTO planning process typically must demonstrate a benefit-to-cost ratio greater than one to proceed to construction. As of 2010, most economic investments had been rejected by ISOs and RTOs [32]. Prior to Order 1000, at least one ISO or RTO has a minimum benefit-to-cost ratio threshold in excess of three [66]. A threshold benefit-to-cost ratio greater than one may lead to the cancellation of a welfare-enhancing investment. Each ISO or RTO proposes its own cost allocation rules subject to FERC approval. Defining contributions based on benefits creates an incentive for a load-serving entity (LSE) to understate an

investment's benefit and free-ride on other contributors [46]. Despite efforts to improve cost allocation, cost allocation may still be the primary barrier for multi-state, multi-utility transmission development [46].

2.4.2. Merchant Transmission Planning

2.4.2.1. Merchant Transmission Theory

The theory of merchant transmission was established in the early 1990s [67,68,69,70,71,72]. The developer of a merchant transmission investment bears the risk of the investment. Figure 8, derived from [67], illustrates how a merchant developer benefits from the investment. In the example, the northern region has generation and the southern region has either no generation or generation that is more expensive than the price at point B . In the absence of congestion, the market would settle at point B . However, with congestion at demand level K , no additional MWs can be supplied to load in the southern region. This creates the area of congestion rent, $K\eta$, the area of congestion cost, ABC , and the shadow price η . The congestion rent is a transfer from southern consumers to the transmission line owner. The congestion cost is the societal deadweight loss of the congestion. Under current market settlement rules, if a merchant transmission developer builds transmission capability δK it is rewarded with revenues of $\eta' * (\delta K)$ where η' is the ex-post shadow price of congestion. The ex-post shadow price of congestion is calculated as $D-E$. If the risk and time adjusted costs of the transmission investment are less than $\eta' * (\delta K)$, the developer proceeds with the investment.

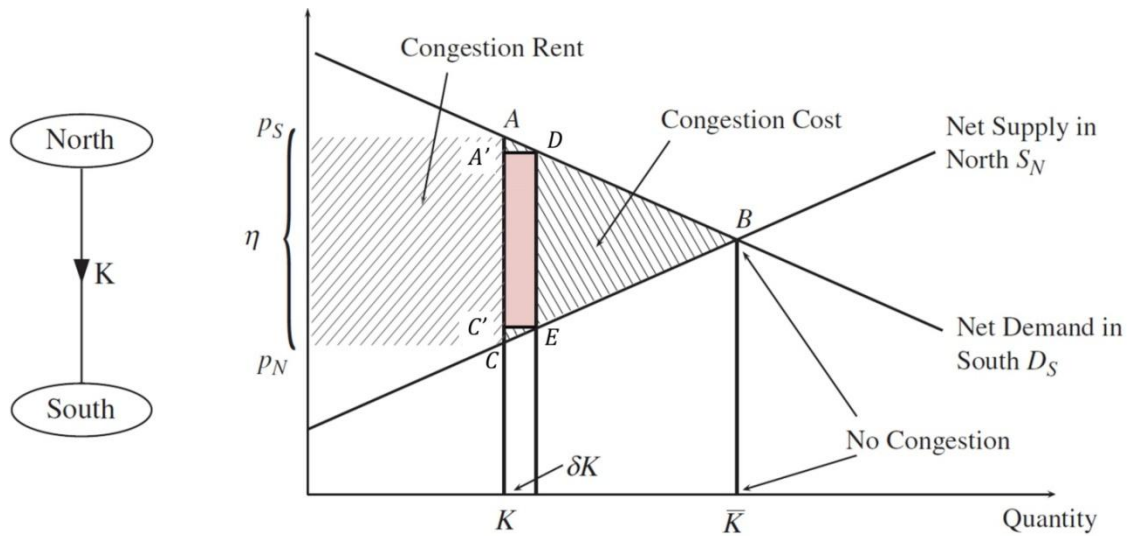


Figure 8: Congestion rent and congestion cost for a transfer between two areas.

Merchant transmission leads to an efficient level of transmission investment if there is no market power, the merchant investment lacks scale economies, the merchant developer receives the incremental benefit of the investment, and well-developed futures markets exist [68,71,72,73]. Under these conditions, regulated transmission investment is not necessary to resolve congestion [67]. Some generators and utilities prefer that merchant transmission make economic transmission investments [74].

The merchant transmission developer faces a number of challenges. The merchant developer has a first-mover disadvantage relative to generation. If a merchant developer announces its intent to build and new generation can be built more quickly than the transmission investment, the new generation can deter construction of the merchant investment. Another challenge is that FTRs alone have not been sufficient to finance a single merchant investment [75]. In areas with capacity markets, controllable merchant transmission can supplement FTR revenues by arbitraging price differences in capacity

markets [76]. In addition, the merchant revenues of Figure 8, $\eta' * (\delta K)$, are less than the societal benefit of the investment, *ADEC*. No evidence was found of non-controllable, AC transmission investments supplementing income with capacity market arbitrage [77].

2.5. Potential Mechanisms to Increase Transmission Capability

The following discussion highlights some of the potential mechanisms to increase transmission capability as well as the challenges of each method. Some methods facilitate traditional transmission investment, thereby increasing transmission capability but reducing utilization. Others increase transmission capability by increasing system utilization.

2.5.1. Aggregating Control and Market Areas

FERC, the Western Governors' Association and others have recognized since at least the 1990s that consolidation of control and market areas would improve the economic efficiency of the electric power sector [78,79]. During the late 1990s and early 2000s, a number of studies quantified the costs and benefits of larger market areas. The integration of PJM, ISONE, and NYISO would save \$440 million per year according to one analysis, negligible amounts according to another, and \$300 million per year according to a third [80]. A FERC study assesses the savings of consolidating operation of the American power system into three to ten RTOs [80]. The study uses the simplified transport transmission model. The RTO scenarios result in annual improvements in societal welfare on the order of \$5 billion per year in 2010 relative to the base case, or five percent of total electricity expenditures. Another study studies the impact of a large RTO in the west using an AC transmission model and a security-constrained optimal power flow (SCOPF) [81]. The study finds that the benefits of integration would justify

the costs and energy prices would drop by more than three percent in all but two control areas and prices would decrease in all but one control area [81].

Integration of control and market areas is challenging. FERC pushed for the formation of large RTOs during the early years of ISO formation to avoid ISO entrenchment [82]. In 2001, it directed PJM, NYISO and ISONE to merge and directed southeastern utilities to form an RTO [83]. However, these directions were avoided. In addition, mandated RTO formation has subsided with the retraction of the Standard Market Design [79,82]. Also, FERC has limited ability to regulated federal power authorities [84].

2.5.2. Incenting Additional Transmission Investment

Three general approaches have been identified to incent transmission investment without changing the structure of transmission ownership or cost allocation methods. First, revenue rules may be modified so the financial interests of regulated TOs are better aligned with societal welfare. Second, the economics of merchant transmission can be improved. Third, investment barriers that plague both regulated and merchant transmission can be mitigated.

2.5.2.1. Incenting Regulated Transmission Investment

FERC Order No. 679, Order No. 679-A, and Order No. 679-B allow a transmission investor to request incentives [85]. Incentives include a rate-of-return adder, accelerated depreciation, and the ability to add the investment to the rate base before completion.

Performance-based regulation may be used to incent transmission investment. For example, the TO could be responsible to pay for system congestion [86]. Few empirical comparisons of rate-of-return and performance-based regulation were identified. One study compares the two techniques using data from 23 electric and gas transmission and distribution utilities in Europe, finding no evidence that rate-of-return regulation leads to lower investment than performance-based regulation [87,88].

2.5.2.2. Incenting Merchant Transmission Investment

Merchant transmission investment may be incentivized by supplementing revenues or changing the market structure. One proposal is to award a merchant developer the reduction in congestion cost (RICC) caused by the investment rather than an FTR [89]. Rather than replace FTRs with RICCs, FTR revenues may be supplemented with capacity payments [75]. This requires the establishment of capacity markets in jurisdictions without them.

Issuance of FTRs is complicated by the requirement that ISOs and RTOs balance the issuance of FTRs with the estimated congestion rent over the life of the FTR. Consequentially, most ISOs and RTOs issue FTRs for periods no more than a few years in the future, burdening the merchant developer with estimating the value of FTRs over the investment lifetime.

Numerous methods propose modifications to the existing market structure to incent merchant transmission development. Both of the methods discussed below require the merchant transmission asset to be controllable and recognize the role of line impedance in congestion mitigation [90,91]. Under current rules, a high impedance,

unconstrained path connecting low-cost and high-cost buses has no financial incentive to invest. The first method assigns marginal or incremental values to both line capacity and line admittance. The first method is equivalent to a merchant TO that pays for the purchase of real power at the source bus and receives payment for the delivery of real power at the destination bus. In the second method, the merchant TO pays for real and reactive power at the source bus and is paid for real and reactive power at the destination bus. It is not clear if the proposed market changes are feasible given that ISOs and RTOs have been under development for more than 10 years and changes disrupt established stakeholders.

2.5.2.3. Removing Barriers to Entry Common to Regulated and Merchant Transmission

Removing barriers to entry may increase investment. One study finds that that public opposition is a more limiting constraint than topographic features or regulation [92]. Subjecting transmission to federal, regional and state-level oversight deters investment [93].

2.5.3. New Transmission Cost Allocation Methods

Before deregulation, transmission investment within a utility's footprint was mainly borne by the utility's customers. As deregulation emerged, the transmission system was increasingly used to wheel power across utility jurisdictions. In ISOs and RTOs, transmission costs are often allocated using the postage stamp method, which distributes costs pro rata among the LSEs based on peak demand. Cost allocation is necessary because the congestion and loss charges collected by the ISO or RTO are insufficient to pay transmission operating and capital costs [94].

Pro rata allocation is contentious as charges are not related to the distance power travels or the path power flows. An LSE tends to resist an investment which does not benefit its customers. ISOs, RTOs and FERC have experimented with new cost allocation rules to ensure that only beneficiaries of a transmission investment contribute towards the project [62,65,66,95].

The cost allocation methods may be classified as PF methods and economic methods. PF methods assess the impact of a given transmission user's generation or demand on power flows through specific assets and then assign costs accordingly. Economic methods redistribute the benefits of welfare-enhancing transmission investments so all entities gain from a transmission investment. Examples of PF methods are transmission-rent constrained economic dispatch [96], tracing [97,98,99,100,101], Z_{bus} [102], distribution factor [94,98,101,103], and equivalent bilateral exchanges [98, 102]. Application of the methods to a common test-system leads to differences in cost allocations, sowing the seeds for contention.

The PF methods vary by the assumptions underlying the methods. Tracing requires the *a priori* assumption that power flowing out of a node is supplied in the same ratio as the sources which feed the node. The equivalent bilateral exchanges method also requires an *a priori* assumption. The transmission-rent constrained economic dispatch, tracing, and distribution factor methods require an arbitrary assignment of costs between generation and load [100,101]. The tracing and Z_{bus} methods do not recognize the benefit of counterflows [98,101,102]. Costs in the Z_{bus} method are dependent on the direction assumed for current [102]. The specific form of the distribution factor method is dependent on the chosen reference bus [102].

The reviewed economic methods are based on game theory. One method distributes the incremental welfare benefit of the transmission investment among users, as credits and charges, ensuring support for a welfare-enhancing transmission expansion [104]. Another method forms coalitions of willing participants to support transmission investments [99].

2.5.4. Consolidation of Transmission Ownership and Operation

One goal of ISO and RTO development is to better coordinate transmission system operation and planning by aggregating operation and planning across multiple TOs. This aggregation leads to transaction costs [105,106]. Centralized ownership, whereby the region's transmission is planned and operated by a single entity, is an alternative to the ISO and RTO structures. In this structure, the single entity is known as a transmission company (TransCo). In theory, the TransCo structure leads to the lowest cost of energy relative to the other structures if a single TransCo covers the entire interconnection. It may not be lowest cost option if it spans only a portion of the interconnection [105]. TransCos are in operation in the United Kingdom, Spain, New Zealand and parts of Australia [107]. In these areas, it is difficult to isolate the effect of adopting the TransCo structure, as the structure was implemented along with other regulatory changes [107]. However, circumstantial evidence supports the TransCo structure [79,105,107,108].

TransCo formation and regulation is challenging. Creation of a TransCo by aggregating privately held TOs is expropriation [109]. In addition, FERC does not have the authority to regulate federal power agencies [110]. Informational asymmetries may exist between the TransCo and the regulator [111].

2.5.5. Increased Controllability of Power Flows

A fully controllable transmission system would allow for the formation of natural markets in which the owner of the controllable transmission asset could charge for use of the asset and forbid access to non-paying entities [52,112]. Under such a scenario, network externalities would disappear [112,113]. Controllability mitigates impediments to transmission investment such as economies of scale, the potential for detrimental investment and investment recovery uncertainty [113].

The impact of controllability may be assessed via simulation of a test-system. Thirty-one studies of controllability were reviewed [114,115,116,117,118,119,120,121,122,123, 124,125,126,127,128,129,130,131,132,133,134,135,136,137,138,139,140,141,142,143]. Fifteen assessments find controllable assets to be a viable investment [114,115,117,118, 119,120,129,134,136,137,138,139,140,141,142]. Of the 31 references, six compare the implementation of controllability to traditional investment options such as transmission line construction [118,134,136,138,140,141]. Of these six, two show controllability to be unequivocally preferential to the other options [118,141]. None of the examined literature evaluates the viability of controllability in a system the size of an ISO or RTO. Despite the findings of these studies, most transmission lines are not controllable.

Increasing the controllability of the transmission system is challenging. Controllability could be used to realize market power and benefit the owner of the controllable asset [91,144,145,146,147]. The cost and reliability of controllers are barriers to implementation [148].

2.6. Potential Methods to Reduce Need for Additional Transmission Capability

Generation, energy storage and demand side management are substitutes for transmission and set an upper bound on future transmission investment. A fourth option, known as *packetized energy*, *the energy internet*, *the digital grid* or renditions thereof, combines elements of generation, distributed generation and demand response.

2.6.1. Locating Generation in Load Centers

Numerous studies identify the ability of new load center generation to reduce the need for distribution system investment [149,150,151,152,153]. While less evidence was found of the link between deployment of generation in load centers and a reduction in transmission system investment, the relationship appears valid [150,153,154]. One study finds that the present value (PV) of transmission investment in Queensland, Australia could be reduced by 31% if coordinated with the deployment of distributed generation. However, none of the identified studies assess the impact of generation and transmission investment on the total cost of energy.

Conventional or renewable generation may serve as load center generation. Locating renewable generation in load centers may be unattractive given a lack of economies of scale and high-quality renewable resources. Land requirements, emissions, noise and cooling water requirements are challenges for locating conventional generation in load centers. One study identifies that 19 of the 22 American counties most at risk for water shortages because of electricity generation are located in the 20 fastest growing metropolitan statistical areas [155,156,157]. Dry-cooling minimizes cooling-water requirements but reduces plant efficiency and increases capital cost, noise levels, and land requirements [158]. Dry-cooling would increase the capital cost of a 500 MW

combined-cycle gas turbine (CCGT) plant by 2-5% [158,159]. A dry-cooling system for a typical CCGT plant would span two football fields while such a system for a coal plant would consume six football fields [158]

2.6.2. Energy Storage

Energy storage sited at the load side of a congested transmission asset can relieve congestion, increase the net utilization of the congested asset, and mitigate the need for additional transmission capability [160]. Providing generation via energy storage has a PV benefit of as much as \$18.4 billion over ten years, or \$400-700 per kW [161].

Deferring transmission and distribution benefit via energy storage has a PV benefit of five billion dollars over ten years, or \$481-1079 per kW [160]. Congestion mitigation via energy storage has a PV benefit of up to \$3.2 billion over ten years. The PV benefit of congestion mitigation increases to \$21 billion over ten years, or \$31-782 per kW, if energy storage is also used to reduce wind energy curtailment [160]. The above benefits are applicable to the United States and do not consider the PV cost of storage.

Congestion relief is projected to require a two to six hour discharge capability, resulting in higher \$/kW costs than other energy storage applications. Meanwhile, the benefits of congestion relief on a dollar per kW basis are the lowest of 19 surveyed applications of energy storage [160].

In addition to the financial challenges of energy storage, energy storage is encumbered by policy uncertainty. It is unclear if energy storage systems can simultaneously receive revenue as regulated and market assets. Some current energy storage technologies would be competitive with transmission if an energy storage asset can simultaneously receive revenue as a regulated and market asset [160].

2.6.3. Demand Side Management

In theory, demand side management can reduce congestion, mitigate the need for additional transmission capability, and increase societal welfare [162,163,164,165]. In practice, demand side management has been slow to develop. Demand side management is challenged by increased system complexity [164], the possibility of near-term and long-term cost increases [164], lack of consumer participation [166], poor alignment with utility incentives [166], and the free rider problem [164]. The challenges faced by demand side management can be categorized as transaction costs. Developments in information and communication technology may reduce the transaction costs and increase the viability of demand side management.

2.6.4. Packetized Energy

Numerous papers have proposed the concept of *packetized energy*, the *energy internet*, the *digital grid* or derivatives thereof [167,168,169,170,171,172,173,174,175,176,177,178, 179,180,181]. The first known work was published in 1997 [167]. Like the nomenclature, the meaning of *packetized energy* is sometimes discordant. However, the bulk of the examined literature has certain commonalities:

- Use of direct load control or variable pricing to realize large amounts of load flexibility
- Use of energy storage to relieve the requirement that instantaneous demand equal supply
- Packetization of energy, with identifying attributes assigned to each packet (i.e. source bus, delivery path, and destination bus)

- Use of energy routers to control loads, energy storage, and packet reception/transmission

Much of the theory of *packetized energy* is inspired by the internet and data centers. Adding load control and energy storage allows infrastructure design to focus more on the average case rather than the worst case [177]. The increased investment in loads and energy storage reduces the investment required for conventional generation, transmission, and distribution. If coupled with the ability to route packet flow, the assignment of packets enables differentiation of electricity by generation type. In addition, the ability to route packets avoids the cost allocation debates of traditional transmission planning, mitigates congestion, and increases utilization. *Packetized energy* is also compatible with the deployment of distributed generation. Finally, some papers design packetized energy to run on top of existing assets, similar to how the internet was initially run using the telephone network [177]. The *packetized energy* network may someday replace the traditional power network, as the internet has done for the telephone network [177].

Most proposals do not address how packets will be routed. Some concede that a synchronous network cannot support control of packet paths [176] and promptly eliminate PF control from the attributes of *packetized energy*. Stripped of packet control, the concept reduces to the deployment of high levels of load control and energy storage. One paper proposed replacing the meshed AC transmission system with an HVDC links [181]. While a meshed system would offer more reliability and options for packet delivery, the paper proposes a star-type or partially-meshed network due to the complexities of fault management in DC networks. A final paper proposed separating large synchronous systems into small systems, asynchronous relative to each other,

coupled with digital grid routers [179]. Every connection between systems would have either a type A port or type B port. A type A port would convert from the AC to DC and then back to AC. The existing AC transmission system would then be used to transport power to the next digital grid router and fed into a type B port. This reduces the stages of power conversion required for inter-system transfers and utilizes existing AC transmission circuits. Within the synchronous areas, PF would be uncontrolled. To packetize energy from source to load, the synchronous areas could be reduced to single buses. This would require the massive deployment of power electronics.

If realizable, *packetized energy* may revolutionize the electric power sector, eliminating many of the regulatory and stakeholder hurdles that currently impede transmission investment. Realizing *packetized energy* through simultaneous deployment of load control, energy storage, and fully-rated controllers would require substantial investment. The benefits of said investment may not be justified and a migration path to *packetized energy* may not exist.

2.7. Power Flow Controllers

Figure 9 shows a two-bus system connected by a single-circuit, lossless transmission line. A simplified expression of the power flow through the transmission line is shown in (Eq. 3) and Figure 10. In the figure, I_{line} is the current that flows between the buses. A PF controller may be used to control PF by changing any of the parameters in the equation. In addition, conversion from and to HVDC may be used to control PF between two AC buses. PF control may be broadly categorized as shunt, series, shunt-series or HVDC. Shunt, series, and shunt-series control respectively inject

voltage/current in shunt with a bus, in series with a line, or both in shunt and in series.
 Much of the following discussion is drawn from [182].

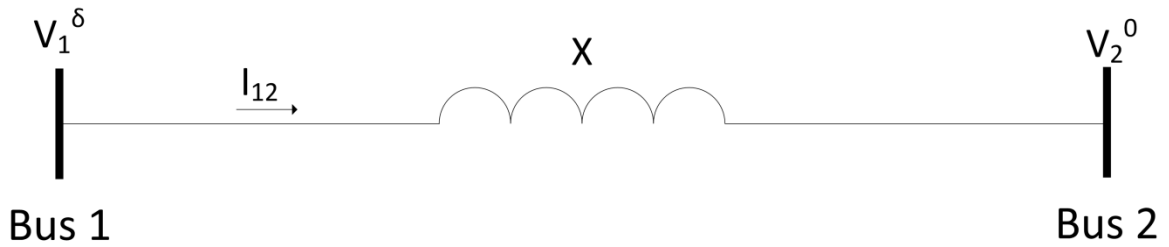


Figure 9: Two-bus system connected by a single transmission line.

$$P = \frac{V_1 V_2}{X} \sin \delta \quad (\text{Eq. 3})$$

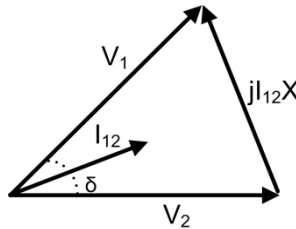


Figure 10: Phasor diagram of the power flow through the transmission line.

2.7.1. Shunt Controllers

A shunt controller can control the magnitude of a bus voltage, V_1 or V_2 in (Eq. 3), or control the voltage profile at a point along a transmission line. Figure 11 shows the connection of a shunt controller at Bus One to change the voltage magnitude of Bus One from V_1 to $(V_1 + V_{1d})$. Figure 12 shows the resulting phasor diagram when the voltage of

Bus One is increased by 10% using a shunt controller. Figure 13 shows the transmission line split in half with the shunt controller at the new bus. Figure 14 shows the resulting phasor diagram, with $\frac{\delta}{2}$ between each original bus and the new bus. Examples of shunt controllers are the shunt mechanically switched capacitor (MSC), the shunt mechanically switched reactor (MSR), the thyristor switched capacitor (TSC), the thyristor switched reactor (TSR), the thyristor controlled reactor (TCR), the static VAR compensator (SVC) and the static compensator (StatCom). All of these controllers are discussed below.

Figure 15 through Figure 20 show the topologies of the shunt controllers.

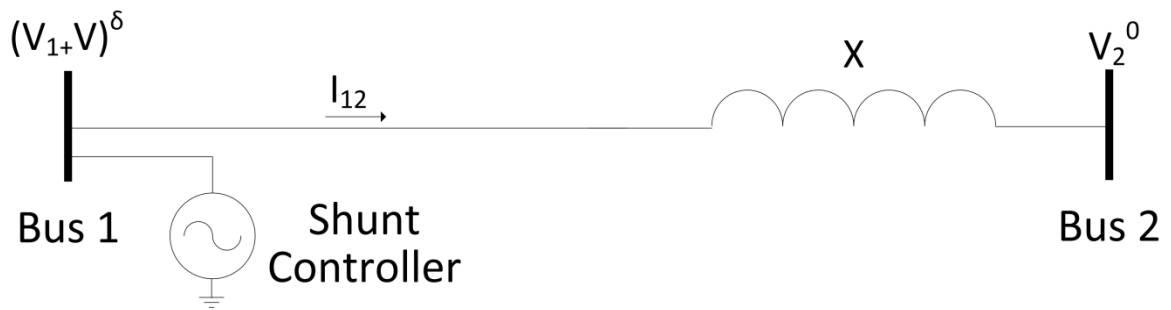


Figure 11: Connection of a shunt controller at Bus One.

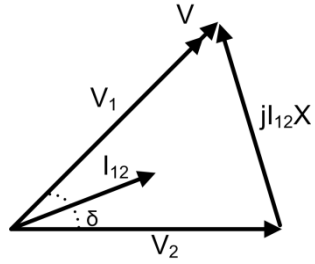


Figure 12: Phasor diagram with a shunt controller installed at Bus One.

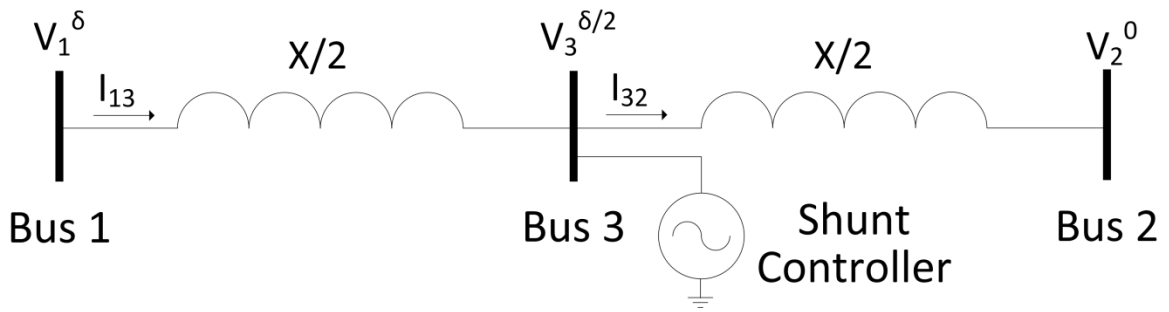


Figure 13: Connection of a shunt controller at the midpoint of the transmission line.

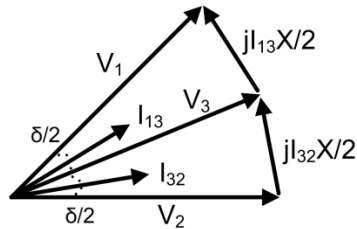


Figure 14: Phasor diagram with a shunt controller at the midpoint of the transmission line.

Figure 15 shows the typical MSC. Multiple MSCs can be used to provide control granularity. Since switching causes deterioration of the mechanical switch, MSCs are preferred for applications requiring infrequent switching.

Figure 16 shows the typical MSR. A circuit breaker is used rather than a switch given the inductive load. Like an MSC, MSRs are preferred for applications requiring infrequent switching.

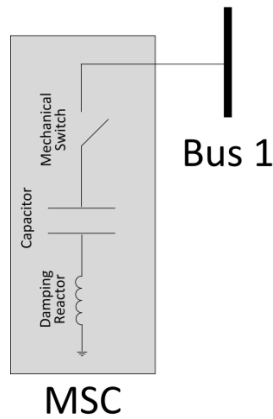


Figure 15: Mechanically switched capacitor (MSC).

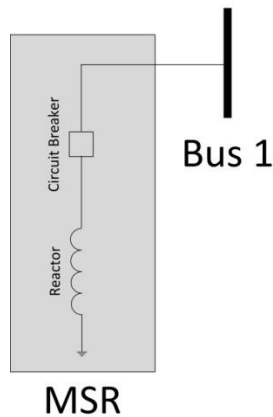


Figure 16: Mechanically switched reactor (MSR).

Figure 17 shows the TSC. The TSC is a shunt capacitor which is switched in and out using a thyristor pair. The use of a thyristor pair, rather than a mechanical switch,

provides longer life. Ideally, the capacitor is connected with no difference between the capacitor voltage and the grid voltage. When this is not feasible, the damping reactor limits the surge current through the capacitor and thyristor.

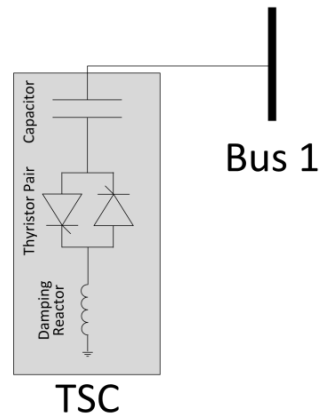


Figure 17: Thyristor switched capacitor (TSC).

Figure 18 shows the TCR. By controlling the delay angle of thyristor conduction relative to the peak bus voltage, the effective inductance of the reactor to fundamental current can be controlled between zero and the inductor's rated value. If the TCR is operated with a delay angle of zero, it is referred to as a TSR. The delay angle can be changed every half cycle, limiting the response time of the TCR.

The TCR produces harmonics if the delay angle is non-zero. Multiple methods exist to reduce the harmonics. If the same delay angle is used for each thyristor, even harmonics are eliminated. In addition, if the three phases are delta-connected and operated symmetrically, the third harmonic and multiples thereof are eliminated.

Alternatively, a TCR can be used in conjunction with one or more TSRs. The TCR provides vernier control of inductance and the TSRs provide lump inductance. This

reduces the harmonic currents. Another option is to use two TCRs, one delta-connected and one wye-connected. Harmonic filters can also be installed to reduce harmonics.

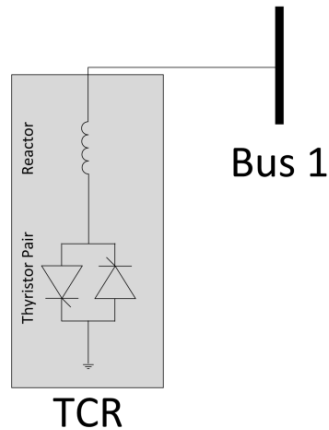


Figure 18: Thyristor controlled reactor (TCR).

An SVC is comprised of a combination of fixed capacitors (FCs), TSCs, and TCRs. One combination is shown in Figure 19. Output is fully capacitive when the TCR delay angle is 180 degrees. Output is zero when the capacitor reactive power matches the inductor reactive power. Output is fully inductive when the TCR delay angle is zero. Response time is improved by adding multiple units that are phase-shifted relative to each other. For applications requiring little to no average VAR output, replacing the FC with one or more TSCs will reduce average losses. However, this will increase the response time relative to an SVC with an FC.

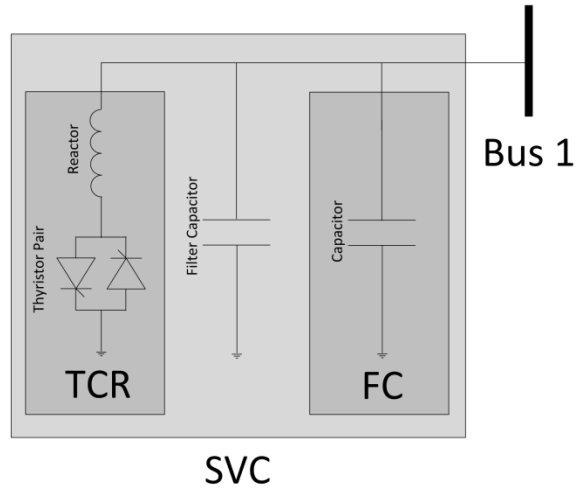


Figure 19: Static VAR compensator (SVC).

The StatCom uses one or more voltage-source converters (VSCs) to mimic the operation of a synchronous condenser. Early StatComs used two-level or three-level converters that were phase-shifted with transformers to produce the required output waveform. Modern StatComs use a modular multilevel topology. This topology uses a stack of submodules to form an arm. The arm generates the output for a single phase. One or more arms can be connected in parallel to provide sufficient capacity. A single-phase representation of the modular multilevel StatCom is shown in Figure 20. Figure 21 shows the topology of a submodule.

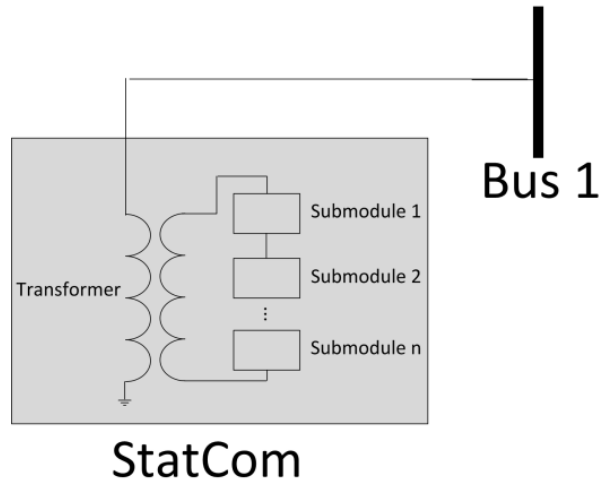


Figure 20: Modular multilevel static synchronous compensator (StatCom).

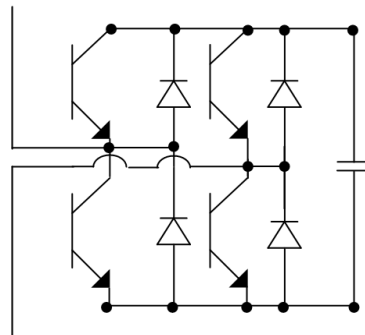


Figure 21: Submodule of a modular multilevel StatCom.

The shunt controllers vary in capability in terms of level of support during faults, potential to resonate with other components of the power system, response time, longevity, and cost. The reactive current of the shunt MSC, shunt MSR, TSC, TCR and SVC are proportional to bus voltage, resulting in a quadratic decrease in reactive power in response to a linear decrease in voltage. This may be problematic since increased reactive power is often required during faults. The StatCom's maximum reactive output current is nearly constant over a wide voltage range, so reactive power output decreases

linearly with a decrease in voltage over a wide bus voltage range. The shunt MSC, shunt MSR, TSC, TCR, TSR and SVC are typically implemented on a per-phase basis, allowing them to provide unbalanced compensation during unbalanced faults. Early StatComs topologies use one or more three-phase VSCs. As a consequence, early StatComs provide limited support during unbalanced faults. The new modular multilevel StatComs use separate converters for each phase and can provide more support during unbalanced faults. When connected, an MSC and TSC may resonate with line reactance. StatComs and SVCs can be used to actively damp resonances. The speed and longevity of the shunt controllers also vary. The shunt MSC and shunt MSR are the slowest shunt controllers and are limited to 2000-5000 switching cycles before switch replacement [183]. The TSC, TSR, TCR, and SVC are the next fastest controllers. The switching cycles of these devices are not as limited as the shunt MSC and shunt MSR. The StatCom response is an order of magnitude faster than an SVC. The switching cycle longevity of the StatCom is high but overall controller reliability is impacted by ancillaries such as the cooling system.

From an equipment cost perspective, the shunt MSC and shunt MSR are the least expensive shunt controllers per VAR at nominal voltage. By contrast, the StatCom is the most expensive shunt controller. However, total project cost of a StatCom may be lower than other controllers because of the cost of substation space and the relationship between voltage and reactive power rating.

2.7.2. Series Controllers

A series controller can alter the line impedance (X) of (Eq. 3). Figure 22 shows the connection of the series controller at Bus One with the controller injecting a series voltage V . Figure 23 shows the phasor impact of injecting a capacitive voltage while Figure 24 shows the impact of injecting an inductive voltage. For most applications, this functionality provides a larger range of PF control than shunt controllers given the limited range of acceptable bus voltages. Series controllers include the series mechanically switched reactor (MSR), series mechanically switched capacitor (MSC), thyristor controlled series capacitor (TCSC), the static synchronous series compensator (SSSC), and the distributed series reactance (DSR). Figure 25 through Figure 29 show the topologies of the five controllers.

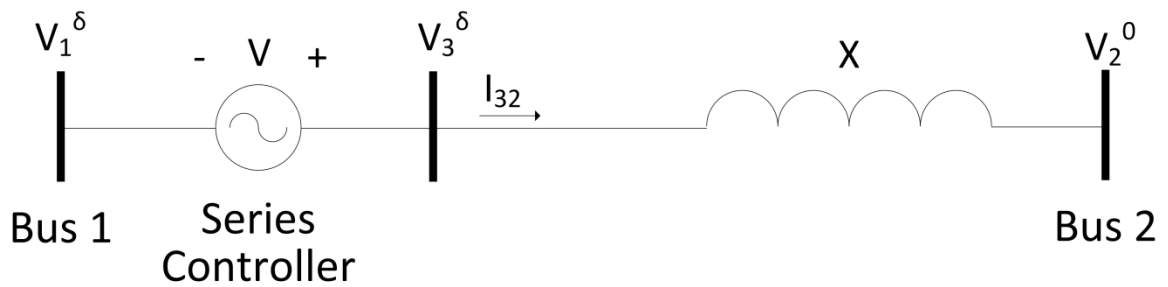


Figure 22: Connection of a series controller at the Bus One side of the transmission line.

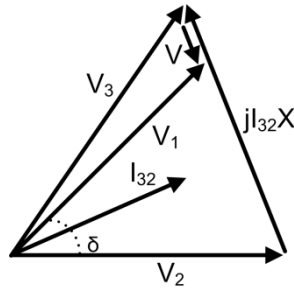


Figure 23: Phasor diagram with a series capacitive controller installed at the Bus One side of the transmission line.

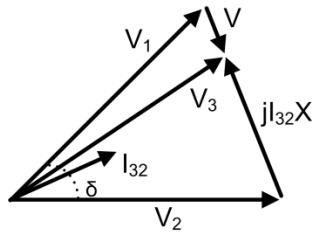


Figure 24: Phasor diagram with a series inductive controller installed at the Bus One side of the transmission line.

The series MSR and series MSC are shown in Figure 25 and Figure 26 respectively. Like their shunt equivalents, the mechanical switches of these controllers limit their response time and longevity. Since an MSC is not typically built to endure the high currents of a fault, protection methods are used to bypass the MSC during the fault and reengage it soon thereafter to increase system stability. The early series capacitors were protected from fault currents using a maintenance intensive spark gap. Modern designs utilize an MOV or thyristor protection. Both are installed on platforms at line potential, requiring space in the substation or along the right-of-way. An MSC can lead to sub-synchronous resonance with the rotating elements of a generator, resulting in potential generator failure and power system instability

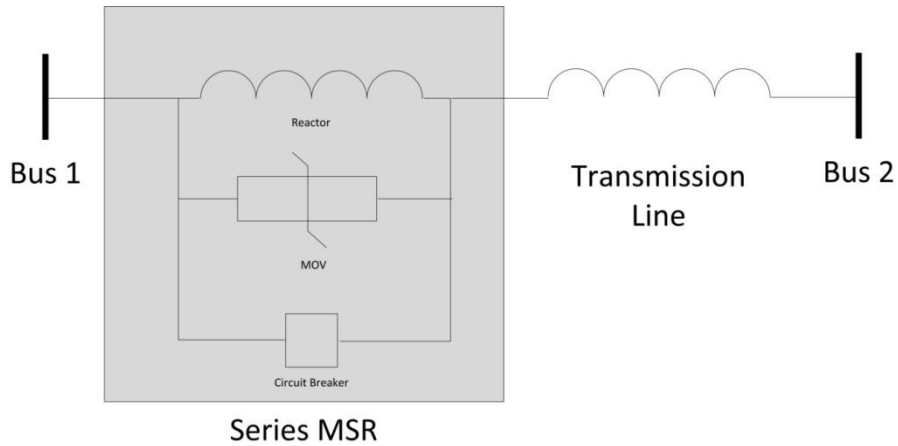


Figure 25: Series mechanically switched reactor (MSR).

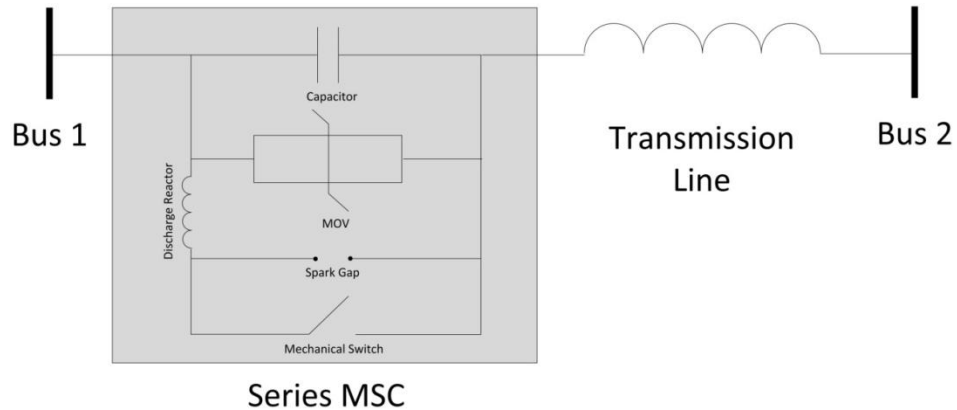


Figure 26: Series mechanically switched capacitor (MSC).

The TCSC, shown in Figure 27, is a series capacitor connected in parallel with a TCR. A TCSC may have one or more series stacked modules. For a configuration where the reactance of the inductor is smaller than the capacitor, a TCR firing angle of 0 to α_{Lim} provides a net inductive impedance and a firing angle of α_{Lim} to $\pi/2$ provides a net capacitive impedance. The TCSC has a resonance point between the two limits. Therefore, the TCSC can inject more reactive power than the nameplate ratings of the capacitor or inductor. Like the shunt TCR, the TCSC produces harmonics. In addition,

the TCSC requires specialized control to operate correctly during startup, shutdown, and faults. Like the series MSC, the TCSC requires an isolation platform, which increases cost and requires additional space at the substation.

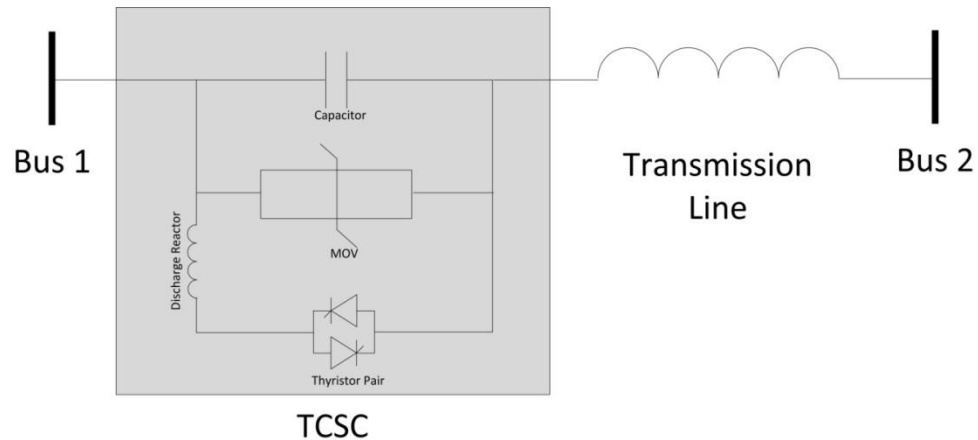


Figure 27: Thyristor controlled series capacitor (TCSC).

The SSSC uses one or more VSCs to emulate a series capacitor or inductor. Figure 28 shows a modular multilevel SSSC similar to a modern StatCom. The SSSC can provide sub-cycle response times and actively mitigate transients. As a voltage source device, sub-synchronous resonance is not an issue. No evidence was found of a stand-alone SSSC installations but the Marcy Convertible Static Compensator (CSC) can be configured to provide SSSC functionality on one or two lines. SSSC designs in the literature propose ground-mounting or mounting the converter on a platform. Construction of the series transformer is challenging given the high basic insulation level and fault current requirements.

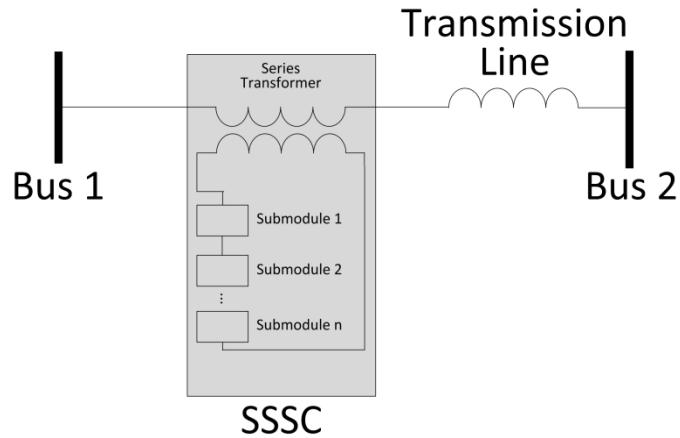


Figure 28: Static synchronous series compensator (SSSC).

Figure 29 shows the DSR. It operates like a series MSR but is fractionally-rated and supported by the line rather than an elevated platform. Deployment of a fleet of modules provides the aggregate capability of the MSR. Each DSR has a single-turn transformer that when operated with the secondary open injects inductive impedance.

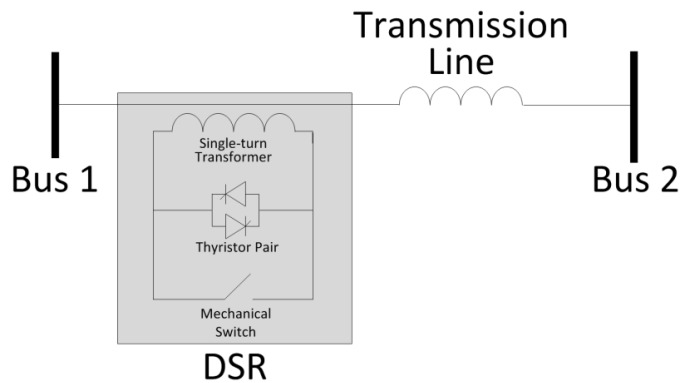


Figure 29: Distributed series reactance (DSR).

The capabilities of the series controllers vary by response time, longevity, and cost. Switching times for the series MSR and series MSC preclude their use to mitigate

transients. The TCSC and DSR have sufficient response times to improve transient stability and damp oscillations. The SSSC has the fastest response time. The series MSR and series MSC are low cost but have limited switching cycles. The TCSC has higher cost than the series MSR or series MSC. Like the StatCom, the SSSC can last many switching cycles but longevity is limited by ancillary components. The cost of the SSSC is unknown given the lack of known deployments but is expected to be higher cost than all other series controllers. The DSR is under development and is expected to have a lower cost and higher reliability than the TCSC and SSSC.

2.7.3. Shunt-Series Controllers

A shunt-series controller changes the angle across the transmission line and may also be able to change the magnitude of the bus voltage at which the controller is connected. This is represented in Figure 30, where the output of the shunt-series controller has voltage V_3 . Figure 31 shows the phasor diagram of a shunt-series controller installed at Bus One. Note, that V can take any value within the dotted circle. Shunt-series controllers include the unified power flow controller (UPFC), the Variable Frequency Transformer™ (VFT), the phase-shifting transformer, the controllable network transformer (CNT), and the fractionally-rated back-to-back (FR-BTB). Figure 32 through Figure 37 show the topologies of the five controllers, with two types of PST controllers shown.

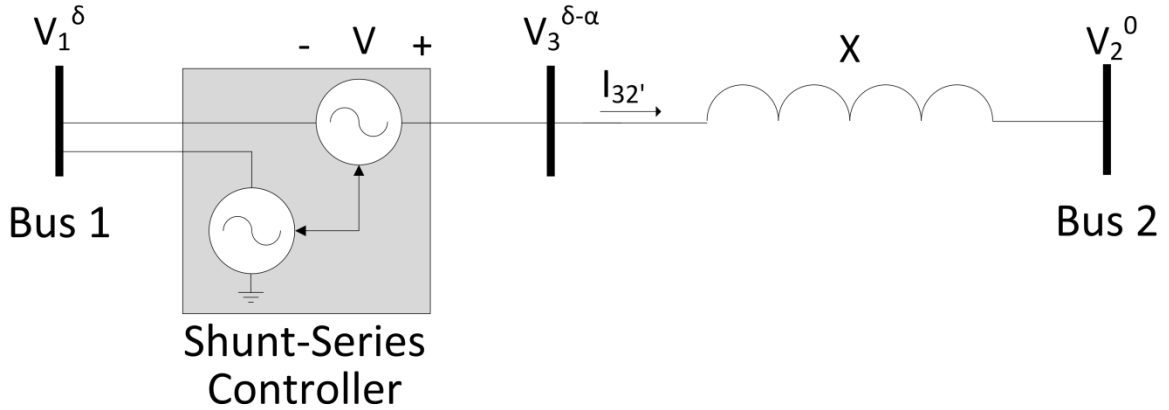


Figure 30: Connection of a shunt-series controller to the power line.

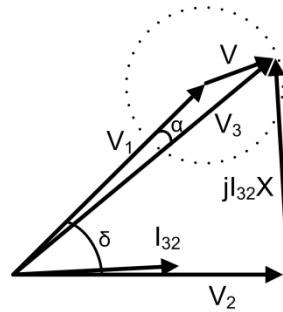


Figure 31: Phasor diagram of a shunt-series controller connected to Bus One and the line between Bus One and Bus Two.

Figure 32 shows an early UPFC topology. The UPFC connects a STATCOM and SSSC through a common DC bus, allowing control of the real and reactive injected power into the line. The UPFC can also control the voltage of the bus to which it is connected. The UPFC has the combined complexity of the SSSC and StatCom.

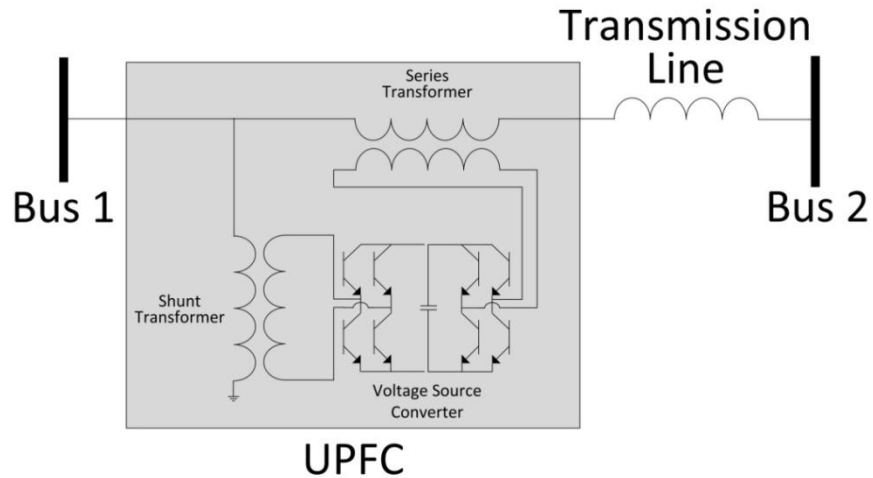


Figure 32: Unified power flow controller (UPFC).

The VFT is shown Figure 33. It provides functionality similar to a BTB without conversion to DC. The VFT is a large doubly fed induction motor developed for power flow control applications. Power flow from the rotor to stator is varied by changing the torque on the rotor. Torque is applied using a drive motor and variable speed drive. The VFT is able to change power flow from full rated output in one direction to full rated output in the other direction.

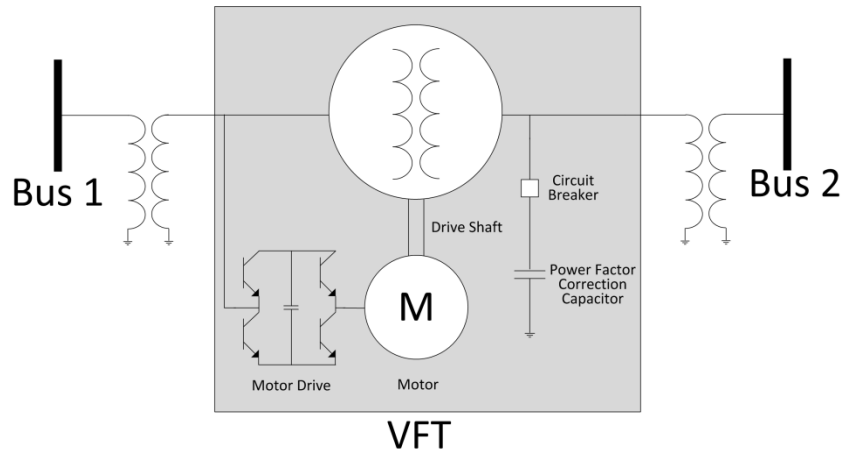


Figure 33: Variable frequency transformer (VFT).

Figure 34 and Figure 35 show the CNT and FR-BTB respectively. Both augment an existing multi-tap transformer with a fractionally-rated converter. Like the UPFC, the CNT and FR-BTB provide simultaneous control of bus voltage magnitudes and line phase angles. Since power flow control typically requires small changes to system parameters, the converter can be fractionally-rated with respect to transformer.

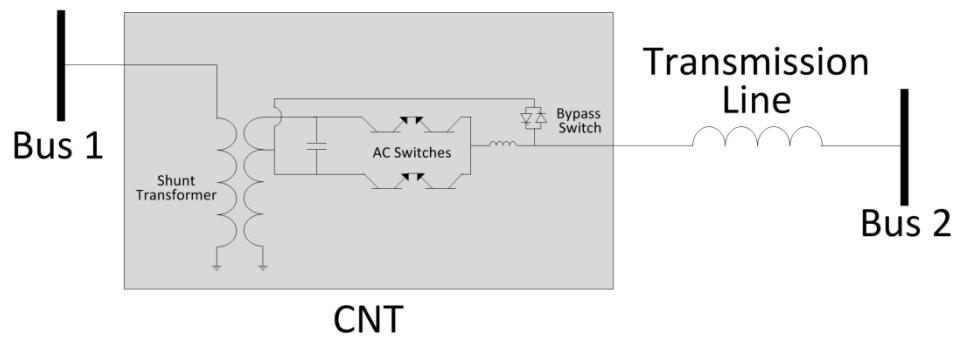


Figure 34: Controllable network transformer (CNT).

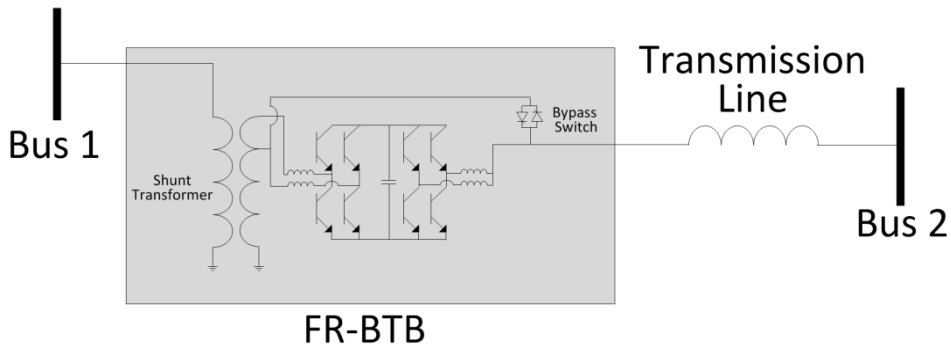


Figure 35: Fractionally-rated back-to-back (FR-BTB).

The PST is also known as the phase-angle regulator or quadrature booster. A typical PST can control the phase angle but not the bus voltage magnitude. Therefore, the locus of feasible values of the injected voltage V , shown in Figure 31, reduces from a circle to the line perpendicular to line current.

Numerous PST topologies exist. The simplest type has a fixed phase angle. In more complicated topologies, mechanical load tap-changers (LTCs) or solid-state switches are used to vary the phase angle. The most common type of PST uses a single core as seen in Figure 36. This single core design requires the full line current to pass through the LTCs, exacerbating fault current management and increasing the cost of the LTCs. A more expensive PST, shown in Figure 37, uses shunt and series transformers to overcome the limitations of a single-core PST. This version couples a wye-connected series transformer with a delta-connected exciting transformer. In another PST type, the mechanical LTCs are replaced by thyristor pairs. As an alternative, voltage source converters could be used to synthesize the quadrature injection voltages.

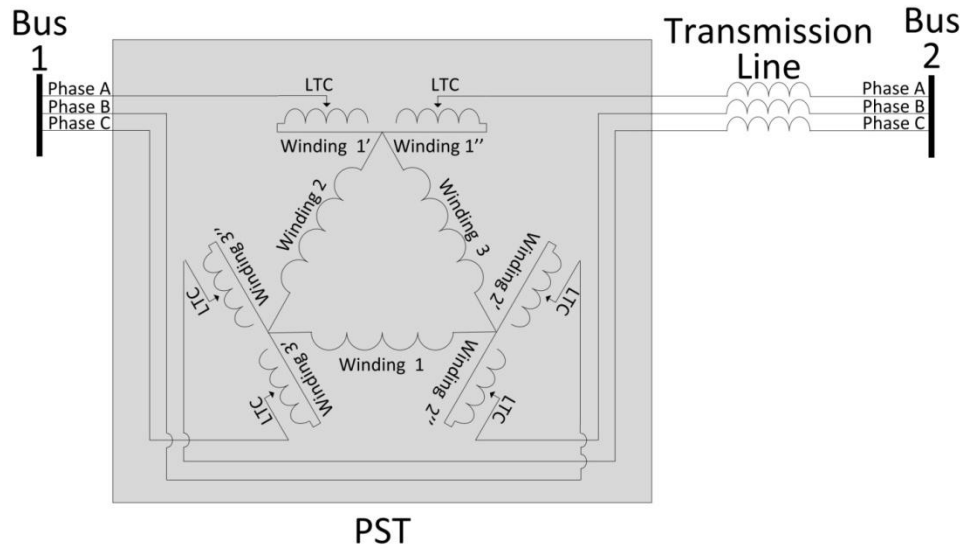


Figure 36: Three-phase diagram of a single core phase-shifting transformer (PST).

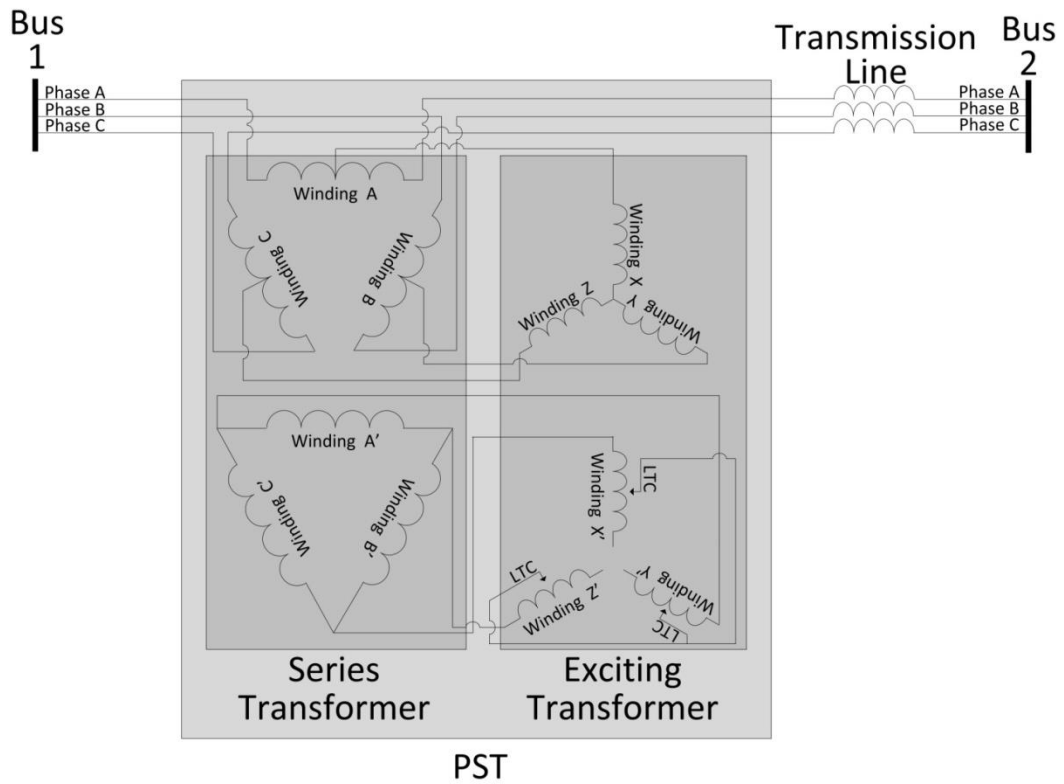


Figure 37: Three-phase diagram of a two core phase-shifting transformer (PST).

The shunt-series controllers can be differentiated by speed, longevity, and control capability. The UPFC, CNT, FR-BTB and VSC-based PST have the fastest response time. The mechanical PST topologies are the slowest, with a response time on the order of seconds. The longevities of the UPFC, CNT, and FR-BTB are limited by the ancillary components rather than the switching devices. The longevities of the mechanical PST topologies are limited by the switching elements. The cost of a large, mechanical PST is low per unit of control capability but it requires more substation space than the other shunt-series controllers. The cost of the VFT is unknown. The UPFC is more expensive than the mechanical PST. The CNT and FR-BTB are under development and are expected to be lower cost than the UPFC.

2.7.4. HVDC Controllers

An HVDC controller can control the voltage, angle and frequency of the input terminal independently of the output terminal, provided power balance is maintained and the controller operates within design limits. Figure 38 shows an HVDC controller embedded in an AC transmission system with the controller output represented as a new bus. Figure 39 shows the phasor diagram of an HVDC controller installed at Bus One and operated at a specific point. In the figure, V_1 is applied to the input of the controller and V_3 is developed at the output. HVDC controllers include the HVDC transmission system and the back-to-back converter (BTB).

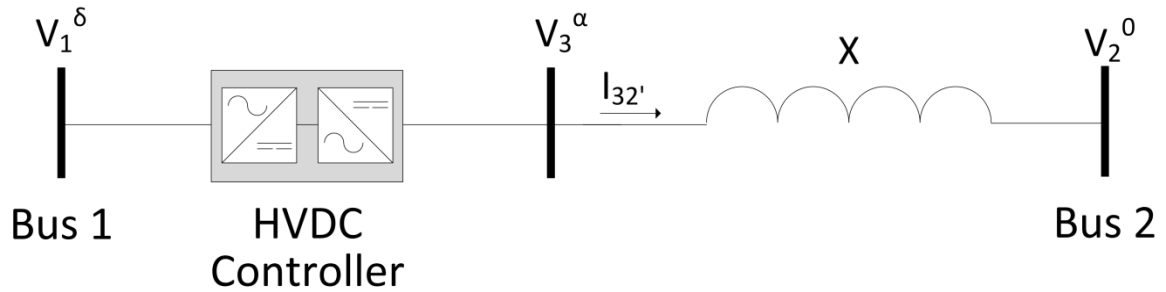


Figure 38: Phasor diagram of an HVDC controller connected between Bus One and Bus Three.

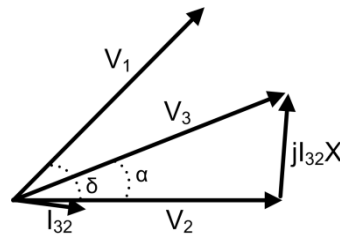


Figure 39: Phasor diagram of an HVDC controller connected to Bus One and supplying the line between Bus Three and Bus Two.

The HVDC transmission system was originally developed to transport power efficiently over long distances. The original HVDC transmission systems used line commutated converters as shown in Figure 40. Line commutated converters absorb reactive power at both terminals and thus require reactive compensation. They also require harmonic filtering. As a result, an HVDC transmission system requires more space at each terminal than other PF controllers. The modular multilevel converter approach has been applied to HVDC systems, as shown in Figure 41. The submodule for HVDC, shown in Figure 42, is distinct from the submodule for the StatCom and the SSSC. The modular multilevel approach eliminates the need for reactive power compensation and reduces or eliminates the filtering requirements. The smaller size

facilitates embedding an HVDC transmission system within an AC transmission system for power flow control. An HVDC transmission system can be configured to limit fault current contributions, an advantage over AC lines. In addition, the receiving terminal an HVDC transmission system has many of the features of a dispatchable generator sited at the terminal [184].

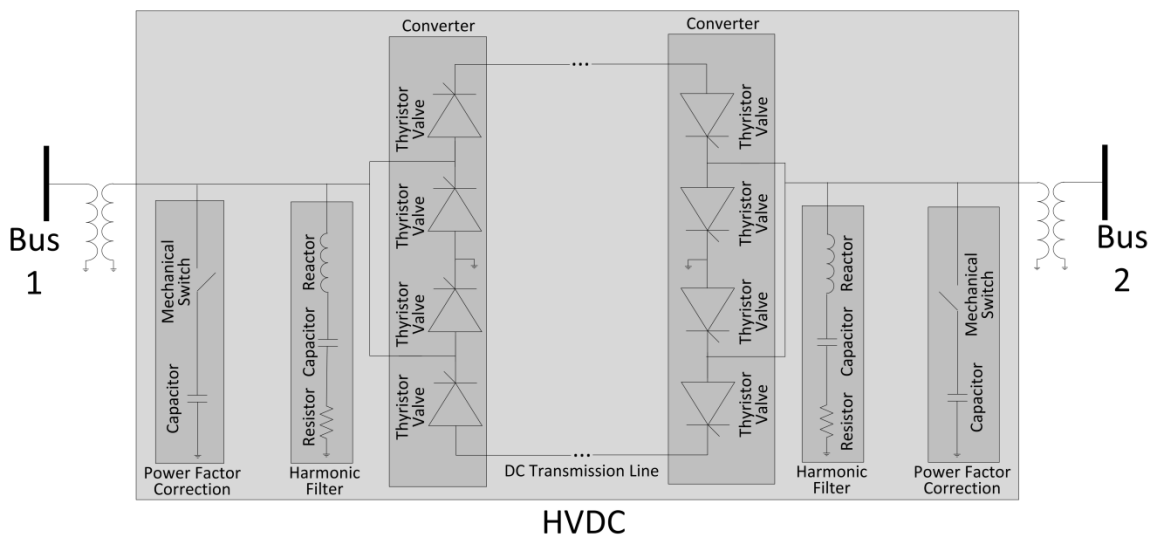


Figure 40: High voltage DC (HVDC) transmission system using line commutated converters.

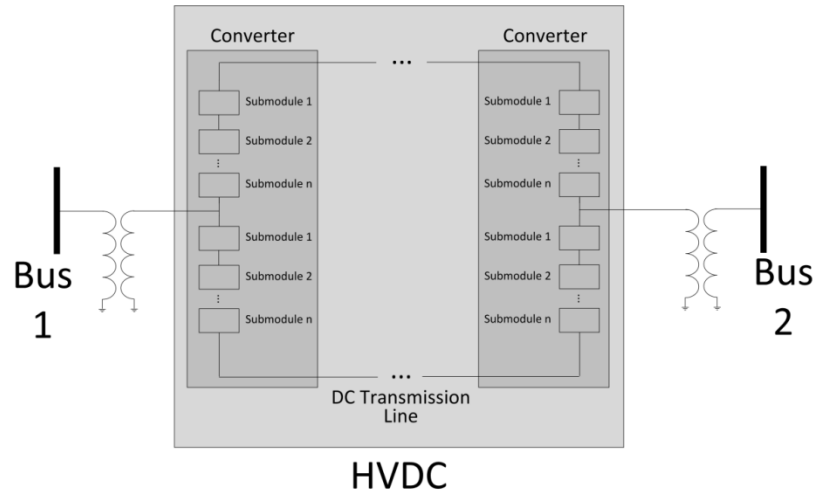


Figure 41: High voltage DC (HVDC) transmission system using modular multilevel converters.

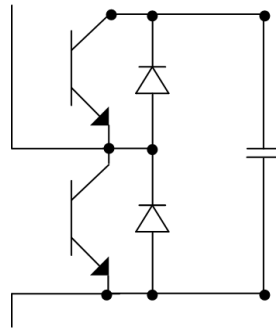


Figure 42: Submodule of a modular multilevel HVDC.

A BTB is an HVDC transmission system with the two terminals directly connected, as shown in Figure 43. Modern BTBs use modular multilevel converters, averting the need for reactive compensation and large filters. BTBs have been primarily deployed to connect asynchronous systems. That said, a BTB can be embedded within a synchronous system to control power flow.

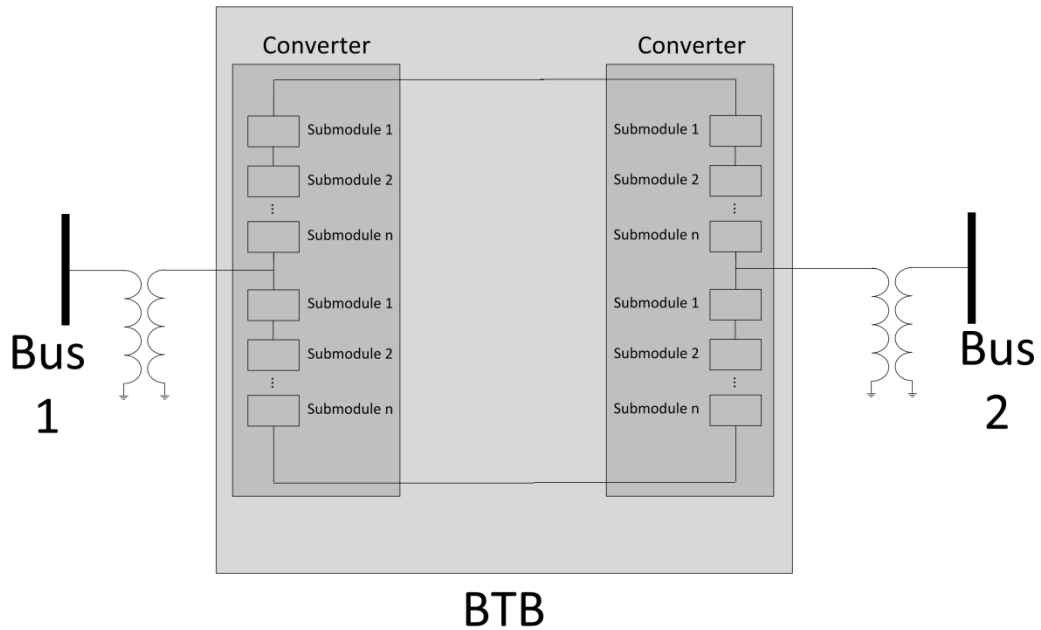


Figure 43: Back-to-back converter (BTB).

HVDC controllers have a number of disadvantages relative to other PF controllers. They are fully rated devices, so control of 1 MVA of power flow requires 2 MVA of control capability. This results in a high cost per unit of controlled power. In addition, HVDC controllers require cooling and other ancillary equipment which impact longevity and reliability.

2.7.5. Level of Power Flow Control in the Current Grid

The number and ratings of BTBs, HVDC systems, CSCs, PSTs, SSSCs, TCSCs, UPFCs, and VFTs in the American power system were estimated. The discussion is limited to PF controllers in which all terminals of the controller are in the same interconnection. All of the identified BTBs in the United States are used to interconnect asynchronous networks [185,186,187,188,189,190]. No evidence was found of deployed SSSCs. The results are taken as a lower bound on the number of deployed PF controllers.

Table 2 presents salient characteristics of the PF controllers in the United States, organized by controller type. TCSC ratings were identified in MVA and no evidence was found specifying the PF control capability of the TCSCs. Total rating of the aggregate fleet of PF controllers is 31.3 GVA which translates into less than +/- 31.3 GVA of controllable power flow as some controllers are listed by total rating not the amount of controllable flow. In comparison, total generation in the United States was 1,040 GW in 2010 [26]. Sources used to generate the table include [185,186,187, 191,192,193,194,195,196,197,198,199,200,201,202,203,204,205,206,207,208,209,210, 211,212,213,214,215].

Table 2: Details on power flow controllers deployed in the United States by type.

Controller Type	Max Interconnection Voltage (kV)	Max Power (MVA)	Number of Units Deployed	Aggregate Rating (MVA)
CSC		2x100	1	200
HVDC			8	10400
PST	345		72	20000
TCSC	500	unknown	9	unknown
UPFC	138	160	1	160
VFT			5	500
Total				31260

2.7.6. Modeling Power Flow Controllers

PF controllers are modeled in the power system at timescales ranging from microseconds to decades. The discussion below focuses on operational models for the PST, TCSC, and SSSC. These controllers are selected as they are the most studied controllers in the surveyed literature for use within a synchronous network over short to medium distances.

2.7.6.1. Power Flow Methods

Traditional PF methods have been modified to accommodate commercial PF controllers. Methods should exhibit strong convergence properties if large numbers of PF controllers are present in the system [125]. DC power flow is used in many commercial tools. However, DC power flow may not converge when used to solve the PF of a system with numerous PF flow controllers [216]. The most prevalent methods to integrate PF controllers in PF are the admittance method and the power injection method. Each method is discussed in brief.

The admittance method is an intuitive approach which modifies the admittance matrix to accommodate the PF controller [217]. For example, a TCSC can be modeled as a change in the line impedance [135,218]. This maintains the symmetry of the Jacobian. Modeling a PST is possible with the admittance matrix method but results in an asymmetric Jacobian [125,135,219]. An asymmetric Jacobian requires more memory and does not permit fast decoupled load flow.

The power injection method computes the real and reactive power injections necessary at the endpoints of the controller-equipped transmission line so that two requirements are met. First, the sum of the real power of the uncontrolled line and the injected real power match the power of a controlled line. Second, the sum of the reactive power of the uncontrolled line and the injected reactive power match the reactive power of a controlled line.

A PST modeled using the power injection method of a PST appears in Appendix A as Figure 82. Models using the power injection method exist for the PST

[122,135,217,218,219,220], TCSC [217,219] and SSSC [217,221]. The sensitivities of the injected real and reactive powers to the bus voltage magnitudes and angles are small for practical controller ratings [219]. Thus, the power injections may be designated as load or generation before each iteration and updated after the iteration based on the revised magnitudes and angles [219]. For this reason, the power injection method is sometimes referred to as the sequential method [125].

If the desired power flows are known, the methods above can be modified to solve for the set points required to realize the desired flow. The controller set points can be added as state variables [220,222,223]. Alternatively, a Newton relaxation method can be implemented within the PF solver [219].

2.7.6.2. Security-Constrained Optimal Power Flow Methods

Security-constrained optimal power flow (SCOPF) is used to minimize production cost while complying with security constraints. SCOPF can be divided into two types, preventive security-constrained optimal power flow (PSCOPF) and corrective security-constrained optimal power flow (CSCOPF) [224]. Both methods dispatch system elements to minimize production cost while complying with security requirements. PSCOPF dispatches the system assuming that post-contingency actions, such as changes to generator set-points, are infeasible. CSCOPF dispatches the system assuming that post-contingency actions are feasible but these actions must be within the bounds of equipment ratings. The CSCOPF typically leads to a lower production cost but is more computationally intensive. The system operator often requires completion of post-contingency actions within a set time of the contingency. The most common post contingency actions are changes to generator set points and startup of quick-start

generators, such as open-cycle gas turbines (OCGTs). The speed of PF controllers is sufficient to allow participation in post-contingency actions.

Without PF controllers, CSCOPF is typically solved with linear programming (LP) by decomposing the original problem into multiple linear problems [225].

CSCOPFs have also been solved directly with non-linear programming (NLP), but direct solutions may not be scalable to large systems. Using decomposition, the problem is broken down into a master problem (MP) and a series of similar sub-problems (SP). If DC power flow is used, the PF is solved within the MP or SP. If AC power flow is used, each MP and SP will iterate between the optimization problem and a PF solver. The master problem minimizes the production cost during secure operation while ensuring that constraints are met. Each sub-problem redispatches generation to ensure that the system is able to serve all load and meet constraints during a given contingency. A total of m sub-problems are run where m is the number of contingencies used to judge system security as defined by [3]. If a sub-problem is found to be infeasible, a constraint is added to the master problem to inform the steady-state generation dispatch. The master problem and sub-problems are iterated until all the subproblems are feasible or the iteration count exceeds a pre-defined limit. This process is shown in Figure 44.

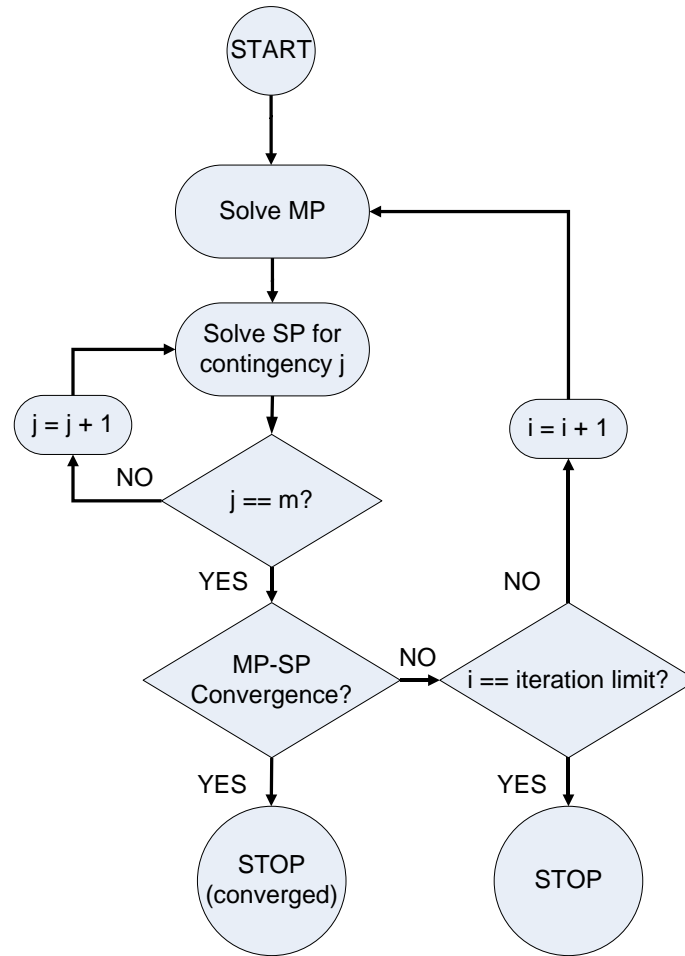


Figure 44: Flowchart for CSCOPF without PF controllers.

The PF methods require exogenous definition of the PF control set points. Therefore, a method is necessary to determine the optimal PF controller set points within the SCOPF. One approach is to further decompose the SCOPF. The first subproblem is commonly solved with a heuristic technique, such as evolutionary programming [218], a hybrid of tabu search and simulated annealing [135], or a genetic algorithm (GA) [131,135]. Another approach is to integrate the non-linear PF within the OPF solution and use a nonlinear solver [221].

2.8. Methods of Transmission Planning Optimization

Methods to optimize transmission planning have existed since at least the late 1950s [226,227,228]. The methods vary by objective, study horizon, the set of transmission expansion choices, and the solver type.

The optimal transmission planning problem is dominated by two major classes of objectives. The first class is the maximization of societal welfare, with societal welfare sometimes approximated as the negative of consumer cost. The second class of objectives is the maximization of system loadability. Some studies in the first class neglect transmission investment cost [121,134,137,229].

The study horizon may consist of a single period of transmission expansion [114,118,121,127,129,130,131,132,133,134,137,229] or multiple periods [230,231,232]. For studies with multiple periods, dynamic planning optimizes the timing of expansion across the periods [231,232] while pseudodynamic planning takes the expansion plan of the prior period as a given [216].

The choice set for expansion may be limited to transmission lines [230,231,232], a single controller type [129,132,133,134,217,229], multiple controller types [114,127,130,131,137], or either transmission lines or a controller [118]. No methods were identified which study the simultaneous planning of transmission lines and controllers.

Solvers may be categorized as mathematical, heuristic, and meta-heuristic [216].

Mathematical solvers, such as linear programming (LP), non-linear programming (NLP), mixed integer linear programming (MILP), and mixed integer non-linear programming (MINLP) guarantee optimality but are limited by a rapid increase in computational time

as a function of problem scale [130,134]. Heuristic solvers such as particle swarm optimization (PSO), genetic algorithm, simulated annealing (SA), and exponential evolutionary programming (EEP) accommodate non-linearities and integer variables well but do not guarantee global optimality [216,218]. Methods incorporating both mathematical and heuristic solvers are called meta-heuristic. Typically, a heuristic solver is used to select a candidate expansion plan and a mathematical solver is run to determine the viability of the candidate [114,118,127,129,131,132,133,137,218,229,230,231,232].

Table 18 of Appendix A presents the major characteristics of a sample of automated transmission expansion methods.

2.9. Operation and Regulation of Natural Gas Transportation Pipelines

Both the natural gas and petroleum pipeline networks are intermeshed and controllable. This discussion excludes the petroleum pipeline network for two reasons. First, natural gas pipeline transportation costs are three to five times the cost of petroleum pipeline transportation, on a per unit energy transported basis [233]. Second, natural gas pipelines became open access in the last 30 years while petroleum pipelines have been regulated as common carriers since the early 1900s.

2.9.1. Fundamentals of Planning and Operation of Natural Gas Pipelines

The majority of natural gas in the United States is sent from production to load centers via a controllable, intermeshed network of transportation pipelines. In the US, there are 300,000 miles of natural gas transportation pipelines distributed across the country as seen in Figure 45 [234]. The figure is sourced from [235]. To maintain velocity and pressure of the transport pipelines, compressor stations are deployed every

150-200 km [233]. The velocity of gas in a transportation pipeline is typically less than 15 m/s [236]. The expected lifetime of a pipeline is 25 years although assets are routinely operated longer than their expected life through active maintenance [236]. Pipeline owners utilize a centralized control center to monitor the transportation pipeline system and ensure delivery of contracted transactions [237]. Construction and operation of transportation pipelines exhibit economies of scale and scope. Scope economies result from the ability to store gas in pipelines via line packing and balance deviations between scheduled deliveries and scheduled withdrawals by aggregating across multiple transactions.

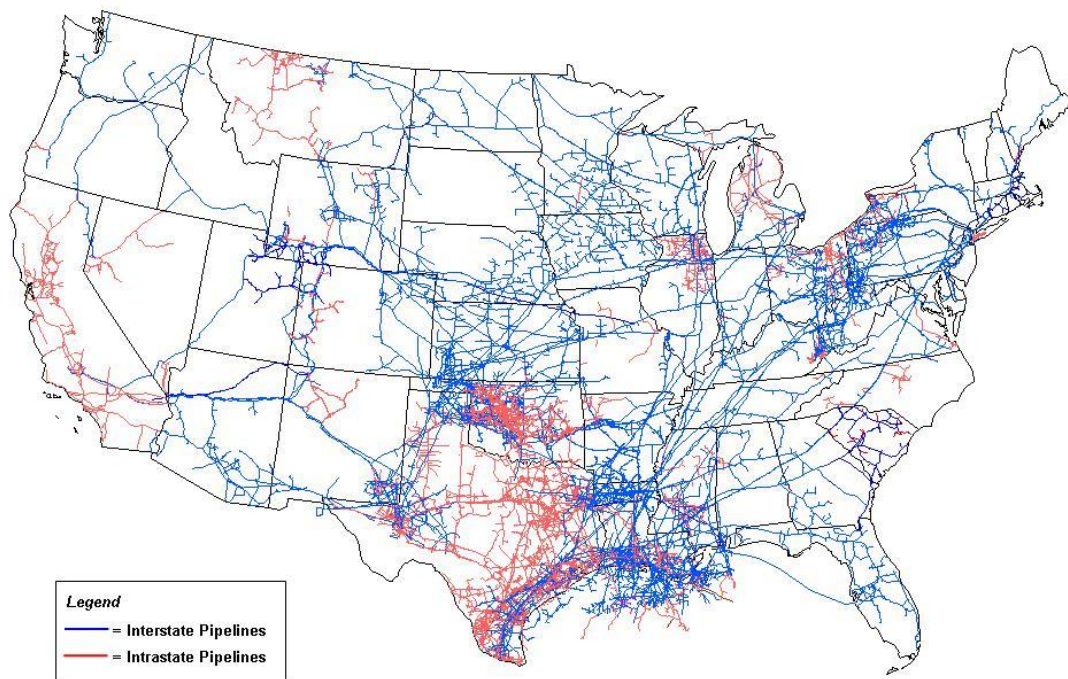


Figure 45: US natural gas transportation pipelines.

2.9.2. Natural Gas Regulation

Initially, town gas and natural gas were transported short distances as a result of limitations in pipeline technology. The first gas pipeline was built in 1872 and operated as a private carrier, meaning that the pipeline owner was able to discriminate who could and could not use the pipeline [238]. In the 1920s, improvements in pipeline technology enabled interstate natural gas transport [239]. Since a state PUC cannot grant monopoly rights to an interstate pipeline, pipelines underwent a period of vertical integration to ensure pipeline investments were viable [240].

Regulation of the natural gas sector began in the 1930s [241]. For more than four decades thereafter, pipeline companies purchased gas from suppliers, managed transport and storage of the gas, and sold gas to distribution companies and large customers [241]. The Federal Power Commission (FPC) and later FERC oversaw rates and new construction [240]. Deregulation of the natural gas sector began in the 1970s as natural gas prices spiked given FERC's inability to process new wellhead applications [241]. Order 636 mandated that pipelines operate as common carriers [242].

Since deregulation, natural gas transmission has adopted either a straight-fixed-variable (SFV) rate structure or a negotiated tariff [243]. Under SFV, firm delivery contracts pay the fixed-cost of the pipeline pro rata based on each contract's percentage of reserved pipeline capacity [240]. All contracts, interruptible and fixed, pay the variable costs of transportation [240]. Existing users are not charged for pipeline capacity additions unless transport costs will increase no more than five percent [244,245]. A natural gas pipeline owner may negotiate a tariff if the pipeline does not have market power and the potential user is given the option to choose a regulated rate

[243]. Long-term contracts have enabled the financing of a number of large, interstate pipelines without cost allocation controversies [244]. Table 3 provides a list of the large pipelines built between 2000 and 2005.

Table 3: Natural gas pipelines built between 2000 and 2005.

Line Length (miles)	Source State/Province	Destination State/Province	Diameter (inches)	Interstate
887	Saskatchewan	Illinois	36	Y
922	Wyoming	California	36	Y
264	Texas	Georgia	42	Y
1088	Texas	California	30	Y
405	New Mexico	California	16	Y
560	Mississippi	Florida	36, 30	Y
716	Wyoming	California	36	Y
253	Wyoming	North Dakota	16, 8	Y
380	Colorado	Kansas	36	Y
254	Texas	Texas	24	N

2.9.3. Relevance for Electricity Markets

While natural gas transportation is similar to electric transmission in many respects, the differences are illuminating. Electric power flows 20 million times faster than natural gas along a path that is largely uncontrollable. Thus, electric power transmission requires high levels of coordination and operating procedures that substitute product tracking for financial instruments. The lack of control impedes the owner of an electric transmission asset from charging based on usage. As a substitute for usage rates, investment costs in the electric transmission sector are largely socialized, cost allocation debates are common, and investment is slow.

2.10. Discussion

This chapter reviews the current state of the transmission system, the drivers for additional transmission capability, and the alternatives to further transmission investment. It describes some of the impediments to transmission investment. It overviews PF controllers and the methods used to simulate operation and planning of a power system equipped with PF controllers. Finally, it reviews the operation and regulation of natural gas pipelines. The aforementioned information will inform the remainder of the research.

CHAPTER 3

METHOD OF INCREMENTAL POWER FLOW CONTROL

3.1. Introduction

This chapter describes incremental power flow (IPF) control and provides an initial assessment of the feasibility and value of using IPF to increase transmission capability. As an incremental solution, IPF control may be used to supplement the power flows resulting from a traditional generator dispatch.

The chapter proceeds in four stages:

- 1) The concept of IPF control is explained.
- 2) The control effort required for IPF control is calculated for a test system.
- 3) The cost of complying with an RPS is computed under three planning scenarios, one of which includes IPF transactions.
- 4) The viability of controlling IPF controllers using hybrid centralized-localized control is assessed to avert the construction of a high-bandwidth, communication network.

3.2. Concept of Incremental Power Flow Control

IPF control is the transfer of an incremental quantity of power from a specified source bus to specified destination bus along a specified path without influencing power flows on circuits outside of the path. The earliest known proposal of the concept was in [246]. In contrast to PF control, which is used to optimize overall system operation or conduct bulk merchant transactions, IPF control may be used to conduct incremental, bilateral power transactions. IPF control is a subset of PF control. In IPF control, the PF controllers are arranged in a specific configuration and operated in a specific manner, as discussed below.

The transformational potential of controllable, merchant assets has been recognized by many luminaries in the fields of power system engineering, economics and public policy. Prof. William Hogan, Research Director of the Harvard Electricity Policy Group, writes:

“If the world were simple, market-based investments in transmission would provide a natural and self-evident approach to transmission expansion. Suppose that an electric transmission network consisted only of transmission lines and valves. In this case, the power would flow down the lines from source to sink, and the valves could make the system completely and continuously controllable in the sense that the actual path of power flows could be assured, no matter what the pattern of power inputs and outputs in the network. In principle, power flows could be

labeled, directed, and tracked. We could charge directly for the power flows on each line. If we did not want the power to flow down a particular line, the valve could be closed for those who did not pay. In this world, there would be no network externalities. The convenient contract-path model of electric power transmission would apply. The owner(s) of a line could charge for its use. In competitive equilibrium, the price of that usage would be equal to the differences in the prices of electricity at the source and sink. Equivalently, the owners of the line could buy at the source and sell at the sink, profiting from the difference in locational prices." [247]

IPF control enables incremental power transactions consistent with Dr. Hogan's vision. For example, consider a derivative of the 138 kV IEEE 39-bus system shown in Figure 46. Generator Six desires to send an incremental 20 MW to the destination bus along the transaction path highlighted in green. Without IPF control, a 20 MW incremental power output from Generator Six results in ten percent of the transmitted power reaching the desired bus. The inability to control flows prohibits transmission line owners from leveraging underutilized capacity in the vicinity of heavily loaded lines. Also, unlike the variety of discordant tracing methods discussed in Chapter Two, IPF control would allow the source, path, and final destination of transacted power to be observable. Parameters for the 138 kV system, as modeled in PSCAD, are shown in Appendix B.

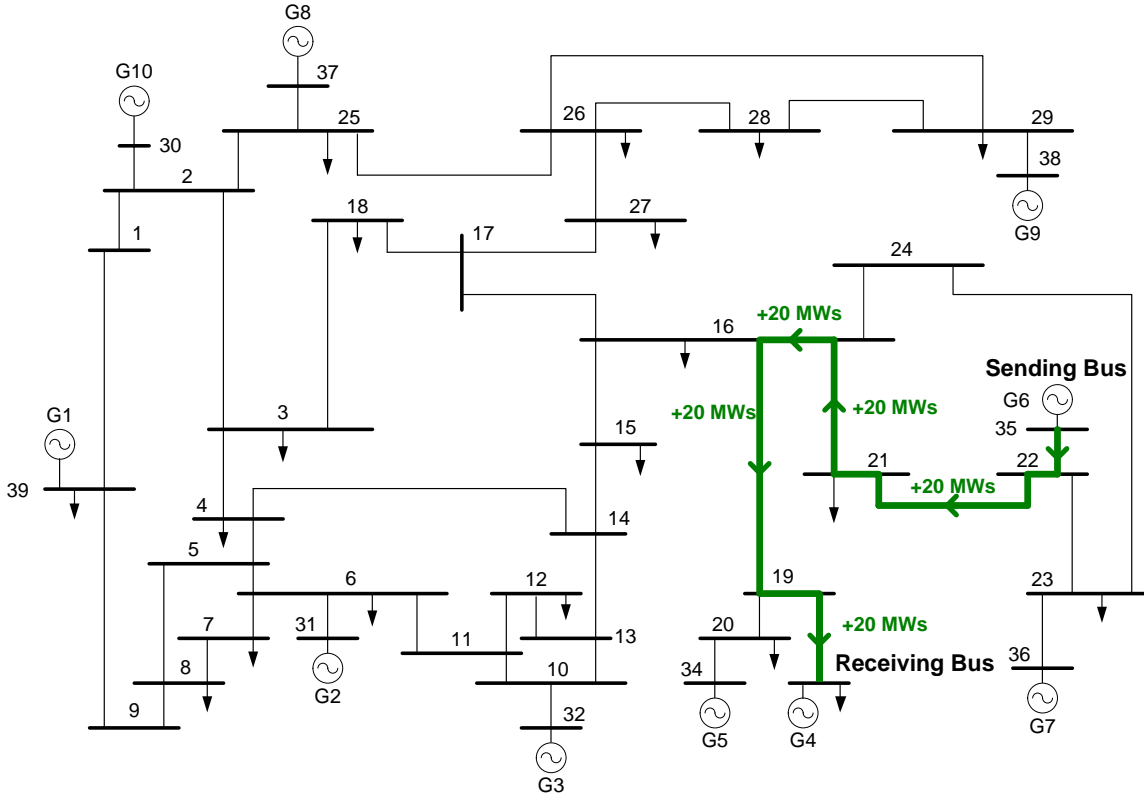


Figure 46: IEEE 39-bus system with desired incremental transaction shown in green.

A concept for realizing IPF control in a meshed network is presented in [246]. The concept perturbs the system state to reach the desired IPF transaction without changing the flows in other lines. Figure 47 shows a part of a meshed network, with the thick line representing the transaction path. If an incremental current is injected at the left end of the transaction path, the additional current ΔI results in a voltage ΔV generated across the line impedance. This in turn causes a change in the current of the adjacent circuits, Circuit One and Circuit Two. One method to ensure that the currents in the adjacent circuits are not perturbed is to inject series voltages in Circuit One and Circuit Two that exactly buck ΔV . It can be seen that ΔV corresponds only to the drop across the line impedance and is small compared to the line voltage. Controllable voltage sources

may be inserted at each circuit intersecting the path to control the current along a specific path.

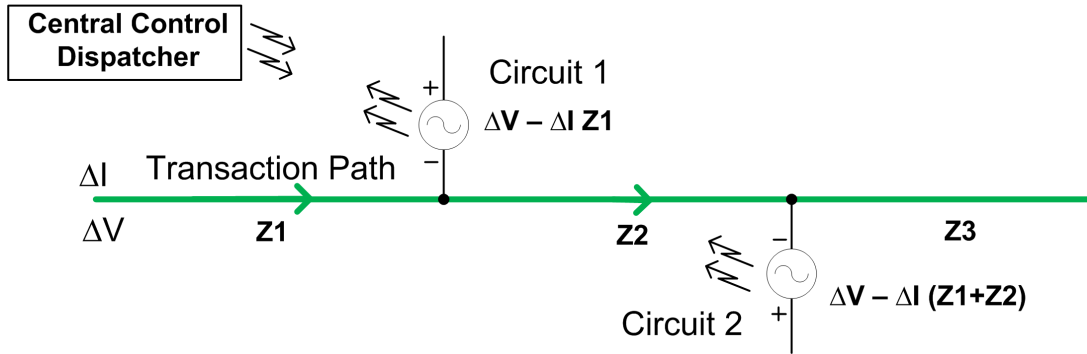


Figure 47: An overview of the method to realize IPF control along a transaction path without changing power flows on adjacent circuits.

To realize the 20 MW IPF transaction shown in Figure 46, a CNT is placed in series with each of the five transmission lines adjacent to the transaction path. The voltage injections required to realize the 20 MW incremental transaction are listed in Table 4. The injection for line 19-20 is not listed as the magnitude required is negligible. The pre-transaction currents of the lines requiring injection are shown in Table 5. CNTs are only required along the transaction path. Superposition can be applied to simultaneously achieve control across multiple paths in the network, even when several line segments are shared [246].

Table 4: Voltage injections required to realize the IPF transaction.

Line₂₂₋₂₃	Line₁₆₋₁₅	Line₁₆₋₁₇	Line₁₆₋₂₄
3.9 kV RMS at 89.8°	1.9 kV RMS at 88.6°	1.9 kV RMS at 88.6°	1.9 kV RMS at 88.6°

Table 5: Pre-transaction currents on lines adjacent to the IPF transaction.

Line₂₂₋₂₃	Line₁₅₋₁₆	Line₁₆₋₁₇	Line₁₆₋₂₄
46 A RMS	222 A RMS	307 A RMS	10 A RMS

3.3. Converter Rating Required for Incremental Power Flow Control

The converter rating required to realize the IPF transaction of Figure 46 is calculated in this section for two types of PF controllers - the BTB and the CNT.

3.3.1. Problem Setup

The converter ratings required to realize the incremental transfer are calculated for a CNT solution and a BTB solution. The BTB solution requires placing a BTB converter in series within each line of the transaction path. The BTB converters are rated to accommodate the entire line power.

The voltage injections required for IPF control are calculated before initiation of the transaction. Following the start of the transaction, the voltage injections are implemented so that the line power flow, P_t , approaches the sum of the pre-transaction flow, P_o , and the transaction flow, P_{trans} , via a decaying exponential as seen in (Eq. 4). In the equations, t_o is the start time of the transaction.

The efficacy of the solution is measured using the performance metric of (Eq. 5), which compares the controlled MW of the transaction, ΔP , to the MVA of converter rating required to realize the transaction, S_i .

$$P_t = P_o + (P_{tran} - P_o) \left(1 - e^{-\frac{(t-t_0)}{\tau}} \right) \quad (\text{Eq. 4})$$

$$M_i = \frac{\Delta P}{S_i} \quad (\text{Eq. 5})$$

3.3.2. Results

The required ratings of each BTB and CNT along the transaction path are shown in Figure 48 and Figure 49 respectively. The aggregate ratings and performance metrics are shown in Table 6, with the aggregate CNT rating nearly three orders of magnitude less than the BTB rating. If scalable to a real system, the CNT may provide IPF control at less cost than conventional PF control techniques.

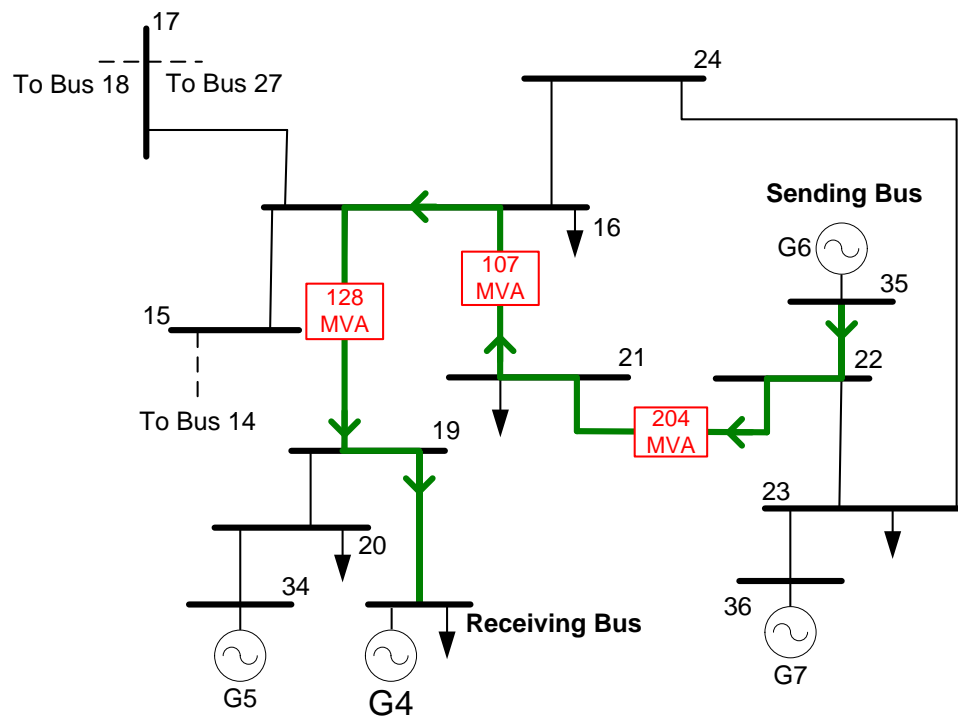


Figure 48: Locations and ratings of BTB converter to realize a 20 MW IPF transaction.

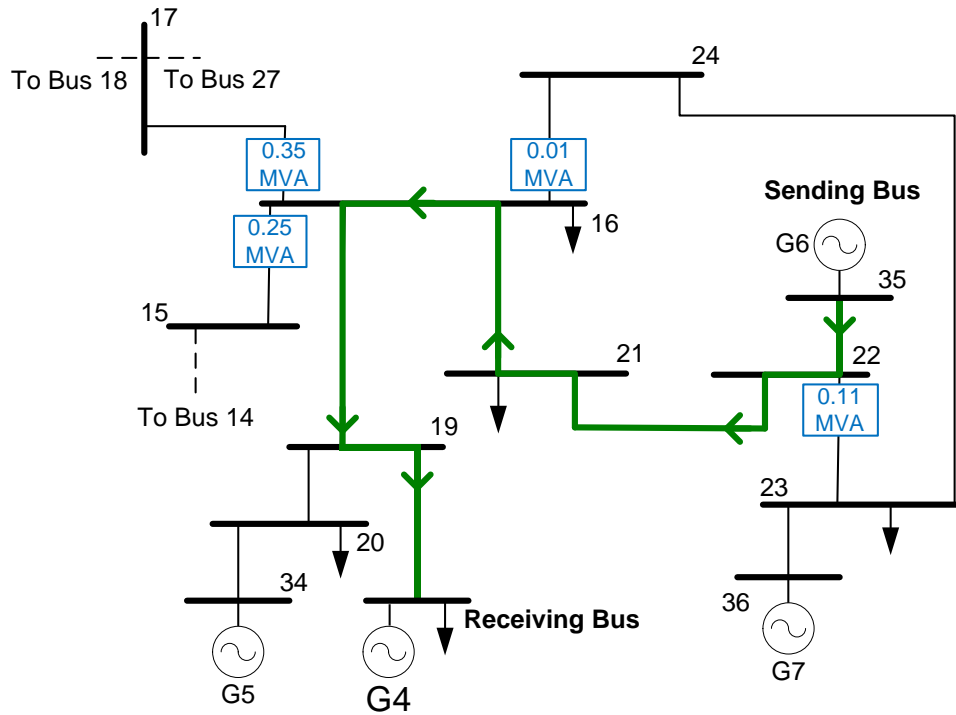


Figure 49: Locations and ratings of CNT converters to realize a 20 MW IPF transaction.

Table 6: Aggregate ratings and performance metrics.

Solution	Aggregate Rating of All Converters (MVA)	Performance Metric (MW controlled per controller MVA)
BTB	439	0.046
CNT	0.72	27.7

Figure 53 and Figure 54 show a sample of the generator power injections and line power flows before and after the initiation of the 20 MW IPF transaction. The transaction is initiated one second into the simulation. Power flows through some of the adjacent circuits deviate from their pre-transaction values during the transition. However, they return to pre-transaction values.

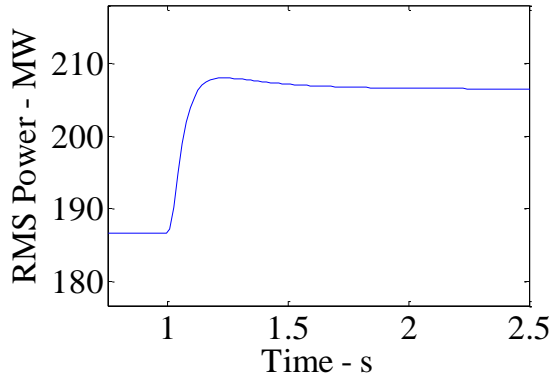


Figure 50: Generator Six output before and during the IPF transaction.

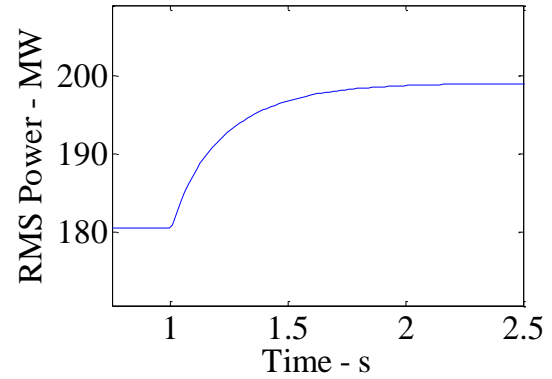


Figure 51: Power through Line₂₁₋₂₂ before and during the IPF transaction.

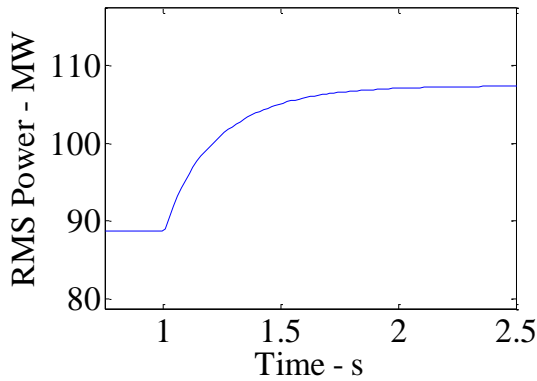


Figure 52: Power through Line₁₆₋₂₁ before and during the IPF transaction.

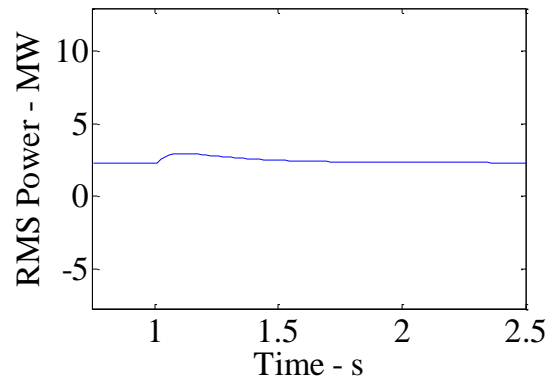


Figure 53: Power through Line₁₆₋₂₄ before and during the IPF transaction.

3.3.3. Discussion

In the above analysis, IPF control realized using fractionally-rated PF controllers has a lower aggregate rating than IPF realized using BTB converters. As discussed earlier, all of the known active merchant transmission investments in the United States use a PF controller rated to control the line power from $-P$ to P , where P is the rating of the transmission line. At first glance, the ability of a converter to control power from $-P$ to P may seem advantageous compared to the smaller control range of a CNT. However, the downside of the BTB is that a fully-rated converter is required even if only an IPF

transaction is desired. In contrast, the control range of the CNT is proportional to the converter rating, allowing the converter rating to be minimized when incremental control is required. Conceivably, a low-rated HVDC line or VFT could be placed in parallel with an AC line to provide vernier control but the economics may be unfavorable. Based on the study results, CNTs and FR-BTBs may achieve IPF control with a lower converter rating than a BTB, HVDC line, or VFT.

3.4. Impact of Power Flow Control and Incremental Power Flow Control on the Cost of RPS Compliance

3.4.1. Motivation

As discussed in Chapter Two, 29 states have enacted binding RPSs and eight states have enacted non-binding RPSs. In some states, the RPS can be met by purchasing renewable energy credits which do not require transmission capability between the renewable generation and the state [248]. When an RPS requirement cannot be met through renewable energy credits, it might be more economical to import renewable energy from a state with high quality renewable resources than generate the energy in-state. Thus, increased penetration of renewable generation may lead to increased inter-area power transactions. The inter-area tie-lines are often long and require substantial capital investment because of the location of the highest quality renewable resources.

3.4.2. Problem Setup

The IEEE 39 bus system is used to quantify the impact of IPF control on the cost of RPS compliance. For the RPS compliance study, loads and generator parameters differ from the IEEE 39 bus system. System parameters are presented in Appendix C. It

is assumed that the entire system is divided into four regions – the Northeast (NE) Region, the Northwest (NW) Region, the Southwest (SW) Region and the Southeast (SE) Region. The regions are broadly representative of the NYISO, MISO-central, SERC Reliability Corporation (SERC) and PJM regions respectively. Figure 54 shows the regional demarcations overlaying the IEEE 39-bus system. It is assumed that the system at Year Zero, the start of the planning horizon, sources one percent of annual energy from renewable generation and that the RPS requires that 20% of energy in Year 19 be sourced from renewable generation. The RPS is incremented by one percent each year between Year Zero and Year 19.

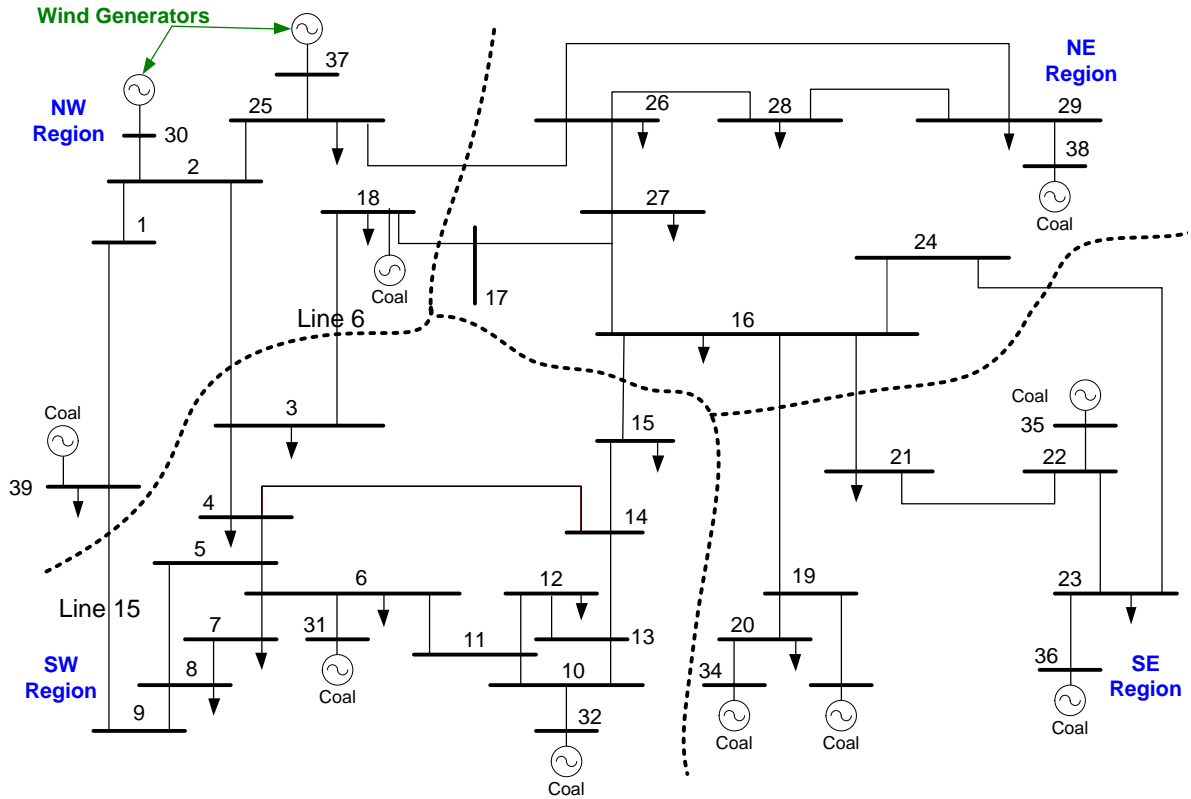


Figure 54: IEEE 39-bus system with regional demarcations.

A number of simplifying assumptions are made. Given that wind energy has been the largest source of intermittent renewable energy in the United States since 2005, wind generation is assumed the sole source of renewable energy for the entire system [249]. All wind energy for the four regions is sourced from the NW Region. The planning process is assumed to have perfect foresight of load and wind production, meaning that transmission investments can be initiated with certainty to overcome future constraints. Therefore, there is no difference between the results of the planning and operational stages.

It is assumed that the Bus 30 and Bus 37 are wind generators, while all other generators in the system use fossil fuels. The inter-area tie-lines are the lines intersected

by the black dotted lines in Figure 54. The study assumes inter-area tie-lines are much longer than the intra-area lines. The study also assumes that upgrading inter-area tie-lines is much more expensive than upgrading intra-area lines. Therefore, intra-area line investment is neglected by assigning infinite capacity to these lines at the start of the planning horizon.

The wind generators and the load buses are assigned diurnal profiles of varying potential wind production and load respectively. Operation over the year is modeled by six time steps of a single day. Since the study is aimed at transmission planning, the worst case day (highest load, lowest wind generation) is chosen as the representative day of the year. The diurnal load profiles are based on the load variations of PJM, NYISO, MISO-central and SERC. The study assumes the NE Region follows the NYISO load profile, the NW Region follows the MISO-central profile, the SW Region follows the SERC profile and the SE Region follows the PJM profile. To generalize the solution, the two wind generators have different potential production profiles. Diurnal wind potential production profiles were sourced from EWITS [250]. The generator at Bus 30 is assigned the diurnal profile of a typical SPP wind plant and the generator at Bus 37 is assigned the profile of a typical MISO-West plant. Figure 55 shows the resulting wind and load profiles [251].

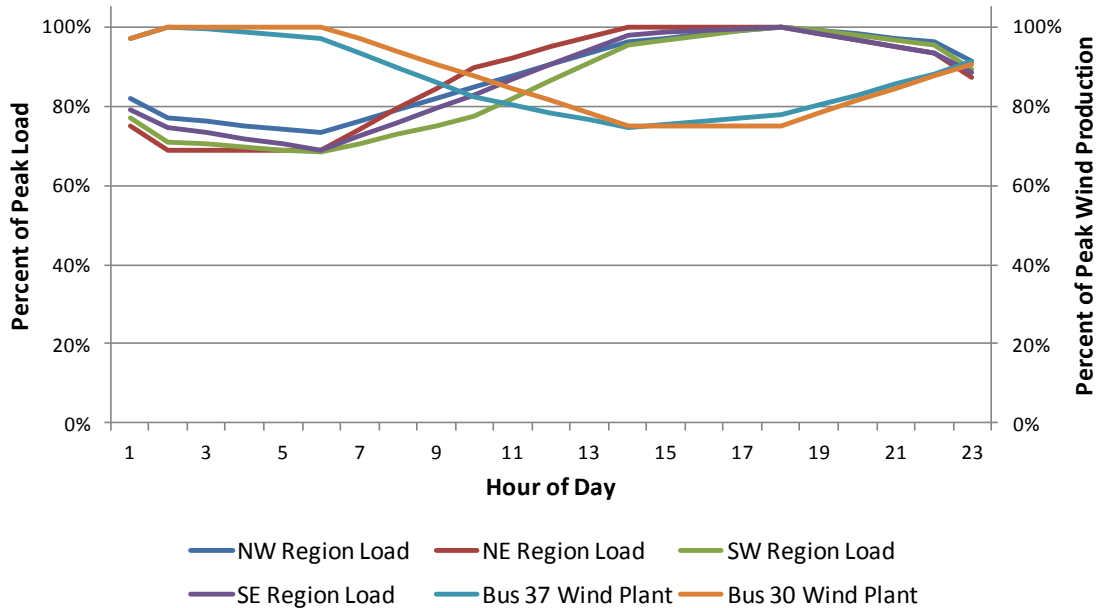


Figure 55: Diurnal variation of loads and wind potential production.

The assumed initial peak system load for Year 0 is 4,880 MW. The distribution of load across the buses is heterogeneous. Load at each bus during each time period increases exponentially at an annual rate of two percent. The average wind capacity factor is 43% while a safety factor of five percent is applied when determining the total wind peak generation capacity. The safety factor is the percentage by which the wind plant capacity is overbuilt to take into account elements which may reduce the energy output of the wind plant, such as failure of the wind plant collector system or turbine unavailability.

Sufficient wind generation is built to satisfy the RPS during each time period of the representative day. For example, in Year 5 when the RPS requires the renewable energy to be six percent of the load, total wind generation capacity is sized so at least six percent of the load during each of the time steps is supplied by the wind generators. As

the typical RPS is enforced annually, an hourly RPS results in more renewable generation than a typical RPS.

For this study, since intra-area transmission line investment is assumed to be negligible, no intra-area congestion is present during any of the time periods. The initial ratings of the inter-area tie-lines are selected to approximate the distribution of historical tie-line loadings. Lines 20, 29 and 30 are rated so they operate at 95% of their rated value during the peak load period of Year Zero. The other tie-lines, namely lines 3, 6, 15, 22, 23 and 25, are rated so they are loaded at 50% of their thermal rating during the peak load period.

The study assumes that all of the wind potential generation at a particular time-step must be delivered in order for the wind plants to meet revenue requirements. If the planning study predicts curtailment will occur during a future year, an investment is made so the curtailment is eliminated in the operational timeframe. The investments are manually selected. MATPOWER, a MATLAB-based OPF software, is used for the simulation.

Three transmission planning cases are considered to avoid curtailment of wind generation.

- Business as Usual (BAU): The utility may build a line of the same rating parallel to an existing constrained line.
- IPF control: The utility may use existing IPF controllers to route power around the constraint, deploy new IPF controllers, or build a line of the same rating

parallel to an existing constrained line. The transmission investment cost includes the cost of line construction as well as the cost of IPF controllers.

- DSR: The utility may use existing DSRs to avoid line congestion, deploy new DSRs, or build a line of the same rating parallel to an existing constrained line. The transmission investment takes into account both the line construction as well as the installation of DSRs.

The simulation algorithm is summarized in the flowchart shown in Figure 56.

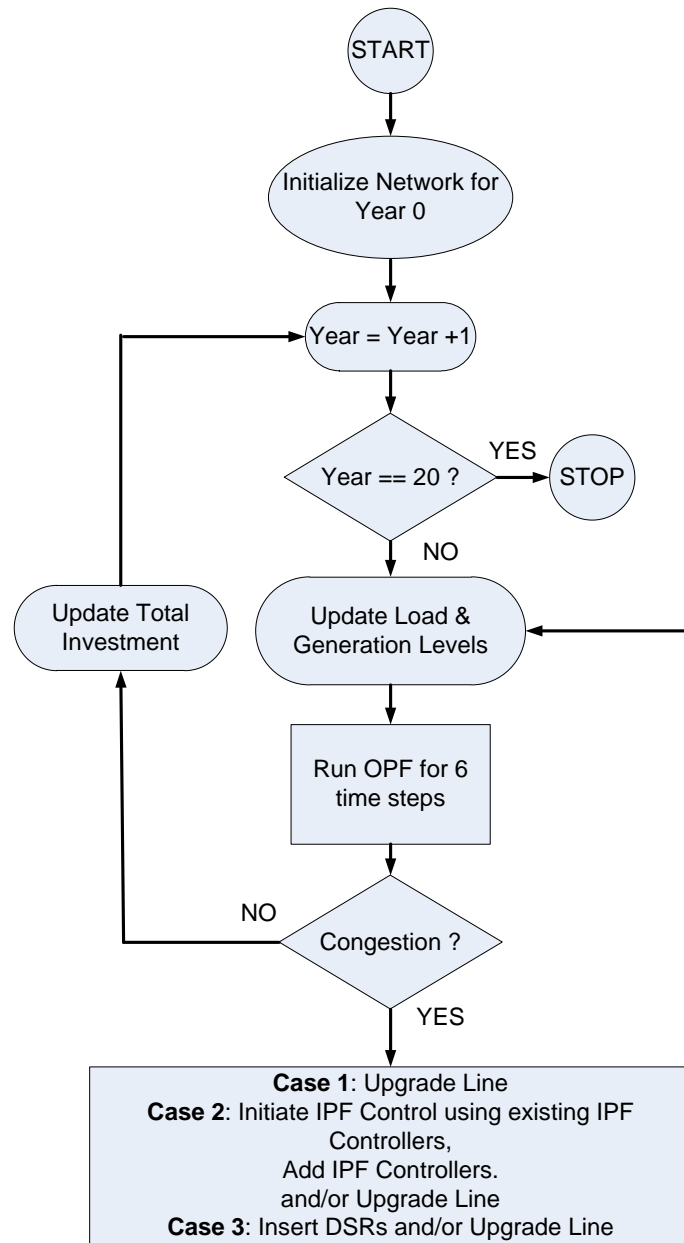


Figure 56: Flowchart for simulation methodology.

For the IPF control case, the OPF of each time-step is first solved in MATPOWER. For time-steps with curtailed wind production, IPF controllers are used to reroute power. A MATLAB function calculates the necessary IPF controller settings and updates the power flows. If existing IPF controllers are unable to eliminate the

curtailment of wind generation, additional IPF controllers are added to use alternative routes. Once IPF control is exhausted, a transmission line is added in parallel with the constrained line.

3.4.3. Results

3.4.3.1. BAU Results

For the BAU case, all regions are assumed to operate under a single OPF and PF controllers are not deployable. Therefore, the only possible method of increasing the network throughput from the NW region to the other regions is to build new tie-lines in parallel with the existing tie-lines. Figure 83 in Appendix D shows the various line upgrades that are required by the system to comply with the RPS under the BAU case. Table 26 in Appendix D shows the transmission investments as a function of time. The total required investment is 186,000 MW-miles.

3.4.3.2. DSR Results

For the DSR case, the upgrades include installation of DSRs as well as adding tie-lines. The cost of one MVA of DSRs is assumed equivalent to 100 MW-miles of transmission line, based on a cost of \$1,000 per MW-mile for transmission an estimated DSR cost of \$100 per kVA [252]. Figure 84 of Appendix D shows the tie-line upgrades required to meet the RPS with DSRs and new lines. Table 27 of Appendix D shows the transmission investments as a function of time. The total investment cost is 90,700 MW-miles, of which 64,100 MW-miles is new transmission line construction.

3.4.3.3. IPF Control Results

For the IPF control case, the potential upgrades include installation of IPF controllers to realize IPF transactions as well as the construction of new tie-lines. IPF control can be realized using series of shunt-series controllers [253]. It is estimated that the cost of one MVA of series voltage compensation is equivalent to the cost of 100 MW-miles, based on a MW-miles cost of \$1,000 and an estimated series voltage compensation cost of \$100 per kVA [148]. Figure 85 of Appendix D shows the tie-line upgrades required to meet the RPS with IPF control.

In the IPF control case, it is possible to utilize the capacity of under-loaded lines to postpone line upgrades. At times, multiple transaction paths are in operation. For example in Year Six, there are five simultaneous IPF transactions, one of which is shown in Figure 86 of Appendix D. The total investment cost to realize these IPF transactions is calculated by determining the total rating of IPF controllers required and then converting to MW-miles.

Table 28 of Appendix D shows the transmission investments as a function of time for the IPF case. Most of the expenditure in the IPF control case is for IPF controllers. The total investment cost incurred is 107,300 MW-miles, of which 36,500 MW-miles is new line construction.

3.4.3.4. Comparison across Cases

The DSR and IPF control cases offer an appreciable reduction in short-term and overall investment compared to the BAU case. Short-term savings result from the deferral of transmission line upgrades. If the investments are not discounted, the total

transmission investment required in the DSR and IPF control cases are 50% and 60% respectively of the BAU case. In addition, transmission line construction for the DSR and IPF control cases is reduced by 66% and 80% respectively compared to the BAU case. If the investments are converted to PV using a ten percent discount rate, the savings of the DSR and IPF cases relative to the BAU case increase. For example, the DSR case demonstrates a 51% reduction in nominal investment compared to BAU but a 58% reduction in PV investment compared to BAU. Figure 87 and Figure 88 of Appendix D show the cumulative transmission investments of the cases for the non-discounted and discounted scenarios respectively.

Table 7: Comparison of total investments.

	Nominal Investment (GW-miles)	Nominal Savings Relative to BAU	Investment PV (GW-miles)	PV Savings Relative to BAU
BAU	186.0		61.6	
DSR	90.7	51%	25.9	58%
IPF Control	107.3	42%	32.7	47%

In the test cases, DSR and IPF control enable the deferral of new line transmission construction. The analysis neglects the lead time required to build a new transmission line. In practice, the lead time for a new line is five to ten years. Given that utilities are required to meet reliability standards, uncertainty may lead to overrating of new transmission lines. Deploying DSRs or IPF controllers on existing lines is expected to require a shorter lead time than constructing a new line. The shorter lead time of DSR and IPF controller installation may allow deployment decisions to be made with more certainty, increasing capital efficiency.

3.4.3.5. Discussion

The analysis suffers from a number of limitations, namely:

- Renewable generation is not currently operated as a firm resource and areas with RPSs experience curtailment.
- The investment decisions were made manually and are non-optimal.
- The system was not subject to $n-1$ reliability requirements.
- The system used in the analysis is simplistic.

Despite the limitations of the proceeding analysis, the preliminary results support a conditional conclusion that IPF control can reduce the cost of RPS compliance. RPS compliance with remote generation is similar to wheeling low-cost power from conventional generators to load centers. Therefore, the above results also suggest that IPF control may be used to increase the transmission capability between low-cost generation and load centers.

3.5. Viability of Realizing Incremental Power Flow Control using a Hybrid Centralized-Localized Control Scheme

3.5.1. Motivation

As discussed in Chapter Two, PSTs are the most common type of PF controller used today. The reference power of a PST can be changed every few minutes via a command from the control center. However, as discussed earlier, there is no evidence that PSTs can support frequent switching without maintenance. Between commands, the typical PST controller regulates tap settings to maintain the PF of the prior command using local information. This represents a hybrid control strategy, utilizing a slower

control loop relying on communications with the control center and a faster loop using local information. The PST can be configured so the local controller maintains the tap settings that were in place prior to the loss of communication. With fixed taps, the PST is a passive asset and does not attempt to force a set power flow.

Realizing IPF control with a power electronic converter would allow a much faster response than a PST. However, the communication infrastructure required to realize centralized, reliable, and sub-cycle control of IPF transactions may deter the ubiquitous adoption of IPF control. In addition, reliance on centralized control may jeopardize system stability should communications fail. For example, stability could be compromised if during a communication outage the IPF controller attempts to maintain the prior real and reactive power set points but the load, generation, or topology has changed. Stability may be easier to demonstrate if during a communication outage the controller appears to be a passive element similar to a PST with fixed taps. The work below explores whether IPF control realized using power electronics controllers can be controlled using a hybrid centralized-localized control scheme similar to the PST.

3.5.2. Problem Setup

The four-bus, 79 kV system shown in Figure 57 is selected to study hybrid control of IPF transactions. This system is selected to capture the dynamics of meshed systems with minimal complexity. The CNT is selected to realize the IPF control, with each CNT modeled as a series voltage source and shunt current source as shown in Figure 58. The CNT have a tap ratio of ± 0.3 . The power transmitted through a CNT-equipped line is dependent on line terminal voltages, line impedance, the angle difference between the line terminals, and the CNT set points (K_0 , K_2 , and Φ).

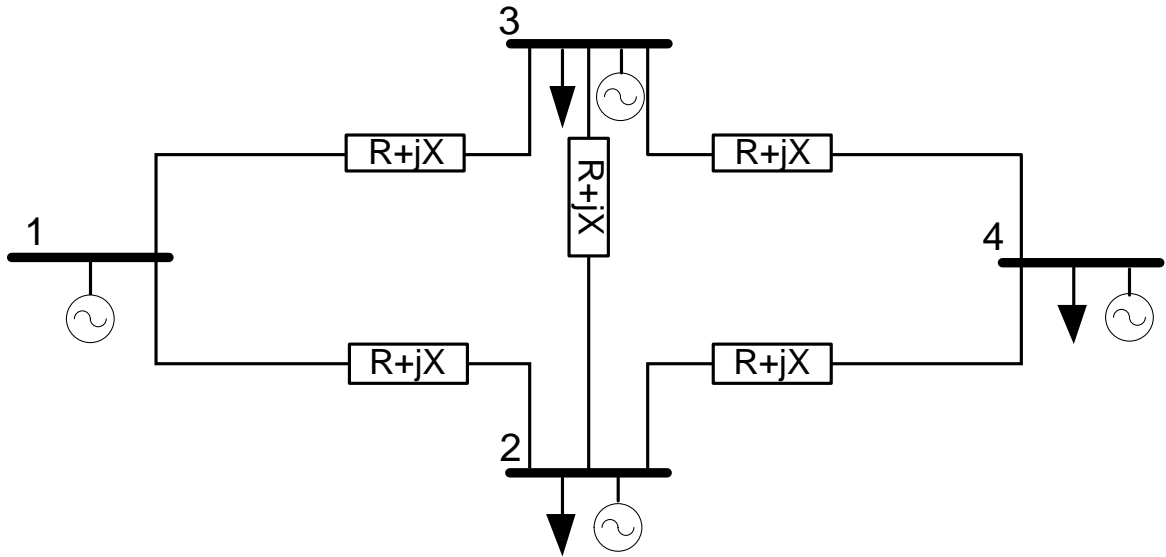


Figure 57: Four-bus system for study of centralized-localized IPF control.

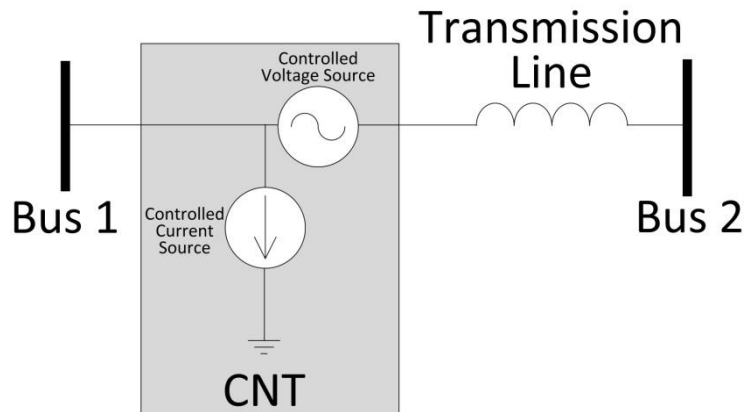


Figure 58: CNT model using voltage and current sources.

Hybrid centralized-localized control of IPF transactions is realized in a two-step process. First, the power dispatch commands to produce the desired incremental transaction(s) are computed for the entire system by a central controller. The power dispatch commands are sent to the CNTs participating in the transaction(s). Second, each participating CNT determines the set points necessary, using local information, to realize

the power dispatch command. Local information is defined as the voltage phasors of the line terminals to which the CNT-equipped line is connected.

Systems with multiple, locally controlled PF controllers have been shown to remain stable if the local controllers utilize decaying exponential control [254,255]. For this simulation, decaying exponential control is used to move each CNT towards the desired transaction power, $P_{command}$, as seen in (Eq. 6). At a given time t , the CNT controller attempts to realize a power level $P_{ref,t}$ closer to $P_{command}$ than at the prior time, $t-1$.

$$P_{ref,t} = P_{t_0} + (P_{command} - P_{t_0}) \left(1 - e^{-\frac{(t-t_0)}{\tau}} \right) \quad \text{(Eq. 6)}$$

If only real power flow control is required and the angle required to realize the commanded power is small, PF can be controlled by changing the angle between the buses. In this case, reactive power flows during the transaction can match the pre-transaction flows by equalizing the transaction and pre-transaction terminal voltage magnitudes. Under this condition, control reduces to solving for the angle, δ_{ref} , necessary to realize the applicable $P_{ref,t}$ as shown in (Eq. 7). Based on this equation, the required d-axis and q-axis voltage injections, relative to the bus voltage to which the CNT is connected (V_j), are calculated as per (Eq. 8) and (Eq. 9). The K_0 and K_2 values corresponding to the d-axis and q-axis voltage injections are solved with (Eq. 10) and (Eq. 11), contingent upon the limits shown (Eq. 12) and (Eq. 13). The parameter Φ is set to zero at all times to simplify the control although maximum control of real power flow may require non-zero values for Φ .

If the power dispatch command changes, the decaying exponential is reset by setting t_o to the current time. The parameter refresh rate, shown in Table 8, defines how frequently the CNT parameters are updated and τ determines the rate of decay of the exponential. If communications with the central controller are lost, the local controller maintains the last calculated K_0 , K_2 , and Φ values. The connection of the local controller to the CNT and neighboring buses is shown in Figure 59.

$$\delta_{ref} = \sin^{-1} \left(\frac{P_{ref} X}{|V_1| |V_2|} \right) \quad (\text{Eq. 7})$$

$$V_d = |V_2| - |V_1| \quad (\text{Eq. 8})$$

$$V_q = |V_2| \tan(\delta_{ref}) \quad (\text{Eq. 9})$$

$$K_0 = \frac{|V_2| - |V_1|}{2|V_1|n} + 0.5 \quad (\text{Eq. 10})$$

$$K_2 = \frac{V_d}{|V_1|n} \quad (\text{Eq. 11})$$

$$0 \leq K_0 \leq 1 \quad (\text{Eq. 12})$$

$$|K_2| \leq K_0 \text{ and } |K_2| \leq 1 - K_0 \quad (\text{Eq. 13})$$

Table 8: CNT local controller parameters.

Parameter	Value
τ	4 sec
Parameter refresh rate	3 Hz

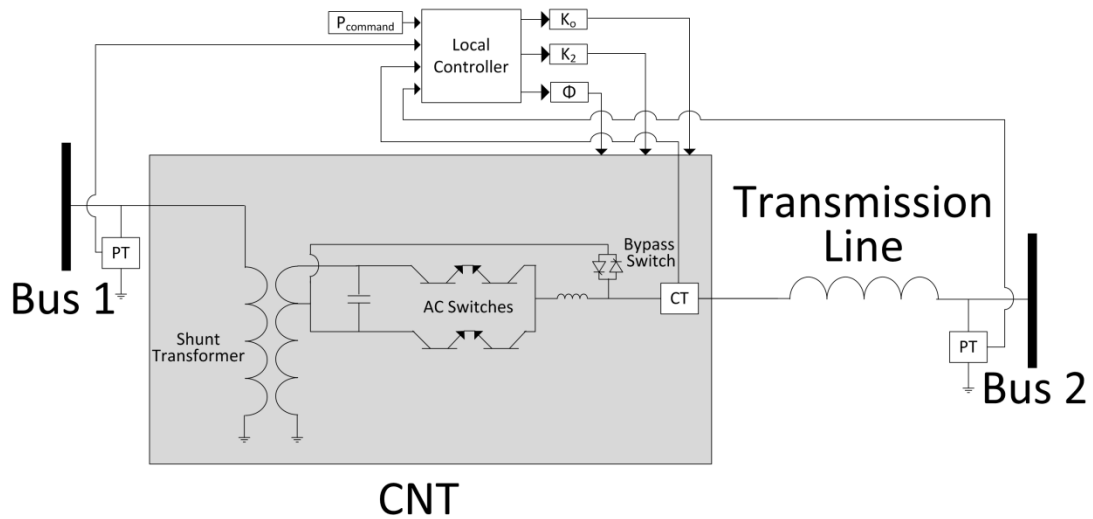


Figure 59: CNT and local controller embedded in a transmission line.

To simulate an IPF transaction, the CNT power dispatch commands were coordinated to direct power from a source bus to a destination bus via a specified path. In coordination with the transaction, a constant power load was switched in at the destination bus to absorb the incremental power. Two simulated IPF transactions are shown in Figure 60, with both transactions occurring on the same path. The first transaction is initiated four seconds into the simulation and intends to increase the power along the path by ten MW. Twenty seconds after the initiation of the first transaction, the second transaction intends to increase PF along the path by another ten MW.

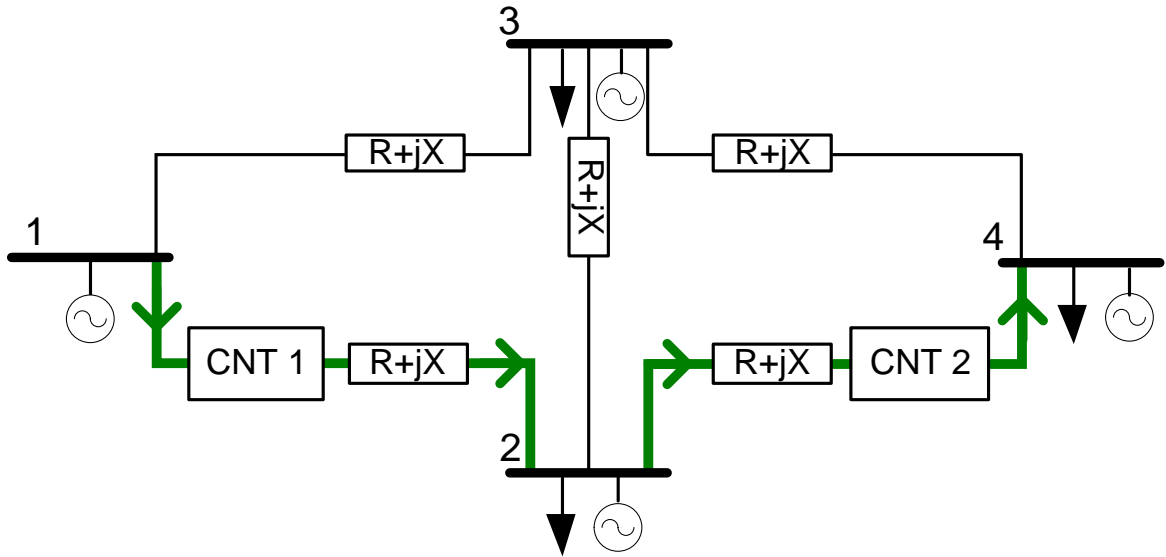


Figure 60: Test-system with CNTs installed to execute transactions along one path.

3.5.3. Results

The line flows for lines along the transaction path are presented in Figure 61 and Figure 62. As desired, flows along the transaction path increase following the decaying exponential profile in accordance with the two ten MW transactions. Flows along non-transaction paths, as seen in Figure 63 through Figure 65, are unchanged. Figure 66 through Figure 69 show the power supplied by the four generators. Generator Two experiences power deviations during the onset of each transaction before returning to pre-transaction levels. This is a consequence of modeling the incremental load as a discrete load rather than a decaying-exponential load. For each transaction, Generator Four settles to a final value 0.5 MW higher than the pre-transaction level, an indication of the non-ideality of the approach. Figure 70 and Figure 71 show the operation of the local controllers of CNT One and CNT Two respectively.

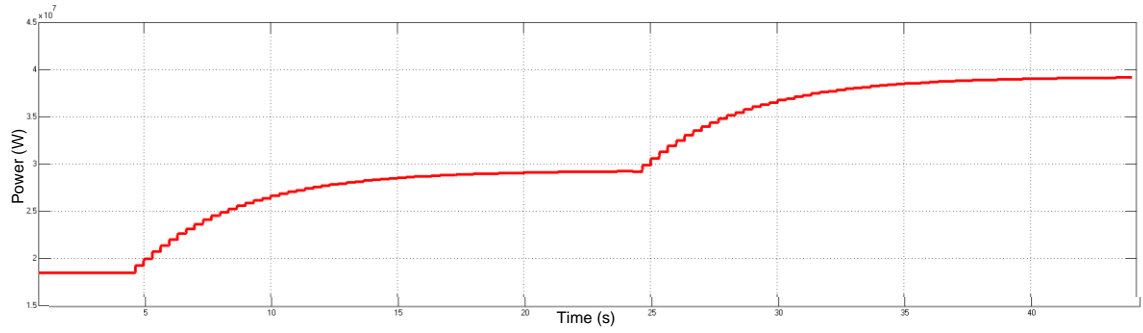


Figure 61: Power flow through Line₁₋₂ of the IPF transaction path.

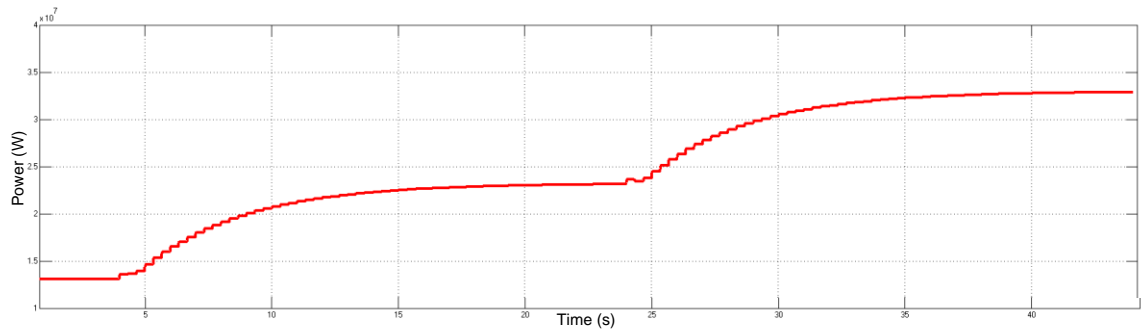


Figure 62: Power flow through Line₂₋₄ of the IPF transaction path.

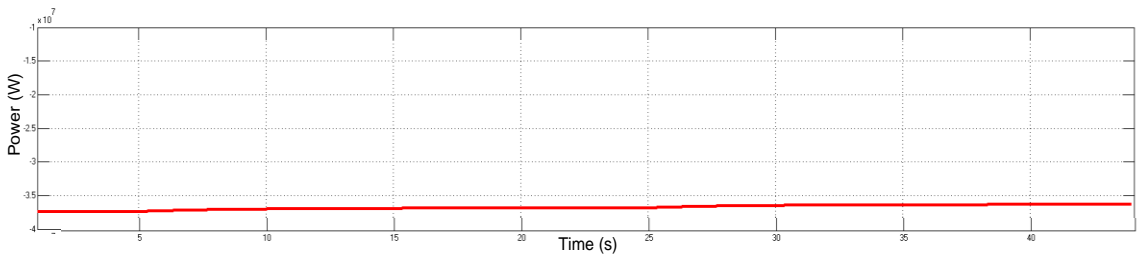


Figure 63: Power flow through Line₃₋₁, which is not part of the IPF transaction path.

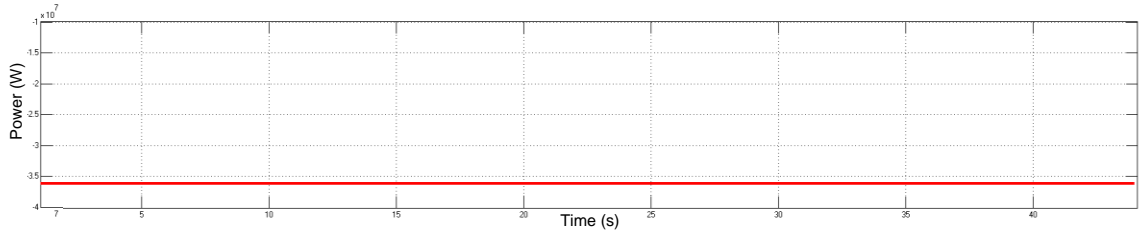


Figure 64: Power flow through Line₃₋₂, which is not part of the IPF transaction path.

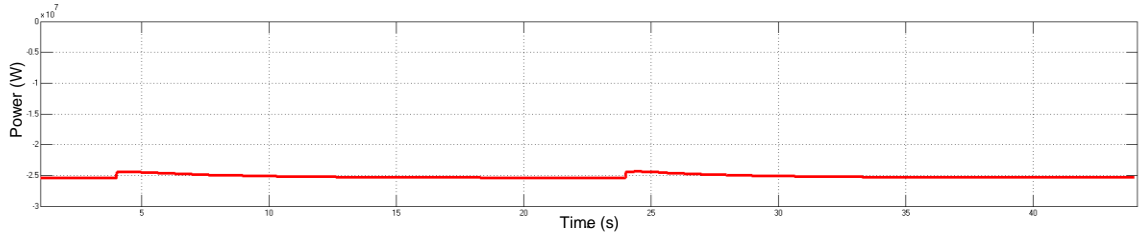


Figure 65: Power flow through Line₃₋₄, which is not part of the IPF transaction path.

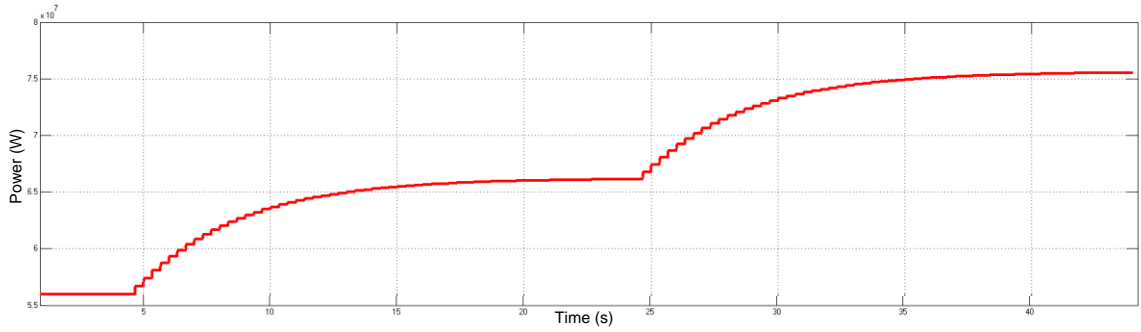


Figure 66: Power supplied by Generator One.

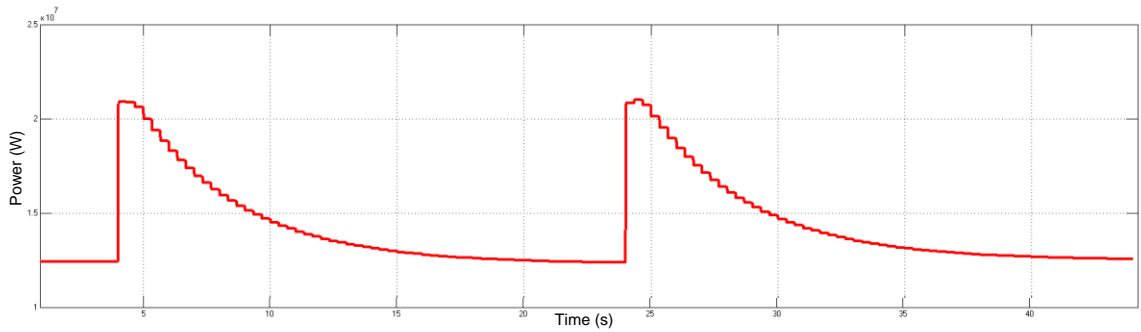


Figure 67: Power supplied by Generator Two.

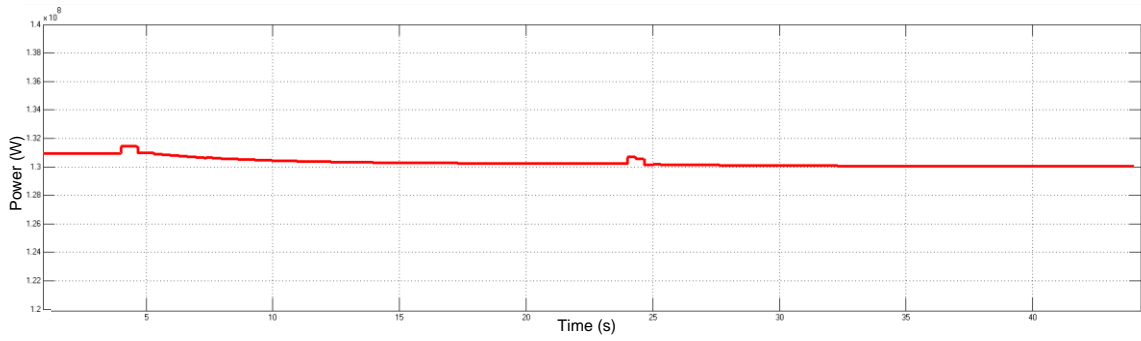


Figure 68: Power supplied by Generator Three.

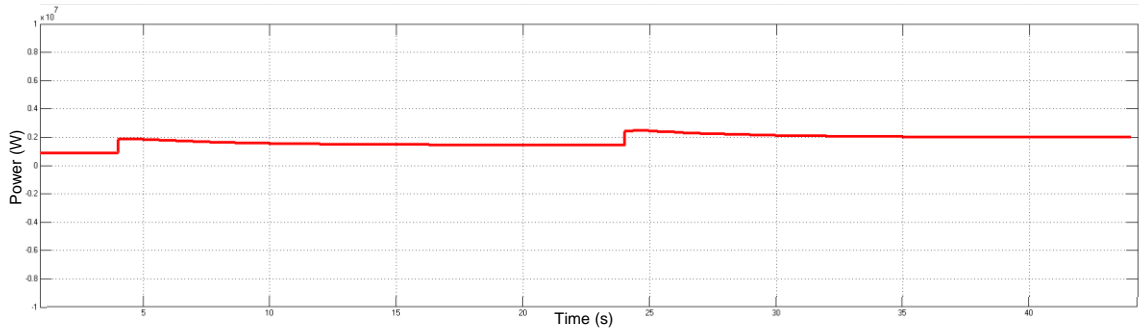


Figure 69: Power supplied by Generator Four.

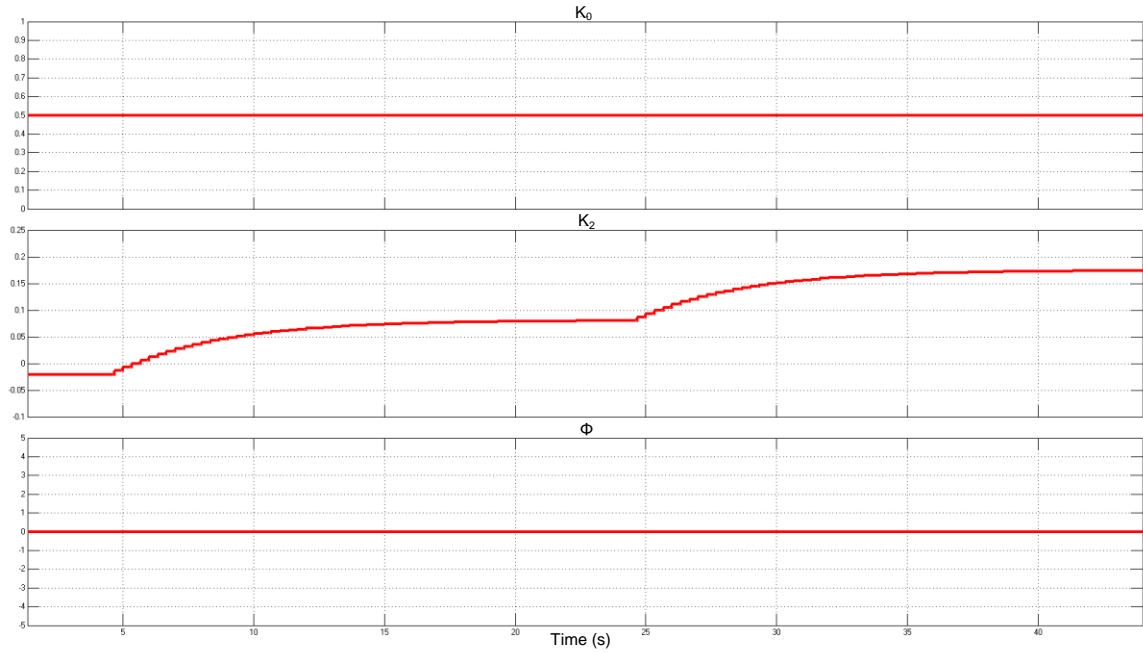


Figure 70: Variation of the set points of CNT One.

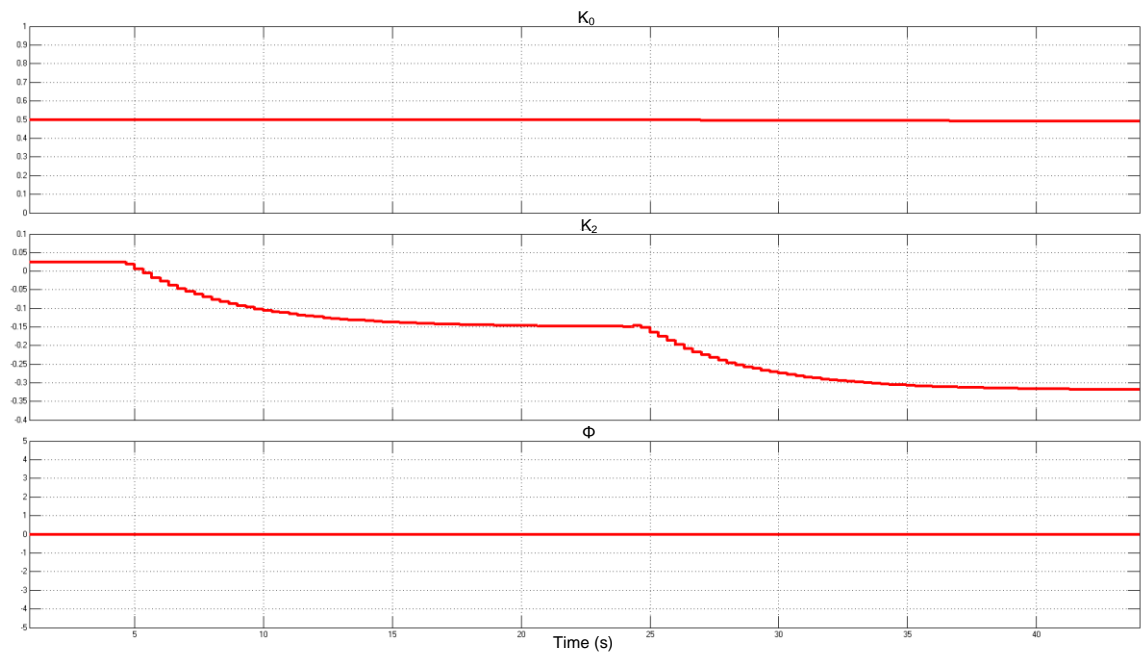


Figure 71: Variation of the set points of CNT Two.

3.5.4. Discussion

Initial results indicate that IPF control is feasible in meshed systems using a hybrid centralized-localized control, avoiding the need for high bandwidth communication between the PF controllers and the control center. If demonstrable at scale, this would decrease the burden of adopting IPF control. Also, this may increase the robustness of IPF control to communication outages.

The demonstrated control method requires measurement of time-synchronized voltage phasors at the terminals of the CNT-equipped line. Low-cost synchrophasors may be an enabling technology for IPF control. In this analysis, terminal phasors were sampled 3 times per second. The sampling frequency may be low enough to transmit the phasor measurements via existing inter-terminal communication equipment used to coordinate line protection.

3.6. Discussion

This chapter overviews the previously proposed concept of *incremental power flow*. It also shows, via preliminary research, that IPF control may be a feasible, low-cost mechanism to increase transmission capability. The preliminary findings, applicable to small test-systems under specific conditions, are as follows:

- Fractionally-rated PF controllers provide incremental control at a lower aggregate rating than traditional solutions such as an HVDC line or BTB.
- IPF control is a lower cost solution than new line construction to meet an RPS.

- A hybrid control scheme using central and local control enables a fleet of distributed IPF controllers to realize IPF transactions without high bandwidth communication between the controllers and the control center.

CHAPTER 4

CORRECTIVE SECURITY-CONSTRAINED OPTIMAL POWER FLOW WITH POWER FLOW CONTROL AND INCREMENTAL POWER FLOW CONTROL

4.1. Introduction

As discussed in Chapter Two, including PF controllers in the SCOPF may reduce the power system production cost. These benefits may increase if the PF controllers may participate in post-contingency actions and the system is dispatched with a CSCOPF that selects generator and PF controller set points. Despite the economic advantages of incorporating PF control into CSCOPF, none of the known CSCOPF tools are compatible with multiple PF controller types. The bulk of the chapter describes a CSCOPF method compatible with PF control and IPF control, development of a CSCOPF tool compatible with PF control, and demonstration of the tool.

The final section of the chapter proposes a revised version of *packetized energy*, called *incremental packetized energy*. *Incremental packetized energy* is expected to exhibit some of the benefits of *packetized energy* but at lower cost. The CSCOPF tool is used to demonstrate the benefits of *incremental packetized energy*.

4.2. CSCOPF Method

A CSCOPF method compatible with PF controllers requires:

- A model for power flows through a circuit equipped with each considered PF controller, and
- A method to simultaneously dispatch generator and PF controller set points.

This section will first describe development of the PF models and proposed method.

4.2.1. Power Flow Equations for Circuits with Power Flow Controllers

As discussed in Chapter Two, there are at least three methods to calculate power flows for a system with PF controllers. The first two methods are based on AC power flow. The first method adds the PF controller to the admittance matrix. The second, the power injection method, does not modify the admittance matrix. Rather, a series PF controller is modeled as a set of real and reactive power injections at the sending and receiving ends of the transmission line. The power injection method is prevalent in the literature but requires solution of a sub-problem between iterations of the Newton-Raphson solution. This leads to non-quadratic convergence of the Newton-Raphson algorithm and has poor convergence when the system is heavily loaded or when PF controllers are prevalent. The third method augments the susceptance or angles of a DC power flow. As with the power injection method, results show that this method provides poor results when the network is heavily loaded or PF controllers are ubiquitous.

Given the above, the preferred method is the admittance matrix method.

However, based on solution times reported in prior work, it was decided that the AC methods were too computationally intensive to allow integration of the CSCOPF into the transmission planning tool. Therefore, the DC power flow method was chosen.

The analysis is limited to series PF controllers. Rather than model a generic series PF controller, specific types of PF controllers are modeled to assess the relative competitiveness of multiple types of series PF controllers. This is important given the lack of prior work comparing the new PF control technologies to each other and the new technologies to established technologies. The following PF controllers are considered:

- Thyristor Controlled Series Capacitor (TCSC),
- Distributed Series Reactance (DSR),
- Phase-Shifting Transformer (PST), and
- Fractionally-Rated Back-to-Back (FR-BTB).

For a circuit l between bus j and bus k equipped with a TCSC, the PF between the line terminals is solved with (Eq. 14)-(Eq. 16). In this formulation, the line impedance without the influence of the TCSC is $X_{0,j,k,l}$. TCSC operation is limited by constraints (Eq. 17)-(Eq. 18) based on the rating of the TCSC [131].

$$P_{j,k,l} = \frac{\sin(\delta_{j,k})}{X_{j,k,l}} = -P_{k,j,l} \quad (\text{Eq. 14})$$

$$\delta_{j,k} = \delta_j - \delta_k \quad (\text{Eq. 15})$$

$$X_{j,k,l} = X_{0,j,k,l} + X_{TCSC\ j,k,l} \quad (\text{Eq. 16})$$

$$X_{TCSC\ j,k,l,min} \leq X_{TCSC\ j,k,l} \leq X_{TCSC\ j,k,l,max} \quad (\text{Eq. 17})$$

$$0 \leq |P_{j,k,l}| \leq P_{TCSC\ j,k,l,max} \quad (\text{Eq. 18})$$

For a line equipped with one or more DSR modules, the PF between the line terminals is solved with (Eq. 14), (Eq. 15) and (Eq. 19). The amount of inductive

injection is limited by the constraints seen in (Eq. 20)-(Eq. 21), where X_{DSR} is the total impedance injected by all DSR modules on the line.

$$X_{j,k,l} = X_{0,j,k,l} + X_{DSR j,k,l} \quad (\text{Eq. 19})$$

$$0 \leq X_{DSR j,k,l} \leq X_{DSR j,k,l,max} \quad (\text{Eq. 20})$$

$$0 \leq |P_{j,k,l}| \leq P_{DSR j,k,l,max} \quad (\text{Eq. 21})$$

For a line equipped with a PST, the PF between the line terminals is found with (Eq. 15), (Eq. 22), and (Eq. 23). PST operation is limited by the constraints seen in (Eq. 24)-(Eq. 25).

$$P_{j,k,l} = \frac{\sin(\delta_{j,k,l})}{X_{j,k,l}} = -P_{k,j,l} \quad (\text{Eq. 22})$$

$$\delta_{j,k,l} = \delta_{j,k} + \alpha_{PST j,k,l} \quad (\text{Eq. 23})$$

$$\alpha_{PST j,k,l,min} \leq \alpha_{PST j,k,l} \leq \alpha_{PST j,k,l,max} \quad (\text{Eq. 24})$$

$$0 \leq |P_{j,k,l}| \leq P_{PST j,k,l,max} \quad (\text{Eq. 25})$$

For a line equipped with a FR-BTB, the PF between the line terminals is found with (Eq. 15), (Eq. 22), and (Eq. 23). FR-BTB operation is limited by the constraints seen in (Eq. 26) and (Eq. 27). [256].

$$\alpha_{FRBTB j,k,l,min} \leq \alpha_{FRBTB j,k,l} \leq \alpha_{FRBTB j,k,l,max} \quad (\text{Eq. 26})$$

$$0 \leq |P_{j,k,l}| \leq P_{FRBTB j,k,l,max} \quad (\text{Eq. 27})$$

For a line without a PF controller, the PF between the line terminals is found with (Eq. 14), (Eq. 15), and (Eq. 28).

$$X_{j,k,l} = X_{0,j,k,l} \quad (\text{Eq. 28})$$

The DC power flows are solved using a set of linear equations based on (Eq. 14) through (Eq. 28) and the requirement that supply equal demand at each bus. The PF solver requires exogenous definition of generator set points, PF controller set points, and load levels.

4.2.2. Corrective Security-Constrained Optimal Power Flow Leveraging Power Flow Control and Incremental Power Flow control

To leverage PF and IPF control in the CSCOPF, the CSCOPF must be capable of dispatching generator and PF controller set points during secure operation and during a contingency. Without PF controllers, DC power flows can be solved within a LP. However, DC power flows cannot be solved within an LP if PF controllers are included. Using the decomposition technique, the PF controller set points are solved as a master problem (MP1) and the cost of operation during secure operation is minimized by solving a sub-problem (SP1). The solution of this approach is then fed into another master-sub-problem pair (MP2, SP2) for the solution of each contingency. The process can be iterated until convergence is reached or the iteration count exceeds a pre-defined level. The process is shown in Figure 72. The process in Figure 72 is augmented with additional constraints to model the IPF transactions.

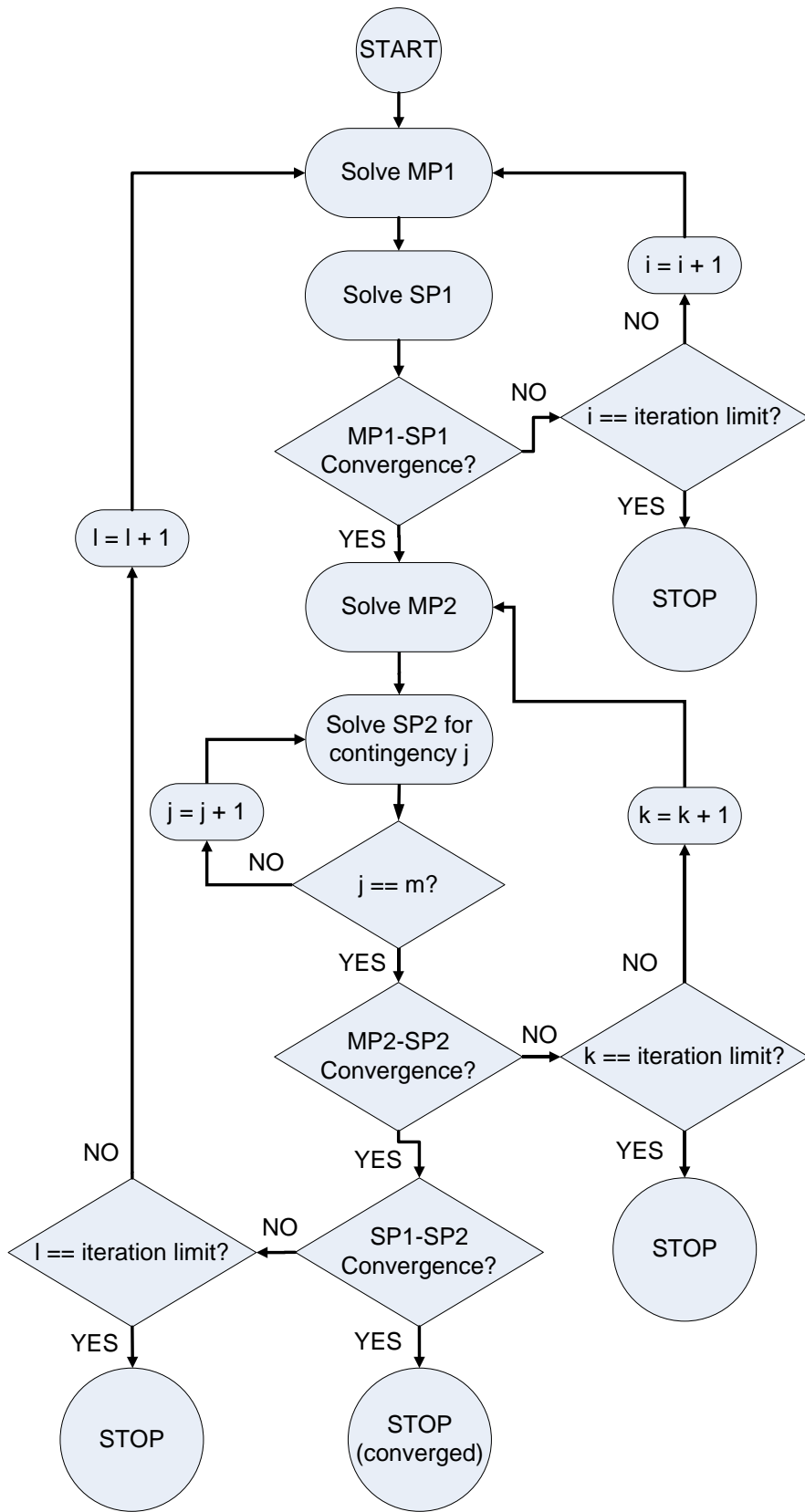


Figure 72: Flowchart for CSCOPF with PF controllers.

Operation of the typical power system requires both unit commitment and generation dispatch. Unit commitment is performed using a security-constrained unit commitment (SCUC) tool. Prior research using unit commitment and OPF tools shows that startup and shutdown costs comprise roughly one percent of the total production cost for a large power system. This result is consistent even for cases with large amounts of intermittent renewable generation that use less accurate renewable production forecasts at the unit commitment stage than the dispatch stage. At the same time, prior research shows that the integrality of the unit commitment problem results in higher computational intensity. The CSCOPF does not model unit commitment for the following reasons:

- The CSCOPF will be embedded within the planning tool, which is itself computationally intensive, and
- The expected cost impacts of startup and shutdown are negligible compared to the expected cost savings of including PF controllers in the planning process.

The CSCOPF minimizes the production cost, shown in (Eq. 29), which is a function of the unit output power and unit production cost. Constraints on the objective function will include system power balance (Eq. 30), circuit flow limits (Eq. 31), TCSC reactance limits (Eq. 32), DSR reactance limits (Eq. 33), PST angle limits (Eq. 34), FR-BTB angle limits (Eq. 35), total circuit reactance (Eq. 36)-(Eq. 38), phase angle across circuits (Eq. 39)-(Eq. 40), bus power balance (Eq. 41), limits on the circuit flows under $n-1$ conditions (Eq. 42), fulfillment of IPF transactions (Eq. 43), generator limits (Eq. 44), and limits on angle differences across circuits (Eq. 45). Limits on the real power through the PF

controllers are subsumed into the circuit flow limits under the assumption that a PF controller deployed on circuit i meets or exceeds the flow limit of circuit i . The method allows the system to simultaneously support IPF transactions and undesigned flows. The notation of (Eq. 29)-(Eq. 40) is based on (Eq. 14)-(Eq. 28), with an additional subscript to accommodate multiple time steps.

$$\sum_{g \in \Omega_{GEN}} \sum_{t \in \Omega_{TIME}} (b_g)(P_{g,t}) \quad (\text{Eq. 29})$$

$$\sum_{d \in \Omega_{LOAD}} P_{d,t} = \sum_{g \in \Omega_{GEN}} P_{g,t} \text{ for } \forall t \quad (\text{Eq. 30})$$

$$0 \leq |P_{j,k,l,t}| \leq P_{j,k,l,t,max} \text{ for } (j, k, l) \in \Omega, \forall t \quad (\text{Eq. 31})$$

$$X_{TCSC j,k,l,t,min} \leq X_{TCSC j,k,l,t} \leq X_{TCSC j,k,l,t,max} \text{ for } (j, k, l) \in \Omega_{TCSC}, \forall t \quad (\text{Eq. 32})$$

$$0 \leq X_{DSR j,k,l,t} \leq X_{DSR j,k,l,t,max} \text{ for } (j, k, l) \in \Omega_{DSR}, \forall t \quad (\text{Eq. 33})$$

$$\alpha_{PST j,k,l,t,min} \leq \alpha_{j,k,l,t} \leq \alpha_{PST j,k,l,t,max} \text{ for } (j, k, l) \in \Omega_{PST}, \forall t \quad (\text{Eq. 34})$$

$$\alpha_{FRBTB j,k,l,t,min} \leq \alpha_{j,k,l,t} \leq \alpha_{FRBTB j,k,l,t,max} \text{ for } (j, k, l) \in \Omega_{FRBTB}, \forall t \quad (\text{Eq. 35})$$

$$X_{j,k,l,t} = X_{0,j,k,l} + X_{TCSC j,k,l,t} \text{ for } (j, k, l) \in \Omega_{TCSC}, \forall t \quad (\text{Eq. 36})$$

$$X_{j,k,l,t} = X_{0,j,k,l} + X_{DSR j,k,l,t} \text{ for } (j, k, l) \in \Omega_{DSR}, \forall t \quad (\text{Eq. 37})$$

$$X_{j,k,l,t} = X_{0,j,k,l} \text{ for } (j, k, l) \notin \{\Omega_{TCSC}, \Omega_{DSR}\}, \forall t \quad (\text{Eq. 38})$$

$$\delta_{j,k,l,t} = \delta_{j,k,t} + \alpha_{j,k,l,t} \text{ for } (j, k, l) \in \{\Omega_{PST}, \Omega_{FRBTB}\}, \forall t \quad (\text{Eq. 39})$$

$$\delta_{j,k,l,t} = \delta_{j,k,t} \text{ for } (j, k, l) \notin \{\Omega_{PST}, \Omega_{FRBTB}\}, \forall t \quad (\text{Eq. 40})$$

$$\sum_{g \in n} P_{g,t} - \sum_{d \in n} P_{d,t} + \sum_{(j,k,l) \in \Omega, k=n} \frac{\delta_{j,k,l,t}}{X_{j,k,l,t}} - \sum_{(j,k,l) \in \Omega, j=n} \frac{\delta_{j,k,l,t}}{X_{j,k,l,t}} = 0 \text{ for } \forall n, \forall t \quad (\text{Eq. 41})$$

$$0 \leq |P_{j,k,l,t}| \leq P_{j,k,l,t,max} \text{ for } (j, k, l) \in \Omega, \forall N - 1 \text{ contingencies}, \forall t \quad (\text{Eq. 42})$$

$$P_{o,j,k,l,t} + \sum_{i \in \Omega_{IPF,j,k,l,t}} T_{i,j,k,l,t} \leq P_{j,k,l,t} \text{ for } \forall t \quad (\text{Eq. 43})$$

$$0 \leq P_{g,t} \leq P_{g,t,max} \leq 0 \text{ for } \forall g, \forall t \quad (\text{Eq. 44})$$

$$|\delta_{j,k,l,t}| \leq \delta_{max} \text{ for } (j, k, l) \in \Omega, \forall t \quad (\text{Eq. 45})$$

The notation for (Eq. 29)-(Eq. 45) (Eq. 45) is as follows:

- b_g is the production cost, including the fuel cost, variable operation cost, variable maintenance cost, and carbon penalty of producing one MWh of energy with unit g ,
- $P_{g,t}$ is the power produced by unit g at time t ,
- Ω_{GEN} is the set of system generators,
- Ω_{TIME} is the set of time steps solved in the CSCOPF,
- $P_{d,t}$ is the power demanded by load d at time t ,
- Ω_{LOAD} is the set of system loads,
- $P_{j,k,l,t}$ is the real power through the l^{th} circuit connecting buses j to k at time t ,
- $P_{j,k,l,t,max}$ is the max power through the l^{th} circuit connecting buses j to k at time t ,
- Ω is the set of all circuits,
- $X_{TCSC j,k,l,t,min}$ is the minimum reactance of the l^{th} circuit connecting buses j to k at time t , including the reactance of the TCSC, when the TCSC operates in full capacitive mode,
- $X_{j,k,l,t}$ is the reactance of the l^{th} circuit connecting buses j to k at time t , including the reactance of any series reactance controller,

- $X_{TCSC j,k,l,t,max}$ is the maximum reactance of the l^{th} circuit connecting buses j to k at time t , including the reactance of the TCSC, when the TCSC operates in full inductive mode,
- Ω_{TCSC} is the set of all circuits with a TCSC,
- $X_{DSR j,k,l,t,max}$ is the maximum reactance of the l^{th} circuit connecting buses j to k at time t , including the reactance of the DSR, when the DSR operates in full inductive mode,
- Ω_{DSR} is the set of all circuits with at least one DSR module,
- $\alpha_{PST j,k,l,t,min}$ is the maximum amount the angle across the l^{th} circuit connecting buses j to k at time t can be reduced by the PST,
- $\alpha_{j,k,l,t}$ is the angle injection of the series phase angle controller installed on the l^{th} circuit connecting buses j to k at time t ,
- $\alpha_{PST j,k,l,t,max}$ is the maximum amount the angle across the l^{th} circuit connecting buses j to k at time t can be increased by the PST,
- Ω_{PST} is the set of all circuits with a PST,
- $\alpha_{FRBTB j,k,l,t,min}$ is the maximum amount the angle across the l^{th} circuit connecting buses j to k at time t can be reduced by the FR-BTB,
- $\alpha_{FRBTB j,k,l,t,max}$ is the maximum amount the angle across the l^{th} circuit connecting buses j to k at time t can be increased by the FR-BTB,
- Ω_{FRBTB} is the set of all circuits with a FR-BTB,
- $X_{0,j,k,l}$ is the reactance of the l^{th} circuit connecting buses j to k at time t , not including the reactance of any series reactance controller,

- $\delta_{j,k,l,t}$ is the angle across the l^{th} circuit connecting buses j to k at time t , including the angle shift of any series phase angle controller,
- $\delta_{j,k,t}$ is the phase angle at bus j minus the phase angle at bus k at time t ,
- n is a system bus,
- $P_{o,j,k,l,t}$ is the real power flow at time t on the l^{th} circuit connecting buses j to k without any of the IPF transactions of the set $\Omega_{IPF,j,k,l,t}$ in operation,
- $T_{i,j,k,l,t}$ is the real power flow of IPF transaction i at time t on the l^{th} circuit connecting buses j to k ,
- $\Omega_{IPF,j,k,l,t}$ is the set of IPF transactions at time t scheduled to use the l^{th} circuit connecting buses j to k ,
- $P_{g,t,max}$ is the maximum real power limit of generation g at time t ,
- δ_{max} is the maximum allowed angle between any buses connected by a circuit, including any angle injected by a series phase angle controller.

4.3. CSCOPF Tool Development

The CSCOPF tool was developed based on the method described above.

Development proceeded in stages to facilitate testing. First, an economic dispatch tool was created to solve generator dispatch without considering network constraints. Then, an OPF tool was developed to dispatch generation given network constraints but without considering contingencies. Then a CSCOPF was developed to dispatch generation and ensure that the system remains normal if any single line is outaged. Then a CSCOPF was developed with the same reliability requirements of the prior CSCOPF but this CSCOPF

could dispatch generation and PF controllers when all assets were online but only PF controllers for contingency action. The final CSCOPF has the same goal as the others but dispatches generation and PF controllers when all assets are online or if an asset is offline. The IPF constraint shown in (Eq. 43) was not included in the CSCOPF tool. The CSCOPF tool was coded in AMPL, a programming language designed to code optimization problems. The problems were solved with IBM ILOG CPLEX 12.5 running on a single machine running the Ubuntu operating system. CPLEX was obtained through the IBM Academic Initiative. Relevant machine specifications include:

- Intel i7-3820 4 core, 8 thread processor
- 6 GB DDR3 SDRAM at 1.6 GHz
- 60 GB SATA III SSD
- LGA 2011 Chipset

Given that the CSCOPF was designed for integration into the planning tool, some simplifying assumptions were made:

- Demand is assumed to be inelastic and constant within each operating hour. This reduces the objective function to the minimization of production cost.
- Feasible PF controller set points are assumed continuous within the limits of the controller rating.
- The system is assumed stable provided that the maximum phase angle difference between adjacent buses, including the effect of phase-shifting controllers, is below a pre-specified limit common to all buses. Some commercial CSCOPF

tools incorporate stability limits via a nomogram, which specifies stability as a function of the generator dispatches and system topology.

4.4. Demonstration

The CSCOPF tool was demonstrated using modified versions of the Garver five-bus system and the IEEE 39-bus system. Costs and loads are assigned to represent operation in 2033. The Garver five-bus system is seen in Figure 73. The systems were simulated with and without PF controllers. For a given system, load was the same with and without PF controllers. The Garver system was loaded to produce congestion. The IEEE 39-bus system was loaded so that the case without PF controllers could not serve additional load when held to $n-1$ constraints. Sufficient wind generation was added to both cases to meet a 33% RPS in the absence of congestion. This is higher than the 20% RPS used for the RPS compliance study in Chapter Three.

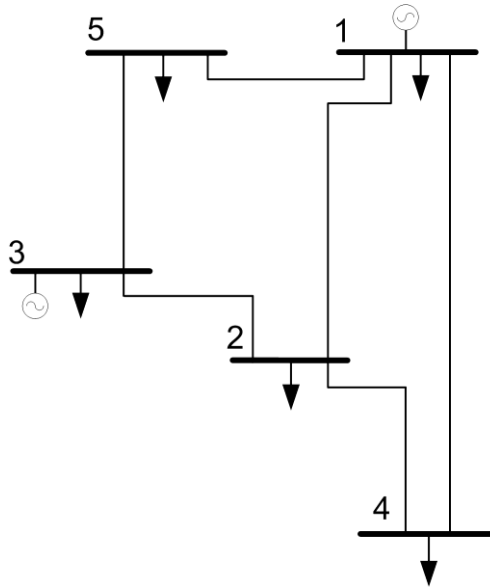


Figure 73: Topology of the Garver five-bus system.

In actual practice, the SCOPF is run numerous times for each operating hour. It is run before the operating hour to update the generation dispatch developed by the SCUC. Then, the SCOPF is then run multiple times within the operating hour to account for changes in load, generation availability, and transmission outages. The demonstration assumes load forecasts are perfect and generators are always available. The pre-operating hour SCOPF is typically run a few hours before the operating hour, so the renewable production forecast is more accurate than the forecast input into the SCUC. For simplification, actual renewable potential production values are input into the CSCOPF. Given that an SCUC is not used, the minimum power of all generation is set to zero to allow the CSCOPF to mimic the SCUC shutdown of unnecessary units.

For the cases with PF controllers, both systems were arbitrarily assigned a mix of TCSCs and PST. Circuits were sampled in groups of two, with the first circuit of each group receiving a TCSC rated for +/- 15% of line admittance and the second two circuit

of each group receiving a PST rated ± 0.1 rad. The cycle was repeated until all circuits were populated with PF controllers.

The Garver system was assigned a mix of coal, natural gas CCGT, natural gas OCGT, natural gas steam turbine, and wind generation to provide the opportunity for congestion. The IEEE 39-bus system was assigned a mix of coal and wind generation, with each unit type matching those used for the RPS compliance study in Chapter Three. However, the unit ratings and line ratings of the 39-bus system were updated to model intra-area congestion and also to enable operation under $n-1$ contingencies. Figure 74 shows the Garver system without PF controllers that was used for the CSCOPF demonstration. More details on the systems are found in Appendix E.

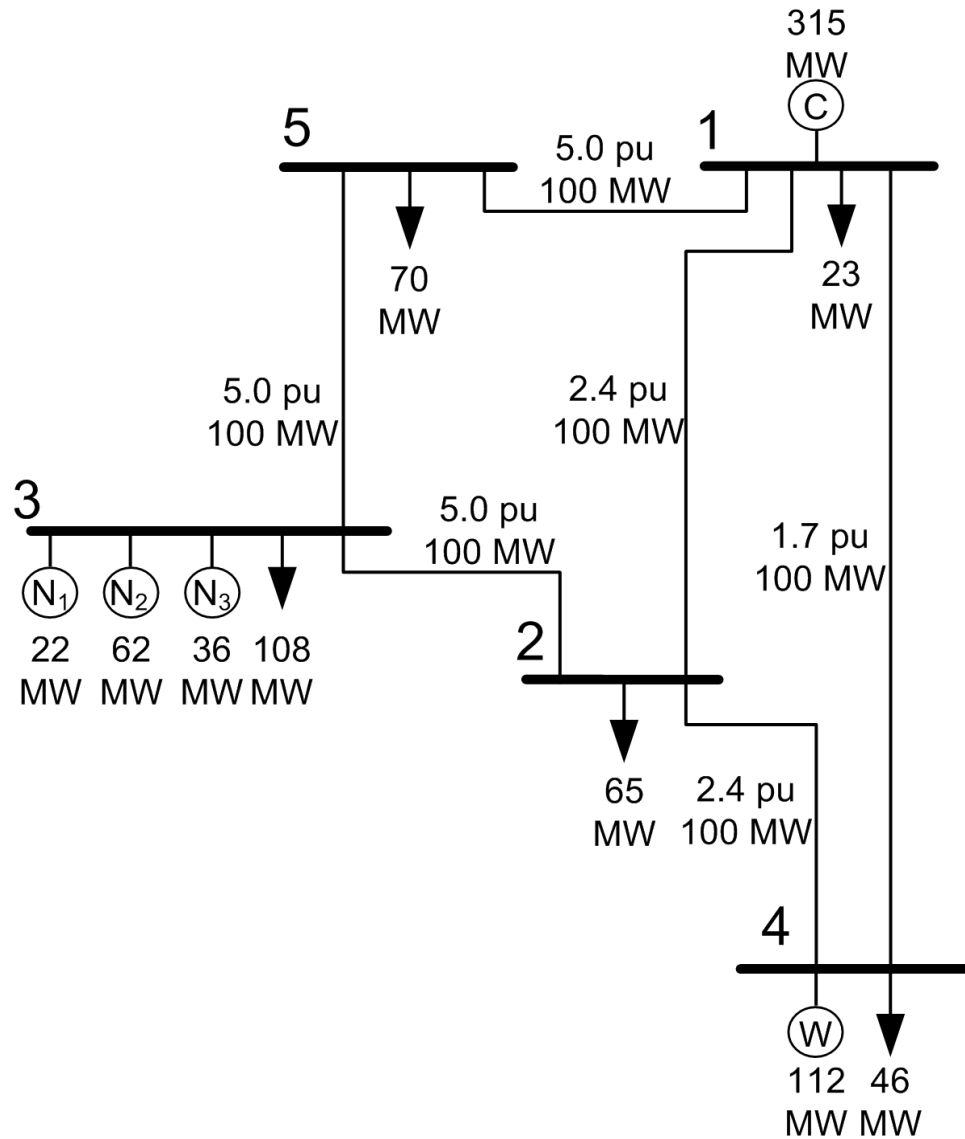


Figure 74: System topology, generation capacity and load for the CSCOPF demonstration cases.

Each system was simulated with and without use of the PF controllers. Table 9 shows the relevant results. PF control reduces the system operating cost of the Garver system by 7% but does not reduce the cost of the IEEE 39-bus system.

Table 9: Results of the CSCOPF demonstration.

Case	Production Cost (\$/hr)	Utilization of Potential Wind Production (%)	Solution Time (s)
Garver	10630	100	0.0678
Garver w/ PF Controllers	9892	100	0.0623
IEEE 39-Bus	268316	100	0.9568
IEEE 39-Bus w/ PF Controllers	268316	100	1.2829

Test cases with ubiquitous PF controllers were infeasible for large PF controller ratings. The limit of feasibility varied by PF controller type but was generally around 20% of line admittance or +/- 0.2 rad if every circuit was equipped with a PF controller. This may be a consequence of the decomposed solution method, which requires convexity of the solution space as described in [224].

4.5. Incremental Packetized Energy

The *packetized energy* concepts discussed in Chapter Two are burdened by high cost, primarily because of the requirement for energy storage and ubiquitous PF control. That said, the synergy of IPF with new developments in load control may provide many of the benefits of *packetized energy* at a fraction of the cost. The proposed reduced-form of *packetized energy*, called *incremental packetized energy* is presented below.

Prior concepts of *packetized energy* required the following components:

- PF control throughout the meshed portions of the transmission and distribution systems,
- Energy storage to decouple the timing of production and consumption, and
- Load control or elastic demand response market to increase the average utilization of assets.

All identified prior work compromises, to some degree, between the ideal of *packetized energy* and the suggested approach. The primary compromise is the level of PF control, as there is a tradeoff between the fraction of the transaction path that can be controller and the cost necessary to realize the control. In the extreme case, where the entire meshed system has PF control, differentiating electrons sharing a common distribution lateral is challenging. Packetization from producer to customer could be realized in the electric sector by equipping each customer with sufficient energy storage to allow all loads on the feeder, except the designated recipient, to stop accepting energy while the packet was transmitted. While such a system may be technically feasible the economic benefits are not obvious given that electrons are non-differentiable. A consumer may rather have a lower cost solution, sourced on average by an electric mix that meets the consumer's preferences, than a higher cost solution that is guaranteed to comply with the consumer's preferences. With this in mind, there may be an opportunity to leverage the insights of *packetized energy* without the cost consequences of forcing the electrical sector to operate exactly like the networking sector.

The cost of energy storage is an impediment to the viability of *packetized energy*. Energy storage for frequency regulation, when properly valued, is becoming competitive to conventional frequency regulation [257]. But using energy storage to smooth the diurnal variability of stochastic renewable generation is uneconomical compared to dispatchable fossil fuel sources [258]. Even if energy storage becomes economical on the diurnal timescale, the synoptic and seasonal timescales also limit renewable penetration and may require storage [257]. Therefore, it would be helpful to eliminate

the energy storage requirement or find ways to allocate the cost of energy storage across multiple applications.

Work with Dr. Thomas and Dong Gu Choi of the Georgia Tech School of Industrial and Systems Engineering has demonstrated a potential means to reduce the cost of energy storage by integrating the electric and light-duty transit sectors and allocating the cost of energy storage among multiple applications [259]. The effort quantifies the benefit of coordinating the charging of GEVs with the variability of wind production. Generation capacity planning and operation were simulated over two decades for the entire Eastern Interconnect. The study assumes two types of GEV charging, uncontrolled and controlled. For uncontrolled charging, the GEV begins charging upon completion of the last journey of the day. For controlled charging, the GEV is available for charging whenever at home. The system operator schedules charging at will provided the vehicles are fully charged each day. The timing of charging is based on surveyed vehicle usage per [260]. Generation capacity is added or retired in each year of the planning horizon to minimize the NPV of electricity expenditures. Multiple cases were simulated including an extreme case with GEV market share and renewable energy requirement as follows:

- 100% GEV market share in 2030, corresponding to 81% of the total light-duty vehicle fleet, and
- 33% of the annual electrical energy in the Eastern Interconnection is sourced from renewable generation.

The extreme case with uncontrolled charging requires 450 GW of additional generation capacity relative to a BAU case. The BAU case consists of CVs for 100% of

the light-duty fleet and the currently legislated Eastern Interconnection RPS mandates, corresponding to 10% of annual demand in 2030. Of the 450 GW of additional capacity, 200 GW is new natural gas capacity. In comparison, if the GEVs are controlled, the extreme case requires an additional 260 GW of capacity relative to the BAU case. The wind capacity requirement remains the same but the natural gas requirement reduces by 95%. This level of improvement is realized without invoking vehicle-to-grid functionality (V2G), avoiding the distribution system impacts and battery degradation of V2G [261]. Also, integrating the electric and light-duty transit sectors has a lower total cost relative to a non-integrated system, providing an impetus for change. Here, total cost is defined as the sum of consumer expenditures for electricity, gasoline, vehicle purchase, home charging infrastructure, and public charging infrastructure. The electricity cost includes the capital cost of new generation, fuel cost, operation and maintenance (O&M), and new transmission to transfer wind energy from areas of high-quality wind resource to load centers. The work suggests that many of the advantages of energy storage can be realized without grid-dedicated energy storage, lowering consumer energy expenditures relative to BAU.

GEVs are one example of a class of loads called flexible loads. Flexible loads, which have been proposed previously and are referred to by various names, are not subject to the reliability requirements of the traditional electrical load [165,168,169,177,178,262, 263,264,265,266,267,268,269,270,271,272]. The power draw of a flexible load could be controlled at will within constraints, such as a requirement that a certain minimum amount of energy be delivered to the flexible load over a specified time. Users are incented to designate loads as flexible loads based on lower energy costs.

Incremental packetized energy combines PF control and flexible loads without the strict requirements of *packetized energy*. Rather than packetizing all energy and controlling the path of all energy from producer to load, *incremental packetized energy* serves flexible loads and uses packet routing only when necessary to overcome congestion in the meshed network. For example, consider a given wind generator that is curtailed by a transmission constraint. At the same time, a fleet of GEVs are connected to a distant bus and are available for charging. If the GEVs are classified as traditional loads, even with PF control, the transmission constraint precludes the injection of power at the wind generator and receipt of power at the GEV bus. However, if the $n-x$ requirement is relaxed, additional power can be sent from the wind generator to the GEV bus. With IPF, the PF controllers may send even more power by piecing together a series of underutilized transmission paths from wind generator to GEV bus. Energy packets are defined in the congested portions of the network as a source bus, a transaction path, a receiving bus, a power level and a duration. If the energy packet is no longer realizable due to changes in generation, transmission, distribution, or load, the energy packet is nullified and a new packet is defined. Multiple simultaneous energy packets can increase the utilization of existing generation, transmission and distribution capacity without the burdensome cost of prior *packetized energy* methods.

Incremental packetized energy can be realized with IPF. However, the benefits of *incremental packetized energy* may be realizable without IPF. By definition, *incremental packetized energy* uses power routing only to overcome congestion. Since there is no requirement to track packets from source to load, PF control can be used rather than IPF. This allows the use of transmission paths which are not contiguous. This said, Chapter

Five discusses why IPF may increase the likelihood that the required transmission investments are made to realize *incremental packetized energy*.

The concept of *incremental packetized energy* is demonstrated using the CSCOPF tool. The Garver five-bus and IEEE 39-bus systems were used for the demonstration of *incremental packetized energy*. The initial loading levels are identical to the levels used for the CSCOPF test cases. The initial load level is considered to be secure load, which must be served subject to the standard CSCOPF security requirements. For each system, flexible load is then added iteratively until either the secure load cannot be served reliably or no more flexible load could be serviced. The demonstration assumes flexible load is added per (Eq. 46), where the flexible load at bus i , denoted $P_{f,i}$, is related to a system-wide constant, α , and the secure load at bus i , which is denoted $P_{s,i}$. The case with PF controllers have +/- 0.1 rad PSTs on all circuits. The ratings of all generators are increased so that the amount of flexible load is not limited by generation limits. This configuration is a lower bound on the total amount of load serviceable via *incremental packetized energy*, as more flexible load may be serviceable when the allocation of flexible load is less rigid than (Eq. 46). Table 10 shows the total load each system can supply relative to the secure load, with results demonstrating a two to three increase in total load.

$$P_{f,i} = \alpha P_{s,i} \tag{Eq. 46}$$

Table 10: Max system load using incremental packetized energy relative to max secure load. The numerator includes secure load and flexible load.

Case	<i>Max System Load with Incremental Packetized Energy</i>	
	<i>Max Secure Load</i>	
5-Bus w/o PF Controllers		3.3
5-Bus w/ PF Controllers		3.3
39-Bus w/o PF Controllers		1.95
39-Bus w/ PF Controllers		2.05

4.6. Discussion

This chapter presents a CSCOPF implementation compatible with impedance-injection and angle-injection IPF control. A CSCOPF tool compatible with four PF controllers was developed and demonstrated on the Garver five-bus and IEEE 39-bus systems. The Garver system with an arbitrary PF controller allocation results in 7% savings in production costs. The 39-bus system with arbitrary PF controller allocation shows no cost savings as a consequence of the lack of generation diversity and congestion.

This chapter also proposes the *incremental packetized energy* concept, which exhibits some of the benefits of *packetized energy* but is expected to have lower cost. By sharing energy storage costs between the electric and light-duty transit sectors, GEVs provide a means to lower consumer total costs, realize load flexibility, and reduce the need for grid-dedicated energy-storage. Meanwhile, IPF control provides the means to utilize spare transmission capacity to serve flexible loads. The proposed concept averts the cost of packetizing all electrical energy. A demonstration of *incremental packetized*

energy shows that a system supplying maximum secure load can serve an additional amount of flexible load equivalent to one to two times the secure load.

CHAPTER 5

TRANSMISSION PLANNING WITH POWER FLOW CONTROL AND INCREMENTAL POWER FLOW CONTROL

5.1. Introduction

The impact of PF control and IPF control depends on the degree and manner to which they are implemented. This chapter proceeds in four parts. First, three transmission planning frameworks are proposed, one compatible with PF control and two compatible with IPF control. Second, an automated planning tool is developed that is compatible with the proposed frameworks as well as the existing centralized transmission planning process. Third, the planning tool is demonstrated for two proposed planning frameworks and the existing centralizing planning process. Fourth, the findings are discussed.

5.2. Proposed Transmission Planning Frameworks

Three transmission planning frameworks are proposed. The first, the revised centralized transmission planning framework (revised centralized framework), integrates PF controllers into the centralized planning process. The second, the *merchant electrical pipeline* (MEP) framework, enables merchant developers to realize IPF transactions on existing transmission assets. The third, the hybrid transmission planning framework (hybrid framework), allows the revised centralized and MEP frameworks to coexist. The

hybrid intends to encourage investment in IPF control while maintaining compatibility with centralized planning

5.2.1. Revised Centralized Transmission Planning Framework

Prior to industry restructuring, a centralized planning process was coordinated by each TO to comply with reliability requirements and improve system economics. Recent FERC orders have transferred the planning process to entities responsible for larger regions, such as ISOs and RTOs in market jurisdictions. FERC has mandated that the planning process consider economic investments. The centralized planning process includes development of a list of candidate reliability and economic investments. To resolve a reliability problem, the least cost candidate is typically constructed. Economic investments are typically constructed only if the proposed solution exceeds a benefit-to-cost threshold. The benefit-to-cost threshold depends on the investment's lead-time, with higher threshold for longer term investments. Once online, the cost of the investment is incorporated into the rate base of the TO that constructed the investment.

The revised centralized framework proposes to include PF controllers in the set of permissible transmission investment choices. This framework allows systems to benefit from PF controllers without introducing the complexity of IPF transactions. Comparing a candidate investment solely deploying PF controllers to one constructing new lines, the PF controller investment is expected to have a shorter lead-time and thus have a lower benefit-to-cost threshold. However, given the multi-stakeholder nature of centralized planning, the lead-time for PF controller deployment on existing transmission assets may be longer than the lead-time for a similar deployment financed by a merchant developer.

5.2.2. Merchant Electrical Pipeline Framework

As shown in Chapter Three, IPF control allows power to be directed from a source bus to a destination bus along a specified transaction path. The term *merchant electrical pipeline* (MEP) is proposed to define a transmission investment developed and owned by a private company to realize an IPF transaction.

As discussed in Chapter Two, natural gas transportation pipelines in the United States are planned and operated by private companies as merchant pipelines. Natural gas pipelines are required to provide open access to all credit-worthy shippers at a published tariff. Before construction, a pipeline developer must demonstrate to FERC that the pipeline meets or exceeds a benefit-to-cost threshold. The pipeline tariff must also be approved by FERC. The pipeline developer may utilize a rate-of-return tariff, market-based rate, or negotiated rate. A negotiated rate allows the shipper and pipeline owner to negotiate a tariff, with the caveat that the shipper may opt for the rate-of-return tariff. Use of market-based rates requires demonstration to FERC that the pipeline will be unable to exercise market power.

Investment to increase the capacity of a natural gas pipeline is borne by the users of the incremental capacity and the benefits of the investment are accrued by the users of the incremental capacity. The rates and quality of service of existing users cannot be impacted by the investment. For a natural gas transportation pipeline, both the original capacity and incremental capacity are typically merchant. The negotiated rates for use of the new capacity have no upper bound. A gas producer may be willing to accept

negotiated rates higher than the rate-of-return tariff to ensure the pipeline is built. This may incent additional investment by providing the pipeline developer a greater fraction of the societal value of the pipeline.

Adding MEP functionality to an existing electric transmission line is similar to adding capacity to an existing natural gas pipeline. However, there are a number of notable differences between a MEP and incremental natural gas pipeline capacity. In the case of a MEP, the original capacity is likely to be regulated while the new capacity is unregulated. It is unclear whether the PUCs and FERC will allow a merchant developer to use regulated transmission assets even if the regulated assets are not impacted. A MEP lacks storage capability and the speed of electrical transmission is faster than a natural gas pipeline. These characteristics require more sophisticated control than a natural gas pipeline.

A MEP planning framework is proposed whereby a MEP is used to create a long-term power purchase option (PPO) between the owner of a MEP and an LSE. The LSE purchases the long-term option to buy a specified amount of power at the source end of the pipeline and have the energy delivered to the LSE via the pipeline. The LSE would have the option to temporarily suspend the pipeline transaction and offer the controllability of the pipeline to the system operator. LSE load in excess of the PPO quantity would be procured through the energy market at the LSE's LMP.

Based on the proposed framework of MEP planning, a developer will build a MEP if the benefit to the LSE exceeds the cost of construction and ownership. Under the rate-of-return tariff or market-based rate in a competitive market, the price of the

delivered energy would be equal to the LMP price at the source end plus the amortized cost of the pipeline capacity plus O&M costs. Under the negotiated rate, the pipeline owner could charge a higher rate than the rate-of-return tariff, capturing more of the societal benefit of the MEP. Similar to the use of negotiated rates for natural gas pipelines, the LSE may be willing to share their benefit to ensure the pipeline is built. Construction of the MEP will be subject to certification that the MEP is non-predatory.

MEP developers may follow a process similar to IPP developers to assess investment value. An IPP developer typically simulates multiple future scenarios, each based on assumed values for future fuel prices, online generators, and network topology. The IPP developer gauges the verity of potential generation and topology changes by monitoring the permitting and regulatory status of potential changes. MEP developers may follow a similar process to vet MEPs under development by others.

As discussed in Chapter Two, current merchant transmission development faces a number of challenges. First, the uncertainty of servicing multi-decade debt using revenues from short-term markets [244] increases the cost of capital for merchant investments. Second, the lead-time and uncertainty of new line construction increases the cost of capital and gives merchant transmission first-mover disadvantage. Linking a MEP with an LSE through a long-term PPO provides long-term revenue certainty and may lower the cost of capital. Avoidance of new transmission line construction reduces the potential for first-mover disadvantage.

5.2.3. Hybrid Transmission Planning Framework

The MEP framework and the existing centralized planning process seem, at least at present, to be complements. Centralized planning seems well suited for the development of a large scale, long-term transmission investment with a high benefit-to-cost ratio. For such an investment, the number of beneficiaries and the magnitude of the net benefits enable transcendence of the cost allocation challenges. However, centralized planning often fails to develop an investment with a less attractive benefit-to-cost ratio. A MEP is well suited for such an investment for two reasons: reduced development time and long-term revenue certainty. The nature of the MEP mitigates cost allocation disagreements, reducing development time. Development time may be further reduced given that the underlying transmission assets already exist. The faster development cycle reduces the uncertainty of forecasted investment benefits and costs. The improved estimates of benefits and costs reduce the investment risk and allow the MEP developer to access lower cost financing, improving the investment's benefit-to-cost ratio. The long-term PPO between the developer and LSE enables revenue certainty, further improving estimated benefits and costs and further reducing the cost of financing.

In the proposed hybrid planning framework, the centralized planning process occurs in parallel with MEP planning. Centralized planning seeks to guarantee reliability and develop economic investments which exceed the benefit-to-cost threshold. Centralized planning is allowed to deploy PF controllers but does not attempt to establish IPF transactions. MEP developers seek to develop investments which arbitrage pricing differentials that exist or are expected to exist despite the centrally planned investments. Despite the existence of centralized planning, viable MEP investments may exist due to

their lower benefit-to-cost threshold. Provided the financials are compelling, a MEP investment may be feasible to alleviate a short-term price differential that will be partially or fully alleviated by an announced centrally planned investment. The centralized planning process assumes that once an MEP investment reaches a certain level of verity, it will be built and operated. This is similar to the way that power plant developers currently incorporate publicly announced generation and transmission investments into their investment screening methodology. If successful, the hybrid framework will provide a lower total cost of energy than the revised centralized framework while ensuring compliance with reliability requirements.

5.3. Implementation

As discussed in Chapter Two, known planning tools are not able to simultaneously include PF controllers and new transmission lines in the set of permissible transmission investment choices. In addition, these tools have not been developed for use with the proposed hybrid framework. This section describes the development of a planning tool that is:

- Able to simultaneously deploy a mix of PF controllers and transmission lines at a higher level of detail than known planning tools, and
- Compatible with the proposed hybrid framework.

The section proceeds in two stages. First, the general structure of the planning tool is described. Then, the specifics required to model each planning framework are described.

5.3.1. General Structure of the Planning Tool

5.3.1.1. Problem Formulation and Permissible Transmission Investment Choices

The planning tool combines a genetic algorithm (GA) and fitness function as shown in Figure 75. The CSCOPF, described in Chapter Four, is embedded in the fitness function. The fitness function evaluates the fitness of the current offspring developed by the GA. The planning tool iterates until the generation counter ($i5$) reaches a pre-defined limit on the number of generations (n) or the number of generations with the same elite individual ($i6$) reaches a pre-defined limit (o).

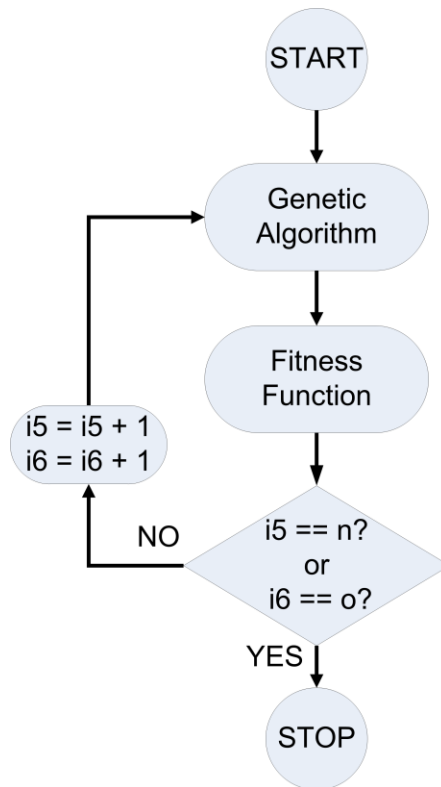


Figure 75: Planning tool overview flowchart.

The transmission planning problem is more computationally intensive than the CSCOPF problem. Perhaps for this reason, the prior works identified in Chapter Two

have limited the planning problem to either deployment of PF controllers or new transmission lines. For the prior works able to deploy new transmission lines, the planning tools solved for the number of new circuits between bus-pairs but did not select the line ratings or circuit parameters of the circuits. In contrast, transmission planners designing a new line select from a higher dimension choice set which includes conductor type, conductor orientation, conductor tension, and the types and ratings of fixed or switched reactive power sources/sinks. In addition, the transmission planner has alternatives other than new line construction. Some examples are:

- Reconductor existing lines,
- Retrofit existing structures to support higher conductor tensioning and thus increasing the thermal rating for a given sag threshold,
- Upgrade system breakers,
- Change system topology by line switching,
- Upgrade peripheral equipment to operate a core asset at rated capability rather than the lower capability at which it has historically been operated (i.e. reconfigure the terminals of a 230 kV line that has been operated at 169 kV),
- Deploy dynamic thermal rating systems,
- Deploy reactive power controllers,
- Deploy PF controllers, including HVDC lines, and
- Deploy new transformers.

The proposed planning tool is intended to:

- Better align with the large choice set of the transmission planner than prior work,
- Simultaneously consider multiple transmission investment options, and
- Allow assessment of the previously proposed transmission planning frameworks.

Consider a transmission planning problem with the choice set shown in Table 11.

Assuming up to two circuits can be built between bus-pairs and ignoring the possibility to reduce the search space by considering the dependencies among planning options, the Garver five-bus system has a total of $9.1e^{67}$ potential transmission plans. The CSCOPF tool can be used to assess the production cost and other pertinent metrics of each transmission plan. To improve accuracy, the CSCOPF would be run for a number of time steps for each planning period of the planning horizon. Assuming a simulation of two time steps per planning horizon, an exhaustive search would require $1.8e^{68}$ CSCOPF evaluations. Given the CSCOPF execution time from Chapter Five, this would require $1.1e^{63}$ days. Given that current planning studies assess systems on the order of 10^4 buses, a method based on exhaustive search is not feasible. GAs can identify near optimal solutions for non-linear problems while evaluating a fraction of the search space [273]. Since GAs do not guarantee optimality, they are identified as meliorization techniques [274]. However, meliorization rather than optimization may be acceptable given the resolution of the proposed planning tool relative to known planning tools.

Table 11: Choice set of the example planning problem.

Planning Option	Choice 1	Choice 1 - Number and List of Options	Choice 2	Choice 2 – Number of Options
New Transmission Line	Line Impedance	10 – 0.05 pu to 0.2 pu at steps of 0.017 pu	Line Rating	5 – 0 to 1000 MW at 250 MW steps
PF Controller	PF Controller Type	5 – none, TCSC, DSR, PST, FR-BTB	Converter Rating	10 – the significance of the steps depends on the PF controller type

The proposed planning tool is compatible with all of the proposed planning frameworks as well as the current centralized planning process. The goal of the planning tool is to minimize the cost of energy (COE) of the planning period given the structure of the planning framework under consideration and reliability requirements. As shown in (Eq. 47), COE is the sum of production cost (C_p), amortized cost of transmission investments made in the planning period ($C_{trans,new}$), amortized cost of transmission in the base case ($C_{trans,base}$), and amortized cost of generation capacity (C_{gen}). Four assumptions are made to facilitate development and reduce computational intensity of the planning tool. First, the planning tool solves the planning problem pseudodynamically. As such, the planning tool makes expansion decisions for the current planning period and does not coordinate expansions among multiple planning periods. Second, load, generation capacity, cost of the investment option, relevant policies and fuel prices are known at the start of the planning period. Third, technologies not commercially available at the start of the planning period are not included in the set of permissible transmission investment choices. Fourth, for reasons discussed below, capacity decisions are exogenous to the

planning period but are incorporated in a limited manner for a multi-period planning study.

$$COE = C_{prod} + C_{trans,new} + C_{trans,base} + C_{gen} \quad (\text{Eq. 47})$$

Some transmission planning methods consider the interdependency of transmission planning on generation planning. In the restructured environment, the interplay of transmission and generation is complex and is typically simulated with game theory. Given the time constant of centralized transmission investments, transmission investments are often planned irrespective of generation or planned considering generation changes over an initial fraction of the lifetime of the transmission asset [275]. Planning of transmission irrespective of generation may not be acceptable if PF control or MEPs are permissible choices, since the time constant of these investments may be similar to the time constant of generator investment. However, endogenous capacity planning will increase the size of the solution space. As a compromise, generation is taken as endogenous within a transmission planning period but can be updated between transmission planning periods. Similarly, transmission investments are exogenous to capacity planning.

Some of the investment options listed above require detailed system information. For example, retensioning requires knowledge of the tension rating of each tower of a transmission circuit and a function describing the cost of achieving a given tension for each tower. In contrast, limiting the search space to new line construction and PF controller installation can be modeled with less detailed information and is thus readily applicable to a large system. Given the combinatorial nature of the planning problem,

limiting the set of permissible transmission investment choices increases the likelihood of finding a solution in an acceptable timeframe. Since new line construction is the mainstay of current transmission investment, the planning tool uses the following set of permissible transmission investment choices:

- Deploy new transmission lines – selecting line impedance and line rating independently,
- Deploy PF controllers – selecting PF controller type and rating independently, and
- Outage existing transmission lines

Constraints are placed on the amount of expansion to limit the size of the solution space. A new transmission line will be allowed between any two buses. The maximum number of circuits between any two buses will be limited to m as seen in (Eq. 52), where l indicates the circuit number between the (j,k) pair of buses and p indicates the planning period. In addition, only one PF controller type, c , may be deployed per circuit as seen in (Eq. 53).

$$\sum_l u_{j,k,l,p} \leq m \text{ for } \forall j, k = \{1, j - 1\}, \forall p \quad (\text{Eq. 48})$$

$$\sum_{t=1}^4 u_{j,k,l,c,p} \leq 1 \text{ for } \forall j, k = \{1, j - 1\}, \forall p \quad (\text{Eq. 49})$$

The cost of new transmission investment is modeled over the planning period as annual payments equal to the product of the original investment cost and a fixed carrying

cost, also known as a fixed charge rate. This method appears consistent with the manner used to finance regulated transmission investments, as evidenced by [276]. All existing transmission assets are assumed to be operational over the planning period and subject to annual payments based on the carrying cost method. The planning tool averts the need to model system operation over the lifetime of a proposed transmission investment by using the carrying cost method and assuming the benefits of investment perpetuate beyond the planning period.

Some rules pertaining to PF controller investment are assumed. Over the study horizon, the planning tool may increase the rating of a given circuit's PF controller. In the case of the DSR, the cost of said enhancement is limited to the cost of the additional DSR modules. However, since the TCSC, PST, and FR-BTB are less modular than the DSR, rating enhancement of these controllers requires investment equivalent to the rated value of the new controller. If the planning tool rebuilds an existing circuit and then equips the new circuit with the same type of PF controller as the prior circuit, the investment in the prior PF controller is assumed to be a sunk cost and not applicable to the new circuit.

5.3.1.2. Genetic Algorithm

Figure 76 shows the flowchart for the GA. The problem structure determines the quality and computational intensity of a solution generated by a given genetic algorithm, with quality defined as the distance from the optimal solution. Automated methods exist to select the most appropriate GA type and parameter values for a given problem. These automated methods are a form of meta-GA, solving the problem with different combinations of GAs type and parameters values. Given the computational intensity of

the planning problem, it was deemed infeasible to use a meta-GA to select the proper GA. Prior literature can serve as a proxy for meta-GA even though prior planning tools have a less complex problem structure than the proposed planning tool. Given the lack of other alternatives, the prior literature was used to inform the structure of the planning tool GA. Once the structure was defined, the GA parameters were varied based on prior work and applied to a sample planning problem representative of each planning framework. A limited number of parameter values were tested. The set of parameters that consistently converged with the lowest generation count were used for the demonstration.

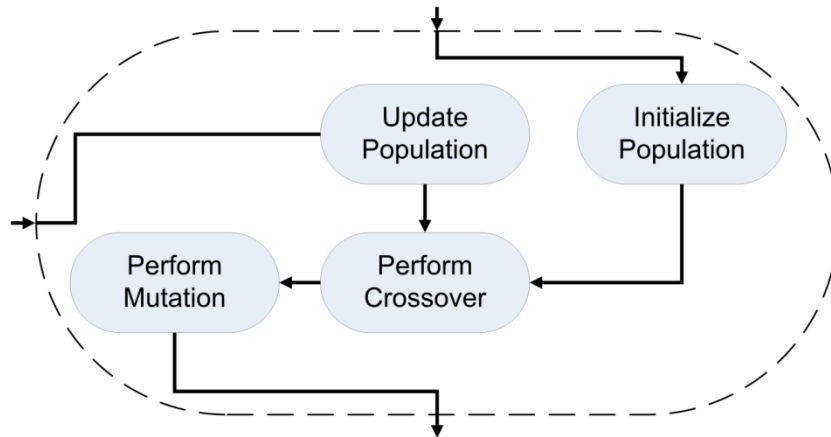


Figure 76: Flowchart for the genetic algorithm.

The GA uses a four-string, decimal codification to represent the investment choices as chromosomes. This approach is seen in prior work which involved selection of multiple power system investment parameters [131,133,139]. Each string represents a different parameter choice for each potential circuit. The four strings correspond to line impedance, line rating, PF controller type, and PF controller rating. Chromosome values

are limited to a string-specific range of integer values. For a five-bus system allowed to build up to 2 circuits per bus-pair, each string has 20 chromosomes. The codification spans potential new circuits as well as existing circuits, allowing the planning tool to reconfigure the system topology. The use of decimal codification induces quantization error, which impacts the results in two ways. First, quantization of the base case may lead to different operational outputs than the base case. Second, a better planning solution may exist if more granular steps are used between parameter values.

The initial population is randomly assigned. Random initialization is typical when applying GAs to small power systems with limited choice sets [277]. Alternatives to random initiation use the existing system as a starting point [230,231,278,279]. The alternatives are able to converge faster. These methods have been applied to large systems with limited choice sets. However, given the complexity of the problem at hand and lack of prior examples, random initiation was chosen to increase the likelihood of solution quality.

The crossover operator combines elements of parents to form new, potentially improved offspring. The crossover operator specifies how parents are chosen and how the genetic material of the parents is combined. Roulette wheel [131,133,139, 280] and tournament selection [230,231,278, 281] are both common in prior work. A form of tournament selection was chosen. A separate tournament is executed to choose each parent. In each tournament, the contender with the highest fitness in a tournament is chosen to be the parent. Based on prior work that chooses multiple parameters using a single GA, parent chromosomes were mixed on a string-by-string basis using random

two-point selection. This avoids mixing genetic material across parameters and increases the likelihood that elite genetic material is passed to the next generation.

The mutation operator introduces genetic material not contained in the population, decreasing the likelihood of converging near a local optimum and increasing the likelihood of converging near a global optimum. The mutation operator was executed once the offspring was created using the crossover operator. In prior work using a mutation operator based on simulated annealing, the probability of mutation is conditioned on whether or not the mutation improves the fitness of the individual [277, 278]. This approach, although seen in prior planning tools, was deemed unacceptable due to the increase in computational intensity. The probability of mutation increased as a function of the number of generations since the elite fitness increased [230,277,279]. This structure allows for unimpeded search of the population when the GA is started but increases the mutation rate as the GA begins to converge. For each chromosome of the offspring, a random number is drawn using the uniform distribution. If this number is less than the generation-specific mutation rate, the chromosome is mutated. The direction of mutation is then assigned via another draw from the uniform distribution. To limit the impact of mutation, mutation is limited to a +/- 1 unit change to the chromosome. This is an approximation of the triangle mutation operator seen in [278]. If the mutated chromosome is outside the allowable range for the string to which it belongs, the sign of the mutation is switched. The mutation process repeats for all chromosomes.

Some research has shown promise using adaptive crossover and mutation probabilities [282]. In this case, the crossover rate is increased if it promotes offspring

fitness relative to the parents. By symmetry, the crossover rate is decreased if it decreases offspring fitness relative to the parents. The mutation rate is adjusted similarly. Experiments conducted with the adaptive method demonstrated poor convergence and high generation counts. Therefore, adaptive crossover and mutation probabilities were not used in the final tool.

The population update operator embeds the offspring within the population. The operator searches the population for the individual with the lowest fitness and replaces this individual with the offspring. This replacement is not conditioned on the fitness of the offspring relative to the individual replaced by the offspring.

5.3.1.3. Fitness Function

Figure 77 shows the flowchart for the fitness function. The fitness function evaluates the annual production cost and the annualized transmission cost of a given individual of the GA. The annualized transmission cost from prior study periods are neglected, as these investments are common to all individuals. For the same reason, the annualized capacity cost is neglected. Annualized transmission and capacity costs are used to calculate the cost of energy once the planning decisions have been made. The production cost is found by running the CSCOPF for each of the T time steps of the planning period. The CSCOPF results are used to calculate the annual production cost (C_{prod}) by adding a weighting coefficient w_t to (Eq. 29), resulting in (Eq. 50). The weighting coefficient is the percent of annual hours represented by time step t . If any time step of the planning period is infeasible, a high fitness value is assigned to penalize the individual. The investment cost is found by comparing the topology of the offspring with the base case.

The investment cost is neglected for the following conditions, as they represent cases where the investment was already made in the base case:

- offspring matches the impedance and line rating of the base case
- offspring outages a circuit that was built in the base case
- a circuit of the offspring has the same line properties as the base case, the same type of PF controller as the base case, and a PF controller of the same or lower rating than the base case

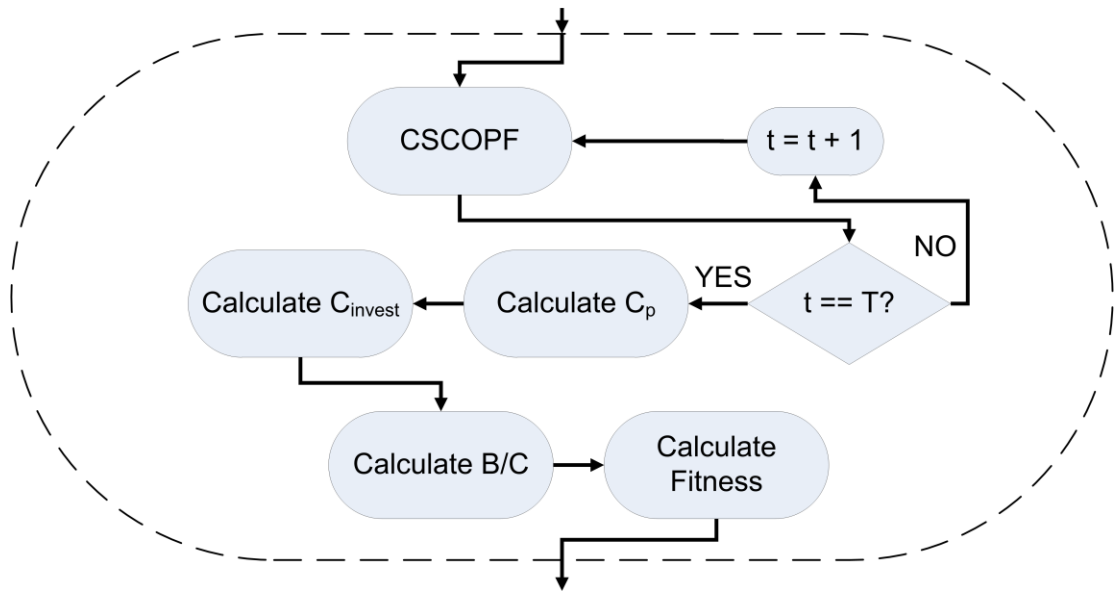


Figure 77: Flowchart for the fitness function.

The fitness function then computes the benefit-to-cost ratio (B/C) of the individual as seen in (Eq. 51), where $C_{trans,new}$ is the annualized cost of the new transmission elements of the individual and $C_{prod,base}$ is the annual production cost of the

base case. If the individual's benefit-to-cost ratio is below the planning framework's threshold ratio, the individual fitness is adjusted downward to deter similar solutions.

$$C_{prod} = \sum_{g \in \Omega_{GEN}} \sum_{t \in \Omega_{TIME}} (w_t)(b_g)(P_{g,t}) \quad (\text{Eq. 50})$$

$$\frac{B}{C} = \frac{(C_{prod,base} - C_{prod})}{C_{trans,new}} \quad (\text{Eq. 51})$$

5.3.2. Planning Tool Design Specific to each Planning Framework

The following sub-sub-sections describe how the tool was designed to ensure compatibility with each of the planning frameworks.

5.3.2.1. Specifics to the Centralized Transmission Planning Process and the Revised Centralized Transmission Planning Framework

For both the centralized planning process and revised centralized framework, a centralized transmission expansion plan (CTEP) will be generated for each planning period. Each CTEP must exceed the benefit-to-cost ratio threshold. The CTEP is assumed to be generated in advanced so the investments are realized by the operational year corresponding to the first year of the planning period. The MISO uses a benefit-to-cost threshold of 1.4 for investments online within two years and a benefit-to-cost threshold of three for investments online within ten years [66]. To capture the varied nature of investment commissioning dates, a benefit-to-cost threshold of two will be assumed for the centralized planning process and revised centralized framework. The

centralized transmission planning process is not permitted to deploy PF controllers while the revised centralized framework is.

5.3.2.2. Specifics to the Hybrid Transmission Planning Framework

The hybrid framework simultaneously supports revised centralized planning and MEP planning. For each planning period, the CTEP is developed assuming the MEPs announced in the prior planning periods are online. The CTEP is announced before the beginning of the MEP planning season. Each pipeline developer integrates the newest CTEP into their investment analysis. Centralized planning and the MEP planning season are assumed to each occur once per planning period.

The MEP planning season begins when a developer commits to build a MEP investment by the year corresponding to the start of the planning period. As part of the commitment, the developer specifies the source bus, the destination bus, the transaction path, location and ratings of the PF controllers, and the contracted capacity. The hypothetical investment must meet two requirements beyond complying with the security constraints. First, the annual LSE benefit must exceed the cost of the investment. Although the pipeline may provide other financial benefits to the system, the only guaranteed source of revenue is the LSE benefit and thus a conservative developer requires LSE benefit to meet or exceed investment and operation costs. Second, the regulator requires that the annual COE must be the same or lower with the investment than without it. The second requirement is to avoid predatory investments and is akin to the regulatory approval of natural gas pipelines. A MEP transaction infeasible under an

n-1 condition may be built provided that the system is compliant with equipment ratings during the contingency while serving all load, including the full load of the benefiting LSE.

Following commitment to an investment, other developers assume the committed investment will be online at the start of the planning period and for all subsequent planning periods. Developers continue to commit to profitable investments until no additional profitable investments exist. Once the final investment is announced, the MEP planning season closes.

Since the LSE is the sole owner of the capacity of a MEP, the LSE has the option to suspend the contracted transaction and offer spare control capacity for the benefit of other market participants. For all cases, spare control capacity will be made available to the system operator

The LSE may wish to suspend the transaction provided two prerequisites are met. First, the reduction in production cost with the suspension in place must be greater than the increase in the LSE's costs. Second, the LSE must have a mechanism to profit from the suspension. Given that the LSE has complete control over the MEP, it may be possible to create a market mechanism by which the LSE foregoes the transaction in exchange for payment. Ideally, prior to each operating hour, each LSE with a MEP would decide independently whether to suspend its transaction. A simplified problem is to compare the savings in production cost with all MEP transactions suspended to the total increase in cost for the LSEs suspending the transactions. If the savings exceed the

cost, all transactions are suspended without determination of the optimal set of suspensions.

It is not clear if a market can be established to allow the exchange of spare control capacity. It is also not clear if the potential savings from such rules justify the transaction costs. However, if new rules are feasible and affordable, said transactions may represent a substantial increase in the benefits of owning a MEP. These estimated revenues could lead to more transmission expansion.

To simplify solution of the MEP planning problem, the set of committed MEPs as a whole are required to improve COE but the requirements on individual investments are neglected. This is reasonable if a controllability market develops to allow LSEs to suspend their PPOs and sell the controllability of their MEPs.

MEP development in the hybrid framework will be limited to controllable investments, as a MEP requires controllability by definition. To reduce scope, a MEP may only be deployed on an existing transmission asset. For a given circuit, the sum of all investments must be compliant with (Eq. 53). However, the capacity of a PF controller may be expanded over time.

5.3.2.3. Capabilities and Limitations of the Proposed Planning Tool

The planning tool developed in this chapter simulates complexity that has not been identified in literature or commercial planning tools. The hybrid framework, which appears to be a salient departure from known precedent in the electric power sector, is grounded in the economic theory of natural gas pipelines and in proven technology.

Despite the complexity of the planning tool, a number of simplifications have been proposed:

- Generator expansion, construction, and retirement are solved exogenous to the planning period. Thus the ability to reduce generation capacity requirements via transmission expansion is not considered. Subsequently, capacity payments made by LSEs to owners of MEPs are not considered.
- Under the centralized planning process, PF controllers are excluded from the set of permissible transmission investment choices.
- Merchant transmission development is nonviable under the centralized planning process and revised centralized framework. This seems reasonable given the current dearth of merchant transmission investments.
- Power system stability is not guaranteed.
- The response of demand to short-term and long-term price variations is neglected.
- The reserve market is not modeled.
- Generator contingencies are not considered as they are typically accounted for in the reserve markets.
- The planning tool is not able to select from the full set of transmission investment choices. Salient options not included in the choice set include HVDC line construction, dynamic thermal rating systems, and system topology changes.
- All market players are assumed competitive and consequentially there is no market power.

- The inputs to the planning tool (forecasted load, generation capacity, cost of the permissible transmission investment choices, policy changes and fuel prices) are assumed to be perfect forecasts.
- The planning tool does not capture the relationship between investment lead-time and benefit-to-cost hurdle rate.
- When used to generate a CTEP, the tool assumes cost allocation issues are surmountable provided a CTEP is welfare-enhancing and meets the benefit-to-cost threshold. This ignores the transaction costs and contentiousness of cost allocation.
- The planning tool does not endogenously balance the economic cost of reliability with the economic benefit. Rather, the reliability requirement is a pre-defined constraint on the solution.
- Deployment of energy storage is not considered.

5.4. Comparison of Frameworks and Demonstration of Planning Tool

This section describes the demonstration of the planning frameworks via application of the appropriately-configured planning tool to a common test system. Each framework is evaluated over a 20-year planning horizon, with two ten-year planning periods per planning horizon. The 20-year horizon spans the duration of most RPS phase-in periods and is consistent with, or longer than, known transmission plans.

The section includes a description of five components of the demonstration:

- Metrics,
- Propositions,

- The test system,
- Unit cost of transmission investment, and
- Results

5.4.1. Metrics

The following metrics will be used to test the transmission planning frameworks:

- **Cost of Energy (COE):** As described in (Eq. 47) on p. 144, COE is the total cost of electricity expenditures over the planning horizon. COE includes the cost of system operation, investment during the planning period, and investment during prior planning periods.
- **Total carbon emissions (TCE):** Total emissions produced by the electric sector over the entire planning horizon. Emissions resulting from the fabrication and installation of transmission assets or generation capacity are not included.

5.4.2. Propositions

To compare the planning frameworks, three propositions were proposed prior to applying the frameworks to the test case:

- **Proposition 1:** The COE will be lower for the revised centralized framework than the centralized planning process.
- **Proposition 2:** The COE will be lower for the hybrid framework than the revised centralized framework.
- **Proposition 3:** When applied to a system with renewable generation subject to curtailment because of congestion, the revised centralized framework and hybrid framework will produce lower emissions than the centralized planning process.

5.4.3. Test System

The Garver five-bus system used for the CSCOPF demonstration is the base case for the framework demonstration. The Garver system has been used to test other transmission planning tools [277,283,284,285,286,287,288,289,290,291,292,293,294]. Two planning periods were considered, 2014-2023 and 2024-2033. A common generation scenario served as the base case for the first planning period of each framework. The generator types and bus assignments used for the CSCOPF demonstration are retained for the planning framework/tool demonstration. Generator costs are adjusted based on the planning period. The wind generator is sized to comply with a 16.67% RPS during the first planning period, if the wind generation is not curtailed.

For production cost studies involving stochastic renewable generation, a common approach is to simulate all hours of each year of the study period [44,45]. This is deemed computationally untenable for a planning study. Instead, two operational hours are simulated for each planning period. One operating hour represents the 10% highest load hours. The other operating hour represents the loading during the remaining 90% of the hours. Loads are scaled in each planning period to represent expected growth in US annual demand over the two planning periods [295]. Load during the hour representative of low-load condition is adjusted using the 2010 ratio of US peak load to annual average load, assuming average load during the high-load period equaled peak load [26]. The base case has no PF controllers.

The assumed generation parameters matched those used for the CSCOPF, which in turn match the current US generation fleet. The assumed production costs are based on

EIA projected fuel prices for each planning period. Variable O&M costs are based on EIA projections [159]. Capacity costs and carbon emissions are calculated as described in Appendix F. A carbon cost of \$0 dollars per ton of carbon is used for the calculation of production costs. The production costs for the first planning period are shown in Table 12. A 15 minute time limit for post-contingency action is assumed, matching the time limit of the CSCOPF demonstration.

Table 12: Production costs for the first planning period.

Generation Type	Production Cost (2010\$/MWh)
Natural Gas CCGT	36.67
Natural Gas OCGT	64.55
Natural Gas Steam Turbine	54.62
Pulverized Coal	29.87
Wind	0.00

The distances between bus-pairs, as specified by Garver in [296], are used. The assumed maximum number of circuits between any bus-pairs is two. All $n-1$ transmission contingencies are included in set of contingency events considered by the CSCOPF. The annualized cost of transmission investments prior to the start of the planning horizon are calculated in the same manner as the cost for transmission investments within the planning horizon.

The planning tool is run for each framework separately. For the first planning period, common generation capacity, transmission topology and load levels are assigned. For subsequent planning period, generation and transmission topology are assigned based

on the results of the prior planning period. Thus, the inputs to planning periods after the first could vary by framework. For the test system, the load in the second planning period is higher than the first planning period, based on expected load in 2033 relative to 2024 [295]. Following completion of the first planning period, the generation scenarios are updated separately for each planning framework, based on the transmission investments made in the prior planning period. The intent of the generation update is to meet load growth and comply with a 33% RPS using minimal generation investment. Surplus natural gas capacity is retired.

Figure 78 shows the transmission network parameters, generation capacities, and peak load levels for the base case. The base case represents the system that will be operated during the first planning period if no investments are made.

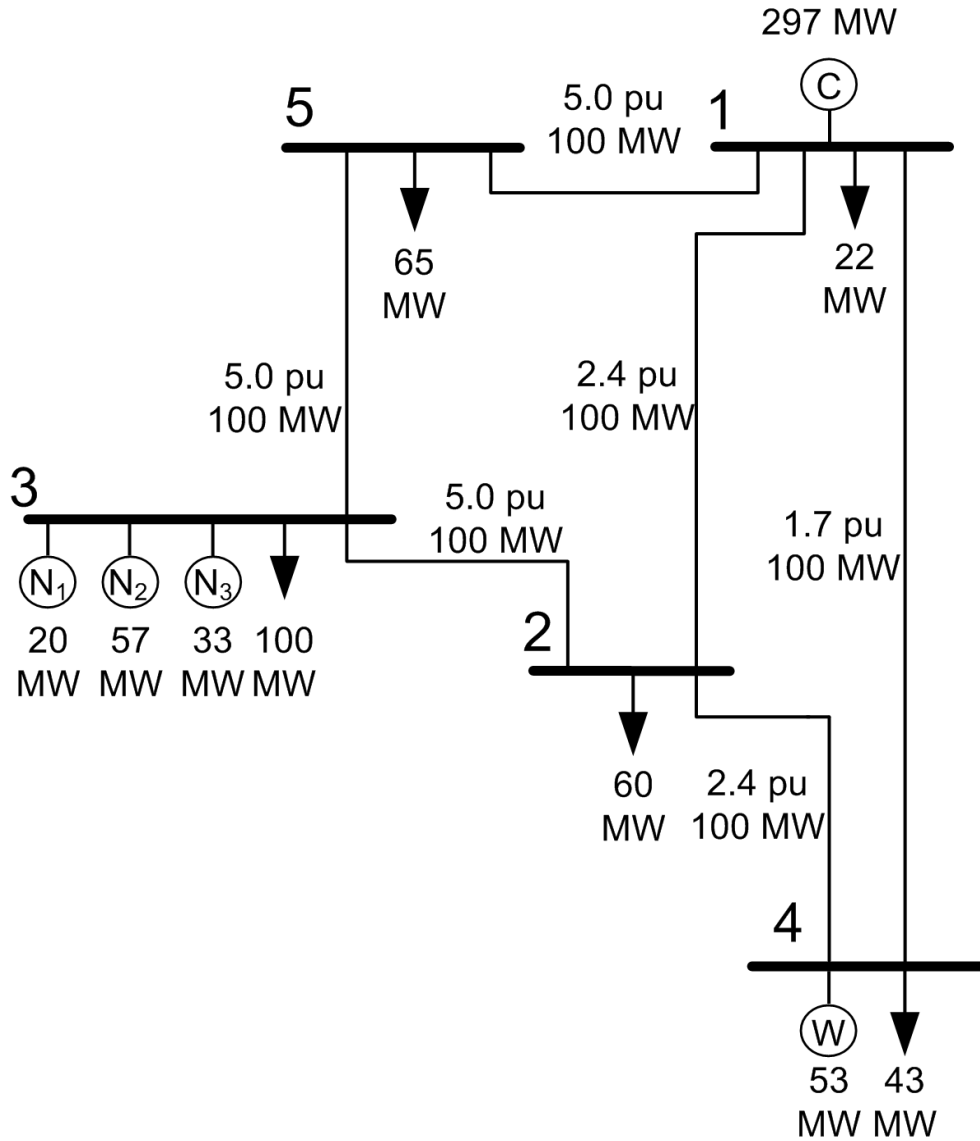


Figure 78: Base case system. The line values represent the admittance and max power flow. The generator types are designated by C, G, and W for coal, CCGT natural gas, and wind respectively. The generator values indicate the generator capacity. The load values indicate the peak load.

5.4.4. Unit Cost of Transmission Investment

The cost of a new or existing transmission circuit is normalized on a \$/MW-mile basis. When in doubt, assumptions are made to lower the effective cost of new transmission so as to not bias the results toward PF controllers. The normalized cost of

transmission, \$3,541/MW-mile (2010\$), is developed using AEP data for a 300 mile, 345 kV line operating at an SIL value of 1 [297]. Except for an AEP 765 kV line, with a cost of \$1,432/MW-mile (2010\$), this cost is the lowest of surveyed costs [298,299,300]. The \$/MW-mile cost is found to increase by no more than 23% if the cost of a new substation is included, provided the line length is at least as long as the minimum distance (20 miles) of the Garver case. Since a new substation would likely not be required if a line is added to an existing bus and the result, the substation cost is neglected.

The costs of the PF controller are modeled as function of impedance for the impedance-injection controllers and injected MVA for the angle-injection controllers. The installed cost of a TCSC cost is modeled as a quadratic function of MVA_r in [139]. This reference is derived from a 2000 Siemens Report to the World Bank that is no longer available. The TCSC cost model is updated to 2010 values using the producer price index (PPI) [301]. The cost-per-phase equation is shown in (Eq. 52), where x is the TSCS MVA_r.

$$C_{TCSC} = (0.0015x^2 - 0.713x + 153.75) \frac{PPI_{2010}}{PPI_{2000}} \quad (\text{Eq. 52})$$

DSR cost is modeled based on pre-commercial estimated material cost as well as a markup. The total cost estimate is \$2,000 (2010\$) for a 47 μH module, irrespective of line current or line voltage. The fleet of modules on a given circuit are assumed to be

dispatchable in real-time from no impedance injection to the aggregate impedance of the fleet.

The PST cost model assumes use of a double core design. Cost is modeled as a function of positive injection angle ($\theta_{max,p}$), negative injection angle ($\theta_{max,n}$), and the power rating of the line to which the PST is connected (F_{max}). The model, shown in (Eq. 53)-(Eq. 56) calculates cost (C_{PST}) as a function of the rating of the shunt ($S_{PST,sh}$) transformer of the PST. The cost parameter of \$10,300/MVA (2010\$) is determined by fitting the model to two recent PST installations – a 1,200 MVA, +/-40 degree unit in Slovenia [302,303] and a 800 MVA, +/-35 degree unit in the United States [304, 305].

$$S_{PST,sh} = \max\left(F_{max}\left(\sin\left(\theta_{max,n}\right)\right), F_{max}\left(\sin\left(\theta_{max,p}\right)\right)\right) \quad (\text{Eq. 53})$$

$$S_{PST,n} = F_{max}\left(\sin\left(\theta_{max,n}\right)\right) \quad (\text{Eq. 54})$$

$$S_{PST,sh} = \max\left(S_{PST,p}, S_{PST,n}\right) \quad (\text{Eq. 55})$$

$$C_{PST} = 10300\left(2S_{PST,sh}\right) \quad (\text{Eq. 56})$$

Similar to the PST, the FR-BTB 2010\$ cost is modeled as a function of maximum injection angles and line rating. The model, shown in (Eq. 57) and (Eq. 58), includes a cost component due to line power rating (F_{max}) and due to converter rating (S_{FRBTB}). The second term is proportional to converter rating. The \$6,667/MVA cost parameter is for a transformer rated one-half the converter rating. The cost parameters are based on hardware prototypes developed as part of the ARPA-E ADEPT project. A markup factor (m) of 1.25 is used to translate from materials cost to customer price.

$$S_{FRBTB} = F_{max} \left(\max \left(\sin(\theta_{max,p}), \sin(\theta_{max,n}) \right) \right) \quad (\text{Eq. 57})$$

$$C_{FRBTB} = (26667F_{max} + (53333 + 6667)S_{FRBTB})m_{markup} \quad (\text{Eq. 58})$$

A common 15% carrying cost is used for all transmission investments. The economical lifetime of the DSR and FR-BTB may be less than the typical 40-year lifetime of transmission lines. Based on [276], the carrying cost of a 40-year transmission line is roughly 14.2%. Asset lifetimes of 10 and 20 years result in carrying costs of 22.8% and 16.2% respectively. It is assumed that PF controllers have a lifetime of at least 20 years, leading to the assumed 15% carrying cost for all investments. The carrying cost assumes annual O&M cost of 3% of the initial investment cost, adjusted annually for 2% inflation.

5.4.5. Results

Under the centralized planning process, no transmission is added during the first planning period or the second planning period. This has two implications. First, the transmission system at the start of the first planning system was sufficient to meet reliability requirements over the course of the planning horizon. Second, reduction of congestion via transmission investment did not meet the benefit-to-cost threshold. The primary result metrics are shown in Table 13. The system topology at the end of the second planning period is shown in Figure 79. There was no wind curtailment in either planning period.

Table 13: Centralized transmission planning process results.

	Planning Period		Annual Costs (2010\$)			
	COE (2010\$)	Emissions (tons CO ₂)	Production	Capacity	Transmission	Total
1st Decade	8.19E+08	9.85E+06	2.81E+07	4.31E+07	1.06E+07	8.19E+07
2nd Decade	1.09E+09	8.44E+06	2.69E+07	7.12E+07	1.06E+07	1.09E+08
Average	9.53E+08	9.14E+06	2.75E+07	5.72E+07	1.06E+07	9.53E+07

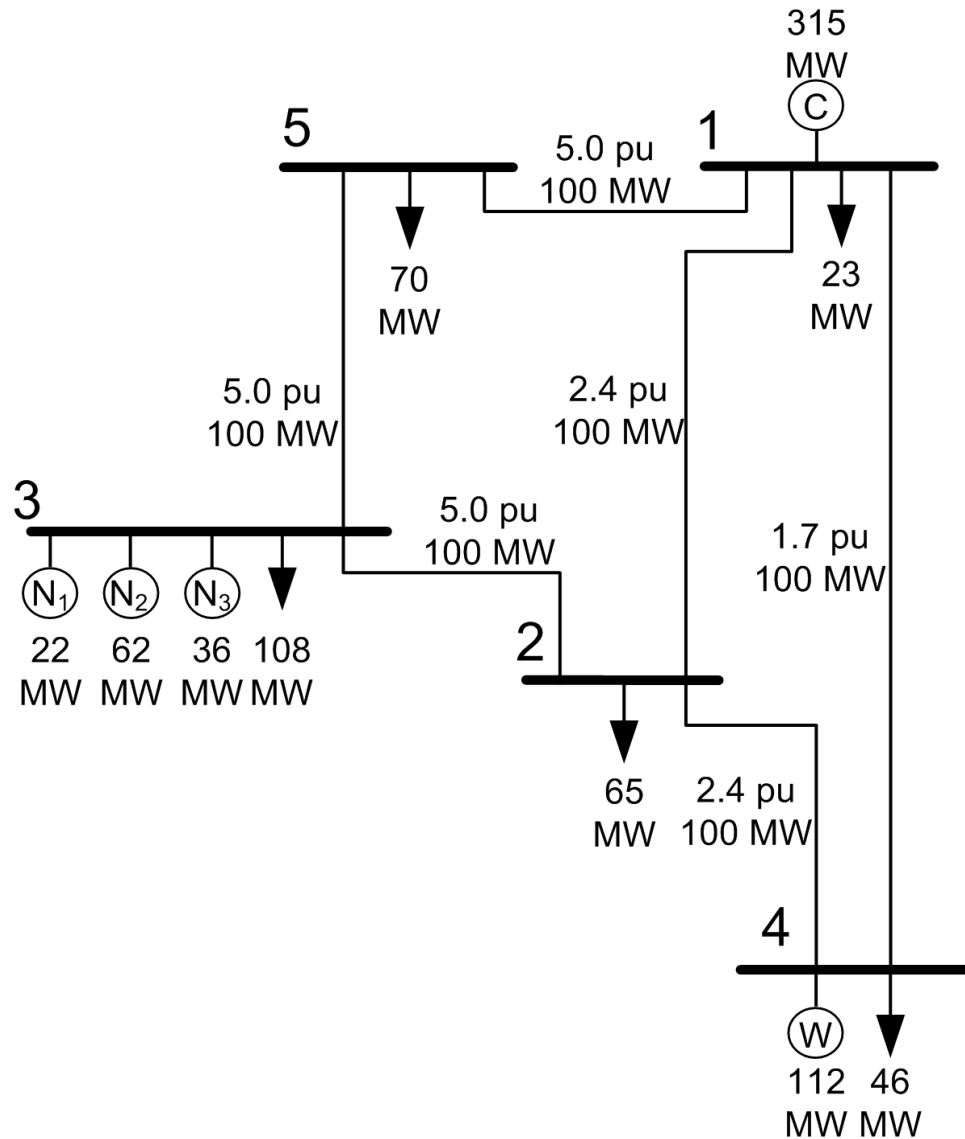


Figure 79: System topology, generation capacity and peak load at the end of the second decade under the centralized transmission planning process.

Under the revised centralized framework, two PSTs are added in the first planning period and two PSTs are added in the second period. The primary metrics are shown in Table 14. The system topologies at the end of the first and second planning periods are shown in Figure 80 and Figure 81 respectively. There was no wind curtailment in either planning period.

Table 14: Revised centralized transmission planning framework results.

	Planning Period		Annual Costs (2010\$)			
	<i>COE (2010\$)</i>	<i>Emissions (tons CO₂)</i>	<i>Production</i>	<i>Capacity</i>	<i>Transmission</i>	<i>Total</i>
1st Decade	8.15E+08	1.01E+07	2.76E+07	4.31E+07	1.08E+07	8.15E+07
2nd Decade	1.02E+09	8.78E+06	2.61E+07	6.50E+07	1.08E+07	1.02E+08
Average	9.17E+08	9.46E+06	2.68E+07	5.41E+07	1.08E+07	9.17E+07

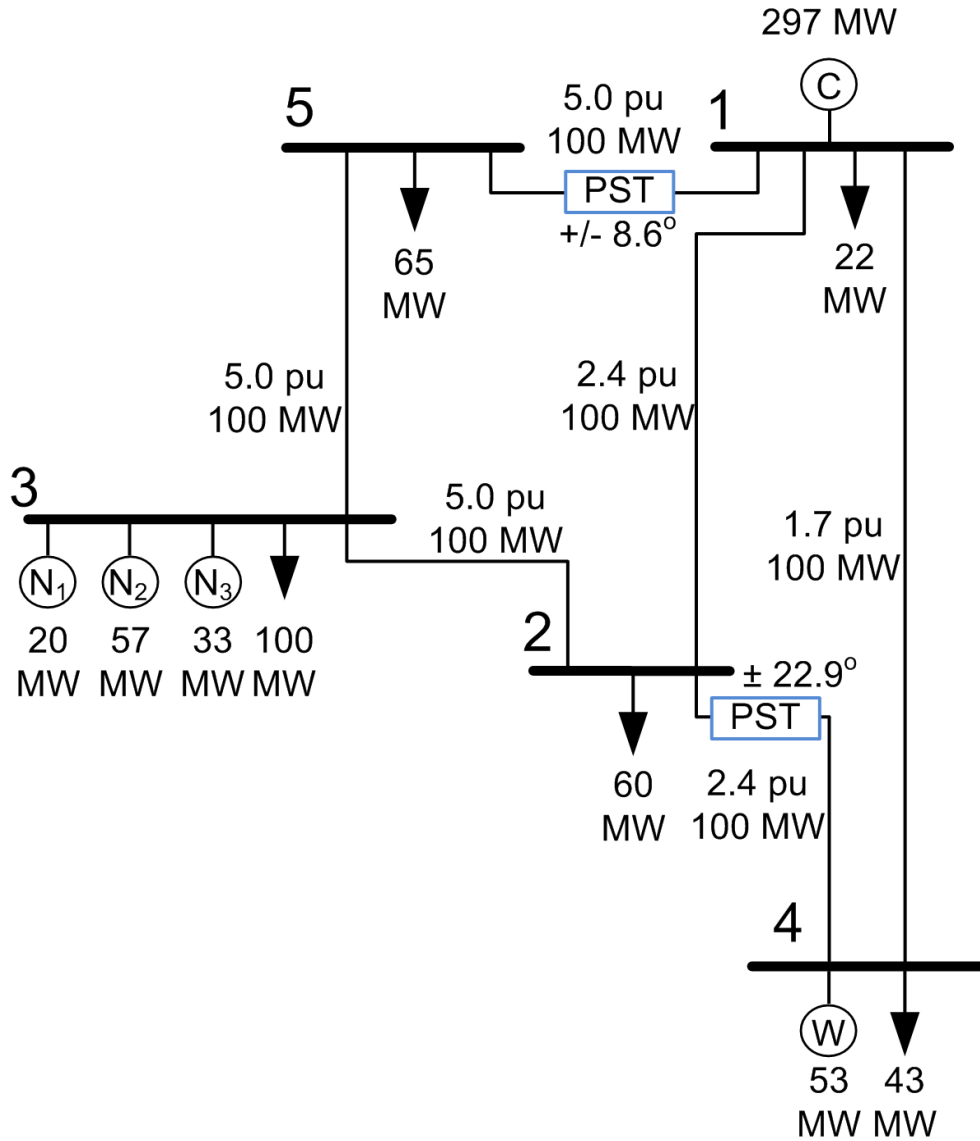


Figure 80: System topology, generation capacity and peak load at the end of the first decade under the revised centralized transmission planning framework. Transmission assets added in the first decade are shown in blue.

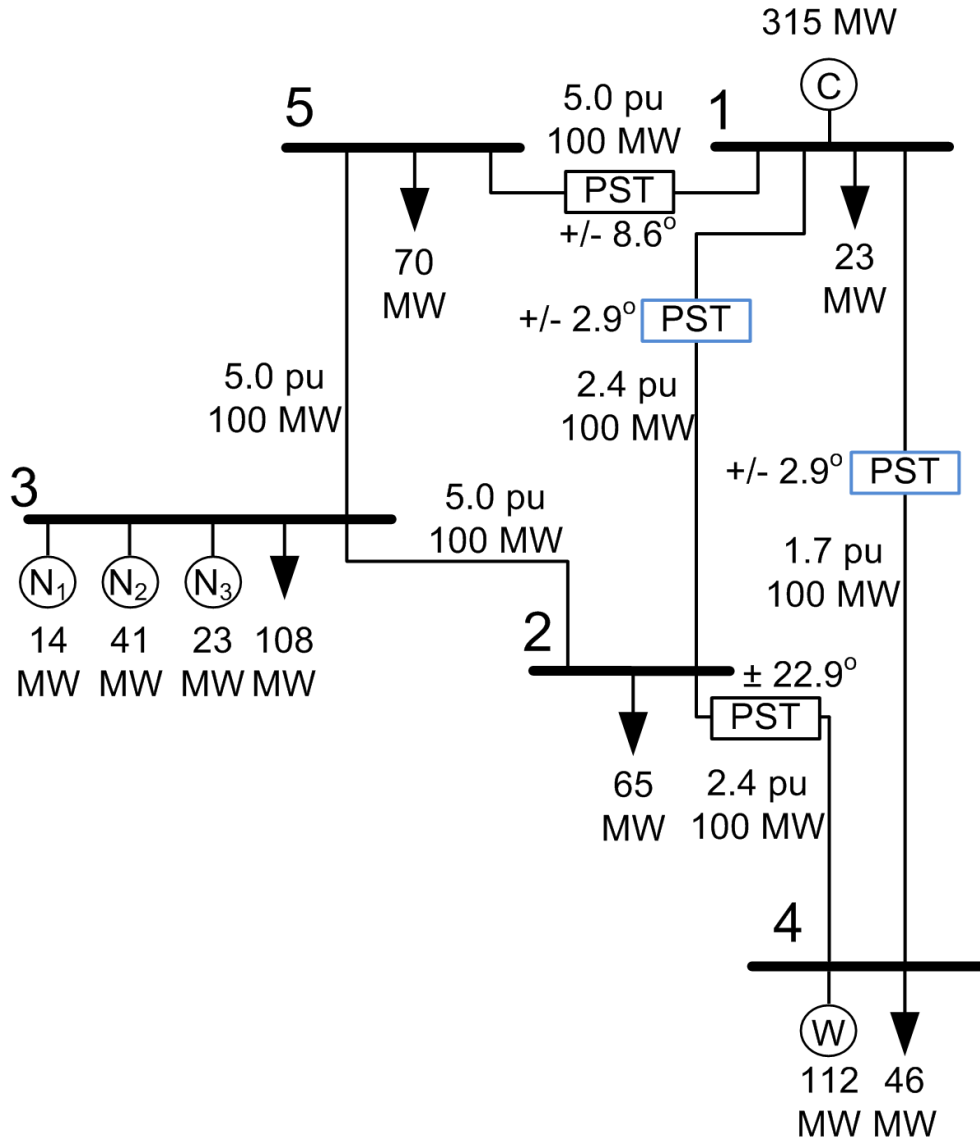


Figure 81: System topology, generation capacity and peak load at the end of the second decade under the revised centralized transmission planning framework. Transmission assets added in the second decade are shown in blue.

Under the hybrid framework, two investment plans are generated per decade, a centralized plan and a MEP plan. In the first decade, the centralized plan matches that found by the revised centralized framework and no MEPs were built. In the second decade, the centralized plan matched the results of the revised centralized plan and no

MEPs were built. The results are shown in Table 15. The system topologies for the first and second decade match those shown above in Figure 80 and Figure 81. There was no wind curtailment in either planning period.

Table 15: Hybrid transmission planning framework results.

	Planning Period		Annual Costs (2010\$)			
	<i>COE (2010\$)</i>	<i>Emissions (tons CO₂)</i>	<i>Production</i>	<i>Capacity</i>	<i>Transmission</i>	<i>Total</i>
1st Decade	8.15E+08	1.01E+07	2.76E+07	4.31E+07	1.08E+07	8.15E+07
2nd Decade	1.02E+09	8.78E+06	2.61E+07	6.50E+07	1.08E+07	1.02E+08
Average	9.17E+08	9.46E+06	2.68E+07	5.41E+07	1.08E+07	9.17E+07

Table 16 compares the costs and emissions over the 20-year planning horizon for all three planning frameworks. The results support the first proposition that the COE under the revised centralized framework will be lower than the centralized planning process. The results do not support the second proposition, that COE under the hybrid framework will be lower than the revised centralized framework, but are insufficient to reject it. The third proposition, that emissions will be lower for cases with wind generation under the revised centralized and hybrid frameworks if wind output is curtailed in the centralized planning process, is not testable given the lack of curtailment in the centralized planning process. The revised centralized and hybrid frameworks avoid constructing new transmission lines over the planning horizon.

Table 16: Comparison of results across frameworks.

	COE		Emissions	
	<i>Absolute (2010\$)</i>	<i>Fraction of Centralized</i>	<i>Absolute (tons CO₂)</i>	<i>Fraction of Centralized Emissions</i>
Centralized	1.91E+09		1.83E+07	
Revised Centralized	1.83E+09	0.962	1.89E+07	1.034
Hybrid	1.83E+09	0.962	1.89E+07	1.034

Each planning period of each framework was solved four times. In all cases, at least two of the four solutions for a given decade and framework were identical and provided the highest fitness of the four solutions.

The planning tool does not quantify the value of fast controllers, like the FR-BTB, to mitigate stability issues. Assuming the PF controller set points are refreshed every 5 minutes, the FR-BTB is more expensive per MVA than the PST to own and operate. This result holds true even if expected PST O&M costs are increased by an order of magnitude. That said, the TCSC and PST may be unacceptable due to their centralized design, substation space requirements, O&M cost, or response time. To quantify the potential impact of the fast controllers, planning with the revised centralized and hybrid frameworks is rerun, with TCSCs and PSTs removed from the set of permissible transmission investment choices. Whether under the revised centralized or hybrid frameworks, no investments were made in either planning period. Thus the results match those of the centralized planning process.

Table 17 shows the average solution time and average search efficiency to complete the planning study for the entire 20-year planning horizon. The search efficiency is a function of the number of CSCOPF runs executed by the planning tool

over the planning horizon (n) and the number of CSCOPF runs which would be required for an exhaustive search ($n_{exhaustive}$).

Table 17: Planning tool solution time and search efficiency by framework.

	Solution Time	Search Efficiency
	<i>hours</i>	$\log_{10}\left(\frac{n}{n_{exhaustive}}\right)$
Centralized	23.2	-31.6
Revised Centralized	113.1	-65.2
Hybrid	156.9	-65.0
Revised Centralized - DSR and FR-BTB only	95.2	-60.9
Hybrid - DSR and FR-BTB only	106.16	-60.8

5.5. Discussion

The primary contributions of this chapter are:

- A *merchant electrical pipeline* (MEP) framework to increase the utilization of existing transmission lines within a merchant framework,
- the hybrid transmission planning framework, allowing the coexistence of centralized planning and MEPs,
- an automated transmission planning methodology compatible with the proposed frameworks and better aligned with the choices facing transmission planners, and
- the development of an automated planning tool based on the proposed methodology.

If viable, the MEP framework may transcend the primary obstacle of merchant transmission investment by guaranteeing long-term income and reducing first-mover disadvantage relative to a generation developer. However, the full value of the framework requires a market for controllability, allowing the LSEs to monetize the option to forego delivery of contracted energy and offer use of the PF controllers. This work has not quantified the value of MEPs in the absence of a market for controllability.

In the test system, the hybrid framework showed no advantage relative to the revised centralized framework. In addition, the automated transmission tool did not deploy fast controllers. It remains to be seen if the hybrid framework shows relative advantage for other system topologies, fuel prices, and load profiles.

The solution time of the planning tool is a critical impediment to practical application. Application of the existing tool with existing assumptions and resolution to a realistic system size of 4,000 buses results in a problem three million orders of magnitude larger than the test problem if using the revised centralized framework. Unless search efficiency shows increasing returns to scale, application of the planning tool is untenable. Suggestions to improve the solution time are discussed in Chapter Six.

CHAPTER 6

CONTRIBUTIONS, FUTURE WORK, AND CONCLUSIONS

6.1. Contributions

The primary contributions of the work are listed below and then described in more detail.

- Proposal of the *merchant electrical pipeline* (MEP) framework, based on the regulatory precedence of natural gas transmission pipelines, which augments existing transmission assets with PF controllers to realize IPF transactions.
- Proposal of a hybrid transmission planning framework, allowing the co-existence of MEP development and centralized transmission planning.
- Proposal of a methodology to perform corrective security-constrained optimal power flow (CSCOPF) in a system with PF controllers or IPF transactions, solving generator set points and PF controller set points when all assets are online and during contingencies.
- Development of a CSCOPF tool based on the proposed CSCOPF methodology.
- Proposal of an automated transmission planning methodology applicable to transmission systems with large numbers of PF controllers and compatible with the centralized, revised centralized and hybrid transmission planning frameworks.
- Development of an automated transmission planning tool consistent with the proposed planning tool methodology.

- Proposal of *incremental packetized energy* to increase transmission, distribution, and generation utilization at a fraction of the cost of conventional *packetized energy*.

6.1.1. Merchant Electrical Pipeline Framework

The MEP framework augments existing transmission assets with PF controllers to realize IPF transactions. The framework creates a long-term power purchase option (PPO) between the owner of the MEP and the LSE receiving the power. The duration of MEP development may be shorter than new transmission line development since a MEP can be constructed by installing PF controllers on existing transmission assets. The combination of the long-term PPO and short development duration may enable the MEP framework to transcend obstacles which have historically inhibited merchant transmission investment.

6.1.2. Hybrid Transmission Planning Framework

A sudden shift from the current centralized planning process to the proposed MEP framework appears untenable. The hybrid framework allows centralized planning and MEP development to co-exist. Centralized planning provides a process to guarantee reliability and ensure that investments with compelling societal benefit are built. MEP development allows savings to be achieved which are currently unrealizable with the centralized planning process, due to the delay and uncertainty induced by the presence of multiple stakeholders and the lack of agreement on how to allocate costs and benefits to stakeholders.

6.1.3. CSCOPF Methodology

The proposed CSCOPF methodology enables PF controllers to participate in the secure, economical operation of the power system. Prior known CSCOPF methods do not allow PF controllers to participate in post-contingency actions. The common alternative has been to rely on PSCOPF which does not leverage the ability of PF controllers to change post-contingency power flows. Incorporating PF controllers into the CSCOPF may result in lower production costs and the ability to reliably serve more load than a PSCOPF or a CSCOPF which does not allow post-contingency operation of PF controllers. In addition, the proposed methodology is compatible with simultaneous operation of undesigned flows and IPF transactions. The ability to simultaneously simulate undesigned flows and IPF transactions may facilitate the realization of the hybrid framework.

6.1.4. CSCOPF Tool Development

The CSCOPF tool is based on the proposed CSCOPF methodology. The tool solves the generator and PF controller set points that minimize production costs while ensuring security. The tool was demonstrated on two test systems. For both test systems, more load was able to be serviced using the CSCOPF than the PSCOPF. In addition, the test systems with PF controllers have production costs equal to or less than otherwise identical systems without PF controllers.

6.1.5. Automated Transmission Planning Methodology

The proposed automated transmission planning methodology is compatible with the centralized, revised centralized, and hybrid frameworks. The methodology simultaneously selects transmission line reactance, transmission line rating, PF controller

type, and PF controller rating. This as an improvement over known transmission planning methods, which are not compatible with the proposed frameworks and typically either select bus-pairs to be connected with a transmission line or the location and rating of PF controllers.

6.1.6. Automated Transmission Planning Tool

The automated transmission planning tool is based on the proposed automated transmission planning methodology. The planning tool is compatible with the centralized planning process, the proposed revised centralized framework, and the proposed hybrid framework. The solution of the hybrid framework assumes the LSEs holding PPOs sell controllability in the controllability market if the benefit of such sale exceeds the benefit of executing the option and receiving delivery. The planning tool was applied to a test system under the centralized planning process, the revised centralized framework, and the hybrid framework. For the test system, the revised centralized and hybrid frameworks provide lower production cost than the centralized framework. The results indicate that the planning tool requires 30-40 orders of magnitude less executions of the CSCOPF than would have been required for an exhaustive search.

6.1.7. Demonstration of Benefit of Packetization

The proposed *incremental packetized energy* concept is expected to exhibit some of the benefits of *packetized energy* at lower cost than existing *packetized energy* concepts. The concept eliminates the need for grid-dedicated energy storage by using flexible loads. A flexibly charged GEV is a sample flexible load. Flexible charging does not require V2G control, avoiding the associated battery degradation and power system impacts. Meanwhile, IPF control provides the means to utilize spare transmission

capacity to serve flexible loads. Demonstration with a test system showed that under peak load conditions, flexible load as large as or greater than the traditional load could be served while simultaneously serving traditional load subject to $n-1$ constraints.

So far, this work has generated one journal publication, six conference papers, one encyclopedia entry and one book chapter, as shown below.

D.G. Choi, F. Kreikebaum, V.M. Thomas, D. Divan, "Coordinated EV Adoption: Double-Digit Reductions in Emissions and Fuel Use for \$40/Vehicle-Year," *Environmental Science & Technology*, vol. 47, no. 18, pp. 10703-10707, 2013.

F. Kreikebaum, D. Das, Y. Yang, F. Lambert, D. Divan, "A distributed, low-cost solution for controlling power flows and monitoring transmission lines," in *IEEE PES Innovative Smart Grid Technologies Europe*, Gothenburg, 2010, pp. 1-8.

F. Kreikebaum, M. Imayavaramban, D. Divan, "An inverter-less static series compensator," in *IEEE Energy Conversion Congress & Expo*, Atlanta, GA, 2010, p 3626-3630.

D. Das, F. Kreikebaum, D. Divan, F. Lambert, "Reducing transmission investment to meet renewable portfolio standards using smart wires," in 2010 IEEE PES Transmission and Distribution Conference and Exposition, New Orleans, LA, 2010, pp. 1-7.

F. Kreikebaum, D. Das, D. Divan, "Reducing transmission investment to meet renewable portfolio standards using controlled energy flows," in *IEEE Conference on Innovative Smart Grid Technologies*, Gaithersburg, MD, 2010, pp. 1-8.

F. Kreikebaum, D. Das, H. Hernandez, D. Divan, "Ubiquitous power flow control on meshed grids," in *IEEE Energy Conversion Congress & Expo*, San Jose, CA, 2009, pp. 3007-3914.

F. Kreikebaum, D. Divan, “Smart Grids, Distributed Control for,” in *Encyclopedia of Sustainability Science and Technology*, R. Meyers, Ed. New York, NY: Springer, 2012.

F. Kreikebaum, D. Divan, “Smart Grids, Distributed Control for,” in *Electrical Transmission Systems and Smart Grids*, M. Begovic, Ed. New York, NY: Springer, 2013.

6.2. Future Work

Further effort is required to test the impact of the proposed frameworks and methodologies in realistic systems. The suggested future efforts are categorized in the list below and then described in more detail.

- Explore the feasibility of MEPs
- Scale the CSCOPF tool to realistic systems
- Scale the planning tool to realistic systems and assess propositions
- Augment the CSCOPF tool to model IPF transactions and the controllability market
- Improve the modeling of stability constraints in the CSCOPF tool
- Improve the modeling of planning tool choices

6.2.1. Explore the Feasibility of Merchant Electrical Pipelines

The MEP framework is proposed based on a limited search of the pertinent regulatory, policy, and planning elements. The framework, as defined, assumes that the precedence of incremental investment in the natural gas pipeline sector can be applied to the electric transmission sector. The MEP framework also requires that the base investment can be regulated while the incremental investment can be merchant. In natural gas, both the base and incremental investments are typically merchant. Further

study is warranted to assess feasibility and determine if framework modifications are required.

6.2.2. Scale the CSCOPF Tool to Realistic Systems

The CSCOPF has not been tested on a system larger than 39 buses. In comparison, realistic systems have orders of magnitude more buses. For example, the PJM LMP model has 10,299 pricing nodes [306]. If solution of realistic systems is not tenable in a reasonable timeframe with the existing CSCOPF tool, modifications are required.

6.2.3. Scale the Planning Tool to Realistic Systems and Assess Propositions

As discussed at the end of Chapter Five, the current planning tool will not solve realistic systems unless search efficiency improves fast enough to offset the increase in search space size. Such an improvement in search efficiency is unexpected. Therefore, other mechanisms are required to scale the planning tool. Some possibilities include constraining the number of feasible bus-pairs. The current planning tool is allowed to connect any given bus with any other bus. Constraining the search space to existing circuits would reduce the order of the search space of a typical 4,000 bus system by 99.97% relative to allowing 2 circuits per bus-pair and all bus-pair combinations. However, this would preclude new connections. To allow new bus-pair combinations without the search space ramifications of allowing every bus-pair combination, a certain percentage of bus-pairs could be designated as hubs. These hubs could be allowed to connect to other hubs. Allowing the development of hub interconnection, modification/rebuild of existing circuits, and construction of circuits parallel to existing

circuits may be an adequate compromise between a solvable search space and an economically desirable solution.

6.2.4. Augment the CSCOPF Tool to Model Incremental Power Flow Transactions and the Controllability Market

The full value of the hybrid and MEP frameworks requires a market for LSEs to monetize the option to forego delivery of contracted energy and offer pipeline controllability to the market. The CSCOPF methodology proposed a method to accommodate IPF transaction but this functionality was not built-into the CSCOPF tool. Instead, the CSCOPF tool assumes all controllability is sold to support overall system optimization. To assess the viability of IPF control in the absence of a market for controllability, it would be helpful to enforce IPF transactions in the CSCOPF tool.

Incorporating the controllability market into to the CSCOPF would enable assessment of the relative attractiveness of the controllability market to IPF control. By embedding a dual-market CSCOPF tool into an agent-based simulation tool, the market power of LSEs can be examined. A high level of LSE market power may deter adoption of the hybrid framework.

6.2.5. Improve the Modeling of Stability Constraints in the CSCOPF tool

The CSCOPF uses a limit on the angle between bus-pairs as a stability constraint. Commercial OPF tools often use nomograms, developed offline, to impose stability constraints. A nomogram may be a more accurate predictor of stability than angle limitations. In addition, using a nomogram rather than a conservative angle limitation may allow a lower cost solution to be identified or a feasible case to be identified that

would otherwise be infeasible. Improving CSCOPF through a nomogram or a similar structure would also better align the CSCOPF with operational precedence. Separate nomograms could be developed depending on whether PF controllers are available to improve stability. The production and investment costs of these cases could be compared to assess the economic viability of deploying PF controllers to improve stability.

6.2.6. Improve the Modeling of Planning Tool Choices

The planning tool is only able to implement some of the transmission investment choices available to planners. HVDC is one of the missing choices. Also, the proposed MEP framework does not permit construction of new transmission lines. This may impede the development of an otherwise viable MEP. Future work could add HVDC as an expansion option. It could also allow merchant transmission pipeline developers to build new transmission lines. This would require adjusting the benefit-to-cost threshold to account for the lead-time implications of transmission line construction. Also, the infeasibility of CSCOPF solutions with ubiquitous, PF controllers of large ratings may mask some preferred planning solutions. In addition, the accuracy of the planning tool results may be improved if the following were considered:

- project specific costs such as the dependency of transmission line cost on terrain type,
- technology and project specific carrying costs,
- fixed costs such as the value of substation space and the cost of substation expansion
- value of the ancillary benefits of fast controllers such as the ability to improve stability, and

- project lead-time.

6.3. Conclusions

This work has reviewed impediments to the deployment of PF control and proposed frameworks and methods which may increase the probability of future deployment of PF control. The primary impediment is the disconnect between the parties investing in PF control and the parties that benefit from the investment. The MEP framework attempts to award an investor with more of the societal benefit of the investment. The hybrid framework seeks to create a structure where conventional, centralized transmission planning can co-exist with the proposed MEPs.

Beyond planning frameworks, this work has proposed methods and developed tools to enable the planning and operation of a power system equipped with PF controllers. These tools are compatible with the proposed frameworks. The CSCOPF tool leverages the controllability of the generators and PF controllers to achieve an equal or lower cost solution than PSCOPF. The automated transmission planning tool can simultaneously deploy new transmission lines and multiple PF controller types and units. As such, it considers a larger choice set than known automated transmission planning tools.

Finally, this work proposes the *incremental packetized energy* concept to realize some of the benefits of *packetized energy* at a fraction of the cost. *Incremental packetized energy* seeks to increase the utilization of generation, transmission, and distribution capacity. Beyond reductions in cost, this concept may facilitate reduction in the environmental impact of energy consumption.

The work has identified a host of unresolved issues, ranging from the regulatory sphere to power system stability. Despite the list of unresolved issues, the societal impact of the concepts discussed could be substantial. The revised centralized framework may be the simplest of the proposed frameworks to realize. If the impact of this framework scales from the demonstration system to the national level, the annual savings in electricity expenditures would be \$13 billion per year (2010\$). *Merchant electrical pipelines* and *incremental packetized energy*, while more complex to realize than the revised centralized transmission planning framework, may result in additional savings.

**APPENDIX A: SUPPLEMENTAL INFORMATION FOR CHAPTER
ONE**

Figure 82 is based on Figure 3 of [135].

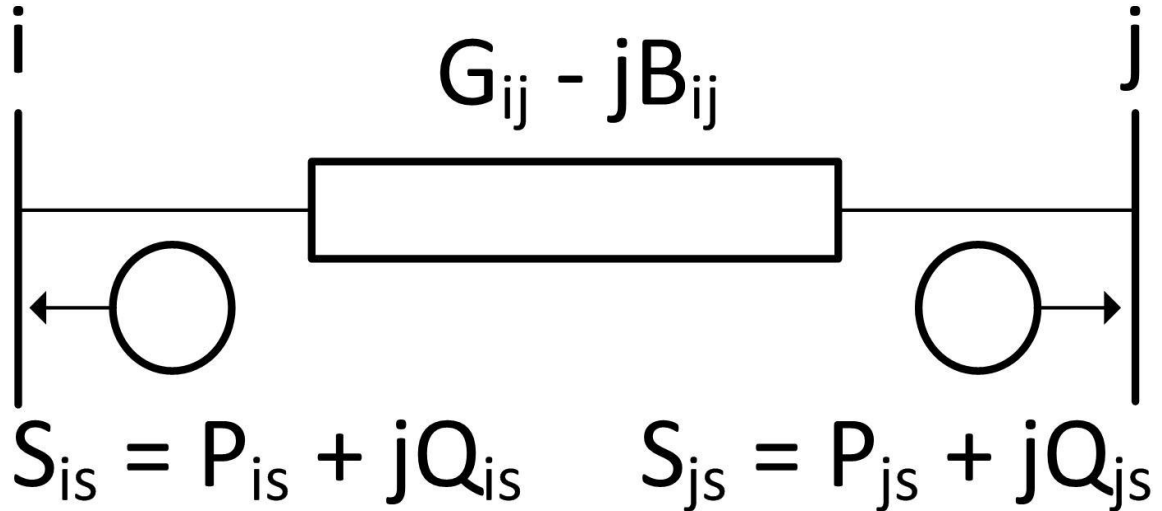


Figure 82: Model of a PF converter connected to Line_{i-j} per the power injection method.

Table 18: Comparison of selected optimal transmission expansion papers.

Ref.	Objective	Multi - Period	Investment Options	Solver(s)	Power Flow Type	Models Line Outages	Load Points per Period	Solves for Number of Controllers or Lines to Install
114	Minimize COE	N	SVC, TCSC, TCVR, TCPST	<i>Mathematical</i> GA –site and rate of controllers, NS – OPF	Un-known	N	11	Y
229	Minimize production cost or congestion rent	N	TCSC	<i>Meta-heuristic</i> Exhaustive search - site controllers SQP - OPF	AC	N	1	N

Table 18 continued

Ref.	Objective	Multi - Period	Investment Options	Solver(s)	Power Flow Type	Models Line Outages	Load Points per Period	Solves for Number of Controllers or Lines to Install
118	Minimize production cost	N	SSSC or new line, not both	<i>Meta-heuristic</i> Indexes – site controllers NS – OPF	DC	Y, <i>n-1</i>	2	Y
121	Minimize congestion cost	N	TCSC	<i>Meta-heuristic</i> Sensitivity analysis – site controllers NS – OPF	Unknown	N	1	N
127	Minimize product of LMP mean and LMP variance	N	StatCom, SSSC	<i>Meta-heuristic</i> GA – site controllers SQP - OPF	Unknown	N	1	Y
130	Maximize loadability	N	TCSC, TCPAR	<i>Mathematical</i> LP - optimize transaction matrix MILP - maximize loadability	DC	N	1	N
129	Maximize ratio of savings to cost	N	PST	<i>Meta-heuristic</i> GA - site and rate controllers LP – OPF	DC	N	1	N
131	Maximize loadability	N	TCSC, TCPST, TCVR, SVC	<i>Meta-heuristic</i> GA – site, select and rate controllers Power Flow – solve load flows	AC	N	1	N

Table 18 continued

Ref.	Objective	Multi - Period	Investment Options	Solver(s)	Power Flow Type	Models Line Outages	Load Points per Period	Solves for Number of Controllers or Lines to Install
132	Maximize loadability	N	UPFC	<i>Meta-heuristic</i> GA – site and rate controllers Power Flow – solve load flows	AC	N	1	N
133	Maximize loadability	N	TCSC	<i>Meta-heuristic</i> GA – site and rate controllers Continuation Power Flow – maximize loadability	AC	N	1	N
134	Minimize cost	Static	Idealized series controller	<i>Mathematical</i> Two-stage Bender's Decomposition	DC	Y	>1	N
137	Minimize cost and/or losses	N	TCSC, TCPAR	<i>Meta-heuristic</i> Rule Based – site controllers NLP - OPF	AC	N	1	N
230	Minimize PV of COE	Y, Dynamic	Lines	<i>Meta-heuristic</i> GA – site and time line additions LP – OPF	DC	N	1	Y
231	Minimize NPV of investment and outage costs	Y, Dynamic	Lines	<i>Meta-heuristic</i> GA – site and time line additions LP – OPF	DC	N	1	Y

Table 18 continued

Ref.	Objective	Multi - Period	Investment Options	Solver(s)	Power Flow Type	Models Line Outages	Load Points per Period	Solves for Number of Controllers or Lines to Install
232	Maximize societal welfare, which includes production cost, demand benefit, and investment cost	Y, Dynamic	Lines	<i>Meta-heuristic</i> GA – site and time line additions OPF – interior point method (likely linear)	DC	N	>1	Y

**APPENDIX B: SYSTEM PARAMETERS FOR QUANTIFICATION
OF CONVERTER RATING REQUIRED TO REALIZE
INCREMENTAL POWER FLOW CONTROL**

Below are the network parameters for the system in Figure 46. S_{base} is 100 MVA.

All lines, generators and loads are assumed online for all simulations. All loads are constant impedance. All generators are voltage sources with ideal source impedances.

Circuit Data

Circuit data is shown in Table 19.

Table 19: Circuit data for the quantification of IPF control effort.

From Bus	To Bus	R (pu)	X (pu)	B (pu)
1	2	0.0219	0.2573	0
1	39	0.0062	0.1564	0
2	3	0.0081	0.0944	0
2	25	0.0438	0.0582	0
2	30	0.0000	0.0000	0
3	4	0.0081	0.1332	0
3	18	0.0069	0.0831	0
4	5	0.0050	0.0802	0
4	14	0.0050	0.0802	0
5	6	0.0012	0.0162	0
5	8	0.0050	0.0699	0
6	7	0.0037	0.0568	0
6	11	0.0044	0.0517	0
6	31	0.0000	0.0000	0
7	8	0.0025	0.0285	0
8	9	0.0144	0.2263	0
9	39	0.0062	0.1564	0
10	11	0.0025	0.0271	0
10	13	0.0025	0.0271	0

Table 19 continued.

From Bus	To Bus	R (pu)	X (pu)	B (pu)
10	32	0.0000	0.0000	0
12	11	0.0015	0.0416	0
12	13	0.0100	0.2718	0
13	14	0.0056	0.0633	0
14	15	0.0112	0.1358	0
15	16	0.0056	0.0582	0
16	17	0.0044	0.0556	0
16	19	0.0100	0.1215	0
16	21	0.0025	0.0420	0
16	24	0.0019	0.0368	0
17	18	0.0044	0.0517	0
17	27	0.0081	0.1087	0
19	20	0.0044	0.0879	0
19	33	0.0000	0.0000	0
20	34	0.0000	0.0000	0
21	22	0.0050	0.0879	0
22	23	0.0038	0.0594	0
22	35	0.0000	0.0000	0
23	24	0.0138	0.2185	0
23	36	0.0000	0.0000	0
25	26	0.0200	0.2019	0
25	37	0.0000	0.0000	0
26	27	0.0088	0.0919	0
26	28	0.0269	0.2973	0
26	29	0.0357	0.3904	0
28	29	0.0088	0.0944	0
29	38	0.0000	0.0000	0

Load data

Load data is shown in Table 20.

Table 20: Load data for the quantification of IPF control effort.

Bus No.	Impedance (pu)
3	1.1027
4	1.1027
6	1.1027
7	1.1027
8	1.1027
12	1.1027
15	1.1027
16	1.1027
18	1.1027
20	1.1027
21	1.1027
23	1.1027
24	1.1027
25	1.1027
26	1.1027
27	1.1027
28	1.1027
29	1.1027
38	1.1027
39	1.1027

Generator data

Generator data is shown in Table 21.

Table 21: Generator data for the quantification of IPF control effort.

Bus No.	Voltage (pu)
30	1.0240
31	0.9687
32	0.9845
33	1.0259
34	0.9687
35	1.0259
36	1.0209
37	1.0329
38	1.0264
39	1.0076

APPENDIX C: SYSTEM PARAMETERS FOR THE RPS COMPLIANCE STUDY

Below are the network parameters for the system in Figure 54. S_{base} is 100 MVA. All lines, generators and loads are assumed online for all simulations.

Circuit Data

Circuit data is presented in Table 22. Rating A is the steady-state line rating. Shunt conductance and shunt susceptance at all buses is zero for all time periods.

Table 22: Circuit data for the first year of the RPS compliance study.

From Bus	To Bus	R (pu)	X (pu)	B (pu)	Rating A (MVA)
1	2	0.0011	0.0130	0.0000	3.00E+03
1	39	0.0004	0.0104	0.0000	3.00E+03
2	3	0.0018	0.0208	0.0000	4.80E+02
2	25	0.0033	0.0040	0.0000	3.00E+03
2	30	0.0000	0.0181	0.0000	3.00E+03
3	4	0.0008	0.0130	0.0000	3.00E+03
3	18	0.0017	0.0208	0.0000	5.00E+01
4	5	0.0005	0.0078	0.0000	3.00E+03
4	14	0.0006	0.0104	0.0000	3.00E+03
5	6	0.0002	0.0026	0.0000	3.00E+03
5	8	0.0022	0.0312	0.0000	3.00E+03
6	7	0.0007	0.0104	0.0000	3.00E+03
6	11	0.0004	0.0052	0.0000	3.00E+03
6	31	0.0000	0.0250	0.0000	3.00E+03
7	8	0.0014	0.0156	0.0000	3.00E+03
8	9	0.0007	0.0104	0.0000	3.00E+03
9	39	0.0023	0.0573	0.0000	5.80E+02
10	11	0.0005	0.0052	0.0000	3.00E+03
10	13	0.0010	0.0104	0.0000	3.00E+03
10	32	0.0000	0.0200	0.0000	3.00E+03

Table 22 continued

From Bus	To Bus	R (pu)	X (pu)	B (pu)	Rating A (MVA)
12	11	0.0016	0.0435	0.0000	3.00E+03
12	13	0.0016	0.0435	0.0000	3.00E+03
13	14	0.0007	0.0078	0.0000	3.00E+03
14	15	0.0015	0.0182	0.0000	3.00E+03
15	16	0.0030	0.0312	0.0000	9.00E+01
16	17	0.0008	0.0104	0.0000	3.00E+03
16	19	0.0051	0.0624	0.0000	4.30E+02
16	21	0.0035	0.0599	0.0000	2.10E+02
16	24	0.0003	0.0052	0.0000	3.00E+03
17	18	0.0020	0.0234	0.0000	5.00E+01
17	27	0.0006	0.0078	0.0000	3.00E+03
19	20	0.0007	0.0138	0.0000	3.00E+03
19	33	0.0007	0.0142	0.0000	3.00E+03
20	34	0.0009	0.0180	0.0000	3.00E+03
21	22	0.0010	0.0182	0.0000	3.00E+03
22	23	0.0005	0.0078	0.0000	3.00E+03
22	35	0.0000	0.0143	0.0000	3.00E+03
23	24	0.0033	0.0521	0.0000	1.30E+02
23	36	0.0005	0.0272	0.0000	3.00E+03
25	26	0.0057	0.0571	0.0000	5.00E+01
25	37	0.0006	0.0232	0.0000	3.00E+03
26	27	0.0007	0.0078	0.0000	3.00E+03
26	28	0.0012	0.0130	0.0000	3.00E+03
26	29	0.0017	0.0182	0.0000	3.00E+03
28	29	0.0005	0.0052	0.0000	3.00E+03
29	38	0.0008	0.0156	0.0000	3.00E+03

Bus Data

All buses are assigned to the same control area. All buses are nominally 345 kV with an allowable voltage range of 0.9 to 1.1 pu.

Bus type key:

- 1 = PQ

- 2 = PV
- 3 = Reference
- 4 = Isolated

Table 23 and Table 24 show the loads for time periods one through three and four through six respectively of the first year of operation.

Table 23: Bus data for the first year of the RPS compliance study for time periods one through three.

Bus No.	Bus Type	Load - T1 (MW)	Load - T1 (MVar)	Load - T2 (MW)	Load - T2 (MVar)	Load - T3 (MW)	Load - T3 (MVar)
1	1	3.5E+02	-3.5E+01	3.3E+02	-3.3E+01	3.5E+02	-3.5E+01
2	1	7.7E+01	-7.7E+00	7.3E+01	-7.3E+00	7.7E+01	-7.7E+00
3	1	7.7E+01	-7.7E+00	7.3E+01	-7.3E+00	7.7E+01	-7.7E+00
4	1	7.7E+01	-7.7E+00	7.3E+01	-7.3E+00	7.7E+01	-7.7E+00
5	1	2.3E+02	-2.3E+01	2.2E+02	-2.2E+01	2.3E+02	-2.3E+01
6	1	7.7E+01	-7.7E+00	7.3E+01	-7.3E+00	7.7E+01	-7.7E+00
7	1	7.7E+01	-7.7E+00	7.3E+01	-7.3E+00	7.7E+01	-7.7E+00
8	1	7.7E+01	-7.7E+00	7.3E+01	-7.3E+00	7.7E+01	-7.7E+00
9	1	7.7E+01	-7.7E+00	7.3E+01	-7.3E+00	7.7E+01	-7.7E+00
10	1	7.7E+01	-7.7E+00	7.3E+01	-7.3E+00	7.7E+01	-7.7E+00
11	1	7.7E+01	-7.7E+00	7.3E+01	-7.3E+00	7.7E+01	-7.7E+00
12	1	1.5E+02	-1.5E+01	1.5E+02	-1.5E+01	1.5E+02	-1.5E+01
13	1	7.7E+01	-7.7E+00	7.3E+01	-7.3E+00	7.7E+01	-7.7E+00
14	1	2.7E+02	-2.7E+01	2.6E+02	-2.6E+01	2.7E+02	-2.7E+01
15	1	7.7E+01	-7.7E+00	7.3E+01	-7.3E+00	7.7E+01	-7.7E+00
16	1	7.7E+01	-7.7E+00	7.3E+01	-7.3E+00	7.7E+01	-7.7E+00
17	1	7.7E+01	-7.7E+00	7.3E+01	-7.3E+00	7.7E+01	-7.7E+00
18	1	0.0E+00	0.0E+00	0.0E+00	0.0E+00	0.0E+00	0.0E+00
19	1	4.2E+02	-4.2E+01	4.0E+02	-4.0E+01	4.3E+02	-4.3E+01
20	1	7.7E+01	-7.7E+00	7.3E+01	-7.3E+00	7.7E+01	-7.7E+00
21	1	4.2E+02	-4.2E+01	4.0E+02	-4.0E+01	4.3E+02	-4.3E+01

Table 23 continued

Bus No.	Bus Type	Load - T1 (MW)	Load - T1 (MVar)	Load - T2 (MW)	Load - T2 (MVar)	Load - T3 (MW)	Load - T3 (MVar)
22	1	7.7E+01	-7.7E+00	7.3E+01	-7.3E+00	7.7E+01	-7.7E+00
23	1	7.7E+01	-7.7E+00	7.3E+01	-7.3E+00	7.7E+01	-7.7E+00
24	1	7.7E+01	-7.7E+00	7.3E+01	-7.3E+00	7.7E+01	-7.7E+00
25	1	7.7E+01	-7.7E+00	7.3E+01	-7.3E+00	7.7E+01	-7.7E+00
26	1	7.7E+01	-7.7E+00	7.3E+01	-7.3E+00	7.7E+01	-7.7E+00
27	1	1.5E+02	-1.5E+01	1.5E+02	-1.5E+01	1.5E+02	-1.5E+01
28	1	1.9E+02	-1.9E+01	1.8E+02	-1.8E+01	1.9E+02	-1.9E+01
29	1	7.7E+01	-7.7E+00	7.3E+01	-7.3E+00	7.7E+01	-7.7E+00
30	3	0.0E+00	0.0E+00	0.0E+00	0.0E+00	0.0E+00	0.0E+00
31	2	0.0E+00	0.0E+00	0.0E+00	0.0E+00	0.0E+00	0.0E+00
32	2	0.0E+00	0.0E+00	0.0E+00	0.0E+00	0.0E+00	0.0E+00
33	2	0.0E+00	0.0E+00	0.0E+00	0.0E+00	0.0E+00	0.0E+00
34	2	0.0E+00	0.0E+00	0.0E+00	0.0E+00	0.0E+00	0.0E+00
35	2	0.0E+00	0.0E+00	0.0E+00	0.0E+00	0.0E+00	0.0E+00
36	2	0.0E+00	0.0E+00	0.0E+00	0.0E+00	0.0E+00	0.0E+00
37	2	0.0E+00	0.0E+00	0.0E+00	0.0E+00	0.0E+00	0.0E+00
38	2	0.0E+00	0.0E+00	0.0E+00	0.0E+00	0.0E+00	0.0E+00
39	2	0.0E+00	0.0E+00	0.0E+00	0.0E+00	0.0E+00	0.0E+00

Table 24: Bus data for the first year of the RPS compliance study for time periods four through six.

Bus No.	Bus Type	Load - T4 (MW)	Load - T4 (MVar)	Load - T5 (MW)	Load - T5 (MVar)	Load - T6 (MW)	Load - T6 (MVar)
1	1	4.3E+02	-4.3E+01	4.5E+02	-4.5E+01	4.3E+02	-4.3E+01
2	1	9.5E+01	-9.5E+00	1.0E+02	-1.0E+01	9.5E+01	-9.5E+00
3	1	9.5E+01	-9.5E+00	1.0E+02	-1.0E+01	9.5E+01	-9.5E+00
4	1	9.5E+01	-9.5E+00	1.0E+02	-1.0E+01	9.5E+01	-9.5E+00
5	1	2.9E+02	-2.9E+01	3.0E+02	-3.0E+01	2.9E+02	-2.9E+01
6	1	9.5E+01	-9.5E+00	1.0E+02	-1.0E+01	9.5E+01	-9.5E+00
7	1	9.5E+01	-9.5E+00	1.0E+02	-1.0E+01	9.5E+01	-9.5E+00
8	1	9.5E+01	-9.5E+00	1.0E+02	-1.0E+01	9.5E+01	-9.5E+00
9	1	9.5E+01	-9.5E+00	1.0E+02	-1.0E+01	9.5E+01	-9.5E+00
10	1	9.5E+01	-9.5E+00	1.0E+02	-1.0E+01	9.5E+01	-9.5E+00

Table 24 continued

Bus No.	Bus Type	Load - T4 (MW)	Load - T4 (MVar)	Load - T5 (MW)	Load - T5 (MVar)	Load - T6 (MW)	Load - T6 (MVar)
11	1	9.5E+01	-9.5E+00	1.0E+02	-1.0E+01	9.5E+01	-9.5E+00
12	1	1.9E+02	-1.9E+01	2.0E+02	-2.0E+01	1.9E+02	-1.9E+01
13	1	9.5E+01	-9.5E+00	1.0E+02	-1.0E+01	9.5E+01	-9.5E+00
14	1	3.3E+02	-3.3E+01	3.5E+02	-3.5E+01	3.3E+02	-3.3E+01
15	1	9.5E+01	-9.5E+00	1.0E+02	-1.0E+01	9.5E+01	-9.5E+00
16	1	9.5E+01	-9.5E+00	1.0E+02	-1.0E+01	9.5E+01	-9.5E+00
17	1	9.5E+01	-9.5E+00	1.0E+02	-1.0E+01	9.5E+01	-9.5E+00
18	1	0.0E+00	0.0E+00	0.0E+00	0.0E+00	0.0E+00	0.0E+00
19	1	5.3E+02	-5.3E+01	5.5E+02	-5.5E+01	5.3E+02	-5.3E+01
20	1	9.5E+01	-9.5E+00	1.0E+02	-1.0E+01	9.5E+01	-9.5E+00
21	1	5.3E+02	-5.3E+01	5.5E+02	-5.5E+01	5.3E+02	-5.3E+01
22	1	9.5E+01	-9.5E+00	1.0E+02	-1.0E+01	9.5E+01	-9.5E+00
23	1	9.5E+01	-9.5E+00	1.0E+02	-1.0E+01	9.5E+01	-9.5E+00
24	1	9.5E+01	-9.5E+00	1.0E+02	-1.0E+01	9.5E+01	-9.5E+00
25	1	9.5E+01	-9.5E+00	1.0E+02	-1.0E+01	9.5E+01	-9.5E+00
26	1	9.5E+01	-9.5E+00	1.0E+02	-1.0E+01	9.5E+01	-9.5E+00
27	1	1.9E+02	-1.9E+01	2.0E+02	-2.0E+01	1.9E+02	-1.9E+01
28	1	2.4E+02	-2.4E+01	2.5E+02	-2.5E+01	2.4E+02	-2.4E+01
29	1	9.5E+01	-9.5E+00	1.0E+02	-1.0E+01	9.5E+01	-9.5E+00
30	3	0.0E+00	0.0E+00	0.0E+00	0.0E+00	0.0E+00	0.0E+00
31	2	0.0E+00	0.0E+00	0.0E+00	0.0E+00	0.0E+00	0.0E+00
32	2	0.0E+00	0.0E+00	0.0E+00	0.0E+00	0.0E+00	0.0E+00
33	2	0.0E+00	0.0E+00	0.0E+00	0.0E+00	0.0E+00	0.0E+00
34	2	0.0E+00	0.0E+00	0.0E+00	0.0E+00	0.0E+00	0.0E+00
35	2	0.0E+00	0.0E+00	0.0E+00	0.0E+00	0.0E+00	0.0E+00
36	2	0.0E+00	0.0E+00	0.0E+00	0.0E+00	0.0E+00	0.0E+00
37	2	0.0E+00	0.0E+00	0.0E+00	0.0E+00	0.0E+00	0.0E+00
38	2	0.0E+00	0.0E+00	0.0E+00	0.0E+00	0.0E+00	0.0E+00
39	2	0.0E+00	0.0E+00	0.0E+00	0.0E+00	0.0E+00	0.0E+00

Generator Data

Generators at Bus 30 and Bus 37 are wind generators. Table 25 indicates generator ratings for the first year of the planning horizon.

Table 25: Generator data for the RPS compliance study.

Bus No.	Max real power output (MW)	Min real power output (MW)	Max reactive power output (MVar)	Min reactive power output (MVar)
18	1.00E+01	0.00E+00	2.00E+01	-2.00E+01
30	0.00E+00	0.00E+00	5.00E+01	-1.00E+02
31	1.10E+03	1.00E+01	2.00E+03	-8.00E+02
32	1.10E+03	1.00E+01	2.00E+03	-8.00E+02
33	1.10E+03	1.00E+01	2.00E+03	-8.00E+02
34	1.10E+03	1.00E+01	2.00E+03	-8.00E+02
35	1.10E+03	1.00E+01	2.00E+03	-8.00E+02
36	1.10E+03	1.00E+01	2.00E+03	-8.00E+02
37	0.00E+00	0.00E+00	5.00E+01	-1.00E+02
38	1.10E+03	1.00E+01	2.00E+03	-8.00E+02
39	1.10E+03	1.00E+01	2.00E+03	-8.00E+02

APPENDIX D: RESULTS FROM THE RPS COMPLIANCE STUDY

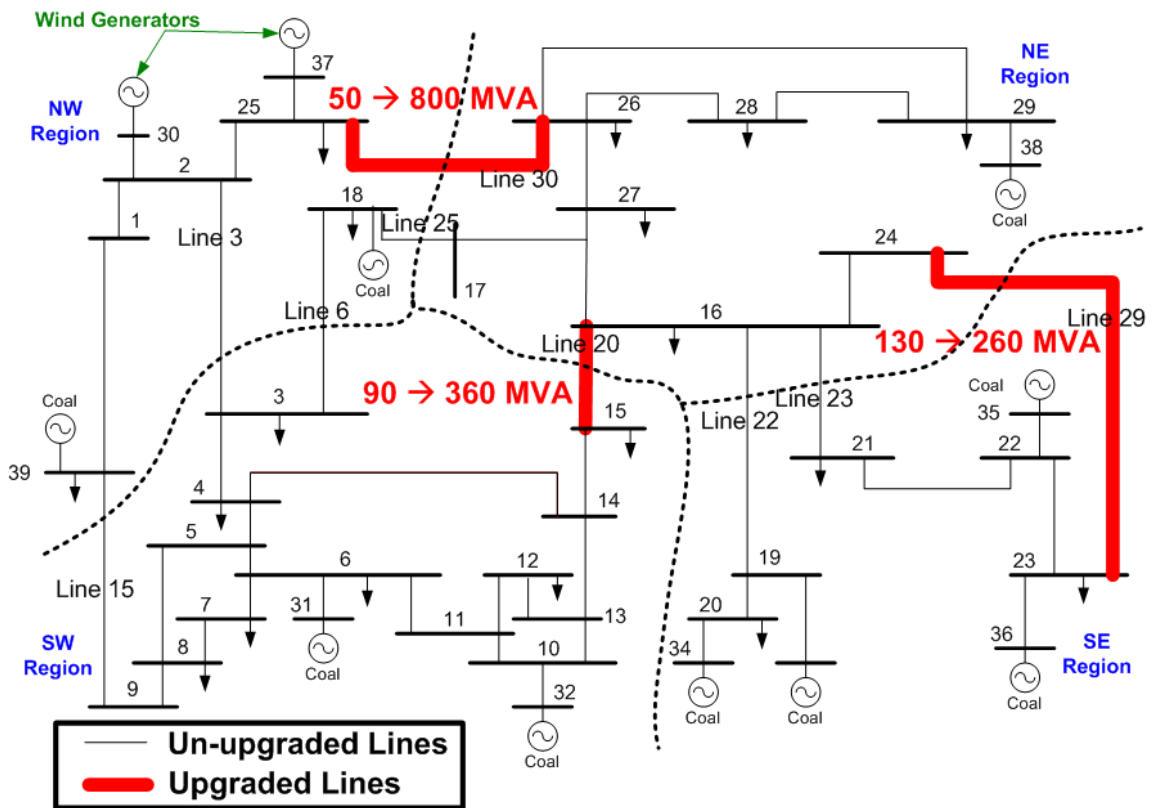


Figure 83: Overview of transmission upgrades required in the BAU case.

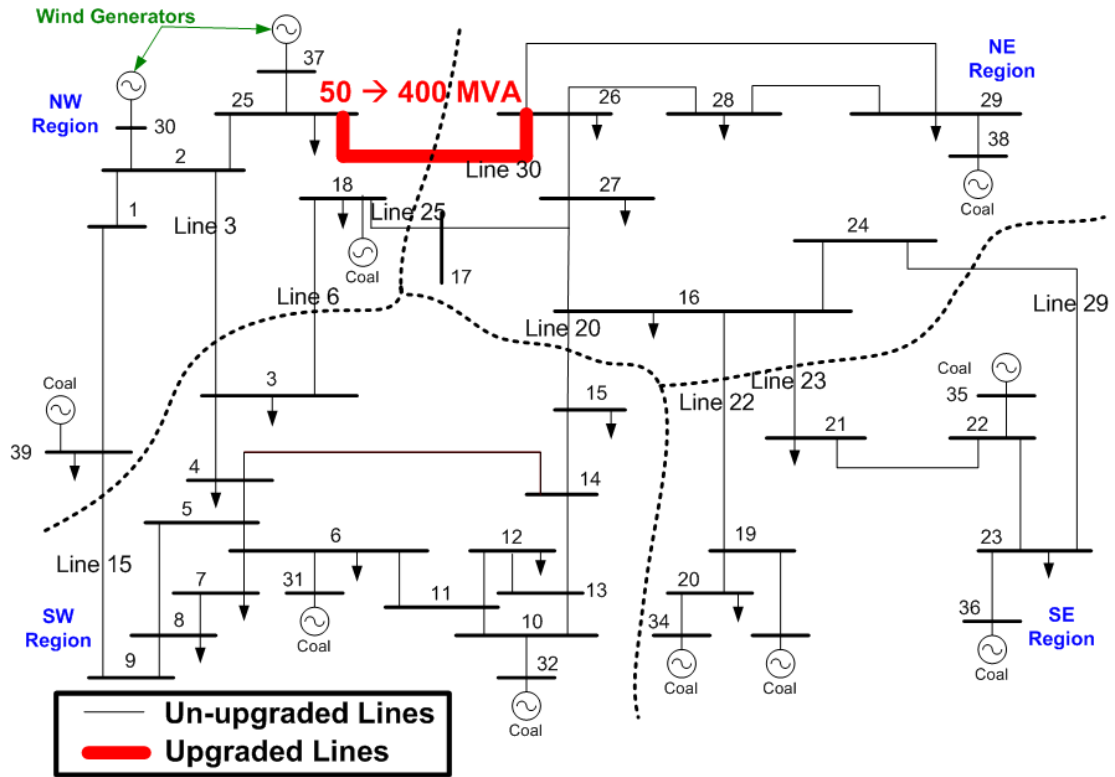


Figure 84: Overview of the transmission upgrades required in the DSR case.

Table 27: Breakdown of the transmission upgrades required for the DSR case.

Year	Line No.	Line Capacity Added (MW)	Line Capacity Added (000s MW-miles)	DSR Modules Installed (MVA)	DSR Capacity Installed (000s equivalent MW-miles)	Total Investment (000s equivalent MW-miles)
6	29	-		6.2	0.62	0.62
	30	-		34	3.40	3.40
7	30	-		18.1	1.82	1.82
8	29	-		5.6	0.56	0.56
	30	-		17.9	1.80	1.80
9	30	-		17	1.70	1.70
10	30	50	9.2	-		9.20
	29	-		5.2	0.52	0.52
11	30	-		1.9	0.20	0.20
12	29	-		4.8	0.48	0.48
	30	-		8.3	0.84	0.84
13	30	100	18.3	-		18.30
14	3	-		4.9	0.50	0.50
	30	-		6	0.60	0.60
15	30	200	36.6	-		36.60
17	29	-		4.4	0.44	0.44
	3	-		4.1	0.42	0.42
18	3	-		8.2	0.82	0.82
	20	-		26.7	2.68	2.68
19	20	-		66.7	6.68	6.68
	30	-		21.6	2.16	2.16
	3	-		3.1	0.32	0.32
Total			64.1		26.6	90.7

Table 28: Breakdown of the transmission upgrades required in the IPF control case.

Year	Line No.	Line Capacity Added (MVA)	Line Capacity Added (000s MW-miles)	Installed IPF Controller Capacity (MVA)	Installed IPF Controller Capacity (000s equivalent MW-miles)	Total Investment (000s equivalent MW-miles)
6	-	-		58.6	5.86	5.86
9	30	50	9.2	-		9.2
	-	-		98.6	9.86	9.86
10	30	100	18.3	-		18.3
12	-	-		140	14	14
15	-	-		167	16.7	16.7
17	20	90	9	-		9
19	-	-		244	24.4	24.4
Total			36.5		70.8	107.3

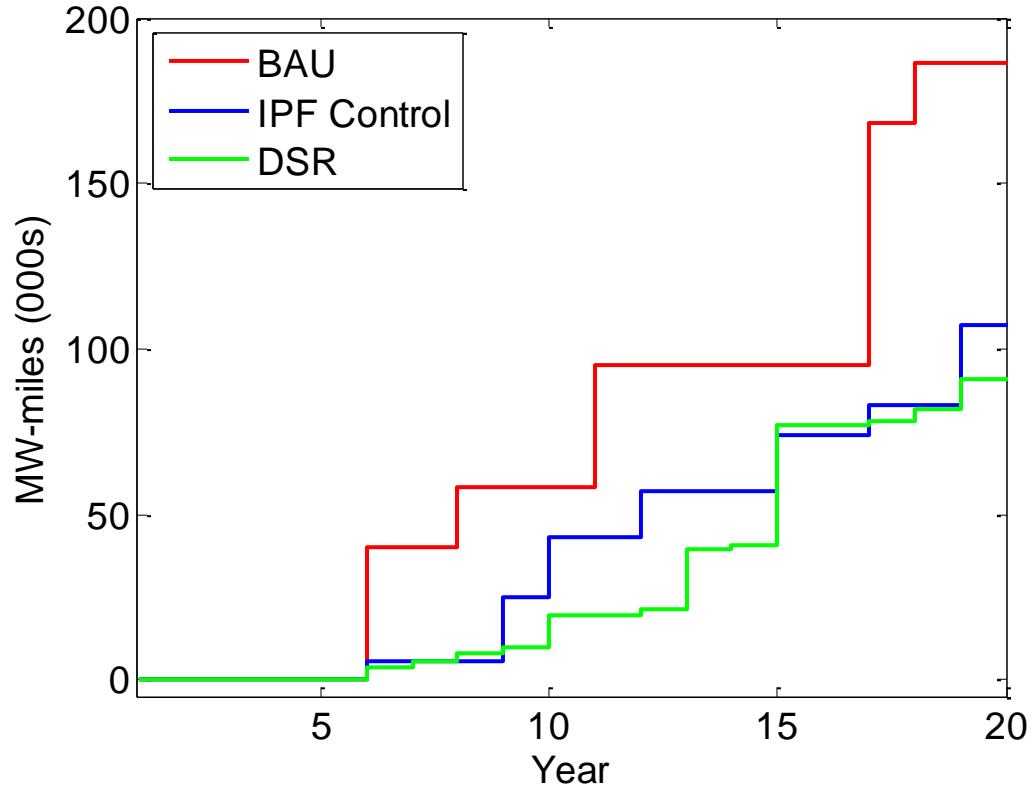


Figure 87: Total non-discounted investment as function of time for the RPS compliance study.

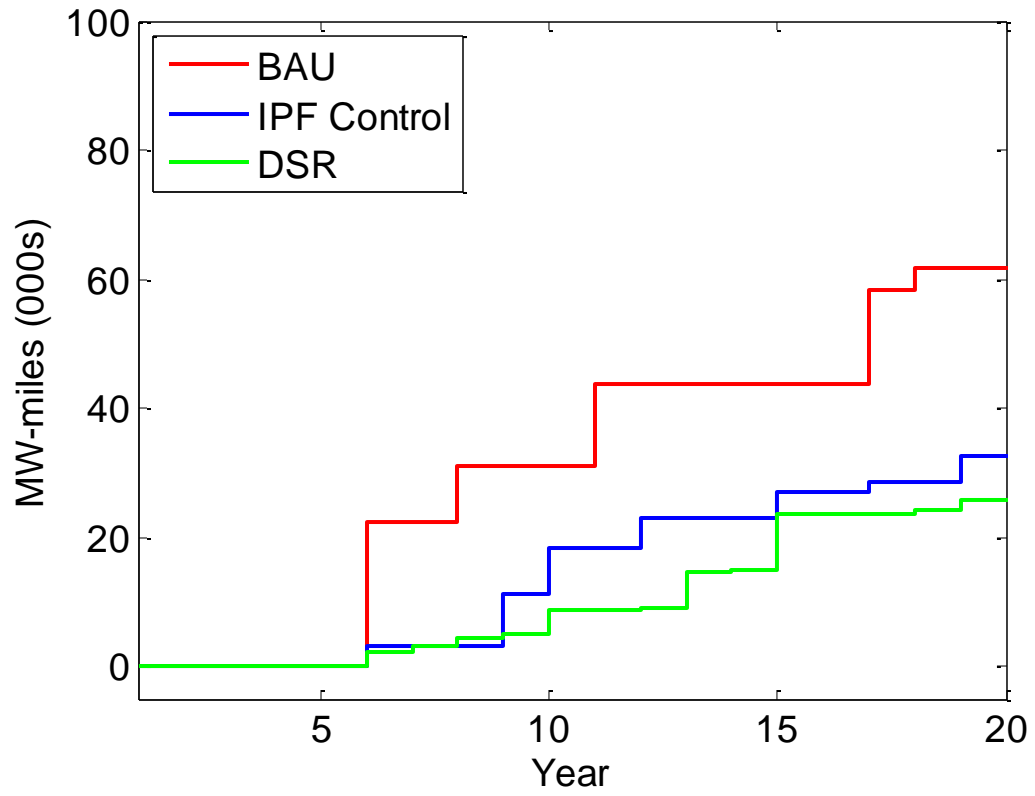


Figure 88: Total discounted investment as function of time for the RPS compliance study.

APPENDIX E: SYSTEM DETAILS FOR THE CSCOPF AND PLANNING TOOL DEMONSTRATION SYSTEMS

Parameters Common to Both Systems

For the cases using the CSCOPF, post-contingency actions are limited to 15 minutes from the onset of the contingency.

Generator Parameters

Ramp rates of 0.07 [307], 0.01, 0.01 [308], and 2.4 pu/min [309] are assumed for the natural gas OCGT/CCGT, natural gas steam turbine, coal, and wind generators respectively. Given the similarity of technologies, the natural gas steam generation is assumed to have the same ramp rate as coal generation. The ramp rates are representative of the installed US generation fleet. New coal plants have a ramp rate of up to 0.05 pu/min [308], which would increase the contingency capability of coal plants over the 15 minute post-contingency window. New CCGT plants have a ramp rate of 0.1 pu/min, but this improvement is unnoticeable in a CSCOPF with a 15 minute window for post-contingency action.

Generator production costs are developed as a function of heat-rate, fuel cost, and variable O&M cost. Heat-rates for natural gas plants are derived for each plant-type based on the capacity-weighted vintage of the current US fleet [310]. The CCGT and OCGT fleet heat-rates are represented by 2011 plants [311]. The natural gas steam turbine fleet is represented by a 1965-1969 vintage plant [312]. The representative coal plant heat-rate is based on survey data [313]. The coal heat-rate is sourced from

respondents reporting bituminous or sub-bituminous coal as the primary fuel. Responses with a heat-rate of more than 100 mmbtu/MWh are filtered out as they may be erroneous. The variable O&M costs are based on EIA estimates for new plants constructed in 2010 [159]. Natural gas steam turbine generation is assumed to have the same variable O&M cost as coal generation. Fuel costs for the CSCOPF demonstration cases are the average of the EIA projection for 2024-2033 [314, 315]. Fuel costs for the planning tool cases are the average of EIA 2014-2023 projections for the first period and the average of 2024-2033 for the second period [314, 315]. Generator heat-rates, fuel costs, variable O&M costs, and total variable costs are reported in Table 29.

Table 29: Generator parameters used for the CSCOPF demonstration cases.

Generator Type	Heat-Rate (mmbtu/MWh)	Fuel Cost 2014- 2023 and 2024-2033 (2010\$/mmbtu)	Variable O&M (2010\$/MWh)	Total Variable Cost 2014-2023 and 2024- 2033 (2010\$/MWh)
Natural Gas CCGT	6.883	4.83 6.17	3.43	36.67 45.90
Natural Gas OCGT	10.320	4.83 6.17	14.70	64.55 78.37
Natural Gas Steam Turbine	10.429	4.83 6.17	4.25	54.62 68.60
Coal	10.673	2.40 2.62	4.25	29.87 32.21
Wind	N/A	N/A	0	0 0

The Garver system does not specify the generator types. To provide price differentiation, five types of generation are assumed: coal generation at Bus One, natural gas CCGT, natural gas OCGT and natural gas steam turbine at Bus Three, and wind at

Bus Four. The coal generator is sized to serve all load. The gas plants are sized iteratively to ensure feasibility of the solution and match the distribution of plant types in the current US system (52% CCGT, 29% OCGT, and 19% steam turbine). The wind generator is sized as discussed below to meet RPS requirements.

For the IEEE 39-bus system, wind generation is sited at the same buses used in Chapter Three for the RPS compliance study. The other generators are coal generators. All coal generators except the swing generator and rated the same value as the original IEEE 39-bus system. The original IEEE 39-bus system does not specify a size for the swing bus generator. The capacity of swing bus generator is solved iteratively starting with a large value. The value is decreased at 100 MW until a solution is no longer feasible if equipped with unlimited transmission capacity. The wind generator is sized as discussed below to meet RPS requirements.

For each system, the aggregate wind capacity is sized to comply with a 33% RPS if all potential wind generation is delivered. The calculation of annual load assumed a ratio of peak load to average load of 37.4%, the average value for the US in 2010 [26]. The wind generation is assumed to have a capacity factor of 40%. The potential wind production in each period is determined based on the capacity factor and an assumed 22.34% ELCC value during the peak period. The ELCC value is derived from the EWITS study [45]. For the IEEE 39-bus system, the wind capacity is split between Bus Two and Bus 25.

Network and Load Parameters

For the Garver system, the network is used as-is, aside from changing the rating of Circuit 1-4-1 from 80 MW to 100 MW. For the Garver CSCOPF demonstration cases, the load is comprised of the Garver base case loads, multiplied by a factor to account for expected growth in US annual demand in 2033 relative to 2013 [295]. In addition, the load at Bus Two and Bus Three is adjusted to 65 MW and 108 MW, to create periods of congestion. For the planning tool demonstration cases, high-load and low-load hours in each planning period are adjusted to reflect expected growth in US annual demand by the end of the planning period.

Most of the generators in the IEEE 39-bus system are connected to the high-voltage transmission system via a single generator step-up transformer. If the transformer is outaged in a contingency, the entire generator becomes unavailable. This could be avoided by modeling the step-up transformer as multiple transformers in parallel, increasing the circuit count. Instead, the generators are assumed to be directly connected to the high-voltage system and the step-up transformers are removed. The IEEE 39-bus case specifies a load at Bus 31, which is on the low-side of the step-up transformer. Upon removal of the transformer, this load is moved to Bus Six. The resulting system has 30 buses. Also, the rating of the generator connected to Bus 20 is increased to match the load at Bus 20 as the loss of Circuit 19-20-1 will lead to an infeasible solution otherwise.

The IEEE 39-bus system does not specify the circuit PF limits. In the RPS compliance study, circuit limits are assumed infinite for intra-area circuits and assigned

finite values for inter-area circuits. However, CSCOPF solution is not feasible with the circuit limits used in the RPS compliance study. Also, assuming infinite intra-area circuit capacity is a simplification. Therefore, new circuit limits are generated.

To generate circuit limits for the IEEE 39-bus system, first all circuits are rated at 9,999 MW to ensure there is no congestion. Then, the CSCOPF is run to determine the maximum PF through each circuit with all assets online or contingency conditions. The circuit limits are then adjusted so that they are 5 MW above the maximum recorded value. The resulting circuit limits are reported in Table 30.

Table 30: Circuit limits for the 39-bus CSCOPF demonstration system

From Bus	To Bus	Rating (MW)	From Bus	To Bus	Rating (MW)
1	2	645	13	14	2455
1	30	645	14	15	1730
2	3	410	15	16	1250
2	25	490	16	17	1085
3	4	1820	16	19	310
3	18	1330	16	21	410
4	5	2610	16	24	460
4	14	1270	17	18	1095
5	6	3215	17	27	525
5	8	1625	19	20	140
6	7	2510	21	22	750
6	11	1815	22	23	560
7	8	2165	23	24	750
8	9	855	25	26	525
9	30	855	26	27	420
10	11	1615	26	28	310
10	13	2265	26	29	410
11	12	460	28	29	410
12	13	450			

APPENDIX F: SYSTEM DETAILS FOR THE PLANNING TOOL

DEMONSTRATION SYSTEM

The test system for the planning tool demonstration is largely based on the Garver system used to demonstrate the CSCOPF tool. However, additional assumptions are made regarding capacity cost and emissions rates.

Capacity Cost

Capacity costs are generated for each plant-type based on the assumption of competitive energy and capacity markets. Under such a scenario, the fixed costs of generation are recouped in the capacity market and variable costs are recouped in the energy market. Wind is procured in the capacity market to meet RPS requirements.

Pro forma analyses are generated for each plant-type to develop a levelized cost of capacity, based on a discount rate of 10%, a corporate tax rate of 35%, and inflation of 2% for fixed O&M costs and capacity payments. The capital costs of the coal and natural gas steam turbine plants are assumed to be fully recouped at the start of the transmission study horizon, collapsing the cost of coal capacity to the fixed O&M cost [159]. New coal and natural gas steam turbine capacity, if required, is assumed to be sourced from mothballed capacity at zero cost. The fixed O&M cost of the natural gas plant is assumed identical to the coal plant. The CCGT and OCGT are assumed financed over a 40 year period. The wind capacity is assumed financed over a 20 year period.

The CCGT, OCGT and wind capacity costs are derived using the overnight cost from [159] and investment factor from [316]. The investment factor accounts for the

cash flows of construction without explicitly modeling the construction years in the pro forma. The costs parameters and resulting levelized capacity cost are shown in Table 31.

Table 31: Plant capacity cost data.

Generator Type	Capacity Cost (2010\$/kW)	Investment Factor	Fixed O&M (2010\$/kW)	Levelized Capacity Cost (2010\$/kW)
Coal	n/a	n/a	29.67	29.67
CCGT	931	1.16	14.39	136.40
OCGT	927	1.12	6.98	124.30
Natural Gas Steam Turbine	n/a	n/a		29.67
Wind	2278	1.25	28.07	417.50

Emissions

Carbon emissions are calculating using the heat-rates from Appendix E and the carbon intensity of the fuels, as specified in [317]. The ratio of sub-bituminous to bituminous coal during the study horizon is assumed to match the US 2011 ratio, as reported in [318].

REFERENCES

- ¹ P. Hines, J. Apt, S. Talukdar. (2012, February 27). *Large blackouts in North America: Historical trends and policy implications* [Online]. Available: http://www.cems.uvm.edu/~phines/publications/2009/hines_2009_blackouts.pdf.
- ² J. Osborne, C. Kawann, “Reliability of the U.S. electricity system: Recent trends and current issues,” LBNL, Report LBNL-47043, August 2001.
- ³ T.E. Dy Liacco, “Real-time computer control of power systems,” *Proceedings of the IEEE*, vol. 62, no. 7, 884-891, 1974.
- ⁴ NYISO. (2011, March 20). *2009 State of the market report: New York ISO* [Online]. Available: http://www.nyiso.com/public/webdocs/documents/market_advisor_reports/2009/NYISO_2009_SOM_Final.pdf.
- ⁵ NERC. (2011, March 23). *Log of TLR trends* [Online]. Available: <http://www.ercot.com/mktrules/protocols/current.html>.
- ⁶ EIA. (2012, February 11). *Sales and revenue data by state, monthly back to 1990, Form EIA-826* [Online]. Available: http://205.254.135.24/cneaf/electricity/page/sales_revenue.xls.
- ⁷ Potomac Economics, “2009 State of the market report for the Midwest ISO,” August 2010.
- ⁸ B. Lesieutre, J. Eto, “Electricity transmission congestion costs: A review of recent reports,” LBNL, Report LNBL-54049, October 2003.
- ⁹ Monitoring Analytics, “2010 State of the market report for PJM: Volume I,” March 10, 2011.

-
- ¹⁰ CAISO. (2012). *2011 Annual Report on Market Issues & Performance* [Online]. Available: <http://www.caiso.com/Documents/2011AnnualReport-MarketIssues-Performance.pdf>.
- ¹¹ California Energy Commission, “Updated California Energy Demand Forecast 2011-2022,” CEC-200-2011-006-SD, 2011.
- ¹² S. Abraham, “National transmission grid study,” DOE, May 2002.
- ¹³ California ISO. (2007, June 15). *Total transfer capability (TTC) methodology* [Online]. Available: <http://www.caiso.com/1bfe/1bfe98134fa0.pdf>.
- ¹⁴ EIA. (2011, March 16). *Table 8: Electricity supply, disposition, prices, and emissions – Annual Energy Outlook 2011* [Online]. Available: http://www.eia.doe.gov/forecasts/aeo/excel/aeotab_8.xls.
- ¹⁵ EIA. (2011, March 17). *Supplemental table 58: Light-duty vehicle stock by technology type – Annual Energy Outlook 2011* [Online]. Available: http://www.eia.gov/oiaf/aeo/supplement/suptab_58.xls.
- ¹⁶ Deutsche Bank, “Electric cars: Plugged in 2,” November 3, 2009.
- ¹⁷ Electrification Coalition, “Electrification roadmap: Revolutionizing transportation and achieving energy security,” November 2009.
- ¹⁸ Electrification Coalition, “Economic impact of the electrification roadmap,” April 2010.
- ¹⁹ W. Short, P. Denholm, “A preliminary assessment of plug-in hybrid electric vehicles on wind energy markets,” NREL, NREL/TP-620-39729, April 2006.
- ²⁰ A. Abel, “Electric transmission: Approaches for energizing a sagging industry,” US Congressional Research Service, RL33875, April 2007.
- ²¹ EEI, “EEI survey of transmission investment: Historical and planned capital expenditures (1999-2008),” May 2005.

²² EEI. (2009, September 9). *Actual and planned transmission investment by shareholder-owned utilities (2004-2013)* [Online]. Available:
http://www.eei.org/ourissues/ElectricityTransmission/Documents/bar_Transmission_Investment.pdf.

²³ EEI. (2012, February 15). *Actual and planned transmission investment by shareholder-owned utilities (2005-2014)* [Online]. Available:
http://www.eei.org/ourissues/ElectricityTransmission/Documents/bar_Transmission_Investment.pdf.

²⁴ EEI. (2013, June 23). *Actual and Planned Transmission Investment By Shareholder-Owned Utilities (2006-2015)* [Online]. Available:
http://www.eei.org/ourissues/electricitytransmission/documents/bar_transmission_investment.pdf.

²⁵ DOE. (2012, January). *RPS policies* [Online]. Available:
http://www.dsireusa.org/documents/summarymaps/RPS_map.pptx.

²⁶ EIA, “Annual energy review: 2010,” DOE/EIA-0384(2010), June 2010.

²⁷ SEIA, GTM Research. (2013, February 15). *U.S. Solar Market Insight™: 2010 Year in Review, Executive Summary* [Online]. Available: <http://www.seia.org/galleries/pdf/SMI-YIR-2010-ES.pdf>.

²⁸ AWEA. (2013, January). *Press Release* [Online]. Available:
<http://www.awea.org/newsroom/pressreleases/officialyearendnumbersreleased.cfm>

²⁹ NREL. (2010, February). NREL FEMA Transmission Lines [Online]. No longer available:
http://www.pasda.psu.edu/uci/FullMetadataDisplay.aspx?file=NREL_FEMATransmission.xml#Identification_Information.

³⁰ NREL. (2010, February). Wind Data [Online]. Available:
http://www.nrel.gov/gis/data_wind.html.

-
- ³¹ NREL. (2010, February 10). Monthly and annual average solar resource potential for 48 Contiguous United States [Online]. Available: <http://www.nrel.gov/gis/>.
- ³² J. Pfeifenberger, “Transmission planning: Economic vs. reliability projects,” presented at the EUCI Conference, Chicago, IL, October 13, 2010.
- ³³ GE Energy, “Final report: New England wind integration study - Executive summary,” December 2010.
- ³⁴ Midwest ISO, “Regional generation outlet study,” November 2010.
- ³⁵ SPP, “SPP WITF wind integration study,” January 2010.
- ³⁶ NREL, “Nebraska statewide wind integration study, April 2008 - January 2010,” NREL/ SR-550-47519, 2010.
- ³⁷ NREL, “Nebraska statewide wind integration study, Report appendix section 8.2 - Part 1,” December 2009.
- ³⁸ C. Loutan, *et al.*, “Integration of renewable resources: Transmission and operating issues and recommendations for integrating renewable resources on the California ISO-controlled grid,” CA ISO, November 2007.
- ³⁹ K. Porter, “Intermittency analysis project: Final report,” CEC, CEC-500-2007-081, July 2007.
- ⁴⁰ R. Davis, B. Quach, “Intermittency analysis project: Appendix A, Intermittency impacts of wind and solar resources on transmission reliability,” CEC, CEC-500-2007-081-APA, 2007.
- ⁴¹ X. Bai, “Intermittency analysis project: Appendix B impact of intermittent generation on operation of California power grid,” CEC, CEC-500-2007-081-APB, 2007.

-
- ⁴² R. Walling, "Analysis of wind generation impact on ERCOT ancillary services requirements - Final report," ERCOT, 2008.
- ⁴³ NYISO, "Growing wind: Final report of the NYISO 2010 wind generation study," 2010.
- ⁴⁴ NREL, "Western wind and solar integration study," Subcontract No. AAM-8-77557-01, 2010.
- ⁴⁵ NREL, "Eastern wind integration and transmission study," Subcontract Report NREL/SR-550-47078, 2010.
- ⁴⁶ J. Pfeifenberger, *et al.*, "Transmission investment needs and cost allocation: New challenges and models," Presented to FERC, December 1, 2009.
- ⁴⁷ M. Chupka, "Transforming America's power industry: The investment challenge 2010-2030," The Edison Foundation, 2008.
- ⁴⁸ S. Douglas, T. Garrett, and R. Rhine, "Disallowance and Overcapitalization in the U.S. Electric Utility Industry," Federal Reserve Bank of St. Louis Review, January/February, pp. 23-32, 2009.
- ⁴⁹ J. Stigler, "The Theory of Regulation," *Bell Journal of Economics and Management Science*, vol. 2, no. 1, pp. 3-21, 1971.
- ⁵⁰ M. Olson, *The Logic of Collective Action: Public Goods and the Theory of Groups*. Cambridge: Harvard University Press, 1965.
- ⁵¹ S. Peltzman "Toward a More General Theory of Regulation," *Journal of Law and Economics*, August 1976, Vol. 19, No. 2, pp. 211-40.
- ⁵² L. Lave, *et al.*, "Deregulation/Restructuring part I: Reregulation will not fix the problems," *The Electricity Journal*, vol. 20, no. 8, pp. 9-22, October 2007.

-
- ⁵³ H. Averch, L. Johnson, "Behavior of the firm under regulatory constraint," *The American Economic Review*, vol. 52, no. 5, pp. 1052-1069, Dec 1962.
- ⁵⁴ H. Thompson, *et al.*, "Economies of scale and vertical integration in the investor-owned electric utility industry," National Regulatory Research Institute, NRRI Report No. 96-05, 1996.
- ⁵⁵ R. Nelson, "Returns to scale from variable and total cost functions: Evidence from the electric power industry," *Economic Letters*, vol. 18, Nos. 2-3, pp. 271-276, 1985.
- ⁵⁶ T. Lyon. (2011, March 13). *Will rate-of-return "adders" increase transmission investment?* [Online]. Available: www.nrel.gov/analysis/seminar/docs/ea_seminar_dec_8.ppt.
- ⁵⁷ M. Morey, "Performance based regulation for independent transmission companies," Envision Consulting, 2003.
- ⁵⁸ P. Joskow, "Transmission policy in the United States," *Utilities Policy*, vol. 13, no. 2, pp. 95-115, June 2005.
- ⁵⁹ D. Shirmohammadi, *et al.*, "Some fundamental, technical concepts about cost based transmission pricing," *IEEE Transactions on Power Systems*, vol. 11, no. 2, pp. 1002-1008, May 1996.
- ⁶⁰ P. Joskow. (2005, March 15). *Patterns of transmission investment* [Online]. Available: <http://econ-www.mit.edu/files/1174>.
- ⁶¹ FERC, "Transmission planning and cost allocation by transmission owning and operating public utilities," NOPR, Docket No. RM10-23-000, June 17, 2010.
- ⁶² FERC, "Transmission planning and cost allocation by transmission owning and operating public utilities," Final Ruling, Docket No. RM10-23-000, July 21, 2011.
- ⁶³ FERC. (2012, January 26). *Final rule on transmission planning and cost allocation by transmission owning and operating public utilities* [Online]. Available:

<http://www.ferc.gov/media/news-releases/2011/2011-3/07-21-11-E-6-presentation.pdf>.

⁶⁴ P. Joskow. (2011, October). *Creating a smarter U.S. electricity grid* [Online]. Available: <http://web.mit.edu/ceepr/www/publications/workingpapers/2011-021.pdf>.

⁶⁵ S. Fink, *et al.*, “Transmission cost allocation methodologies for regional transmission organizations,” NREL, Subcontract Report NREL/SR-550-48738, 2010.

⁶⁶ Midwest ISO, “Midwest ISO FERC electric tariff,” Third Revised Volume No. 1.

⁶⁷ P. Joskow, J. Tirole, “Merchant transmission investment,” *The Journal of Industrial Economics*, vol. 53, no. 2, pp. 233-264, June 2005.

⁶⁸ W. Hogan, “Contract networks for electric power transmission,” *Journal of Regulatory Economics*, vol.4, no. 3, pp. 211-242, 1992.

⁶⁹ F. Wu, *et al.*, “Folk theorems on transmission access: Proofs and counterexamples,” *Journal of Regulatory Economics*, vol. 10, no. 1, pp. 5-23, July 1996.

⁷⁰ H. Chao, S Peck, “A market mechanism for electric power transmission,” *Journal of Regulatory Economics*, vol. 10, no. 1, pp. 25-59, 1996.

⁷¹ J. Bushnell, S. Stoft, “Electric grid investment under a contract network regime,” *Journal of Regulatory Economics*, vol. 10, no. 1, pp. 61-79, July 1996.

⁷² J. Bushnell, S. Stoft, “Improving private incentives for electric grid investment,” *Resource and Energy Economics*, vol. 19, no. 1-2, pp. 85-108, March 1997.

⁷³ I. Vogelsang, “Transmission pricing and performance-based regulation,” Carnegie Mellon Conference on Electricity Transmission in Deregulated Markets: Challenges, Opportunities, and Necessary R&D Agenda, 2004.

⁷⁴ J. Sterling, “Merchant transmission,” in *IEEE Power Engineering Society Summer Meeting*, Chicago, IL, vol. 3, 2002, pp. 1071-1072.

⁷⁵ E. Krapels. (2011, March 14). *Merchant transmission* [Online]. Available: http://www.hks.harvard.edu/hepg/Papers/Krapels_Merchant.Transmission_3-03.pdf.

⁷⁶ H. Elahi, *et al.*, “The Linden variable frequency transformer merchant transmission project,” presented at CIGRE, Paris, France, August, 2008.

⁷⁷ J. Graves, “Merchant transmission,” in *IEEE Power Engineering Society Summer Meeting*, Chicago, IL, vol. 3, 2002, pp. 1062-1063.

⁷⁸ NYSERDA, “Guide to estimating benefits and market potential for electricity storage in New York (With emphasis on New York City),” Final Report 07-06, 2007.

⁷⁹ F. Sioshansi (Ed.), *Competitive Electricity Markets: Design, Implementation, Performance*. Oxford: Elsevier, 2008.

⁸⁰ ICF Consulting, “Economic assessment of RTO policy,” February 2002.

⁸¹ Tabors Caramanis & Associates, “RTO West benefit/cost study: Final report presented to RTO West filing utilities,” 2002.

⁸² M. Bailey, *et al.*, “Energy market consolidation and convergence: Seams issues revisited,” *The Electricity Journal*, vol. 14, no. 10, pp. 54-65, December 2001.

⁸³ FERC, “Order provisionally granting RTO status,” Docket No. RT01-2-000, July 12, 2001.

⁸⁴ NERC, “Reliability assessment 2001-2010: The reliability of bulk electric systems in North America,” 2001.

⁸⁵ S. W. Snarr, “FERC rate incentives for transmission infrastructure development,” *The Electricity Journal*, vol. 23, no. 2, pp. 6-17, March 2010.

⁸⁶ T.-O. Leautier, "Regulation of an electric power transmission company," *Energy Journal*, vol. 21, no. 4, pp. 61-92, 2000.

⁸⁷ C. Cambini, L. Rondi. (2009, March 23). *Incentive regulation and investment decisions of European energy utilities* [Online]. Available: http://www.webmeets.com/files/papers/EARIE/2009/127/CR_energy_23_March_2009.pdf.

⁸⁸ P. Joskow, "Incentive regulation in theory and practice: Electricity distribution and transmission networks," January 21, 2006.

⁸⁹ J. Hayden, R. Michaels, "Merchant transmission redux," *Public Utilities Fortnightly*, September 2006, pp. 58-61.

⁹⁰ R. Baldick, "Border flow rights and contracts for differences of differences: Models for electric transmission property rights," *IEEE Transactions on Power Systems*, vol. 22, no. 4, pp. 1495-1506, November 2007.

⁹¹ R. P. O'Neill, *et al.*, "Towards a complete real-time electricity market design," *Journal of Regulatory Economics*, vol. 34, no. 3, pp. 220-250, 2008.

⁹² S. P. Vajjhala, P. S. Fischbeck "Quantifying siting difficulty: A case study of US transmission line siting," *Energy Policy*, vol. 35, no. 1, pp. 650-671, January 2007.

⁹³ T. Lyon, "Why rate-of-return adders are unlikely to increase transmission investment," *The Electricity Journal*, vol. 20, no. 5, pp. 48-55, June 2007.

⁹⁴ H. Rudnick, R. Palma, J. Fernandez, "Marginal pricing and supplement cost allocation in transmission open access," *IEEE Transactions on Power Systems*, vol. 10, no. 2, pp. 1125-1132, May 1995.

⁹⁵ Midwest ISO, "Business practices manual: Transmission planning," BPM-020-r3, 2010.

⁹⁶ H.A. Gil, *et al.*, “Nodal price control: a mechanism for transmission network cost allocation,” *IEEE Transactions on Power Systems*, vol. 21, no. 1, pp. 3-10, February 2006.

⁹⁷ J. Guo, *et al.*, “Revenue reconciliation for spot pricing: Implementation and implication,” *Electric Power Components & Systems*, vol. 32, no. 1, pp. 53-73, January 2004.

⁹⁸ F.D. Galiana, *et al.*, “Transmission network cost allocation based on equivalent bilateral exchanges,” *IEEE Transactions on Power Systems*, vol. 18, no. 4 pp. 1425-1431, November 2003.

⁹⁹ J.W.M. Lima, *et al.*, “An integrated framework for cost allocation in a multi-owned transmission system,” *IEEE Transactions on Power Systems*, vol. 10, no. 2, pp. 971-977, May 1995.

¹⁰⁰ A.J. Conejo, *et al.*, “Z-bus loss allocation,” *IEEE Transactions on Power Systems*, vol. 16, no. 1, pp. 105-110, February 2001.

¹⁰¹ D. Lima, *et al.*, “An overview on network cost allocation methods,” *Electric Power Systems Research*, vol. 79, no. 5, pp. 750-758, May 2009.

¹⁰² A.J. Conejo, *et al.*, “Zbus transmission network cost allocation,” *IEEE Transactions on Power Systems*, vol. 22, no. 1, pp. 342-349, February 2007.

¹⁰³ W.Y. Ng, “Generalized generation distribution factors for power system security evaluations,” *IEEE Transactions on Power Apparatus and Systems*, vol. PAS-100, no. 3, pp. 1001-1005, March 1981.

¹⁰⁴ P.A. Ruiz, *et al.*, “An effective transmission network expansion cost allocation based on game theory,” *IEEE Transactions on Power Systems*, vol. 22, no. 1, pp. 136- 144, February 2007.

¹⁰⁵ F. Lévêque, *et al.*, “Comparing electricity transmission arrangements: Revisiting the main arguments from the economic literature to shed light on the EU 3rd Directive debate,” July 2008.

¹⁰⁶ P. Joskow, “Regional transmission organizations: Don’t settle for nth best ($N \gg 1$),” presentation, September 21, 2001.

¹⁰⁷ M. Pollitt. (2007, August). *The arguments for and against ownership unbundling of energy transmission networks* [Online]. Available: <http://www.eprg.group.cam.ac.uk/wp-content/uploads/2008/11/eprg0714.pdf>.

¹⁰⁸ M. Pollitt, J. Bialek. (2011, May 8). *Electricity network investment and regulation for a low carbon future* [Online]. Available: <http://www.dspace.cam.ac.uk/bitstream/1810/194734/1/0750%26EPRG0721.pdf>.

¹⁰⁹ D. Balmert, G. Brunekreeft. (2009, September). *Unbundling, deep ISOs and network investment* [Online]. Available: http://www.unecom.de/documents/discussionpapers/UNECOM_DP_2009_07.pdf.

¹¹⁰ H. Yamin, “Restructuring and regional transmission organizations in competitive electricity markets in the US,” in *Large Engineering Systems Conference on Power Engineering*, Montreal, QC, 2003, pp. 7-11.

¹¹¹ J.R. Boyce, A. Hollis, “Governance of electricity transmission systems,” *Energy Economics*, vol. 27, no. 2, pp. 237-255, 2005.

¹¹² W. Hogan, “Market-based transmission investments and competitive electricity markets,” in *Electric choices: deregulation and the future of electric power*, A. Kleit, Ed. Plymouth, UK: Rowman & Littlefield, 2007.

¹¹³ G. Brunekreeft. (2003, September 15). *Market-based investment in electricity transmission networks: Controllable flow* [Online]. Available: <http://www.econ.cam.ac.uk/electricity/publications/wp/ep29.pdf>.

¹¹⁴ A.A. Alabduljabbar, J.V. Milanović, “Assessment of techno-economic contribution of FACTS devices to power system operation,” *Electric Power Systems Research*, vol. 80, no. 10, pp. 1247-1255, October 2010.

-
- ¹¹⁵ N. Mithulananthan, N. Acharya, "A proposal for investment recovery of FACTS devices in deregulated electricity markets," *Electric Power Systems Research*, vol. 77, no. 5-6, pp. 695-703, April 2007.
- ¹¹⁶ S. N. Singh, A. K. David, "Optimal location of FACTS devices for congestion management," *Electric Power Systems Research*, vol. 58, no. 2, pp. 71-79, June 2001.
- ¹¹⁷ G.B. Shrestha, Wang Feng, "Effects of series compensation on spot price power markets," *International Journal of Electrical Power & Energy Systems*, vol. 27, no. 5-6, pp. 428-436, June-July 2005.
- ¹¹⁸ P. Attaviriyapap, A. Yokoyama, "Economic benefit comparison between series FACTS device installation and new transmission line investment in the deregulated power system using probabilistic method," in *International Conference on Probabilistic Methods Applied to Power Systems*, Stockholm, 2006, pp. 1 - 7.
- ¹¹⁹ K. Mwanza, *et al.*, "Economic evaluation of FACTS for congestion management in pool markets," in *IEEE Power Tech*, Lausanne, 2007, pp. 2053 - 2058.
- ¹²⁰ Z. Yu, D. Lusan, "Optimal placement of FACTS devices in deregulated systems considering line losses," *International Journal of Electrical Power & Energy Systems*, vol. 26, no. 10, pp. 813-819, December 2004.
- ¹²¹ Kwang-Ho Lee, "Optimal siting of TCSC for reducing congestion cost by using shadow prices," *International Journal of Electrical Power & Energy Systems*, vol. 24, no. 8, pp. 647-653, October 2002.
- ¹²² Y. Xiao, Y. H. Song, "Power flow studies of a large practical power network with embedded facts devices using improved optimal multiplier newton-raphson method," *European Transactions on Electric Power*, vol. 11, no. 4, pp. 247-256, July/August 2001.
- ¹²³ Y. Xiao, *et al.*, "Power injection method and linear programming for FACTS control," in *IEEE Power Engineering Society Winter Meeting*, Singapore, vol. 2, pp. 877-884.

-
- ¹²⁴ S. Arabi, P. Kundur, "A versatile FACTS device model for powerflow and stability simulations," *IEEE Transactions on Power Systems*, vol. 11, no. 4, pp. 1944-1950, November 1996.
- ¹²⁵ C.R. Fuerte-Esquivel, E. Acha, "A newton-type algorithm for the control of power flow in electrical power networks," *IEEE Transactions on Power Systems*, vol. 12, no. 4, pp. 1474-1480, November 1997.
- ¹²⁶ G.N. Taranto, *et al.*, "Representation of FACTS devices in power system economic dispatch," *IEEE Transactions on Power Systems*, vol. 7, no. 2, pp. 572-576, May 1992.
- ¹²⁷ S. Rahimzadeh, M. T. Bina, "Looking for optimal number and placement of FACTS devices to manage the transmission congestion," *Energy Conversion and Management*, vol. 52, no. 1, pp. 437-446, January 2011.
- ¹²⁸ B. Venkatesh, H. B. Gooi, "Optimal siting of united power flow controllers," *Electric Power Components and Systems*, vol. 34, no. 3, pp. 271-284, 2006.
- ¹²⁹ P. Paterni, *et al.*, "Optimal location of phase shifters in the French network by genetic algorithm," *IEEE Transactions on Power Systems*, vol. 14, no. 1, pp. 37-42, February 1999.
- ¹³⁰ A. Sharma, *et al.*, "Combined optimal location of FACTS controllers and loadability enhancement in competitive electricity markets using MILP," in *IEEE Power Engineering Society General Meeting*, 2005, pp. 670-677.
- ¹³¹ S. Gerbex, *et al.*, "Optimal location of multi-type FACTS devices in a power system by means of genetic algorithms," *IEEE Transactions on Power Systems*, vol. 16, no. 3, pp. 537-544, August 2001.
- ¹³² D. Arabkhaburi, *et al.*, "Optimal placement of UPFC in power systems using genetic algorithm," in *IEEE International Conference on Industrial Technology*, Mumbai, 2006, pp. 1694-1699.

¹³³ W. Feng, G.B. Shrestha, "Allocation of TCSC devices to optimize total transmission capacity in a competitive power market," in *IEEE Power Engineering Society Winter Meeting*, Columbus, OH, 2001, pp. 587-593.

¹³⁴ J. Mutale, G. Strbac, "Transmission network reinforcement versus FACTS: An economic assessment," *IEEE Transactions on Power Systems*, vol. 15, no. 3, pp. 961-967, August 2000.

¹³⁵ W. Ongsakul, P. Bhasaputra, "Optimal power flow with FACTS devices by hybrid TS/SA approach," *International Journal of Electrical Power & Energy Systems*, vol. 24, no. 10, pp. 851-857, December 2002.

¹³⁶ K.M. Rogers, T.J. Overbye, "Some applications of distributed flexible AC transmission system (D-FACTS) devices in power systems," in *North American Power Symposium*, Calgary, AB, 2008, pp. 1-8.

¹³⁷ P. H. Kim, *et al.*, "Optimal placement of FACTS in northern power transmission system of Vietnam using an OPF formulation," in *2007 Large Engineering Systems Conference on Power Engineering*, Montreal, QC, 2007, pp. 112-117.

¹³⁸ B. Chong, "Congestion management using FACTS controllers," Ph.D. dissertation, School of Engineering, University of Warwick, 2008.

¹³⁹ L.J. Cai, *et al.*, "Optimal choice and allocation of FACTS devices in deregulated electricity market using genetic algorithms," in *IEEE PES Power Systems Conference and Exposition*, New York, NY, 2004, pp. 201-207.

¹⁴⁰ A. L'Abbate, *et al.*, "Economics of FACTS integration into the liberalised European power system," in *IEEE Power Tech*, Lausanne, 2007, pp. 885-890.

¹⁴¹ R.M.G. Castro, *et al.*, "Application of FACTS in the Portuguese transmission system: investigation on the use of phase-shift transformers," in *IEEE Power Tech Proceedings*, Porto, vol. 4, 2001.

-
- ¹⁴² K. Mwanza, Y. Shi, "Congestion management: Re-dispatch and application of FACTS," Thesis, Department of Energy and Environment, Chalmers University of Technology, 2006.
- ¹⁴³ T.T. Lie, H. Hailong, "Optimal dispatch in pool market with FACTS devices," in *IEEE Power Engineering Society General Meeting*, New York, NY, pp. 135-140.
- ¹⁴⁴ National Electricity Code Administrator, "Entrepreneurial interconnectors: safe harbour provisions," November 1998.
- ¹⁴⁵ R. O'Neill, *et al.* "Dispatchable transmission in RTO markets," *IEEE Transactions on Power Systems*, vol. 20, no. 1, pp. 171-179, February 2005.
- ¹⁴⁶ M. Rosenzweig, J. Bar-lev, "Transmission access and pricing: Some other approaches," *Public Utilities Fortnightly*, pp. 20-26, August 1986.
- ¹⁴⁷ D. Shirmohammadi, *et al.*, "Evaluation of transmission network capacity use for wheeling transactions," *IEEE Transactions on Power Systems*, vol. 4, no. 4, pp. 1405-1413, November 1989.
- ¹⁴⁸ D. Das, "Dynamic control of grid power flow using controllable network transformers," Ph.D. dissertation, School of Electrical and Computer Engineering, Georgia Institute of Technology, Atlanta, GA, 2012.
- ¹⁴⁹ J.A. Peças Lopes, *et al.*, "Integrating distributed generation into electric power systems: A review of drivers, challenges and opportunities," *Electric Power Systems Research*, vol. 77, no. 9, pp. 1143-1238, July 2007.
- ¹⁵⁰ R.E. Brown, *et al.*, "Siting distributed generation to defer T&D expansion," in *IEEE/PES Transmission and Distribution Conference and Exposition*, Atlanta, GA, 2001, vol. 2, pp. 622-627.
- ¹⁵¹ D. T-C. Wang, *et al.*, "Evaluating investment deferral by incorporating distributed generation in distribution network planning," in *16th Annual Power Systems Computation Conference*, Glasgow, 2008, pp. 1-8.

¹⁵² G.R. Pudaruth, F. Li, “Costs and benefits assessment considering deferral of assets expansion in distribution systems,” in *42nd International Universities Power Engineering Conference*, Brighton, 2007, pp. 872-878.

¹⁵³ R. Beach, P. McGuire. (2011, May 4). *Response to Dr. Severin Borenstein’s January 2008 paper on the economics of photovoltaics in California* [Online]. Available: http://votesolar.org/linked-docs/borenstein_response.pdf.

¹⁵⁴ J. Zhao, J. Foster. (2011, March 25). *Investigating the impacts of distributed generation on transmission expansion cost: An Australian case study* [Online]. Available: http://www.uq.edu.au/economics/eemg_/pdf/02.pdf.

¹⁵⁵ B. Sovacool, K. Sovacool, “Identifying future electricity-water tradeoffs in the United States,” *Energy Policy*, vol. 37, no. 7, pp. 2763-2773, July 2009.

¹⁵⁶ OMB, “OMB Bulletin No. 10-02: Update of statistical area definitions and guidance on their uses,” December 1, 2009.

¹⁵⁷ US Census Bureau, “Estimates of population change for metropolitan statistical areas and rankings: July 1, 2008 to July 1, 2009,” CBSA-EST2009-05 March 2010.

¹⁵⁸ GAO, “Energy-water nexus: Improvements to federal water use data would increase understanding of trends in power plant water use,” GAO-10-23, October 2009.

¹⁵⁹ DOE. (2013, February 18). *Assumptions to the Annual Energy Outlook 2012* [Online]. Available: [http://www.eia.gov/forecasts/aeo/assumptions/pdf/0554\(2012\).pdf](http://www.eia.gov/forecasts/aeo/assumptions/pdf/0554(2012).pdf).

¹⁶⁰ Sandia National Labs, “Energy storage for the electricity grid: Benefits and market potential assessment guide,” Report SAND2010-0815, February 2010.

¹⁶¹ EPRI, DOE, “EPRI-DOE handbook of energy storage for transmission & distribution applications,” Report 1001834, December 2003.

¹⁶² E. Bompard, *et al.*, “The role of load demand elasticity in congestion management and pricing,” in *IEEE Power Engineering Society Summer Meeting*, Seattle, WA, 2000, vol. 4, pp. 2229-2234.

¹⁶³ N. Lu, T. Nguyen, “Grid FriendlyTM appliances - Load-side solution for congestion management,” in *IEEE PES Transmission and Distribution Conference and Exhibition*, Dallas, TX, 2006, pp. 1269-1273.

¹⁶⁴ G. Strbac, “Demand side management: Benefits and challenges,” *Energy Policy*, vol. 36, no. 12, pp. 4419-4426, December 2008.

¹⁶⁵ T.D. Mount, *et al.*, “Integrating Wind Power: Can Controllable Load Substitute for Transmission Upgrades?,” 44th Hawaii International Conference on System Sciences (HICSS), Manoa, HI, 2011.

¹⁶⁶ J.-H. Kima, A. Shcherbakova, “Common failures of demand response,” *Energy*, vol. 36, no. 2, pp. 873-880, February 2011.

¹⁶⁷ H. Saitoh, *et al.*, “An autonomous decentralized control mechanism for power flow in an open electric energy network,” *Electrical Engineering in Japan*, vol. 121, no. 4, pp. 28-37, 1997.

¹⁶⁸ M. Alizadeh, A. Scaglione, R.J. Thomas, “From Packet to Power Switching: Digital Direct Load Scheduling,” *IEEE Journal on Selected Areas in Communications*, vol. 30, no. 6, 1027-1036, 2012.

¹⁶⁹ R. Katz, *et al.*, “An information-centric energy infrastructure: The Berkeley view,” *Sustainable Computing: Informatics and Systems*, vol. 1, no. 1, pp. 7-22, 2011.

¹⁷⁰ L.H. Tsoukalas, R. Gao, “From smart grids to an energy internet: Assumptions, architectures and requirements,” in *Electric Utility Deregulation and Restructuring and Power Technologies*, Nanjing, China, 2008, pp. 94-98.

¹⁷¹ GE (2013, February 18). *Energy Internet* [Online]. Available: http://www.itsyoursmartgrid.com/solutions/energy_internet.html.

-
- ¹⁷² X. Yi, *et. al.*, “Energy router: Architectures and functionalities toward Energy Internet,” in *IEEE International Conference on Smart Grid Communications*, Brussels, Belgium, 2011, pp. 31-36.
- ¹⁷³ Z. Jianhua, W. Wenye, S. Bhattacharya, “Architecture of solid state transformer-based energy router and models of energy traffic,” in *IEEE PES Innovative Smart Grid Technologies (ISGT)*, Washington, DC, 2012.
- ¹⁷⁴ J. Toyoda, H. Saitoh, “Proposal of an open-electric-energy-network (OEEN) to realize cooperative operations of IOU and IPP,” in *Proceedings of International Conference on Energy Management and Power Delivery*, Singapore, 1998, pp. 218-222.
- ¹⁷⁵ V. Krylov, D. Ponomarev, A. Loskutov, “Toward the power InterGrid ,” in *IEEE International Energy Conference and Exhibition*, 2010, Manama, Bahrain, pp. 351-356.
- ¹⁷⁶ M.M. He, *et. al.*, “An Architecture for Local Energy Generation, Distribution, and Sharing,” in *IEEE Energy 2030 Conference*, Atlanta, GA, 2008.
- ¹⁷⁷ R. Katz (2013, February 18). “*Smart Grid*”: *R&D for an Intelligent 21st Century Electrical Energy Distribution Infrastructure* [Online]. Available: http://cra.org/ccc/docs/init/Energy_Grid.pdf.
- ¹⁷⁸ B. Zhang, J. Baillieul, “A packetized direct load control mechanism for demand side management,” in *IEEE 51st Annual Conference on Decision and Control*, Maui, HI, pp. 3658-3665, 2012.
- ¹⁷⁹ R. Abe, H. Taoka, D. McQuilkin, Digital Grid: Communicative Electrical Grids of the Future, *IEEE Transactions on Smart Grid*, vol. 2, no. 2, pp. 399-410, 2011.
- ¹⁸⁰ H. Takashi, *et. al.*, “Power Packetization and Routing for Smart Management of Electricity,” in *AIAA 10th International Energy Conversion Engineering Conference*, Atlanta, GA, 2012.

¹⁸¹ Y. Matsumoto, S. Yanabu, "Internet Style Electric Energy Network Architecture," in *5th WSEAS/IASME International Conference on Electric Power Systems, High Voltages, Electric Machines*, Tenerife, Spain, 2005, pp. 332-337.

¹⁸² F. Kreikebaum, D. Divan, "Smart Grids, Distributed control for," in *Encyclopedia of Sustainability Science and Technology*, R. Meyers, Ed. New York, NY: Springer, 2012.

¹⁸³ N. Hingorani, L. Gyugyi, *Understanding FACTS: Concepts and technology of flexible AC transmission systems*. New York, NY, IEEE Press, 1999.

¹⁸⁴ R. O'Neill, "Merchant transmission: A new approach to transmission expansion," in *IEEE Power and Energy Society General Meeting*, Minneapolis, USA, 2010, pp. 1-5.

¹⁸⁵ ABB. (September 2010). *HVDC classic - Reference list* [Online].
[http://www05.abb.com/global/scot/scot221.nsf/veritydisplay/a0f3c70bc17b846fc12577a8004da670/\\$file/pow-0013%20rev10%20lr.pdf](http://www05.abb.com/global/scot/scot221.nsf/veritydisplay/a0f3c70bc17b846fc12577a8004da670/$file/pow-0013%20rev10%20lr.pdf).

¹⁸⁶ ABB. (November 2010). *HVDC light and SVC light: Reference List* [Online].
[http://www05.abb.com/global/scot/scot221.nsf/veritydisplay/62bd98e2630cef66c12577de003bb947/\\$file/pow-0027%20rev11%20lr.pdf](http://www05.abb.com/global/scot/scot221.nsf/veritydisplay/62bd98e2630cef66c12577de003bb947/$file/pow-0027%20rev11%20lr.pdf).

¹⁸⁷ Siemens. (2011). *HVDC - High voltage direct current power transmission* [Online]. Available: http://www.energy.siemens.com/hq/pool/hq/power-transmission/HVDC/HVDC_References.pdf.

¹⁸⁸ IEEE AC/DC System Dynamics Task Force, "Dynamic performance characteristics of North American HVDC systems for transient and dynamic stability evaluations," *IEEE Transactions on Power Apparatus and Systems*, Vol. PAS-100, No. 7, pp. 3356-3364, July 1981.

¹⁸⁹ P. Hassink, *et al.*, "Second & future applications of stability enhancement in ERCOT with asynchronous interconnections," in *IEEE Power Engineering Society General Meeting*, Tampa, FL, 2007, pp. 1-7.

¹⁹⁰ K. Bergmann, *et al.*, “Digital simulation, transient network analyzer and field tests of the closed loop control of the Eddy County SVC,” *IEEE Transactions on Power Delivery*, vol. 8, no. 4, pp. 1867-1873, October 1993.

¹⁹¹ M. Thompson, *et al.*, “AEP experience with protection of three delta/hex phase angle regulating transformers,” in *Power Systems Conference: Advanced Metering, Protection, Control, Communication, and Distributed Resources*, Clemson, SC, 2007, pp. 96-105.

¹⁹² WECC. (2009, June 16). *Unscheduled flow (USF) FAQ* [Online]. Available: <http://www.wecc.biz/committees/StandingCommittees/OC/UFAS/Shared%20Documents/USF%20FAQ.doc>.

¹⁹³ WECC. (2011, March 20). *Regional reliability plan: Key facilities list* [Online]. Available: <http://www.wecc.biz/library/Library/Reliability%20Coordination/Key%20facilities%20list%202007.pdf>.

¹⁹⁴ WAPA. (March 20, 2011). *Chapter Two: Threads in the distance: Power, transmission and demand* [Online]. Available: <http://www.wapa.gov/about/pdf/histcha2.pdf>.

¹⁹⁵ WAPA. (2010, May). *Transfer capacity study yellowtail-south* [Online]. Available: http://www.oatioasis.com/LAPT/LAPTdocs/Yellowtail_South.pdf.

¹⁹⁶ EPE, “El Paso electric company 2011-2020 system expansion plan,” 9/17/2010.

¹⁹⁷ CAISO. (2011, March 20). *Study methodology* [Online]. Available: <http://www.caiso.com/docs/09003a6080/2a/7d/09003a60802a7d64.pdf>.

¹⁹⁸ WECC. (2010, June 9). *Associated material for 2020 HSI base case* [Online]. Available: <http://www.wecc.biz/committees/BOD/TEPPC/TAS/SWG/SWG28July/Lists/Minutes/1/2020%20Base%20Case%20Sig%20Additions.pdf>.

¹⁹⁹ WECC. (2012, February 27,). *WSCC unscheduled flow administrative subcommittee meeting minutes* [Online]. Available:

http://www.wecc.biz/committees/StandingCommittees/OC/UFAS/Lists/Calendar/Attachments/9/UFASMinutes_Aug00.pdf.

²⁰⁰ XCEL Energy. (2011, March 21). *SPS planning criteria and study methodology* [Online]. Available: <http://www.xcelenergy.com/SiteCollectionDocuments/docs/AttachmentRCriteria12-7-07Rev1FINAL.pdf>.

²⁰¹ NYISO, “NYISO operating study: Summer 2006,” April 2006.

²⁰² NYISO, “NYISO operating study: Winter 2004-2005,” November 2004.

²⁰³ ReliabilityFirst, “Eastern interconnection reliability assessment group RFC-NPCC (RN) study procedures manual, Version 2,” 2010.

²⁰⁴ ISONE. (2011, March 21). *Reference document for base modeling of transmission system elements in New England* [Online]. Available: http://www.isone.com/rules_proceeds/isone_plan/system_elements_modeling_guide_rev3.pdf.

²⁰⁵ PJM, “PJM manual 03: Transmission operations, Revision: 37,” 2010.

²⁰⁶ NERC, “2008 Summer reliability assessment,” May 2008.

²⁰⁷ SPS, “10 year transmission plan and 20 year strategic vision,” 2009.

²⁰⁸ E. Pratico, et al, “First multi-channel VFT application - The Linden project,” in *IEEE PES Transmission and Distribution Conference and Exposition*, New Orleans, LA, 2010, pp. 1-7.

²⁰⁹ B.A. Renz, et al., “AEP unified power flow controller performance,” *IEEE Transactions on Power Delivery*, Vol. 14, No. 4, pp. 1374-1381, October 1999.

-
- ²¹⁰ J. Sun, "Operating characteristics of the convertible static compensator on the 345 kV network," in *IEEE PES Power Systems Conference and Exposition*, New York, NY, 2004, vol. 2, pp. 732-738.
- ²¹¹ APS, "Feasibility study - final APS contract no. 52055," 2008.
- ²¹² NYISO, "NYISO operating study: Summer 2010," 2010.
- ²¹³ A.S. Mehraban, *et al.*, "Installation, commissioning, and operation of the world's first UPFC on the AEP system," in *1998 International Conference on Power System Technology*, Beijing, 1998, vol. 1, pp. 323-327.
- ²¹⁴ Siemens. (2009, October). *Reactive power compensation - Reference list* [Online]. Available: http://www.energy.siemens.com/co/pool/hq/power-transmission/FACTS/Siemens_Reference_List_FACTS.pdf.
- ²¹⁵ S. Meikandasivam, *et al.*, "Performance of installed TCSC projects," in *2010 India International Conference on Power Electronics*, New Delhi, 2011, pp. 1-8.
- ²¹⁶ G. Latorre, *et al.*, "Classification of publications and models on transmission expansion planning," *IEEE Transactions on Power Systems*, vol. 18, no. 2, pp. 938-946, May 2003.
- ²¹⁷ Y. Xiao, *et al.*, "Power flow control approach to power systems with embedded FACTS devices," *IEEE Transactions on Power Systems*, vol. 17, no. 4, pp. 943-950, Nov 2002.
- ²¹⁸ J. Jayakumar, K. Thanushkodi, "Application of exponential evolutionary programming to security constrained economic dispatch with FACTS devices," *Asian Journal of Scientific Research*, vol. 1, no. 4, pp. 374-384, 2008.
- ²¹⁹ M. Noroozian, G. Andersson, "Power flow control by use of controllable series components," *IEEE Transactions on Power Delivery*, vol. 8, no. 3, pp. 1420-1429, July 1993.

-
- ²²⁰ Z.X. Han, "Phase shifter and power flow control, *IEEE Transactions on Power Apparatus and Systems*," Vol. PAS-101, No. 10, pp. 3790-3795, October 1982.
- ²²¹ X-P. Zhang, E.J. Handschin, "Optimal power flow control by converter based FACTS controllers," in *International Conference on AC-DC Power Transmission*, London, 2001, pp. 250-255.
- ²²² D.J. Gotham, G.T. Heydt, "Power flow control and power flow studies for systems with FACTS devices," *IEEE Transactions on Power Systems*, vol. 13, no. 1, pp. 60-65, February 1998.
- ²²³ C.R. Fuerte-Esquivel, E. Acha, "Newton-raphson algorithm for the reliable solution of large power networks with embedded FACTS devices," *IEE Proceedings of Generation, Transmission and Distribution*, vol. 143, no. 5, pp. 447-454, September 1996.
- ²²⁴ F. Capitanescu, L. Wehenkel, "A New Iterative Approach to the Corrective Security-Constrained Optimal Power Flow Problem, *IEEE Transactions on Power Systems*, vol. 23, no. 4, 1533-1541, r2008.
- ²²⁵ B. Stott, O. Alsac, A.J. Monticelli, "Security analysis and optimization," *Proceedings of the IEEE*, vol. 75, no. 12, pp. 1623-1644, 1987.
- ²²⁶ J.L. Whyson, *et al.*, "Computer program for automatic transmission planning," *AIEE Transactions of the Power Apparatus and Systems*, vol. 81, no. 3, pp. 774-780, April 1962.
- ²²⁷ r1633- C.J. Baldwin, *et al.*, "A model for transmission planning by logic," *AIEE Transactions of Power Apparatus and Systems*, vol. 78, no. 4, pp. 1638-1643, December 1959.
- ²²⁸ J.K. Dillard, H.K. Sels, "An introduction to the study of system planning by operational gaming models," *AIEE Transactions of Power Apparatus and Systems*, vol. 78, no. 4, pp. 1284-1289, December 1959.

-
- ²²⁹ N. Acharya, N. Mithulananthan, “Locating series FACTS devices for congestion management in deregulated electricity markets,” *Electric Power Systems Research*, vol. 77, no. 3-4, pp. 352-360, March 2007.
- ²³⁰ A.H. Escobar, *et al.*, “Multistage and coordinated planning of the expansion of transmission systems,” *IEEE Transactions on Power Systems*, vol. 19, no. 2, pp. 735-744, May 2004.
- ²³¹ I.J. Silva, *et al.*, “Genetic algorithm of Chu and Beasley for static and multistage transmission expansion planning,” in *IEEE Power Engineering Society General Meeting*, Montreal, QC, 2006, pp. 1-7.
- ²³² R. Fu, *et al.*, “A new congestion monitoring index constrained multistage transmission expansion planning under market environment,” in *Third International Conference on Electric Utility Deregulation and Restructuring and Power Technologies*, Nanjing, 2008, pp. 978-983.
- ²³³ V. Chandra, *Fundamentals of Natural Gas - An International Perspective*. Tulsa, Oklahoma: PennWell, 2006.
- ²³⁴ EIA (2012, February 10). *About U.S. Natural Gas Pipelines – Transporting Natural Gas* [Online]. Available: http://www.eia.gov/pub/oil_gas/natural_gas/analysis_publications/ngpipeline/fullversion.pdf.
- ²³⁵ EIA. (2012, February 10). *U.S. Natural Gas Pipeline Network, 2009* [Online]. Available: http://www.eia.gov/pub/oil_gas/natural_gas/analysis_publications/ngpipeline/ngpipelines_map.html.
- ²³⁶ S. Mokhatab, *et al.*, *Handbook of Natural Gas Transmission and Processing*. Burlington, MA: Gulf Professional Publishing, 2006.
- ²³⁷ Natural Gas Supply Association. (2012, February 10). *The Transportation of natural gas* [Online]. Available: <http://www.naturalgas.org/naturalgas/transport.asp>.

-
- ²³⁸ J. Makhholm, "Seeking competition and supply security in natural gas: The US experience and European challenge," NERA Economic Consulting, June 2007.
- ²³⁹ J. Speight, *Natural Gas - A Basic Handbook*. Houston, TX: Gulf Publishing Company, 2007.
- ²⁴⁰ C. A. Dahl, T. K. Matson, "Evolution of the U.S. natural gas industry in response to changes in transaction costs," *Land Economics*, vol. 74, no. 3, pp. 390-408, August 1998.
- ²⁴¹ Public Policy for the Private Sector, "Development of competitive natural gas markets in the United States," Note No. 141, 1998.
- ²⁴² J. Leitzinger, "A retrospective look at wholesale gas: Industry restructuring," *Journal of Regulatory Economics*, vol. 2, no. 1, pp. 79-101, 2002.
- ²⁴³ H. Werntz, "Let's make a deal: Negotiated rates for merchant transmission," *Pace Environmental Law Review*, vol. 28, no. 2, pp. 421-479, 2011.
- ²⁴⁴ J. Makhholm, "Electricity transmission cost allocation: A throwback to an earlier era in gas transmission," *The Electricity Journal*, vol. 20, no. 10, pp. 13-25, December 2007.
- ²⁴⁵ EIA, "Energy policy act transportation study: Interim report on natural gas flows and rates," DOE/EIA-0602(95), 1995.
- ²⁴⁶ H. Johal, D. Divan, "From power line to pipeline - Creating an efficient and sustainable market structure," in IEEE Energy 2030 Conference, Atlanta, GA, 2008, pp. 1-7.
- ²⁴⁷ W. Hogan, "Market-based transmission investments and competitive electricity markets," in *Electric choices: deregulation and the future of electric power*, A. Kleit, Ed. Plymouth, UK: Rowman & Littlefield, 2007.
- ²⁴⁸ Department of Energy. (2012, February 29). *Renewable energy certificates* [Online]. Available:

<http://apps3.eere.energy.gov/greenpower/markets/certificates.shtml?page=0>

²⁴⁹ EIA, “Annual Energy Review 2011,” DOE/EIA-0384(2011), 2012.

²⁵⁰ DOE (2011, July 5). *Obtaining the eastern wind dataset* [Online]. Available: <http://www.nrel.gov/wind/integrationdatasets/eastern/data.html>.

²⁵¹ R. Zavadil, “Eastern interconnection wind integration and transmission study, technical review committee meeting #2,” October 8, 2008.

²⁵² D. Divan, W. Brumsickle, “A distributed static series compensator system for realizing active power flow control on existing power lines,” *IEEE Transactions on Power Delivery*, vol. 22, no. 1, pp. 642-649, January 2007.

²⁵³ F. Kreikebaum, *et. al.*, “Ubiquitous power flow control in meshed grids,” in *Energy Conversion Congress and Exposition*, San Jose, CA, 2009, pp. 3907-3914.

²⁵⁴ J. Sastry, “Direct AC control of grid assets,” Ph.D. dissertation, School of Electrical and Computer Engineering, Georgia Institute of Technology, Atlanta, GA, 2011.

²⁵⁵ H. Johal, “Distributed Series Reactance: A new approach to realize grid power flow control,” Ph.D. dissertation, School of Electrical and Computer Engineering, Georgia Institute of Technology, Atlanta, GA, 2008.

²⁵⁶ D. Das, D. Divan, R.G. Harley, “Increasing inter-area available transfer capacity using controllable network transformers,” in *Energy Conversion Congress and Exposition*, Atlanta, GA, 2010, pp. 3618-3625.

²⁵⁷ EPRI, “Electricity Energy Storage Technology Options: A White Paper Primer on Applications, Costs and Benefits,” 1020676, December 2010.

²⁵⁸ EPRI, “Electricity Energy Storage Technology Options: A White Paper Primer on Applications, Costs and Benefits,” 1020676, December 2010.

²⁵⁹ D.G. Choi, *et al.*, “Coordinated EV Adoption: Double-Digit Reductions in Emissions and Fuel Use for \$40/Vehicle-Year,” *Environmental Science & Technology*, vol. 47, no. 18, pp. 10703-10707, 2013.

²⁶⁰ USDOT FHA (2013, January 18). *2009 NHTS - Version 2.1* [Online]. Available: <http://nhts.ornl.gov/download.shtml>.

²⁶¹ F. Kreikebaum, *et al.*, “Increasing the likelihood of large-scale grid-enabled vehicle (GEV) penetration through appropriate design choices,” in *IEEE Vehicle Power and Propulsion Conference*, Chicago, IL, 2011.

²⁶² A. Brooks, *et al.*, “Demand Dispatch,” *IEEE Power and Energy Magazine*, vol. 8, no. 3, pp. 20 – 29, 2010.

²⁶³ M. Caramanis, J.M. Foster, “Management of electric vehicle charging to mitigate renewable generation intermittency and distribution network congestion,” in *48th IEEE Conference on Decision and Control*, Shanghai, China, pp. 4717-4722, 2009.

²⁶⁴ NREL, “An Evaluation of Utility System Impacts and Benefits of Optimally Dispatched Plug-In Hybrid Electric Vehicles,” NREL/TP-620-40293, 2006.

²⁶⁵ L. Göransson, S. Karlsson, F. Johnsson, “Integration of plug-in hybrid electric vehicles in a regional wind-thermal power system,” *Energy Policy*, vol. 38, no. 10, pp. 5482-5492, 2010.

²⁶⁶ J.E. Hernandez, F. Kreikebaum, D. Divan, “Flexible electric vehicle (EV) charging to meet renewable portfolio standard (RPS) mandates and minimize green house Gas emissions,” *IEEE Energy Conversion Congress and Exposition*, Atlanta, GA, pp. 4270-4277, 2010.

²⁶⁷ F. Kreikebaum, D. Divan, “Overlaying a parallel market to increase renewable penetration,” *IEEE Energy Conversion Congress and Exposition*, Atlanta, GA, pp. 687-694, 2010.

²⁶⁸ A. Papavasiliou, S. S. Oren, “Coupling Wind Generators with Deferrable Loads,” in *IEEE Energy2030*, Atlanta, Georgia, 2008.

-
- ²⁶⁹ A. Papavasiliou, S. Oren, "Supplying renewable energy to deferrable loads: Algorithms and economic analysis," in *IEEE Power and Energy Society General Meeting*, Minneapolis, MN, 2010.
- ²⁷⁰ N. Roterling, M. Ilic, "Optimal Charge Control of Plug-In Hybrid Electric Vehicles in Deregulated Electricity Markets," *IEEE Transactions on Power Systems*, vol. 26, no. 3, pp. 1021-1029, 2011.
- ²⁷¹ A. Shortt, M. O'Malley, "Impact of optimal charging of electric vehicles on future generation portfolios," in *IEEE PES/IAS Conference on Sustainable Alternative Energy (SAE)*, Valencia, Spain, 2009.
- ²⁷² J. Wang, "Impact of plug-in hybrid electric vehicles on power systems with demand response and wind power," *Energy Policy*, vol. 39, no. 7, pp. 4016-4021, 2011.
- ²⁷³ C.B. Lucasius, G. Kateman, "Genetic algorithms for large-scale optimization in chemometrics: An application," *Trends in Analytical Chemistry*, vol. 10, no 8, pp. 254-261, 1991.
- ²⁷⁴ H.P. Schwefel, "On the evolution of evolutionary computation," in *Computational Intelligence: Imitating Life*, J.M. Zurada, R.J. Marks II, C.J. Robinson (Eds.), Piscataway, NJ: IEEE Press, 1994.
- ²⁷⁵ D. Woodfin (2013, February 6). *Economic Planning - Theory and Current Practice* [Online]. Available: http://www.ercot.com/content/meetings/cmwg/keydocs/2011/0304/Economic_Planning_theory_and_practice_for_CMWG_PLWG_rev1.ppt.
- ²⁷⁶ Energy and Environmental Economics Inc. (2013, February 6). *TEPPC Capital Cost Model* [Online]. Available: http://www.wecc.biz/committees/BOD/TEPPC/Versions/100117_TEPPC_E3_ProForma.xls_2.0.xls.

-
- ²⁷⁷ R.A. Gallego, A. Monticelli, R. Romero, "Transmission system expansion planning by an extended genetic algorithm," *IEE Proceedings Generation, Transmission and Distribution*, vol. 145, no. 3, pp. 329-335, 1998.
- ²⁷⁸ E.L Da Silva, H.A. Gil, J.M. Areiza, "Transmission network expansion planning under an improved genetic algorithm," *IEEE Transactions on Power Systems*, vol. 15, no. 3, pp. 1168 – 1174, 2000.
- ²⁷⁹ J. Kennedy, R. Eberhart, *Swarm Intelligence*, San Diego, CA: Academic Press, 2001.
- ²⁸⁰ R.C. Leou; S.Y. Chan, "A Multiyear Transmission Planning Under a Deregulated Market," *IEEE TENCON*, Hong Kong, pp. 1-4, 2006.
- ²⁸¹ D.E. Goldberg, K. Deb, J.H. Clark, "Genetic algorithms, noise, and the sizing of populations," *Complex Systems*, vol. 6, no. 4, pp. 333-362, 1992.
- ²⁸² Wen-Yang Lin, Wen-Yuan Lee, Tzung-Pei Hong, "Adapting Crossover and Mutation Rates in Genetic Algorithms," *Journal of Information Science and Engineering*, vol. 19, pp. 889-903, 2003.
- ²⁸³ P. Sánchez-Martín, A. Ramos, and J. Francisco Alonso, "Probabilistic Midterm Transmission Planning in a Liberalized Market," *IEEE Transactions on Power Systems*, vol. 20, no. 4, pp. 2135-2142, 2005.
- ²⁸⁴ S. de la Torre, A. Conejo, J. Contreras, "Transmission Expansion Planning in Electricity Markets," *IEEE Transactions on Power Systems*, vol. 23, no. 1, pp. 238-248, 2008.
- ²⁸⁵ N. Alguacil, A. Motto, A. Conejo, "Transmission Expansion Planning: A Mixed-Integer LP Approach," *IEEE Transactions on Power Systems*, vol. 18, no. 3, pp. 1070-1077, 2003.
- ²⁸⁶ M.J. Rider, A.V. Garcia, R. Romero, "Power system transmission network expansion planning using AC model," *IET Generation, Transmission & Distribution*, vol. 1, no. 5, pp. 731-742, 2007.

-
- ²⁸⁷ G.B. Shrestha, P.A.J. Fonseca, "Optimal transmission expansion under different market structures," *IET Generation, Transmission & Distribution*, vol. 1, no. 5, pp. 697-706, 2007.
- ²⁸⁸ J. Contreras, *et. al.*, "An incentive-based mechanism for transmission asset investment," *Decision Support Systems*, vol. 47, no. 1, pp. 22-31, 2009.
- ²⁸⁹ R. Romero, R.A. Gallego, A. Monticelli, Transmission system expansion planning by simulated annealing, *IEEE Transactions on Power Systems*, vol. 11, no. 1., pp. 364-369, 1996.
- ²⁹⁰ R. Romero, M.J. Rider, I. de J. Silva, "A Metaheuristic to Solve the Transmission Expansion Planning," *IEEE Transactions on Power Systems*, vol. 22, no. 4, pp. 2289-2291, 2007.
- ²⁹¹ X. Min, Z. Zhong, F.F. Wu, "Multiyear Transmission Expansion Planning Using Ordinal Optimization," *IEEE Transactions on Power Systems*, vol. 22, no. 4, pp. 1420-1428, 2007.
- ²⁹² G.C. Oliveira, A.P.C. Costa, S. Binato, "Large scale transmission network planning using optimization and heuristic techniques," *IEEE Transactions on Power Systems*, vol. 10, no. 4, pp. 1828-1834, 1995.
- ²⁹³ R. Romero, A. Monticelli, "A zero-one implicit enumeration method for optimizing investments in transmission expansion planning," *IEEE Transactions on Power Systems*, vol. 9, no. 3, pp. 1385-1391, 1994.
- ²⁹⁴ R.A. Gallego, A. Monticelli, R. Romero, "Comparative studies on nonconvex optimization methods for transmission network expansion planning," *IEEE Transactions on Power Systems*, vol. 13, no. 3, pp. 822-828, 1998.
- ²⁹⁵ EIA (2013, February 19). Annual Energy Outlook 2012: Electricity Supply, Disposition, Prices, and Emissions, Reference case [Online]. Available: <http://www.eia.gov/oiaf/aeo/tablebrowser/#release=AEO2012&subject=6-AEO2012&table=8-AEO2012®ion=0-0&cases=ref2012-d020112c>.

²⁹⁶ L.L. Garver, "Transmission Network Estimation Using Linear Programming," *IEEE Transactions on Power Apparatus and Systems*, vol. PAS-89, no. 7, pp. 1688-1697, 1970.

²⁹⁷ AEP (2013, February 19). Transmission Facts [Online]. Available: <http://www.aep.com/about/transmission/docs/transmission-facts.pdf>.

²⁹⁸ PG&E (2012, December 14). PG&E's Approximate Unit Costs for Generation Interconnection Projects [Online]. Available: www.caiso.com/2383/2383ca232f20.xls.

²⁹⁹ SCE (2012, December 14). 2011 SCE Generator Interconnection Unit Cost Guide [Online]. Available: www.caiso.com/2b25/2b25b8e528cc0.xls.

³⁰⁰ SDG&E (2012, December 14). SDG&E Preliminary Draft Unit Cost Guide [Online]. Available: www.caiso.com/2b25/2b25b89526df0.xls.

³⁰¹ BLS (2013, February 13). Producer Price Index Industry Data - Original Data Value [Online]. Available: http://data.bls.gov/images/buttons/download_button_xls.gif.

³⁰² ELES (2013, February 10). Networked with Future: ELES Summary Annual Report [Online]. Available: http://www.eles.si/en/files/eles/userfiles/ANG/About_ELES/Annual_reports/ELES_Annual-Report-2010.pdf.

³⁰³ IBE (2013, February 10). News: Successful Connection of the Divača Phase Shifting Transformer into the 400 kV Transmission Network [Online]. Available: http://www.ibe.si/portal/page?_pageid=54,939627&_dad=portal&_schema=PORTAL.

³⁰⁴ F. Esselman (2013, February 10). Upper Midwest APDA "Arrowhead Weston" [Online]. Available: http://oasis.midwestiso.org/documents/ATC/Upper_Midwest_APDA_A-W_presentation053008.pdf

³⁰⁵ MN OAH (2012). [Online]. <http://www.oah.state.mn.us/cases/arrowhead/mpbrief.html>.

³⁰⁶ PJM (2013, February 12). PJM Bus Model as of December 19, 2012 [Online]. Available: <http://www.pjm.com/~media/markets-ops/energy/lmp-model-info/lmp-model.ashx>.

³⁰⁷ Northwest Power Planning Council (2011, June 5) *Natural Gas Combined-cycle Gas Turbine Power Plants* [Online]. Available: http://www.westgov.org/wieb/electric/Transmission%20Protocol/SSG-WI/pnw_5pp_02.pdf.

³⁰⁸ Platts Resource and Consulting, “Coal-Wind Integration: Strange Bedfellows May Provide a New Supply Option,” RPS-3, 2003.

³⁰⁹ N. Miller, P.E. Marken, “Facts on grid friendly wind plants,” in *IEEE Power and Energy Society General Meeting*, Minneapolis, MN, 2010.

³¹⁰ EIA (2013, February 25). *Form EIA-860* [Online]. <http://www.eia.gov/electricity/data/eia860/xls/eia8602011.zip>.

³¹¹ Brattle Group, CH2M Hill. (2013, February 25). *Cost of New Entry Estimates for Combustion-Turbine and Combined-Cycle Plants in PJM* [Online]. Available: http://www.brattle.com/_documents/UploadLibrary/Upload971.pdf.

³¹² N. Petchers, *Combined Heating, Cooling and Power Handbook: Technologies and Applications : an Integrated Approach to Energy Resource Optimization*. Lilburn, GA: Fairmont Press, 2003.

³¹³ EPA (2012). *eGRID2012* [Online]. Available: http://www.epa.gov/cleanenergy/documents/egridzips/eGRID2012V1_0_year09_DATA.xls.

³¹⁴ EIA (2013, January 29). *Annual Energy Outlook 2012: Natural Gas Supply, Disposition, and Prices, Reference case* [Online]. Available: <http://www.eia.gov/oiaf/aeo/tablebrowser/#release=AEO2012&subject=8-AEO2012&table=13-AEO2012®ion=0-0&cases=ref2012-d020112c>.

³¹⁵ (2013, January 29). *Annual Energy Outlook 2012: Coal Supply, Disposition, and Prices, Reference case* [Online]. Available: <http://www.eia.gov/oiaf/aeo/tablebrowser/#release=AEO2012&subject=7-AEO2012&table=15-AEO2012®ion=0-0&cases=ref2012-d020112c>.

³¹⁶ T. Levin, V.M. Thomas, A.J. Lee, “State-scale evaluation of renewable electricity policy: The role of renewable electricity credits and carbon taxes,” *Energy Policy*, vol. 39, no. 2, 2011.

³¹⁷ EPA (2013, February 10). Unit Conversions, Emissions Factors, and Other Reference Data [Online]. Available: <http://www.epa.gov/cpd/pdf/brochure.pdf>.

³¹⁸ EIA (2013, February 5). *Annual Energy Review 2011: Table 7.2 Coal Production, 1949-2011* [Online]. Available: <http://www.eia.gov/totalenergy/data/annual/xls/stb0702.xls>.